Proceedings of the I·R·E

A Journal of Communications and Electronic Engineering

Illinois U Library

July, 1950

Volume 38 Number 7

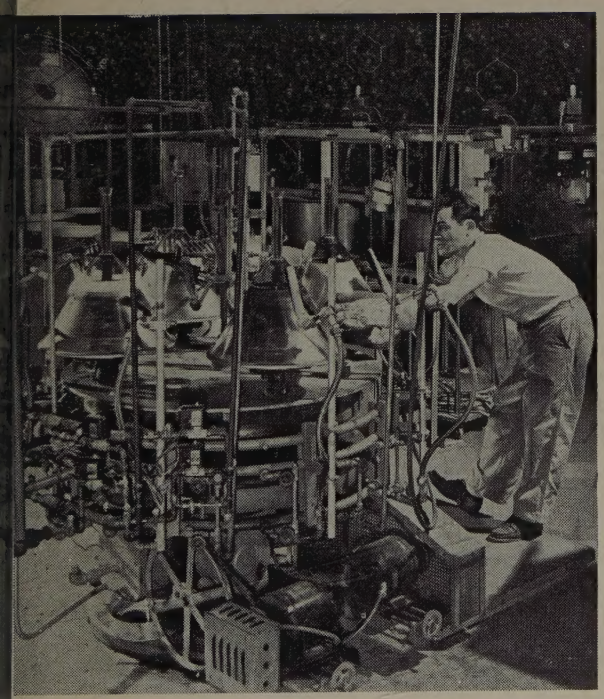

Allen B. DuMont Laboratories, Inc.

EVOLUTION OF PICTURE-TUBE TECHNIQUE

Present-day manufacture of metal-cone glass-face large picture tubes for television contrasts strikingly with the methods of prewar days.

PROCEEDINGS OF THE I.R.E.

Management of Research and Development

Crystal Counters

The Recording Storage Tube

Distributed Amplifiers

Wide-Band Phase Splitting Networks

Detection of a Pulse Superimposed on Noise

Contact Potential Difference for Oxide-Coated Cathode Diodes

Microwave Attenuators

Microwave Attenuation Statistics

The Permittivity of Air at 10 Centimeters

The Beacon Technique in Ionosphere Propagation (Abstract)

Low-*Q* Microwave Filters

Adjustable Electronic Filter Networks

Wide-Band Waveguide Filter Design

Slot Radiators

Surface Waves in Dipole Radiation

Triple-Tuned Coupled Circuits

Abstracts and References

TABLE OF CONTENTS, INDICATED BY BLACK-AND-WHITE MARGIN, FOLLOWS PAGE 32A.

The Institute of Radio Engineers

NEW and *preferred* AMPEREX tubes

for COMMUNICATIONS and INDUSTRIAL Applications

High Frequency · High Power · Proven Life

preferred **FOR HIGH FREQUENCY OPERATION to 150 Mc.**

preferred **FOR GREATER EFFICIENCY**
High Pervience • Thoriated Filaments •
Low Filament Inductance • Specially Coated Grids •
Low Grid Lead Inductance

preferred **ESPECIALLY IN GROUNDED GRID CIRCUITS—**
Minimized Filament-Plate Capacitance

preferred **FOR ECONOMY**
Low Initial Cost • Low Operating Cost

Types
492/5757 and 492-R/5758
(water cooled) (air cooled)

Filament — Thoriated Tungsten	
Voltage	5.0
Current (Amps.)	110
Amplification Factor	28
Maximum Ratings — Class "C" Telegraphy	
Plate Voltage	7500
Plate Current (Amps.)	2
Plate Dissipation (Kw.)	5
Typical Power Output (Kw.)	8.5
Frequency (Mc.)	100
Efficiency	75%
Inter-electrode Capacitances (mmf)	
Grid-Plate	21
Grid-Filament	30
Plate-Filament	0.6

Detailed characteristic sheets available on request

NEW!

TYPE 501-R/5759

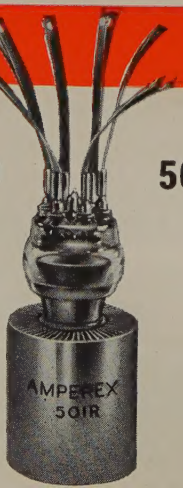

TYPE 502-R/5761

Write for descriptive data sheets

re-tube with AMPEREX

AMPEREX ELECTRONIC CORP.
25 WASHINGTON STREET, BROOKLYN 1, N. Y.
In Canada and Newfoundland: Rogers Majestic Limited
11-19 Brentcliffe Road, Leaside, Toronto, Ontario, Canada

BOARD OF DIRECTORS, 1950*

Raymond F. Guy
President

R. A. Watson-Watt
Vice-President

D. B. Sinclair
Treasurer

Haraden Pratt
Secretary

Alfred N. Goldsmith
Editor

B. E. Shackelford
Senior Past President

Stuart L. Bailey
Junior Past President

1950

Ben Akerman (6)
W. R. G. Baker
T. H. Clark
J. V. L. Hogan (2)
T. A. Hunter (5)
H. E. Kranz (4)
F. H. R. Pounsett (8)
J. E. Shepherd
J. A. Stratton

1950–1951

A. V. Eastman (7)
W. L. Everitt
D. G. Fink
F. Hamburger, Jr. (3)
H. J. Reich (1)
J. D. Reid (5)

1950–1952

W. R. Hewlett
J. W. McRae

●

Harold R. Zeamans
General Counsel

●

George W. Bailey
Executive Secretary

Laurence G. Cumming
Technical Secretary

●

Changes of address (with advance notice of fifteen days) and communications regarding subscriptions and payments should be mailed to the Secretary of the Institute, at 450 Ahnaip St., Menasha, Wisconsin, or 1 East 79 Street, New York 21, N. Y.

All rights of republication, including translation into foreign languages, are reserved by the Institute. Abstracts of papers, with mention of their source, may be printed. Requests for republication privileges should be addressed to The Institute of Radio Engineers.

*Numerals in parenthesis following Directors' names designate Region number.

PROCEEDINGS OF THE I.R.E.

Published Monthly by

The Institute of Radio Engineers, Inc.

VOLUME 38 — *July, 1950* — NUMBER 7

PROCEEDINGS OF THE I.R.E.

William R. Hewlett, Director-at-Large, 1950–1951 722
Radio Is Big Business! ..... Orestes H. Caldwell 723
3657. Management of Research and Development ..... Ralph I. Cole 724
3585. Correction to "Frequency Analysis of Variable Networks" ..... Lotfi A. Zadeh 725
3658. Crystal Counters ..... Robert Hofstadter 726
3659. The Recording Storage Tube ..... R. C. Hergenrother and B. C. Gardner 740
3660. Distributed Amplifiers: Practical Considerations and Experimental Results ..... William H. Horton, John H. Jasberg, and Jerre D. Noe 748
3661. The Design of Wide-Band Phase Splitting Networks ..... W. Saraga 754
3662. Detection of a Pulse Superimposed on Fluctuation Noise ..... Bernard M. Dwork 771
3663. The Measurement of Contact Difference in Potential on Certain Oxide-Coated Cathode Diodes ..... I. E. Levy 774
3664. Microwave Attenuators for Powers up to 1,000 Watts ..... H. J. Carlin and E. N. Torgow 777
3665. Microwave Attenuation Statistics Estimated from Rainfall and Water Vapor Statistics ..... Howard E. Bussey 781
3666. The Permittivity of Air at a Wavelength of 10 Centimeters ..... W. Eric Phillips 786
3667. The Beacon Technique as Applied to Oblique Incidence Ionosphere Propagation ..... J. T. deBettencourt and H. Klemperer 791
3668. Low-*Q* Microwave Filters ..... John Reed 793
3669. Continuously Adjustable Electronic Filter Networks ..... Glenn E. Tisdale 796
3670. Design Relations for the Wide-Band Waveguide Filter ..... Seymour B. Cohn 799
3671. Slot Radiators ..... Nicholas A. Begovich 803
3672. On the Existence of a Surface Wave in Dipole Radiation over a Plane Earth ..... T. Kahan and G. Eckart 807
3673. An Analysis of Triple-Tuned Coupled Circuits. Norman W. Mather 813
Contributors to the PROCEEDINGS OF THE I.R.E. 822
Correspondence:
3674. Cathode Neutralization of Video Amplifiers. Roger D. Thompson 825
3675. Progression of Microwave Radio Scintillations at Wind Speed on an Overwater Path ..... A. W. Straiton and H. W. Smith 825

INSTITUTE NEWS AND RADIO NOTES SECTION

Technical Committee Notes 827
Industrial Engineering Notes 829
IRE People 831
Books:
3676 "Recent Advances in Radio Receivers" by L. A. Moxon ..... Reviewed by S. W. Seeley 832
3677. "Acoustical Designing in Architecture" by Vern O. Knudsen and Cyril M. Harris ..... Reviewed by Leo L. Beranek 832
3678. "Television Simplified" by Milton S. Kiver ..... Reviewed by Nathan Marchand 832
3679. "How To Become a Radio Amateur," published, (1950) by the American Radio Relay League 832
Sections 833
3680. Abstracts and References 835
News-New Products 30A
Section Meetings 33A
Student Branch Meetings 35A
Membership 39A
Positions Open 50A
Positions Wanted 52A
Advertising Index 63A

Copyright, 1950, by The Institute of Radio Engineers, Inc.

EDITORIAL DEPARTMENT

Alfred N. Goldsmith
Editor

E. K. Gannett
Technical Editor

Mary L. Potter
Assistant Editor

●

ADVERTISING DEPARTMENT

William C. Copp
Advertising Manager

Lillian Petranek
Assistant Advertising Manager

●

BOARD OF EDITORS

Alfred N. Goldsmith
Chairman

PAPERS REVIEW COMMITTEE

George F. Metcalf
Chairman

Responsibility for the contents of papers published in the PROCEEDINGS OF THE I.R.E. rests upon the authors. Statements made in papers are not binding on the Institute or its members.

MEMBER AUDIT BUREAU OF CIRCULATIONS

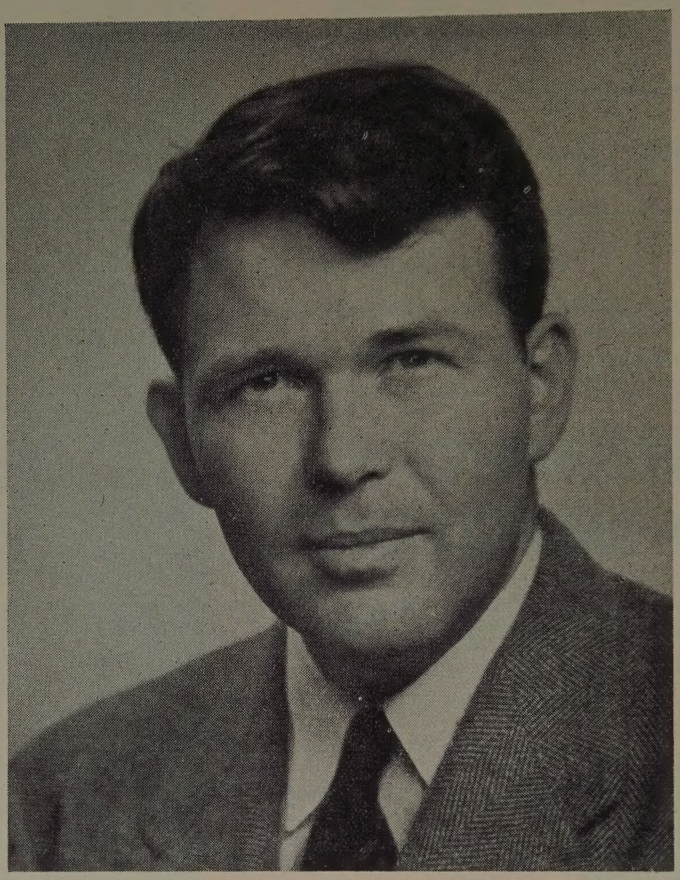

William R. Hewlett

DIRECTOR-AT-LARGE, 1950–1951

William R. Hewlett was born at Ann Arbor, Mich., in 1913. He was graduated from Stanford University in 1934 with the A.B. degree. After a year of graduate work at Stanford, he enrolled at the Massachusetts Institute of Technology, where he received the degree of Master of Science in 1936.

Mr. Hewlett then returned to Palo Alto, Calif., and for the next few years was engaged in electro-medical research, particularly in the field of electro-encephalography. He was at the same time occupied with part-time graduate work at Stanford, receiving the E.E. degree in 1939. That year he and David Packard organized the Hewlett-Packard Company in Palo Alto for the development and production of various kinds of electrical measuring equipment.

In 1942 he was called to active duty in the Army, and was assigned to the Technical Division of the Office of the Chief Signal Officer in Washington, D.C., for the next three years. He was then transferred to the New Development Division of the War Department's Special Staff, where he served as the head of the Electronics Section. In 1945 he was a member of the Compton Mission, which was sent to Japan immediately after surrender to form a quick appraisal of the Japanese scientific war effort. In December of that year he returned to the Hewlett-Packard Company, and has continued his activities there.

Mr. Hewlett was made an Associate Member of the Institute in 1938, a Senior Member in 1947, and in 1948 was elected a Fellow. He is the present Chairman of the San Francisco Section of IRE. Mr. Hewlett is also a member of Sigma Xi, AIEE, and of the Commission on Radio Standards and Methods of Measurement of the URSI.

Engineers are not only capable and successful technologists. They are also powerful stimulators of industry and commerce and may well be proud of the part they play in the welfare of their homeland.

A radio and television pioneer, and a former Federal Radio Commissioner, who is presently the Editor of *Tele-Tech*, here presents impressive statistics showing what the IRE membership are contributing to the national productivity. Their work constitutes an outstanding and encouraging accomplishment.—*The Editor.*

Radio Is Big Business!

ORESTES H. CALDWELL

Now when Uncle Sam is conducting a census of his big family of 153,000,000, it is appropriate for the radio-television industry to size up its own magnitude, as an aid to future planning. It is estimated that in 1950 we will sell $3,000,000,000 worth of radio and television products to American purchasers.

Dependable accurate radio-industry statistics are needed to eliminate the wide discrepancies one finds between the statistical estimates of supposed industry authorities.

Having compiled the statistics of radio and its branches over the past twenty-eight years, I am putting down below my own present best estimate of the industry's outlook for 1950, compiled with the help of specialists in each division:

	At Manufacturers' Selling Price	*At Final or Customers' Price*
6,000,000 television sets	$ 900,000,000	$1,600,000,000
12,000,000 radio sets	260,000,000	500,000,000
Broadcast, recording and studio equipment	200,000,000	200,000,000
Mobile, airplane, police and taxi radio	100,000,000	100,000,000
Replacements, accessories, instruments	190,000,000	250,000,000
Government purchases	350,000,000	350,0000,00
Radio and television total	$2,000,000,000	$3,000,000,000
Electronics—industrial, scientific and medical	100,000,000	100,000,000
Industry total	$2,100,000,000	$3,100,000,000

There you have the tremendous magnitude of our industry today—over 95 per cent of it radio and television! For the total "electronics" or noncommunication applications gross up to a bare 5 per cent of the industry's output at manufacturers' selling prices, or 3 per cent of output at final selling prices. Stated another way relatively, the present size of "industrial electronics" compares approximately with that of Rhode Island in the U.S. picture.

In the past there has been some disposition to call this huge industry of ours by the name of its 5 per cent industrial component. But no longer should loyal radio-engineers and members of the IRE let the small $100-million electronic tail wag the $3-billion radio-TV dog!

We need better radio-industry statistics to evaluate our markets truly and accurately.

In fairness, too, we should call our industry and our markets by their right names. For this is, after all, *the radio-television industry*, and nothing else!

Management of Research and Development*

RALPH I. COLE†, SENIOR MEMBER, IRE

I. Introduction

IT CAN HARDLY be denied that whatever progress modern industry is making towards product improvement, as well as towards new inventions, is being spurred by organized research and development. This does not imply that individual inventors are not contributing to scientific advancement, but, rather, that their over-all effort is small in comparison with the industrial and governmental progress. Directing of large groups of individuals in any field of endeavor requires efficient management, and this is especially true of research and development. Now, by *management* is meant the guidance of scientific or engineering organizations in accordance with applicable technical and administrative policies, said policies being derived to co-ordinate and thus facilitate the work effort to achieve the greatest possible technical progress consistent with the mission.

II. Factors to Take into Consideration in Organizing Research and Development Activity

A. In this guidance, an intimate knowledge of the capabilities of the men serving you is of paramount importance. Thus assignments must be adjusted and based upon what the worker is able to grasp, rather than solely upon decisions that do not take into account the fitness of the man for the job. It can thus be seen that management's responsibility is to possess a deep insight into the type of activity involved in order that the correct match of the capability of the man to the requirements of the job can be obtained.

B. In no other field of activity is the encouragement of nebulous ideas of greater importance than in research and development. It is these ideas that are the seeds of future projects and a part of the storehouse of knowledge which, when mixed with the results of basic sciences, enables an engineer to secure a fresh approach to the most difficult problems. Often, the lack of a fresh approach has led to blind alleys with resulting lack of achievement towards the end goal. The development of scientific vision results in the ability to do long-range planning from nebulous ideas and is achievable only by straight thinkers who have the ability to step out and adapt new scientific principles to their problem.

C. Too often rules and regulations that are perfectly sound for administrative or production personnel prove inadequate for the research and development type owing to the lack of flexibility. This is fairly obvious when one considers that the full outcome of research and development is unpredictable and that the potentialities of the end result usually lead to possible applications in other fields, as well as to the solution sought. Thus, management's responsibility for maintaining the greatest possible flexibility of program is a serious one and requires frequent review of the individual project's relationship to any master plan.

D. It is observed that there are many methods of organizing technical research and development groups, such as according to end function, component, techniques, or individual systems. Each type or organization has its advantages and it is difficult to state if any one is superior, provided that similar categories of work are accomplished within the same immediate section of the organization. This latter premise is of extreme importance in order to avoid overlapping of jobs and duplication of effort. Furthermore, management's ability to follow work progress is at optimum when it is possible to look to one group as the authority on any one subject.

E. In no other field of activity is decentralization of the line of technical authority more important than in research and development. This immediately poses the problem of separation of the technical direction from the administrative control in order to reduce to a minimum the chains of command dealing with purely technical aspects. At the same time, the administrative control must be adequate to insure compliance with all basic policies and provide the atmosphere to accomplish true scientific work.

F. As important as the proper background for initiation of a project is the establishment by management of a means of insuring proper project continuity and a means for reporting thereon. Each echelon of management must insure that status reporting is given its proper emphasis in order that top management can determine its net value to the long-range picture. Too often a change in the end goal is not reflected down to the worker, with the result that proper use cannot be made of the completed project. The exact manner in which this matter is handled is dependent upon the organization but, as a general rule, the reporting period should be frequent in order to insure complete co-ordination.

III. Facilities for Research and Development

A. In establishing proper facilities to accomplish research and development, care must be taken to insure flexibility for the changes in mission as they occur. One aspect, therefore, that management must watch is that allowance be made for periodic expenditures of capital funds to gear the facilities to the mission. Thus, it is not sufficient merely to allocate funds to individual projects with no thought to new capital outlays necessary to accomplish the work. Being mindful of this problem, management must anticipate, considerably in advance, the change in facilities required due either to obsolescence or to a new requirement, and they must see that the new facilities are available prior to the initiation of new projects.

B. The smooth flow of incoming components and supplies is one of the more vexing problems for which management must be continuously on the alert. Too often, the enthusiasm of the engineer or scientist is dampened by the obstacles encountered in obtaining even the most minor component. When it is realized that it is difficult in many instances to properly anticipate requirements on any individual project, one can realize that the responsibilities of management to plan for a nebulous future are indeed great. Only by frequent re-examination of this problem can an organization speedily eliminate bottlenecks as they develop, and thus expedite this phase of the over-all activity.

C. As so often is the case, what at first approach appears to be a minor problem often develops into a major headache. For example, in providing automotive transportation for either field testing or administrative travel, management is responsible for seeing that delays are kept to a minimum and that high-grade scientists and/or engineers do not double as truck drivers, a job for which they are usually poorly equipped. Furthermore, only by having a separate team of drivers can an organization insure maximum safety in the transportation of its personnel.

D. One of the major resources of a research and development organization is the technical library. Keeping such a library up to date not only entails the full-time duties of a suitably trained library staff, but also requires close co-ordination with the scientific staff to insure maximum utilization of the facility provided. One of the ways that the library staff can assist in this matter is to issue periodic abstracts of new books and articles received, thereby calling to the attention of a busy worker material that may have a bearing on the subject under investigation. This in itself is not enough, however, and the research and development staff must be encouraged to outline their *advance* requirements to the library in order that the time of all concerned may be conserved. For example, before an engineer embarks upon a new phase of a project, he should request from the library a survey of the background material in this field, and his request should be explicit enough for the librarian to carry out intelligently his or her task so that the work does not have to be re-

* Decimal classification: R010. Original manuscript received by the Institute, February 10, 1950.
† Watson Laboratories, Air Materiel Command, Red Bank, N. J.

done when the study is turned over to the project leader. It is this phase of library operation that is usually the weakest and it is therefore the responsibility of management to insure that all scientific personnel are properly briefed on what is expected of them.

IV. Charting of Progress in Research and Development

A. It has previously been mentioned that management must insure that the periodic status and technical reporting on any project is adequate to enable proper decisions to be made by higher authority. It is of equal importance, however, to insure that the keeping of internal records is complete and up to date. For this purpose, it is considered essential that project record books explain in considerable detail the experiments conducted, not only to insure that future workers will not duplicate, but, of equal importance, to insure that patent records can be duly authenticated.

B. Not to be confused with status reporting are technical and memorandum reports. These latter reports summarize in considerably more detail the description of the experiments conducted and the results obtained, as well as recommendations for future action. As in the case of project record books, the memorandum and technical reports serve as background material for the planners of new projects and, if properly prepared, furnish an adequate chronological history on the subject covered. Too often these reports, whether prepared within the organization or by contractors, do not reach the proper project leader and, hence, their value is never fully realized. It is considered management's responsibility to see that a distribution system is set up, insuring that all persons having a finite interest in the subject are made aware of the existence of said report, and to encourage the employee to make further investigation of the contents thereof.

C. It is considered an old axiom that the rapidity of man's progress is directly related to his ability to interchange ideas. Project seminars are one of the most effective mediums of such interchange of information, and at the same time afford the project leader an opportunity to gain confidence in self-expression. By encouraging such conferences, management is definitely building future executives and at the same time insuring technical growth of their personnel. In addition, it is considered good policy on the part of management to encourage formal technical education for their staff in order that they may be technically alert to the new findings of science and take advantage of the "know how" that others have derived.

V. Place of Administrators in Research and Development

A. In order to insure the most efficient management, men specially trained in administration should be utilized wherever possible in a research and development organization to relieve the strain on the technical staff. By thus considering administration to be just as specialized as project engineering, management can insure getting the most out of all personnel in an atmosphere that breeds mutual respect and generally loyal "esprit de corps." Among some of the duties which can best be achieved by administrators either in whole or in part are the following:

1. Budget co-ordination.
2. Fiscal matters.
3. Administrative problems relating to hiring of personnel.
4. Correspondence follow up; follow through on due date.
5. Administrative arrangements required for conferences and demonstrations; procurement of supplies; arrangement for transportation both technical and administrative; reproduction of printed matter; management of services such as dispensary, restaurant, etc.

VI. Personnel Policies

A. In order to insure the future growth and perpetuation of any research and development organization, it is considered important that provision be made for special promotion of men with talent. It is recognized that this is often difficult to do, but at the same time the competition is such that if these personnel cannot properly be taken care of they will go elsewhere to seek advancement. For this reason, management should use every means at their control, such as efficiency reports, to insure that outstanding personnel are given the maximum possible responsibilities and that, conversely, older personnel who have stagnated are, if retained, placed in such positions as do not prevent the advancement of junior men.

2. Personal contact by all echelons of supervisory personnel with their workers does much to promote a high "esprit de corps" and, hence, make for more efficient management. When the worker is made to feel that he is part of a big family, he invariably develops a team spirit. Of the many means of achieving this personal contact, staff meetings, as well as technical inspections of the worker's laboratory, are considered the most productive.

VII. Conclusion

From the foregoing, it is seen that management as such has much to contribute to the proper functioning of a research and development organization. It is not to be considered a yoke around the worker's neck, but rather a source of mutual assistance which generates the team spirit. It must be emphasized that supervisory personnel must continually earn the right to hold their job in the eyes of their workers and must never consider that their job is a sinecure. Alert management stresses the common responsibilities of workers and supervisors to bring this mutual respect.

CORRECTION

Two errors in the paper, "Frequency Analysis of Variable Networks," by Lotfi A. Zadeh, which appeared on pages 291–299, of the March, 1950, issue of the Proceedings of the I.R.E., have been brought to the attention of the editors by the author.

They are as follows: (1) In Fig. 1, on page 294, the symbols $H_0(j\omega; t)$, $H_1'(j\omega; t)$, $H_1''(j\omega; t)$, etc., should read $H_0(j\omega)$, $H_1'(j\omega)$, $H_1''(j\omega)$, etc.

(2) Equation (47) on page 297, should read $H = H_f - P\{H\}$.

Crystal Counters*

ROBERT HOFSTADTER†

Summary—This paper gives a general account of the recently discovered conduction type counters. Among the topics discussed are: The nature of the counting phenomenon, preparation of crystals, types of useful crystals, experimental technique, polarization, speed, limitations and comparisons with other types of counters.

I. Introduction

COUNTING ionizing particles with the aid of solids is a relatively novel technique in modern physics. One aspect of this technique has recently been described in this journal.[1] This paper will deal with that second part of the counting technique in which induced conduction of insulating crystals is brought about by ionizing particles.

The first practical crystal counter using AgCl was described by van Heerden[2] in 1945. Subsequently further work was performed, for the most part in this country, on AgCl, diamond, and other materials. A review paper by the author summarizing these developments appeared in 1949.[3] Since publication of that review there have been several new developments, including the discovery of sulphur and germanium counters, and the possible new development of alkali-halide conduction counters.[4] An historical note was given in the literature[3] and will not be repeated here.

II. The Mechanism of Detection

1. *Generalities*

The conventional particle detector which is most like the crystal conduction counter is the ionization chamber. Indeed, a suitable name of the crystal counter might be "solid ionization chamber." This resemblance may be understood from the following discussion centered about Fig. 1. The figure shows an energetic beta particle entering the crystal from the left (point A). Free electrons are produced in the crystal by a process analogous to ionization in a gas. Positive ions are also produced in equal number when the electrons leave their normal sites. Although in a gas the electrons are actually set loose in vacuum, in the crystal the electrons are elevated to the conduction band, shown at the top of Fig. 2. In both cases the free electrons and ions are formed close about the track of the incident beta particle. To appreciate the number of electrons produced, we cite as an example that a 1-Mev electron will form about 1.2×10^5 secondary electrons in AgCl and about 3×10^4 secondary electrons in a gas.

In a gas the positive ions move about

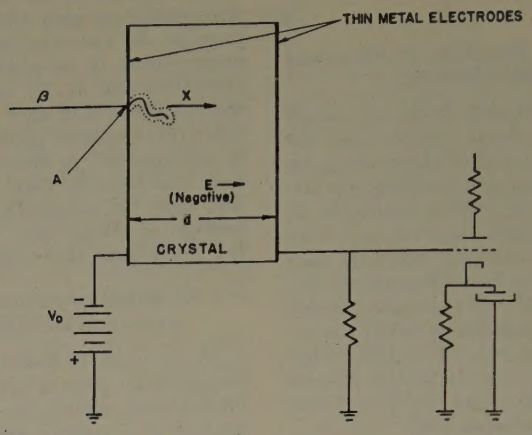

Fig. 1—A schematic diagram of a crystal conduction counter.

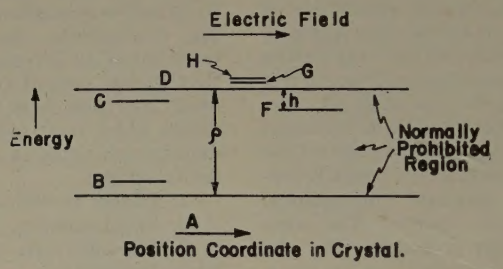

Fig. 2—The energy states for an insulating crystal. Conduction band is above; normally filled band is below. Traps are shown at F and BC represent localized energy states of impurity atoms.

with a speed considerably smaller than that of the electrons. In a solid it is possible that the positive ions or "holes" do not move at all. In AgCl at low temperatures, it is known that the ions do not move. We shall assume in the subsequent paragraphs that the positive ions or holes do not move.

Since an electric field exists across the crystal of Fig. 1, the cloud of electrons, instantaneously formed about the track of the particle, will drift across the crystal. Any individual electron will be accelerated by the field, and will gain speed and energy. It will soon suffer a collision with the ions of the lattice and give up its energy. It will start again and repeatedly go through the same process until either (a) it reaches the neighborhood of the positive electrode, or (b) it is captured by a "trap." Once captured by a trap, the electron is immobilized. Examples of traps, which are capture sites for free electrons in crystals, are impurity atoms, interstitial atoms, vacancies (F centers), lattice defects, cracks, or crystal boundaries. Those electrons which are trapped may be released at a later time, but this time is usually so long (hours, days) that we shall not discuss the electron release mechanism at present.

In a weak field the electrons will drift with a small average velocity

$$w = vE \qquad (1)$$

where w is the velocity, v the mobility, and E the electric field. The mobility v is a constant of the material at a given temperature and is defined by this equation. Sooner or later the electron will be captured before it reaches the positive electrode, if the average velocity w is small. In this case of small velocities, the electron spends a long time near a trap and is eventually sucked in. When the velocity is high, the secondary electron may move by a trap so quickly that there is very little probability that the electron will be stopped. Thus, for high velocities, which means high electric fields, most electrons will reach the positive electrode.

These remarks may be partially condensed into the formula

$$\lambda = vET \qquad (2)$$

where λ is the average distance moved by a cluster of electrons formed at a point in the crystal in the electric field E. T is a characteristic time of the crystal, which indicates the average time an electron may spend in the conduction band before being trapped. λ is called the "Schubweg"[5] and will be observed later to be a most important quantity.

Now when an electron starts near the negative electrode and moves the entire distance within the crystal to the positive electrode, it is easy to see that the charge induced on grid G is the charge of one electron. However, if an electron should move

* Decimal classification: 621.375.2×539. Original manuscript received by the Institute, April 12, 1950.
† Palmer Physical Laboratory, Princeton University, Princeton, N. J.

[1] J. W. Coltman, "The scintillation counter," Proc. I.R.E., Vol. 37, pp. 671–685; June, 1949.
[2] P. J. van Heerden, Dissertation, "The Crystal Counter," Utrecht; 1946.
[3] R. Hofstadter, "Crystal counters," *Nucleonics*, vol. 4, no. 4, p. 2, 1949; vol. 4, no. 5, p. 29, 1949.
[4] Private communication from F. Stöckman (Göttingen). Stöckmann has written a short account of developments in crystal counters in the periodical *Die Naturwissenschaften*, vol. 36, p. 82, 1949.
[5] N. F. Mott and R. W. Gurney, "Electronic Processes in Ionic Crystals," Oxford University Press, New York, N. Y., 1st Ed., p. 119; 1940.

only one-half the distance to the positive electrode and be trapped at a midway point, then the induced charge is not that of one electron, but is just half the electronic charge. It has been shown theoretically[6] that the effective charge q induced on the grid is such that

$$q = e\frac{\Delta x}{d} \tag{3}$$

where Δx is the distance the electron moves before being trapped and d the thickness of the crystal. Equation (3) has also been tested empirically by Hecht,[7] in another regard, who confirms this relation. In (2) it does not matter where the electron starts or ends its travel; it merely travels the distance Δx.[8]

The voltage pulse produced at G, due to a single secondary or "ionization" electron, is

$$V = \frac{e\Delta x}{Cd} \tag{4}$$

where C is the combined capacitance to ground of the grid, crystal, and associated connections. By an analysis similar to that of Hecht[7] or Mott and Gurney[5] it may be shown[3] that the voltage pulse, due to a beta particle entering the crystal of Fig. 1 at point A, is

$$V = \frac{n_0 e}{C}\frac{\lambda}{d}(1 - e^{-d/\lambda}). \tag{5}$$

In this equation n_0 represents the number of electrons released by the beta particle near the negative electrode. The other quantities have already been defined. The fact that the beta particle penetrates the crystal to a small extent is neglected, although it is simple to take this penetration into account.[3] The curve of Fig. 3 shows a behavior of V as a function of λ/d. As might be expected, the voltage pulse saturates at the value n_0e/C when all secondary electrons released near the negative electrode reach the positive electrode.

When the field is weak, by (2), λ is small and (5) becomes

$$V = \frac{n_0 e\lambda}{Cd}. \tag{5a}$$

In this case the pulse size is directly proportional to the number of secondary electrons produced by the ionizing event. This type of behavior is commonly used, e.g., when the incoming particle is heavy and energetic and so deposits a large energy in the crystal.[9]

When an ionizing event releases n_0 electrons at a point x_0 from the positive electrode, the resulting voltage pulse has the form

$$V = \frac{n_0 e\lambda}{Cd}(1 - e^{-x_0/\lambda}). \tag{5b}$$

It may be seen that (5) is a special case of this relation referring to that situation when $x_0 = d$.

If electrons are released uniformly within the crystal by a penetrating particle, whose range is larger than the crystal thickness, the saturation value of the voltage pulse is $n_0e/2C$, since the average distance moved by an electron is $d/2$. The curve giving the pulse size as a function of λ/d is similar, though not the same as that of Fig. 3.[3] The curve for such events is given in Fig. 4 and its expression in (5c):

$$V = \frac{n_0 e}{C}\frac{\lambda}{d}\left[1 - \frac{\lambda}{d}(1 - e^{-d/\lambda})\right]. \tag{5c}$$

By (2) λ is proportional to E so that the curves of Fig. 3 and Fig. 4 may equally well be plotted against the electric field.

In the detection of gamma rays, fast beta particles are produced within the crystal by the photoelectric, pair production, and Compton processes. Such beta particles will further produce clusters of secondary electrons around their tracks. There are two reasons why such beta particles will not provide uniform pulses, even though the original gamma ray beam is homogeneous: (a) the position (x_0) in the crystal where the beta particle is formed occurs at random, and (b) the energy of a Compton beta particle is not unique. Δx, because it may be limited by the electrodes, will clearly depend on (a), unless the displacement is very small. (See (5b).) By using a weak electric field, this effect may be minimized at the usual expense of decreasing the pulse size [$(\Delta x/d)\to 0$]. The spread in pulse height due to formation of electrons at different positions may thus be reduced, although reason (b) remains fully effective. However an idea of the pulse distribution can be obtained when it is assumed that (1) all ionizing events produce an equal number of secondary electrons, and (2) the events are distributed uniformly over the crystal. In this case the number of pulses (dN) lying within the range of dQ at Q, where Q is the charge pulse, is

$$dN = \alpha d\frac{dQ/n_0e}{1 - \frac{d}{\lambda}\frac{Q}{n_0e}}, \tag{6}$$

where α is a constant.[3] The resulting distribution of pulse heights cuts off at a value of

$$\frac{Q_{max}}{n_0e} = \frac{\lambda}{d}(1 - e^{-d/\lambda}) \tag{7}$$

because the particles move only the average distance given by the right-hand side of (7).

Equations (5), (5a), (5b), (5c), and (6) give the pulse height formulas most often used in the case of crystal conduction counters. We may summarize this section by noting that pulse heights and pulse distributions behave according to (5), (5a), (5b), (5c), and (6) which apply also to the case of the gaseous ionization chamber.

2. *Remarks on* λ

The performance of a crystal conduction counter, apart from polarization effects to be discussed later, depends on the quantity λ. If for a given crystal λ is of the order of magnitude of a few tenths of a millimeter to one centimeter, the crystal is likely to be a good counter. If λ is very small the crystal has no chance to count with present elec-

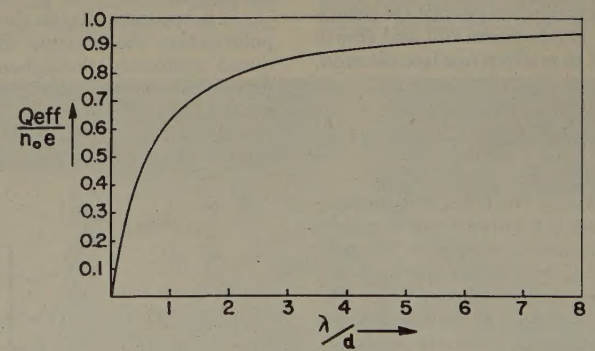

Fig. 3—Pulse size plotted against λ/d. Particle penetrates very small fraction of crystal near negative electrode. The curve is a representation of (5) of the text with $Q_{eff} = CV$. λ is proportional to the electric field.

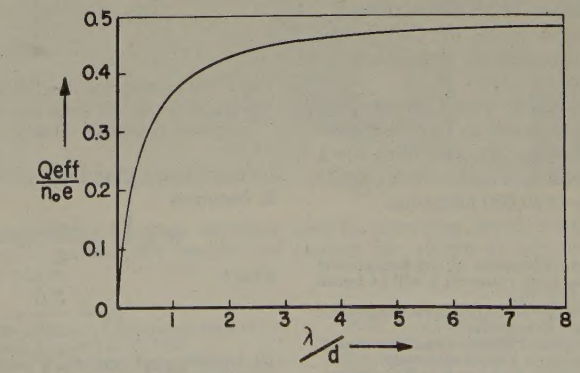

Fig. 4—Pulse size plotted against λ/d for a penetrating particle. The curve corresponds to (5c) of the text with $Q_{eff} = CV$. λ is proportional to the electric field.

[6] W. Shockley, "Currents to conductors induced by a moving point charge," *Jour. Appl. Phys.*, vol. 9, pp. 635–637; October, 1938.

[7] K. Hecht, "Zum Mechanismus des lichtelektrischen Primärstromes in isoherenden Kristallen," *Zeit. für Physik*, vol. 77, p. 235; 1932.

[8] If the positive holes moved the expression corresponding to (3) is

$$q = \frac{\Delta x_- + \Delta x_+}{d} \tag{3a}$$

where Δx_- and Δx_+ are the distances moved respectively by the electron and positive hole.

[9] H. G. Voorhies and J. C. Street, "Star production by negative-μ-mesons in a silver chloride crystal," *Phys. Rev.*, vol. 76, p. 1100; October, 1949.

tronic techniques since V, in (5a), becomes so small that it cannot be measured above the noise introduced by the amplifier circuit.

It is possible to make reasonable estimates of λ for various crystals likely to be conduction counters.[9] A tabulation of such values is given in Table I.[10]

TABLE I

Material	*T(°K)*	*E(volts/Cm)*	*λ(Cm)*
AgCl	77	5×10^3	11.0
AgBr	77	5×10^3	2.1
TlBr	77	5×10^3	6.2
LiF	77	1×10^4	>10.0
LiF	300	1×10^4	0.11
KCl	77	1×10^4	0.28
KCl	300	1×10^4	0.000
KBr	77	1×10^4	0.07
NaCl	77	1×10^4	0.60

Among the materials of the Table, AgCl and AgBr are known to be counters. A mixture of TlBr-TlI has also been proved a counter.[11] The author has had a recent letter from F. Stöckmann of Gottingen which states that alkali halide crystals have been observed to count under the proper conditions. Calculations have not been made for many other crystal types and so it is not possible to predict values of λ.

3. *Remarks on n_0*

It is evident that n_0 helps to determine the size of the observed voltage pulse and hence is a most important constant of the material. It appears that about 5 to 10 electron volts are required to free one secondary electron in the silver halides.[2,12,3] The corresponding quantity is unknown for any other solids except diamond,[13] where the required energy is about 10 electron volts.[14] If we call p the minimum energy (in principle, the energy gap between full and empty bands) required to produce one free electron, then

$$n_0 = \frac{H}{p}\psi \leqq \frac{H}{p}. \tag{8}$$

In this equation H is the energy of the incident particle, and ψ a quantity that gives a measure of how much energy is "wasted" in the crystal, i.e., how much energy is not used in producing free electrons. When ψ is unity no energy is wasted in the above sense. If ψ is zero, no free electrons are produced. The experimentally measurable quantity is $\epsilon=(H/n_0)=(p/\psi)$, the energy per free electron.

It is possible in principle to calculate ψ from the band theory of solids. Although a calculation has been made by Georgesco[28] for AgCl and S, unfortunately details are not given in his paper.

In a gas, ϵ is usually about 30 ev. It is interesting that it is easier to "free" an electron in some solids than in a gas. With $H=1$ Mev, $p=4.9$ ev/electron and $\epsilon=0.6$ (AgCl) (8) shows that $n_0=120{,}000$ electrons.

[10] A more complete discussion of the background required in computing such values of λ will be found in footnote reference 3, p. 10.

[11] R. Hofstadter, "Thalium halide crystal counter," *Phys. Rev.*, vol. 72, p. 1120; 1947.

[12] K. A. Yamakawa, "Silver bromide crystal counter," Thesis, Princeton University, 1949.

[13] For sulphur the value is about 5 ev (Georgesco).

[14] A. J. Ahearn, "Conductivity induced in diamond by alpha particle bombardment and its variation among specimens," *Phys. Rev.*, vol. 73, p. 1113, 1948.

4. *Polarization*

One of the serious handicaps in using solid conduction counters is that in some crystals a space charge or surface charge gradually builds up as the ionization inside the material increases, thereby reducing the pulse size. In a gas the positive ions left behind by the released electrons drift to the negative electrode and are quickly neutralized. In the gas the positive ions therefore do not build up a cumulative stationary space charge. In some solids, e.g., AgCl, AgBr, the positive holes are stationary at the low temperatures where these materials are used as counters. Not only the positive sites, but also the negative electrons can be responsible for polarization since the electrons can be trapped at internal points of the crystal.

A simple example may make the situation clear. Consider a crystal, shown in Fig. 5, which is receiving gamma rays throughout its volume. Assume that the electric field across the crystal is large so that the pulse size is saturated and electrons are carried across the crystal between the point of their formation and the positive electrode.

It is apparent that in the initial stages of polarization the positive sites will be produced uniformly throughout the crystal.[15] If we call the volume density of positive space charge p_0 then the field within the crystal will be modified and will be a function of p_0. A simple calculation in electrostatics[3] shows that the existing electric field E becomes

$$E = \frac{V_0}{d} - \frac{2\pi p_0}{K}(d - 2x) \tag{9}$$

where

$$p_0 = \frac{NH}{\epsilon\tau}e. \tag{10}$$

In these equations V_0/d is the applied electric field without polarization, K is the dielectric constant, ϵ the energy to produce an ion pair, τ the volume of the crystal, and H the energy given up by the gamma ray in the crystal. Fig. 6 shows the applied field and the modified field as a function of the position (x) in the crystal. To the left of center, the field is actually larger than the initial field, while in the right half of the crystal the field is smaller. Evidently the pulse shape will be distorted and the pulse size affected.

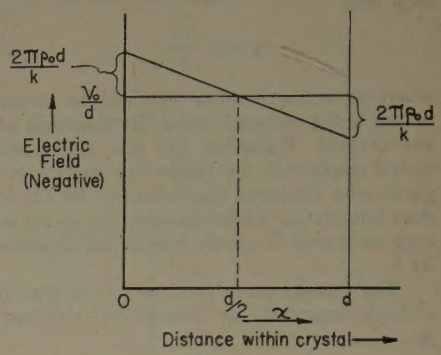

Fig. 6—The sloping line shows the electric field after polarization in a crystal bombarded as shown in Fig. 5. A positive space charge, p_0, has been produced uniformly inside the crystal. K is the dielectric constant. The horizontal line represents the initial electric field, $E=V_0/d$, before polarization occurs.

Some representative numbers will show at what level of counting such effects may be expected: If $V_0/d=5{,}000$ volts/cm, $\tau=0.5$ cm^3, $d=0.5$ cm, $K=12$, $\epsilon=7.6$ ev/ion pair, $H=0.5$ Mev, the number of pulses required to reduce the field to one fifth of its original applied value at the point $x=\frac{3}{4}d$, is 16×10^6. In this small field the pulse size will start to drop in accordance with a behavior like that given by Figs. 3 and 4.

Since electrons will now be trapped in the right-hand half of the crystal, the space-charge effects in that part of the crystal will be partially nullified. It is clear that the subsequent behavior is more complicated than the initial behavior.

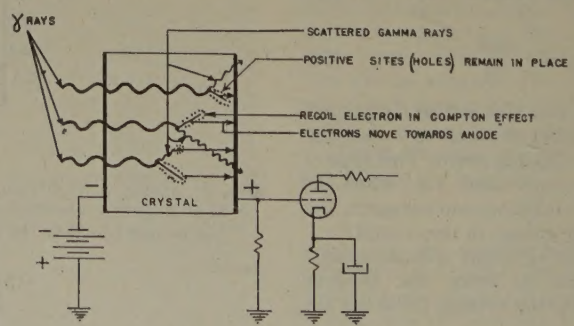

Fig. 5—Crystal bombarded by gamma rays. Electrons are drawn to region of positive electrode. Positive sites are distributed uniformly and are left behind by the electrons. The crystal polarizes slowly.

The effects of polarization can be overcome by periodically reversing the electric field[16,17] under certain conditions. If the

[15] It is assumed that the gamma ray beam is weakly attenuated throughout the crystal.

[16] L. F. Wouters and R. F. Christian, "Effects of space-charge on the detection of high energy particles by means of silver chloride crystal counters," *Phys. Rev.*, vol. 72, p. 1127; 1947.

[17] K. G. McKay, "Electron bombardment conductivity in diamond," *Phys. Rev.*, vol. 74, p. 1606; 1948. See also R. R. Newton, "Space-charge effects in bombardment conductivity through diamond," *Phys. Rev.*, vol. 75, p. 234; 1949.

secondary conduction electrons travel only a short distance before being trapped, both they and their positive sites produce a reversed field. However, if an equal number of secondary electrons can be moved in the opposite direction, by reversal of the field, the effects of the first polarization can be neutralized.

Infrared radiation permits the positive space charge to be neutralized.[18] In this case it is probable that trapped electrons are released by the light, subsequently find their parent ions, and so neutralize them. The effects of visible light in removing polarization have also been studied with diamonds.[19,20]

Newton[17] has given a theoretical explanation, based on space charge effects, of the current versus time relations observed by McKay[17] in bombarding diamond with soft electrons. Newton's results are more detailed but the basic idea is in general agreement with the ideas of polarization presented here and in a previous paper by the present author.[3]

III. Experimental Technique

1. *Materials*

At the present time the crystalline materials which are known to detect single ionization events are AgCl,[2] AgBr,[12,3] diamond,[21–23] ZnS,[24] HgS,[25] S,[26] CdS,[27,28] TlBr-TlI,[11] and solid Argon.[29,30] In addition, one liquid material has been used as a counter-liquid argon.[29,30] Stockman[31] has stated that some alkali halide crystals count single events also. Stibnite and carborundum were also shown to count by Ahearn.[25] The semiconductor germanium[32] has been used to count alpha particles.

2. *Preparation and Handling of Crystals*

It would be most desirable to have crystal counting samples which do not require special treatment before being used for counting. Although this is true for some materials, it is unfortunately not the case for the silver or thallium halide crystals. These halides count only at low temperatures and have to be annealed before use. Crystals of diamond, ZnS, CdS, and S apparently do not need annealing before use, or at any rate, heat treatment has not been applied to such crystals in any published work. Nevertheless the natural crystals which count have to be selected and as a rule are rather uncommon, particularly with respect to beta, particle or gamma ray counting. Certain luminescent type Cds crystals require suitable preparation with green light or with ionizing particle radiation before they count with the very large pulses of which they are capable.

The preparatory treatment of crystals of AgCl, AgBr, TlBr-TlI has been described by several authors.[1,12 11,3,33] A typical treatment of AgCl is to heat the crystal at a fairly slow rate to 400°C and subsequently to reduce this temperature over a period of a day or more to room temperature. Careful handling of the crystal in mounting it is desirable. Haynes[34] has described a procedure for producing strain-free AgCl crystals. From his work it appears that traps occur at or near strained regions, and hence it seems desirable to avoid introduction of strains by rough handling or thermal shocks. Nevertheless, it has not been shown definitely that at low temperatures, strains trap electrons. An investigation of this point seems highly desirable and is of fundamental interest. A procedure which avoids handling and which produces annealing-in-place has been described by Hofstadter.[3] The usual method by which strains have been studied in this work has been by means of polarized light. Clear proof of the efficacy of annealing by heat treatment in the case of the silver and thallium halides has been given by several authors.[2,12,11,3]

3. *Apparatus*

The crystal holder required in working with room temperature crystals is extremely simple. The crystal can be pressed between two plates, for example, with screw pressure, and an output lead taken from one.[23,35,36] High voltage is brought to the other electrode. The main points appear to be to use good insulation and to avoid the introduction of stray capacitance by unnecessarily large electrodes. One must also be sure that the electrode assembly does not behave as an ionization chamber. For this reason it may be advisable to put the counter in vacuum. This procedure has been adopted by Ahearn. Leakage effects due to bad atmospheric conditions are also avoided by enclosure in vacuum.

In work with low temperature counters a vacuum chamber is definitely desirable. Although various stratagems have been used in order to avoid vacuum operations, for example, by placing the crystal in liquid air, the new difficulties introduced by such procedures invariably are more formidable than a simple vacuum chamber and system. A typical apparatus, used by the author, is shown in Fig. 7 and a diagram of the chamber in Fig. 8. The photograph shows the crystal holder in the center of the chamber. The crystal holder forms the lower end of a metal dewar vessel which protrudes as shown into the chamber. The clips which serve both as electrodes and for holding the crystal in place may be seen towards the front of the holder. At the middle are the rear electrode

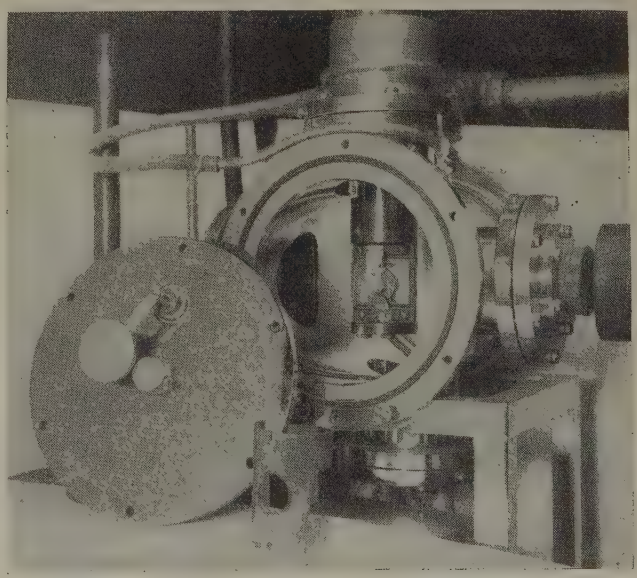

Fig. 7—An experimental vacuum chamber used in studying crystals at low or elevated temperatures. A radioactive source and shutter are shown at left on the inside face of the cover plate.

[18] A. C. Chynoweth, "Removal of space charge in diamond crystal counters," *Phys. Rev.*, vol. 76, p. 310; 1949.
[19] R. K. Willardson, A. C. Damask, and G. C. Danielson, *Bull. Amer. Phys. Soc.*, Paper T, 7; presented, Chicago Meeting, November, 1949.
[20] R. K. Willardson and G. C. Danielson, "Effect of light on a diamond conduction counter," *Phys. Rev.*, vol. 77, p. 300; January, 1950.
[21] G. Stetter, "Durch Korpuskularstrahlen in Kristallen hervorgerufene Elektronenleitung," *Verh. Deut. Phys. Ges.*, vol. 22, p. 13; March, 1941.
[22] D. E. Wooldridge, A. J. Ahearn, and J. A. Burton, "Conductivity pulses induced in diamond by alpha particles," *Phys. Rev.*, vol. 71, p. 913; June, 1947.
[23] L. F. Curtiss and B. W. Brown, "Diamond as a gamma ray counter," *Phys. Rev.*, vol. 72, p. 643; October, 1948.
[24] A. J. Ahearn, "Conductivity pulses induced in single crystals of zinc sulfide by alpha particle bombardment," *Phys. Rev.*, vol. 73, p. 524; June, 1948.
[25] A. J. Ahearn, "A search for crystals that exhibit conduction of pulses under alpha particle bombardment," *Phys. Rev.*, vol. 75, p. 1966; June, 1949.
[26] M. Georgesco, "Détection des particules ionisantes par les cristaux de soufre," *Compt. Rend.*, vol. 228, pp. 383–385; January, 1949.
[27] R. Frerichs, "The photoconductivity of incomplete phosphorus," *Phys. Rev.*, vol. 72, pp. 594–601; October, 1947.
[28] H. Kallman and R. Warminsky, "Über den Verstarkungeseffekt der Elektrischen Leitfähigkeit von Cadmium Sulfide bei Bestrahlung mit α-Teilchen, Elektronen und γ-Quanten," *Ann. der Phys.*, vol. 4, p. 69; September, 1948.
[29] N. Davidson and A. E. Larsh, Jr., "Conductivity pulses in liquid argon," *Phys. Rev.*, vol. 74, p. 220; July, 1948. Also, vol. 77, pp. 706–711; March, 1950.
[30] A. W. Hutchinson, "Ionization in liquid and solid argon," *Nature*, vol. 162, pp. 610–611; October, 1948.
[31] Private communication.
[32] K. G. McKay, "Germanium counter," *Phys. Rev.*, vol. 76, pp. 1536–1537; November, 1949. Also C. Orman, H. Y. Fan, G. J. Goldsmith, and K. Lark-Horovitz, "Germanium *P-N* barriers as counters," *Bull. Amer. Phys. Soc.*, vol. 25, paper 18; March, 1950.
[33] J. C. Street, Brookhaven Conference Report on High-Speed Counters, August 14–15; 1947.
[34] J. R. Haynes, "Technique for obtaining increased range and mobility of free electrons in silver chloride," *Rev. Sci. Instr.*, vol. 19, p. 51; January, 1948.
[35] G. J. Goldsmith and K. Lark-Horovitz, "Cadmium sulfide as a crystal counter," *Phys. Rev.*, vol. 75, p. 526; February, 1949.
[36] S. G. Zizzo and J. R. Platt, "Detection of X-ray quanta by a cadmium sulfide crystal counter," *Phys. Rev.*, vol. 76, p. 704; September, 1949.

and a flat plate of crystalline quartz. The quartz serves as insulator and relatively good thermal conductor at low temperatures. The terminal strips are made of micalex which can withstand the high temperatures used in annealing. The lead-in bushings for wires to the electrodes are also made of micalex. A shield, shown outside and below the chamber is generally placed about the holder so that the crystal is surrounded on practically all sides by material at low temperature. The shield is so constructed that particles may enter from front or side. An unobstructed view directly through the sides of the crystal is also permitted by the cutaways seen in the shield. This view has been useful in studying strain patterns in the crystal. To measure temperature a thermocouple is attached to the outside of the shield. Glass-kovar seals are used to bring all electrical connections into the system with the exception of the thermocouple wires which are carried through with wax seals. Conventional coaxial connectors are soldered to the central wire in the glass-kovar seals. On the cover plate (inside facing reader) a radioactive button[37] of P^{32} is shown, together with a brass shutter which can be moved in or out of the beam by a "Hermeflex" bellows seal. The ports on the left and right of the chamber allow light to be passed into the crystal and viewed at the same time.

[37] Cs^{137} which has a prominent internal conversion line at 0.63 Mev is more desirable than P^{32}.

There is much flexibility in the type of apparatus which may be used for studying the pulses electronically. However all systems will use an oscilloscope, amplifier, a delay of some sort and a triggered or "slave" sweep device. The delay is necessary so that one may see the start of the pulse; the delay compensates for the time it takes the sweep circuit to get started. Two simple combinations of these elements are given schematically in Figs. 9 and 10. Fig. 9 shows a rather economical way of studying the pulses. The delay is produced by a lumped constant line labeled "delay line" in the figure. A Western Electric line with a rise time of 0.15 microsecond and a delay of 4.8 microseconds has been found to be most useful. However the pulses are usually limited in height by amplifier overload into the low impedance of this delay line. Fig. 10 shows the delay line replaced by a length of coaxial line L and an auxiliary amplifier A. With this arrangement the pulse is sent down the line at the low power level of the preamplifier output. No distortion is observed in the range of frequencies used and the signal can be amplified to the overload point of the main (501) amplifier (100 volts) working into an infinite load. Much larger deflection of the cathode-ray beam is thereby obtained. The amplifier A must be fast enough so that its rise time is appreciably smaller than the length of the line. The lower arrangement is excellent for avoiding distortion of large pulses.

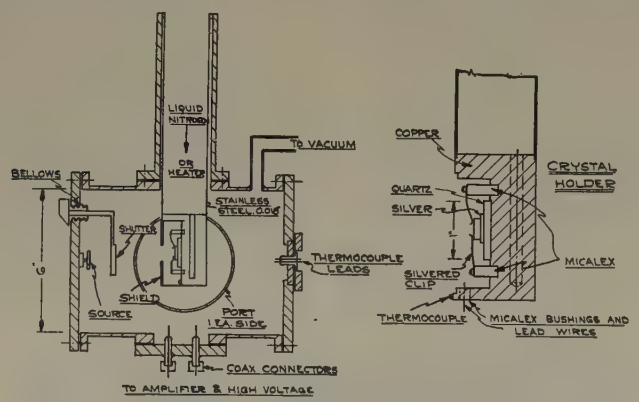

Fig. 8—Diagram of chamber shown in Fig. 7.

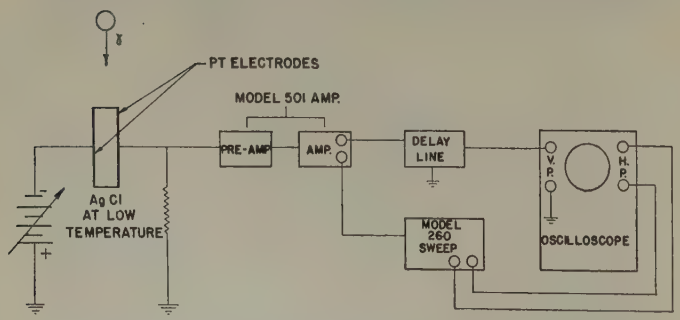

Fig. 9—Block diagram of simple system for observing pulses on oscilloscope.

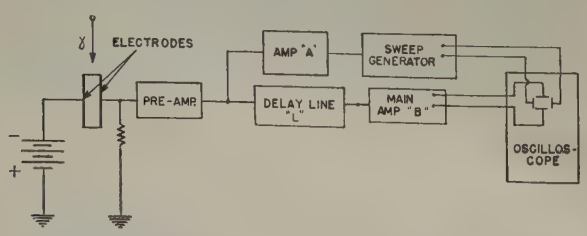

Fig. 10—Block diagram of system which permits large undistorted pulse shapes on oscilloscope screen.

In Fig. 9 the main amplifier is a Model[38] 500 or 501 which is useful for studying the shapes of the pulses. From these shapes mobility measurements are derived.

If one is interested in counting pulses or measuring pulse heights and their distribution it is advantageous to use a slower amplifier, Model 100 (rise time 0.5 μsec, gain 10^6, max. undist. output+150 volts) for which the noise is considerably lower than that of the Model 500 or 501 where the noise level is equivalent to a signal from a 30 kev beta particle entering the crystal. Because of the lower energy/ion pair figure for a crystal than for an ionization chamber, the resultant output signal may be expected to be larger in the former. Nevertheless, the pulse is still rather small (a few millivolts) and therefore a large amplification is required for reasonable display on a screen or for counting. Shot noise in the input amplifying tube and input resistor noise fix a lower level to the size of pulse one may study. Van Heerden[2] and Elmore[39] have shown how the signal-to-noise ratio is an optimum for a given amplifier input tube when the amplifier frequency characteristic is shaped properly. Elmore shows that with a 6AK5 tube, a smallest pulse equivalent to appearance of 100 electrons at its grid, can be detected above noise when the rise time and "clipping" time (time constant of differentiating RC network) are 40 microseconds and 16 microseconds, respectively. When the capacitance of the crystal is considered, the minimum detectable pulse is probably about 200 electrons. At six electron volts/ion pair this would be the equivalent of a 1.2 kev beta particle, which is a low enough energy so that one has other troubles in detecting and observing it. Nevertheless, a high accuracy in determining pulse height is possible when the noise is reduced to this low level. The Model 100 amplifier has been converted by many workers into the optimum type for signal-to-noise ratio by small modifications of the RC constants.

One may count 160 random pulses per second with a slow amplifier and only lose one per cent of the counts due to pile-up.[39] For a great many problems, this rate is high enough. In searching for crystal counting specimens this rate is perfectly satisfactory and so also in studying energy/ion pair in crystals. Where fast counting is required, e.g., coincidence work, measurement of short time intervals, mobility measurements, and the like, a more rapid rise time is required,

[38] W. C. Elmore and M. L. Sands, "Electronics: Experimental Techniques," McGraw-Hill Book Co., New York, N. Y.; 1949.

[39] W. C. Elmore, "Electronics for the nuclear physicist," *Nucleonics*, vol. 2, p. 16; 1948.

perhaps of the order of 0.1 or 0.2 μseconds (Model 500 or 501). One has to put up with the high noise level and can study only larger pulses of the order of 30 kev and larger.

The actual counting of pulses can be carried on with conventional scalers and registering equipment. Single- and multi-channel discriminators are also of great importance in studying pulse height distributions.[38]

4. *Annealing Procedure for Silver or Thallium Halide Crystal*

After a silver or thallium halide crystal is prepared by standard techniques of sputtering, evaporation, painting, or developing electrodes on it, it may be introduced into the vacuum chamber. The crystal should be clean and excessive pressure should not be applied by the clips when mounting it in place. It is not necessary to exercise special caution in introducing it by virtue of the following procedure in which annealing is carried out in the vacuum chamber. (For materials which sublime this procedure would require change. Crystals of this type will give trouble in almost any type of annealing operation.) The vacuum chamber is closed and a high vacuum $<10^{-4}$ or 10^{-5} mm Hg obtained. A small heater coil is lowered into the interior of the dewar vessel in which the subsequent cooling by liquid nitrogen is carried on. The heater employed, (in this case, air) is used to bring the crystal to a temperature of 400°C for AgCl and about 380° when the crystal is AgBr. The dewar is held at this temperature for a few hours and the temperature is gradually decreased by running a variac, which feeds the heater, slowly to zero voltage. A small clock motor can be used for this purpose. The entire annealing procedure may be carried out automatically over a period of about 20 hours in which no attention is required except filling of a liquid air trap occasionally. Perhaps a faster cooling rate can be used. When the crystal is at room temperature, the dewar is gradually filled with liquid nitrogen and the temperature is reduced to 77°K. Van Heerden has used less than an hour for the cooling period.

At this temperature the crystal will be remarkably sensitive to gamma, beta, or alpha radiation. Although the initial procedure is lengthy, it appears that the annealing operation need not be repeated for a long while. If the crystal is kept in the dark, it may be cooled many times to low temperature and will each time give the same pulse shapes and heights. Yamakawa[12] has shown how several successive coolings do not change the strain pattern or produce new crystal boundaries, provided that the cooling interval lasts at least half an hour.

5. *Cautions*

There are many ways in which it is possible to impair the counting efficiency of a silver or thallium halide conduction counter. An electric field placed across the crystal at any but low temperatures will result in electrolytic activity in the crystal and may do permanent damage to it. When the field is applied at low temperature all light must be avoided; otherwise, photoconductivity is produced and polarization of the crystal will ensue. Except when using red or yellow light to study polarization or strain patterns in the crystal, the writer believes it good policy to keep light away from the crystal at all times after depositing it in the vacuum chamber.[40] When viewing the crystal the field should be turned off. Van Heerden has justifiably warned against using electrodes of materials other than silver, platinum, or gold. Chemical reactions occur with other metals such as iron, copper, or nickel. As stated previously, to obtain the best signal-to-noise ratio the capacitance of the electrodes should be kept as low as possible.

After a large amount of radiation has been absorbed by a crystal without a period of returning the specimen to room temperature, peculiar effects many sometimes be observed.[41] Large spurious pulses and numerous smaller ones (hash) can be observed. It is believed that a surface charge forms near the electrodes so that electrons from the metallic electrodes are enabled to enter and leave the crystal. We do not think such behavior occurs under normal operation. An infrared bathing of the crystal might release the high concentrations of trapped electrons near the electrodes and so eliminate this effect. This procedure has not been attemped as far as the author is aware.

Fig. 11—Above (left) halide powder in glass mold. Above (middle and right) two crystals grown by Bridgman method. Below crystal counter samples cut from molds and ingots of type shown above.

6. *Crystal Growth*

In work with crystal conduction counters it is desirable to move those secondary electrons which are created in the conduction band as far as possible before being trapped. The boundaries of separate crystals act as walls with regard to electron motion, and so a powdered sample may not be expected to give as large pulses as a larger crystal sample. It is not certain that larger crystals will give large induced conductivity pulses, for there may be invisible crystal boundaries within the sample. In many cases an etch technique will serve to bring out the boundaries. Examination in polarized light also reveals crystal boundaries within a transparent sample. The X-ray technique of studying crystals is the most reliable, because it may uncover microscopic or submicroscopic crystal boundaries. Crystals composed of a multitude of microcrystals have been called "mosaic" crystals by Ewald. Many studies of mosaic crystals have been carried out by Darwin, Moseley, Mark, Kirkpatrick, Davis, and others. Further discussion of mosaic crystals and references to the original literature are given in reference[3].

It is, accordingly, important to use single crystals in work with conduction counters. The problem of obtaining such crystals is by no means simple. In some cases, e.g., diamond and probably ZnS,[42] only natural crystals are available and these must do. However, in other cases, e.g., CdS, AgCl, AgBr, TlBr-TlI, the alkali halides and probably sulphur, single crystals can be grown from the melt or by sublimation, and very good samples may be obtained for conduction counter work. Furthermore the artificially grown crystals may be made of very much higher purity than naturally occurring specimens. In certain cases impurities may be added deliberately for study of their effects or for preparation of new types of counters.[43]

It is appropriate therefore to discuss the question of crystal growth. Although there are many methods of growing crystals, in the last few years, the Bridgman[44] method has become almost predominantly the single technique used.[45] This method is simple and reliable and will be described briefly below.

The crystal material, for example silver halide powder, is placed in a circular pyrex tube drawn to a point at its lower end. A photograph showing such tubes is given in Fig. 11. The filled tube is lowered into the furnace and the powder melted. A platinum wire may be used to suspend the tube while in a furnace. Nichrome wire is suitable for noncorrosive vapors. A wire yoke can be

[40] Of course, special studies or activation with light are not included in this prohibition.

[41] W. L. Whittemore and J. C. Street, "Silver chloride used as an ionization detector for cosmic rays," *Phys. Rev.*, vol. 73, p. 543; March, 1948.

[42] Moderately large ZnS crystals have been prepared synthetically by D. Reynolds of Batelle Memorial Institute.

[43] K. A. Yamakawa, "A suggested slow neutron crystal counter," *Phys. Rev.*, vol. 75, p. 1774; June, 1949.

[44] P. W. Bridgman, "Physical properties of single crystals of tungsten, antimony, bismuth, tellurium, cadmium, fine, and tin," *Proc. Amer. Acad. Arts. Sci.*, vol. 60, p. 305; October, 1925.

[45] The Kyropoulos method has been used very successfully for alkalihalide crystals and is extremely rapid compared with the Bridgman technique. The latter technique, however, requires little manipulation but much time.

wound around the fired open end of the tube and the suspending wire attached to its middle. A glass crossbar may also be used for attaching the suspending wire. After the powder has melted the apparent volume of halide powder will have contracted considerably. More powder is added until the desired volume is obtained.

The temperature of the furnace in the region where the crystal is first placed (upper half or upper third) is now adjusted to be about 10–20°C above the melting point. The tube should be examined, through a window or by opening the furnace and drawing the tube out, to see whether all the material is liquid. If so, the tube should now be replaced and lowered slowly through the vertical furnace. A clock motor or a motor and separate gear train adjusts the rate of lowering. A rate of one inch a day is about normal for the halides, although slower lowering rates generally produce better results.

There will normally be a temperature gradient in the furnace if it is wound uniformly. For near the ends the temperature will be lower than in the middle. Hence somewhere below the middle of the furnace the melt will pass through a zone of freezing, where the material crystallizes. The layers of crystal are added as the melt drops lower in the furnace. After a sufficient time, depending on the length of the sample, the entire melt will have crystallized. On many occasions the resulting crystal will be one large single crystal. It is generally found that the purer the starting material is, the greater the ease in growing single crystals.

It is desirable to keep the temperature distribution in the furnace as nearly fixed as possible. If time variations of temperature occur, the freezing zone may move up and down and remelt previously crystallized material. To obtain a constant set of conditions, a simple temperature controller will do (±1°C). If the furnace is kept in a room where the temperature remains constant (basement room) within a degree or two, it has been found unnecessary to have a temperature controller. A constant voltage transformer serving the input of the furnace heater coil suffices to keep the temperature conditions stable. For AgCl and AgBr whose melting temperatures are 455°C and 434°C, respectively, a temperature variation of one degree or so does not seem to impair the quality of the crystals. For crystals of lower melting points, the variation may be more serious, although even in cases where organic crystals of naphthalene, stilbene, dibenzyl, whose melting points are in the range 56° to 125° satisfactory crystal specimens have been obtained without the use of a temperature controller. The main point seem always to start with a well purified sample.

In the case of the halides, after the crystal has been formed by lowering into the bottom of the furnace, the furnace is cooled to room temperature at a more or less uniform rate over a period of about a day. The sample can then be removed. If one has started with impure material it will be observed that the material at the top is usually darker in color and strikingly nonuniform when compared to the material underneath.[46] Starting from the lower tip, a AgBr crystal will appear pale yellow and uniform until near the top. The top portions contain the impurity forced out of the crystal matrix during solidification. The lower parts contain the once-purified material. In the case of crystals of low density (~1.0 gm/cc) such as naphthalene, anthracene, stilbene, which are used in scintillation counter work, the impurities (sometimes dirt, filter paper, and cork) will be found at both bottom and top.

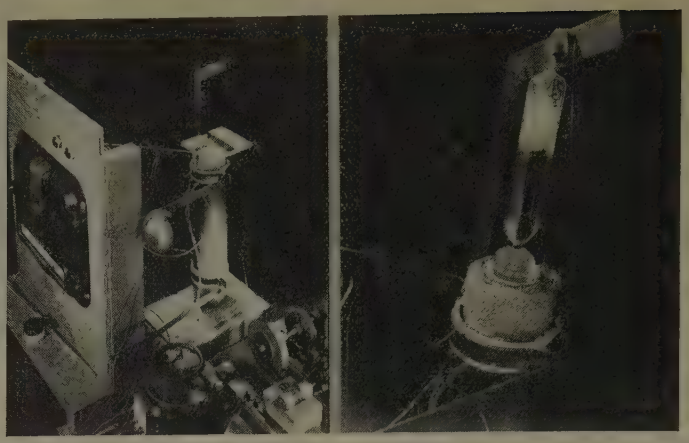

(a) (b)

Fig. 12—(a) Small crystal growing apparatus. Temperature controller at left, furnace and gear train at right. Sample is lowered into furnace by wire moving over pulley. (b) Closeup showing glass mold and partially melted crystal material preparatory to lowering in furnace.

The middle and lower portions of the halide crystals can be remelted for a second and even a third crystallization. The best results are obtained with crystals which have been subjected to more than one crystallization. However, if the material is sufficiently pure at the beginning, only one crystallization is required. Fig. 11 shows samples of AgBr crystals in the glass mold after removal from the furnace. Sections may be cut out using a diamond or carborundum cutting wheel. In many cases, the cut sections will simply fall out of the glass ring. When a silver halide crystal appears to be stuck to the glass, a simple rinsing with hypo will usually free it.

The surfaces of the cut crystals can now be etched with hypo to remove grinding dust and to relieve strains. The crystals should then be washed carefully with water, preferably distilled water at room temperature. After drying, electrodes can be put on by sputtering or by evaporation of a metal film or also by treatment with developer.[33,34] In many cases, aquadag electrodes are suitable.

When crystals are grown too rapidly, an irregular pitting occurs on the cylindrical surfaces and bubbles grow in the crystal near the surface. A slow rate of lowering will usually eliminate such troubles. A clean glass mold should be used in growing crystals.

In growing crystals which sublime or which have large vapor pressures at the melting point, the melt may be formed in vacuum and the pyrex mold sealed while the sample is still under vacuum. A glass hook can be formed above the seal-off and used for suspending the crystal. In this case platinum is unnecessary for the suspending wire because the halide fumes are enclosed in the tube. One must be certain to remove all air and adsorbed water vapor while melting the specimen in vacuum.

Crystals have been grown successfully in rectangular tubes provided the corners are not sharp. A radius of curvature of $\frac{1}{8}$ inch is satisfactory.[47]

Two views of a small crystal growing apparatus[48] are shown in Fig. 12 (a) and (b). In the particular case shown a temperature controller is located at the left of Fig. 12 (a) and was employed because of large temperature fluctuations in the room. The particular material shown is stilbene, growing in a sealed tube. A bulb at the base, followed by a constriction connecting with the main rectangular crystal mold, insures that generally only one seed crystal grows into the larger rectangular volume. In the case of the silver halides such a bulb is not necessary, although it is possible that a further improvement in quality might be obtained with its use.

Many silver halide crystals which are grown imperfectly will not be single crystals, i.e., crystal boundaries will be seen on the surface when the sample is examined in reflected light. In order to see these boundaries, the crystal must first be etched with a weak hypo solution. Fig. 13 shows an AgCl crystal with many crystal boundaries. One will not obtain satisfactory counting results in using such a specimen. Crystal boundaries can also be seen by placing the crystal between crossed polaroid plates. However, the strain boundaries tend to confuse the pattern and the etch test is probably more reliable. A combination of these two tests gives a greater amount of information.

When a silver halide crystal has been

[46] R. H. McFee has given a theory, and also its experimental confirmation, of the method by which impurities are removed from a crystal during solidification (see *Jour. Chem. Phys.*, "Foreign ion rejection in the growth of sodium chloride single crystals from the meet," vol. 15, p. 856; 1947).

[47] Rectangular precision tubes of this type may be obtained from the Fisher-Porter Co., Philadelphia, Pa.

[48] This apparatus was used by the author and J. A. McIntyre while working at the University of California (Radiation Laboratory).

prepared by the method outlined, it will be found that it shows no electrolytic or electronic conduction at low temperatures. If a sample is taken from one of the upper portions of a mold or if prepared from material which is not pure, the crystal will exhibit so large a conductivity at low temperatures that it will be useless as a counter. Material which is intermediate in purity may show spurious pulses due to a weak electrolytic or electronic conductivity which generally appears at higher voltages.

It has been found that crystals taken directly from the mold will often not count well, if at all. Annealing of these crystals however always produces a good counter. Presumably the crystal is strained by the contact with the glass wall.

Good crystals of KRS-5, thallium iodide-thallium bromide, have been made by the Bureau of Standards by techniques of slow cooling of the melt, not involving motion of the crystal mold.

Crystals of CdS have been prepared by Frerichs[27] in a quite different manner. Pure CdS was prepared by heating Cd metal shavings in an atmosphere of H_2S enclosed in a quartz tube. Although the crystals so obtained were very small, since they are prepared by a sublimation method, they must be very pure. Crystals of ZnS have been made by Reynolds (Battelle Memorial Institute) by a similar method.

IV. Discussion of Useful Crystals

1. *Diamond*

Ahearn,[49] Curtiss and Brown,[23] Corson and Wilson,[50] Birks *et al*,[51] Willardson[19] *et al* and others have investigated various diamonds. It appears that the numerous diamonds which count alpha particles show a surprisingly large variation of pulse size for a given energy of alpha particle depending on the particular region of the crystal struck by the alpha particle. Since the alpha particles penetrate only about a ten microns depth of crystal, it is perhaps reasonable to consider that local variations do occur within this distance of the surface. Polishing of a diamond surface, if carried sufficiently far to give an optically flat face, might remove the unknown variation of surface conditions, although it is possible that new effects could be introduced by the polishing operation. The same type of local variation in the related field of photoconductivity has been found by Achyuthan.[52]

Ahearn[53] has found that the largest pulses were produced at a flaw in the case of one particular diamond. Since the nature of the flaw is unknown, we cannot draw further conclusions from this observation. However, it is apparent that the counting of alpha particles by a surface may offer a powerful tool for investigation of irregularities on that surface.

[49] A. J. Ahearn, "Conductivity induced in diamond by alpha particle bombardment and its variation among specimens," *Phys. Rev.*, vol. 73, p. 1113; May, 1948.
[50] D. L. Corson and R. R. Wilson, "Particle and quantum counters," *Rev. Sci. Instr.*, vol. 19, p. 207; April, 1948.
[51] L. S. Birks, H. P. Gauvin, and E. J. Brooks, Memorandum, Naval Research Laboratory; June 4, 1948.
[52] K. Achyuthan, "Directional variations of photoconductivity in diamond," *Proc. Ind. Acad. Sci.*, vol. A 27, p. 171; February, 1948.
[53] A. J. Ahearn, Rochester Report on "High Speed Counters," July, 1948.

Fig. 13—Etch pattern of a rolled sample of AgCl. This crystal is unsuitable for conduction counting because of the large number of small crystals shown by the etch pattern. Diameter of crystal is 1¼ inches.

The effect of impurities on counting in diamond is also poorly understood. The impurity in any particular diamond is usually unknown, and its distribution an unknown of higher order. There seems to be a disagreement in the literature as to whether gem quality diamonds, which are presumably pure, make better counters than poorer, colored crystals. Under such conditions it is difficult to discuss the efficiency of diamond counters. It is even unknown at the present time whether gamma counting diamonds will count alpha particles and vice versa.

Friedman[54] *et al* have suggested that the counting property may be correlated with the ultra-violet transmission of the diamond. The ultra-violet transmission has been used as a criterion to separate diamonds into two classes: I and II. Type I is usually ultra-violet opaque (although exact delimitations of the region of opacity are rarely given) and Type II, ultra-violet transparent. Friedman finds that the Type II diamonds make better gamma counters than those of Type I. A repetition of this experiment with other diamonds unfortunately has not appeared in the literature. It is therefore not clear at the present time whether Friedman's observation applies more generally.

Hofstadter[55] has given an interpretation of Friedman's result in terms of a series of experiments of Raman[56] and his school, who have studied diamonds in great detail, including their fluorescence, birefringence and photoconductivity. Lonsdale[57] has criticized this interpretation and a further discussion of Lonsdale's views is given in the literature.[3] At the present time there is an obvious need to make further conclusive experiments on the efficiency of Types I and II diamond counters.

[54] H. Friedman, L. S. Birks, and H. P. Gauvin, "Ultraviolet transmission of counting diamonds," *Phys. Rev.*, vol. 73, p. 186; January, 1948.
[55] R. Hofstadter, "Remarks on diamond crystal counters," *Phys. Rev.*, vol. 73, p. 631; March, 1948.
[56] C. V. Raman, et al, "First and Second Symposia on the Structure and Properties of Diamond," *Proc. Ind. Acad. Sci.*, vol. 19A, p. 189, 1944; and vol. 24A, p. 1, 1946.
[57] K. Lonsdale, "Remarks on diamond crystal counters," *Phys. Rev.*, vol. 73, p. 1467; June, 1948.

McKay[17] has studied the conduction of diamond under bombardment by electrons in the energy range from 3 to 14 electron kilovolts. In this region he finds that the Hecht relation (Eq. (5)) holds quite well when the polarization, due to space charge, of the crystal is small. He also finds that the holes in diamond move with a mobility of the same order as that of the electrons. McKay finds further, that in the particular diamond studied, the average time T, of Eq. (2), which an electron spends in the conduction band is of the order of 4×10^{-8} second. Ahearn[49] and McKay agree in finding that it takes about 10 ev to free one electron for the conduction band in diamond. By assuming a cross section between 10^{-16} and 10^{-17} cm^2 for a trap, McKay finds a concentration between 2×10^{16} and 2×10^{17} traps per cubic centimeter in the diamond studied. Although this concentration of traps is considerably higher than one finds in AgCl ($10^{13}-10^{14}$ per cm^2), McKay thinks the number reasonable. Such a high concentration of traps in alkali halides could explain the inability of many alkali halides to act as crystal conduction counters. There is little definite confirmatory evidence of this kind for the alkali halides. The nature of the traps is not determined by McKay's work.

Polarization in Diamond. To keep the diamond free of a cumulative polarization field, McKay has used an alternating voltage so that the self-reversals annul the effect of space charge. The effectiveness of this procedure has already been noted. Chynoweth[18] and Willardson[19,20] have also removed polarization charges with infrared radiation.

The most encouraging results regarding the polarization of crystal conduction counters by ionizing radiation have recently been reported by Willardson and Danielson.[20] These authors have found that some diamonds may be activated by violet light so that the space-charge field appears to be completely eliminated. At any rate, for practical purposes, the crystal may be used indefinitely to count particles without showing polarization effects, such as reduction of counting rate. It appears that the external

field must be left on at all times. A detailed explanation of this phenomenon is unknown, although Willardson and Danielson believe that the boundaries of the energy bands have been changed by the space charge.

These authors also have reported a confirmation of Chynoweth's[18] result that infrared illumination of a polarized diamond restored the full counting rate and pulse height of the crystal when unpolarized. An effect of this kind had previously been suggested.[3] Chynoweth used the entire spectrum of radiation obtained from a Nernst lamp (1–10 microns). Willardson and Danielson have achieved a similar effect on one of their diamonds (Q) using red light (6500Å). With other diamonds the red or violet light illumination produced almost no effect. It would be interesting to use a "light probe" on these diamonds to see whether (a) the effect has local variations, and (b) the effect is directional.

It seems likely that under illumination electrons and holes are being freed from their respective trapping sites and are recombining to eliminate the space charge. In fact, it appears that it is only necessary that electrons be freed from traps to eliminate the space charge, because the electrons will, after a sufficient time, find all the empty holes. However, in the presence of a strong field this may not occur.

Figs. 14 and 15 show the results of the investigation of Willardson and Danielson. It is possible that the small increase at the start of irradiation is due to an initial attractive field building up in the left half of the crystal as shown in Fig. 6. The peculiar "kink" in the curve of Chynoweth may also be due to such a phenomenon.

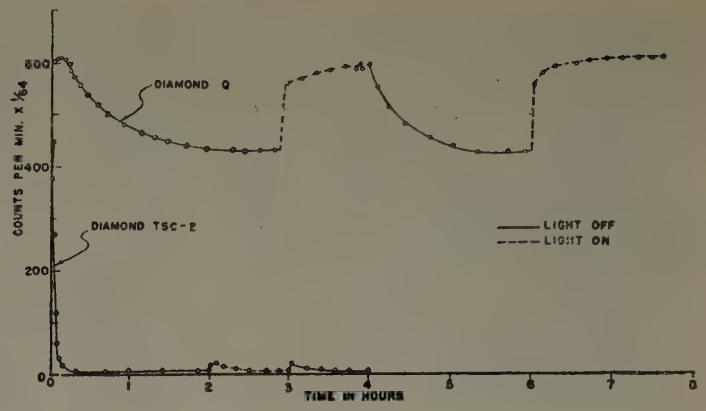

Effect of red light on counting rate (λ =6500A, E_A =10 kv/cm, $Co^{60}\gamma$).

Fig. 14—Effect of red light in removing space charges from diamonds (Willardson and Danielson).

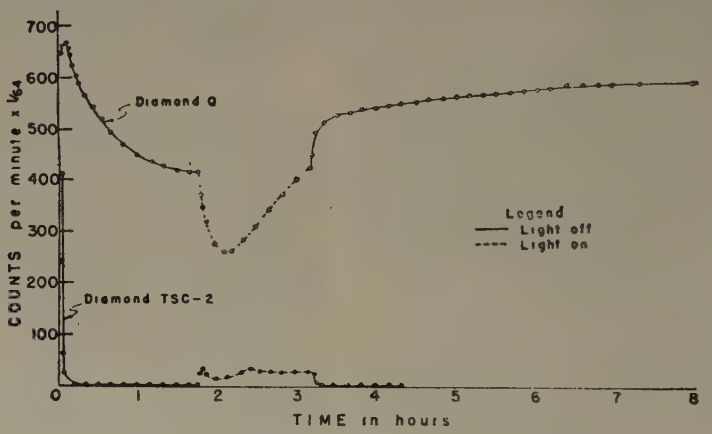

Effect of violet light on counting rate (λ =4047A, E_A =10 kv/cm, $Co^{60}\gamma$).

Fig. 15—Effect of violet light in affecting space charge in diamonds (Willardson and Danielson).

2. *Zinc Sulfide* (*ZnS*)

This material has been investigated with success by Ahearn.[24] ZnS crystals operate at room temperature as counters for alpha particles. The pulses are however a good deal smaller than in diamond. The latter behavior may possibly be due to the poor specimens studied. It is not known whether ZnS will count electrons and gamma rays, although it is probable. Of interest in Ahearn's work is the fact that the sphalerite investigated had an analyzed impurity content of 0.1 per cent of germanium. Nevertheless the crystal counted. This means that certain impurities do not behave as electron traps.

3. *Cadmium Sulfide* (*CdS*)

This material appears to have quite remarkable properties and has therefore lately been the object of much study. A bibliography of some of the recent work on CdS may be found in an article by Frerichs.[58] The fact that the material is not in common use is partially due to the small size of available specimens (~1 mm×0.2 mm×10 mm). Frerichs and Warminsky[27,59] and Warminsky and Kallmann[28] have done the pioneer work on this material. Not only does this crystal material behave as a conduction counter at room temperature but it may also, under different circumstances, perform as a scintillation counter emitting red light. Kallmann[60] has given a comprehensive report on CdS crystals, some of the main points of which will be discussed below. The practical possibilities for CdS crystals are considerable since a single alpha particle may provide a 10-volt pulse in some crystals, thus eliminating need for an amplifier.

Kallmann makes a division of CdS crystals into two groups. The first is the nonluminescent group and the second a luminescent group. The nonluminescent and luminescent types behave quite differently from the point of view of conduction counting and photoconductivity. A nonluminescent crystal has the properties of an ordinary crystal counter, say, like AgCl at low temperatures. In this case the pulse is proportional to the energy, the electrons which are set free in the conduction band requiring an energy per ion pair of 10 ev or so, and the electrons drift across the crystal to the positive electrode where they are stopped. In other words the behavior is similar to that of an ionization chamber. In the luminescent type of CdS crystal, electrons are not removed from the conduction band, a large number being able to remain in the band. While in the conduction band the crystal has the properties of a semiconductor or even a metal. That is, some of the electrons moving about in the conduction band will drift to the electrodes. The neighboring metallic electrode(s) have electrons distributed in its energy band up to a certain maximum energy, the so-called Fermi level. This level generally lies below the lowest edge of the conduction band of an insulator such as CdS. Electrons which have been excited to the CdS band by radiation and which approach the surface, near the electrodes, will drop into the more stable energy levels of the metal electrode. The electrode therefore builds up a negative space charge while the insulator (CdS) builds up a positive space charge near the electrode. The electric field developed by this double-layer distribution of charge lowers the potential energy of electrons in the CdS until the lower edge of the conduction band approximately meets the Fermi level. At this point equilibrium exists and it is now possible, on application of an electric field, for electrons to pass from the metal into the crystal and vice versa. Therefore excitation of a luminescent CdS crystal by ionizing radiation can result in a semipermanent conduction phenomenon in which the total amount of flowing charge is

[58] R. Frerichs, "On the conductivity proposed in cds crystals by irradiation with gamma rays," *Phys. Rev.*, vol. 76, p. 1869; December, 1949.

[59] R. Frerichs and R. Warminsky, "Die Messungen von β-und γ-Strahlen durch innieren photoeffekt in Kristall phosphoren," *Naturwissenschaften*, vol. 33, p. 251; October, 1946.

[60] H. Kallmann, "On conductivity in different types of cadmium sulfide crystals and on its application," Signal Corps Eng. Report E-1306; May 30, 1949.

enormously greater than the directly liberated charge of the ionizing radiation. This phenomenon has been called "multiplication" by Kallmann. In other words, the radiation may set loose a conduction chain of electrons in the crystal, the current so produced lasting a long time. To be effective, it is clear that a luminescent crystal must be prepared so that electrons are already in its conduction band. In this way it will be made similar to a semiconductor or metal. The preparation of the crystal can obviously be carried out by previous irradiation with green light or by fast electrons, gamma rays, or alpha particles.

The condition that permits the electrons to remain in the conduction band for a long time without capture has been attributed by Kallmann to the capture by traps of the positive sites left behind by release of electrons. The impurity activating atoms in the fluorescent CdS (which are necessary for its luminescent properties) are designated as the centers which trap the positive charges. So trapped, the positive sites are rendered relatively ineffective for recapturing their lost electrons. Hence the electrons may exist in the conduction band without interference. In the absence of a field, the electrons in the conduction band may still not leave the crystal because of the resultant positive space charge of the crystal. They are therefore not lost to the electrodes except for the relatively small number that are responsible for the "bridge" effect at the boundaries.

When infrared light illuminates the fluorescent CdS crystals, they lose their multiplicative properties completely. This behavior is due to the fact the positive charges are released from the trapping centers and wander about until they recombine with the electrons in the conduction band. Presumably there should be an emission of luminescent light accompanying the infrared stimulation. Such an effect apparently has not been looked for. After infrared treatment the crystals behave like the nonluminescent ones, until they receive enough radiation or green light to prepare them for the multiplicative behavior we have described.

The enormous multiplication of charge in CdS crystals was first observed by Frerichs. Table II, taken from Kallmann's report, shows a comparison of the behavior of luminescent and nonluminescent CdS crystals. The results are given in direct-current terms under uniform alpha particle bombardment for both types of crystals. Note the enormous effect in crystal No. 53, compared with other crystals of the nonluminescent variety.

Kallmann has shown that CdS crystals are probably proportional devices for registration of ionizing events. He has examined the pulse distribution obtained with alpha particles and has obtained by differentiation of the experimental integral bias plot the resulting curve shown in Fig. 16.

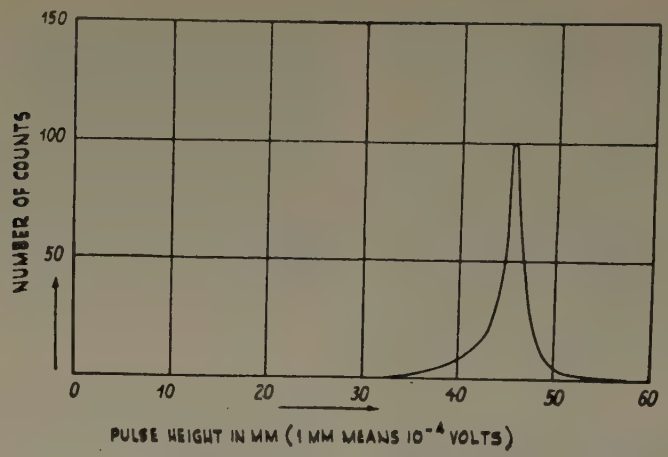

Fig. 16—Derivative of integral bias curve for alpha particles on CdS (Kallmann).

The rise time of pulses in CdS is small (10^{-6} seconds) in the non-luminescent crystals. In luminescent CdS crystals the rise time is longer and can be, of course, enormously longer, depending on the previous treatment of the crystal. There appear to be many other interesting properties of CdS crystals which we cannot describe for lack of space. Not the least of these is the notable after effect of a single alpha particle pulse in luminescent CdS, in which conductivity persists longer than 0.1 second after the original excitation. The reader is referred to Kallmann's account and to Frerich's recent paper.[58] In the latter paper one will also find an energy level diagram which represents the most complete distribution of traps and impurity states now known for CdS. It is very interesting to note that Mott and Gurney,[5] (pp. 186–187), have explained a conductivity phenomenon observed by Lehfeldt in AgCl which strongly resembles CdS "multiplication."

Goldsmith and Lark-Horovitz[35] have also studied CdS conduction counters and have reported rise times of less than 0.2 microsecond at voltage differences of greater than 70 volts. The thickness of crystal studied is not stated, but is estimated by the author at a few tenths of a millimeter. In some crystals surface leakage or other unexplained effects occurred at high voltage gradients. Surprisingly large pulses (12 mv) were obtained for 5-Mev alpha particles, considering the fast rise time observed. The fast rise times suggest primary non-multiplicative behavior.

Zizzo and Platt[36] have succeeded in detecting individual 45 kev X-ray quanta in a small CdS crystal. The crystal had a thickness of 0.07 mm and flat faces of 1 mm² area. Aquadag electrodes were used. The small input capacitance of 8 $\mu\mu$f, including the capacitance of the input grid of the amplifier, was achieved by careful mounting of parts and by use of a small input tube HY 114B. In addition to counting of individual quanta a continuous current could be observed in the crystal due to the arrival of many quanta in a short time. In the arrangement used 10^5 counts/minute were equivalent to a crystal current of 6×10^{-11} ampere. It is shown by Zizzo and Platt how the CdS crystal may perform conventional X-ray detection with very simple means. The order of magnitude of energy per ion pair seems to be less than 14 electron volts and perhaps as little as 3 ev/ion pair. A low value would tend to be consistent with the observations of Frerichs, Goldsmith and Lark-Horovitz and Kallmann. The use of a small crystal of the kind used should allow "good geometry" experiments without the necessity of using slits. Zizzo and Platt do not report any unusual behavior or evidence for stimulation of CdS crystals, thus indicating that their sample was probably of the non-luminescent type.

Gildart and Ewald[61] (Paper 12, March 1950) in a recent abstract have measured the mobility of CdS by irradiating with square wave pulses of ultraviolet light or X rays and observing the conductivity rise and fall as well as the luminescence rise and fall. In this way they measured a mobility of 60 cm²/volt sec for a polycrystal of CdS. They have also been able to measure the density of electrons in the conduction band$\sim10^{11}$ per cm³, but do not say whether this refers to the normal or to some stimulated excited state. The possibility of making such measurements is most interesting. They have also determined the lifetime in the conduction band $T=\sim10^{-3}$ sec and the Schubweg $\lambda=25$ cm, a very large value.

TABLE II

Crystals with Small Luminescence Current in Amp Under Alpha Particle Bombardment *Crystal No.*		*Crystals with Strong Luminescence* Current in Amp Under Alpha Particle Bombardment *Crystal No.*	
1	30.0×10^{-8}	51	1.5×10^{-6}
2	1.0×10^{-8}	52	1.0×10^{-5}
3	20.0×10^{-8}	53	5.0×10^{-4}
4	1.5×10^{-8}	54	5.0×10^{-8}

4. *Sulphur*

Following the calculations of Wasastjerna,[62] Georgesco[26] computed the energy (ϵ) required to produce a free electron in the conduction band of A_gCl. His computations yielded a value of 7.5 ev, which is remark-

[61] L. Gildart and A. W. Ewald, "Electron mobilities in conducting phosphors," *Bull. Amer. Phys. Soc.*, vol. 25, paper 12; March, 1950.

[62] J. Wasastjerna, "Calculation of physical properties of crystals," *Soc. Scient. Fennica Comm. Phys.-Math.*, vol. 8, p. 21; 1936.

ably close to the experimental value (7.6 ev) we have already quoted. He further computed a value for sulphur and arrived at a value of 5 ev.

To test the theory, Georgesco examined several sulphur crystals with conventional techniques. His results show that all of the 14 sulphur crystals chosen for study counted alpha particles. Three of the crystals also counted beta particles. Furthermore, his measurements of alpha particle pulse heights show a strict proportionality with energy, and he has been able to resolve the two alpha particle groups of uranium. The order of magnitude of the energy ϵ measured by Georgesco is 5 volts and so agrees well with the theory.

A brief statement is made by Georgesco that directional effects are present in the counting of particles in sulphur. However, the facts are not given in sufficient detail to form a complete picture of this type of effect. Further peculiarities appear as the electric field is raised. The pulses grow larger with increasing field strength but finally become constant and eventually disappear. The statement is also made that the crystals are perfectly insulating so that they may be used at room temperature.

5. *Silver and Thallium Halides*

We have thus far described crystals which function as counters at room temperature. We come now to those materials which are useful only at low temperatures. More published material is available on the halides than on any other group of conduction counters. Among the halide materials are the first practical counters, devised by van Heerden;[2] who used crystals of AgCl prepared synthetically by a method of crystal growth due to Kyropoulos.[6§] AgCl crystals must be pure in order to operate, since impurities produce an electronic conductivity which persists even at low temperatures. The purification obtained by crystal growth out of the melt seems to be quite adequate, particularly if repeated more than once.[11,3] AgCl cannot be used as a counting material at room temperature because of its electrolytic conductivity which in a short time, depending on the current, effects permanent changes in the material.

The technique used with low temperature crystals has been described in the preceding section. We shall now consider the results obtained in using these materials as counters. The only published material in which application has been made of the counting properties of AgCl is that by Voorhies and Street[9] who studied cosmic-ray star production by negative μ-mesons in such crystals. Since their results are in general agreement with the known properties of this counting material, we may pass on to a general account of the observed behavior.

Speed of Response. In these crystals two events are clearly separated in time if the pulse due to one is over before the other has begun. The time duration of a pulse in a solid conduction counter depends on when the secondary electrons stop moving, i.e., when they are permanently trapped. For large applied fields the time is not greater than that required for electrons to traverse the whole crystal. It has been shown that in AgCl and AgBr crystals the pulse duration for an applied field of 5,000 volts/cm is of the order of 0.7 microsecond,[3] and may be as low as 0.2 microsecond,[9] if the secondary electrons are not required to move through the whole crystal. When electrons do traverse the whole crystal the rise time (τ = time electrons are in motion) of a pulse is of the order

$$\tau = \frac{d}{vE}, \qquad (11)$$

where d is the thickness, v the mobility, and E the electric field strength. Measurements supporting this equation are given in the literature.[3]

It is not to be expected, however, that infinitely long rise times will be obtained by decreasing the electric field in which secondary electrons move. For an electron will eventually be captured while it is in the conduction band. The average time of such a capturing event will therefore determine the rise time in a small field. This time which has been called T previously is quite long for AgCl$\sim$1.0 or 2.0×10^{-6} seconds, but appears to be much shorter$\sim4\times10^{-8}$ seconds in diamond. Thus in diamond it is not possible to increase the length of rise time beyond a fixed value by varying the field.

The dependence of the rise time of a pulse on the electric field is given in Fig. 17. Actual measurements of mobility in AgCl and AgBr[3] (Fig. 18) support the general ideas presented. The results of these measurements indicate at 77°K values between 100 and 300 cm²/volt per second, although the theory of Frohlich and Mott would require larger values of the order of 1,000 cm²/volt per second for AgCl crystals. It is desirable that further experiments on the silver halides be performed to clear up this point. Mobility measurements made by observing rise times in crystals offer an accurate method for checking the theory of polar crystals and the interaction of electrons with the lattice vibrations. From the point of view of the solid state, a new tool is herewith available for probing the structure of polar and other crystals.

Although we have seen that the resolving time is less than a microsecond, it is not possible at the present time to use AgCl crystals for fast counting purposes because

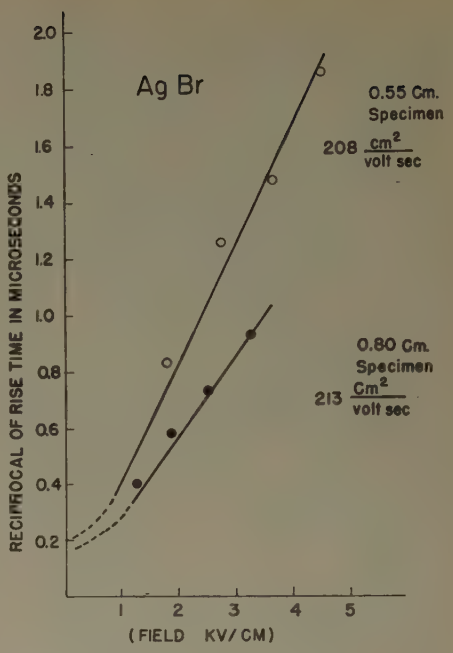

Fig. 18—Experimental curves of reciprocal of rise time versus electric field for AgBr. Data are for 77°K (Yamakawa).

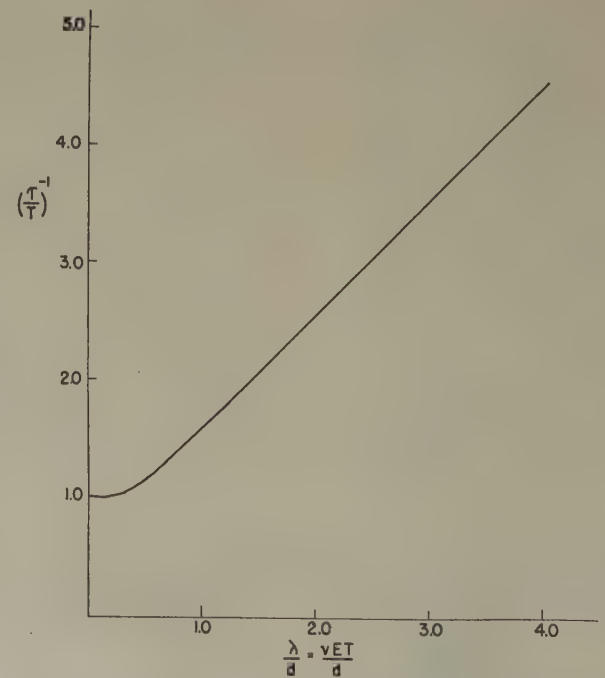

Fig. 17—Theoretical curve showing reciprocal of ratio of rise time (θ) to free time (τ) before trapping plotted against λ/d. λ is proportional to electric field.

§ S. Kyropoulos, "Dielektrizitätskonstanten regulärer Kristalle," *Zeit. f. Phys.*, vol. 63, p. 849; August, 1930.

of the large internal polarization which result. Nevertheless, events which occur within a microsecond of each other may be clearly resolved. The resolution of a μ-meson pulse and the pulse of its decay electron is a case in point. (See Fig. 19, due to Voorhies and Street.)

Polarization. Yamakawa[12] has studied the polarization[64] produced by P^{32} beta particles in a crystal of AgBr. He used a ten-channel discriminator to study the distribution of pulse sizes while the polarization effects were building up. His results are shown in Fig. 20. It is to be noticed that no large changes are produced until after about 3,000 seconds of counting. The pulse distribution then changes quite rapidly with further counting. This behavior can be understood in terms of the saturation curve of the type of Fig. 3. The reversed electric field builds up proportionally with the number of ionizing events, but its effect is only realized effectively when the actual field (applied field minus reversed field) reaches the region of the knee of the saturation curve. It may be calculated[3] that about 10^6 P^{32} beta pulses are required to produce a drastic reduction in pulse size. Yamakawa finds that about 8.3×10^5 pulses produce a large reduction effect. It may be concluded that the theory and experiment are in at least rough agreement on these matters.

It has previously been mentioned on several occasions that infrared radiation of the crystal might release trapped electrons to neutralize the positive holes during gamma or beta counting. Apparently no studies of this phenomenon have been made with AgCl or AgBr, although diamond shows depolarization under infrared illumination. The polarization of AgCl at low temperatures is one of the serious drawbacks in using this material, for depolarization usually requires a warm-up to room temperature and then a subsequent cooling. One of the main advantages of the halide counters is their high specific gravity (AgBr 6.5, TlBr-TlI$\sim$7.0) which makes them very useful for counting gamma rays. Removal of the polarization difficulty by infrared radiation could therefore be an important stimulus to the eventual use of these metal halides.

Polarization is of somewhat smaller importance in the case of TlBr-TlI since the dielectric constant is of the order of 35 for this material. It may be seen from (9) that a larger dielectric constant enables a larger number of events to be counted without producing a serious effect. For AgCl and AgBr the dielectric constant is about 12.

In the counting of alpha particles the positive sites remaining after ionization all lie very close to the negative electrode where the particles enter. Consequently their effect is largely neutralized[3] by negative charge drawn to the electrode from the power supply which maintains the applied voltage difference. With alpha particles of energy 5 Mev, probably 10^8–10^9 particles can be counted before serious change in pulse size is noted. It is theoretically possible to obtain reversed pulses on removal of the electric field. For a discussion of this point see the literature.[3]

[64] See footnote reference 3, page 33, where these results are reported.

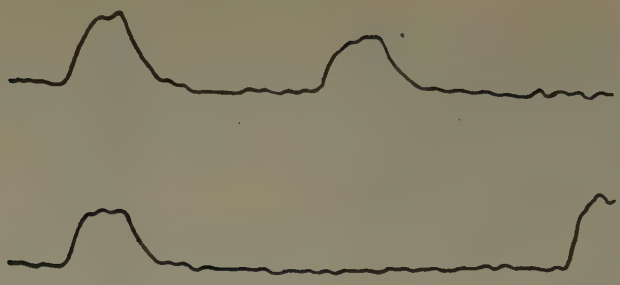

Fig. 19—Meson decay events in AgCl (Voorhies and Street).

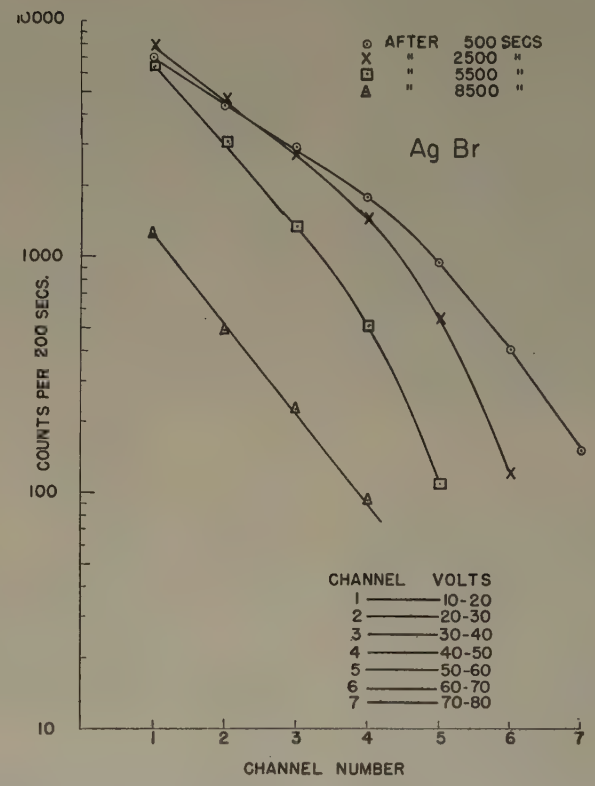

Fig. 20—Ten-channel discriminator curves of AgBr pulses due to P^{32} beta particles. The lower curves show the large drop-off in counting rate when the crystal polarizes (Yamakawa).

Energy per Ion Pair Measurements. The energy per ion pair may be measured when the energy H of the particle and the combined capacitance C of the input and crystal are known. For the pulse height V may be measured (5) when the pulses are saturated. In this case we have

$$V_{sat} = \frac{n_0 e}{C} \quad \text{or} \quad n_0 = \frac{CV}{e}. \tag{12}$$

We then obtain n_0 and from (8)

$$\epsilon = \frac{H}{n_0} = \frac{p}{\psi} \tag{13}$$

where ϵ is the experimentally measurable quantity for energy per ion pair.

Any difficulties arising from additional or undesired trapping of electrons in AgCl crystals will tend to produce too large a value for the energy per ion pair. It is easily possible with some commercial samples having cracks, strains, and impurities to obtain 50 or 100 ev/ion pair. However it has been demonstrated by many investigators that for AgCl the value is 7.6 ev or lower.[2] In AgBr Yamakawa[12,3] finds 5.8 ev. Since ϵ is important in determining pulse size (through n_0) it is desirable to obtain crystals free of boundaries, cracks and strains.

A rough idea of expected values of ϵ appears to be obtainable from the known energy gaps (p). For AgCl and AgBr the p values are 4.88 ev and 3.95 ev. The significance of this is that the ψ values appear to be close to unity. This is apparently the case in sulfur also.

Proportionality of Pulses with Energy. At saturation (12) holds, which states that the pulse size is proportional to n_0. By (13) n_0 is proportional to the energy spent by an ionizing particle in a crystal. In principle the conduction counter therefore appears to be linear, which is to say that the pulse height is proportional to incident energy. Van Heerden has done the best work to prove

point and his results are reproduced in Fig. 21. By using almost monoergic beta particles (0.4 Mev) he obtained the distribution of pulse heights given in the figure. The maximum is expected and its width appears to be satisfactorily explained in terms of the energy per ion pair and inhomogeneity of incident beta particles which have lost only a fraction of their energy in the crystal. Georgesco[26] has shown that sulphur crystals are also proportional with respect to energy of the incident particle.

By using a cylindrical counter the low energy tail might be avoided, since the beta particle, however scattered, will end up in the crystal. The cylindrical counter with small entrance hole for beta particles has been proposed,[3] but to date seems not to have been tried.

Mixtures. Three cases of counting by mixed crystals are known. (1) Yamakawa has prepared and investigated a mixture of LiBr and AgBr. (See below under neutron counting for further details.) (2) Yamakawa and the author[3] have made mixed crystals of NaCl-AgCl which count even when the NaCl content is as high as 15 per cent by weight. Thus even though NaCl has not been observed to count, a large "impurity" of it in AgCl does not cause counting to cease although the observed pulses are smaller than in pure AgCl crystals. (3) The case of TlBr-TlI has already been discussed.

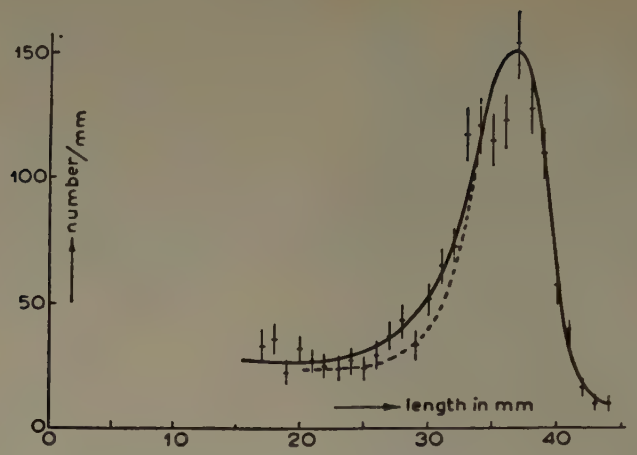

Fig. 21—Van Heerden's pulse distribution for 0.4 Mev data particles on AgCl. The tail at the left is due principally to back scattering of beta particles. The dashed curve shows what is expected theoretically.

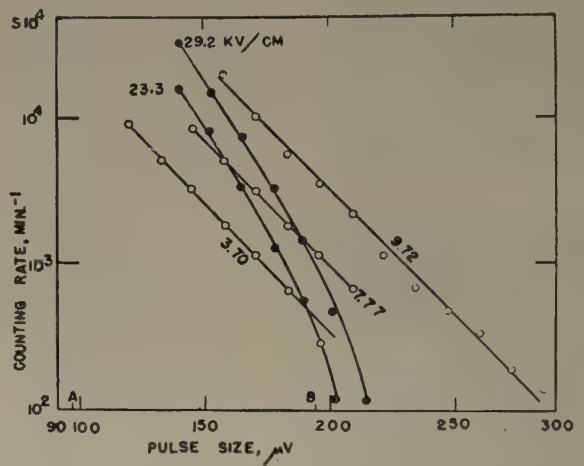

Fig. 22—Gamma ray counting with liquid argon (Davidson and Larsh). *A* and *B* indicate maximum pulse sizes for polonium alpha particles for 9.6 and 28.9 kv/cm, respectively. Dots refer to 0.36 mm gap and circles refer to 1.08 mm gap.

6. *Argon*

Liquid and solid argon have been investigated by Davidson and Larsh[29] and by Hutchinson.[30] The first authors have principally employed alpha particle excitation and the latter gamma irradiation. As might be expected from the properties of gaseous counters, oxygen is to be avoided. Less than 1 per cent of dissolved oxygen is enough to destroy the counting property. Nitrogen does not appear to be a serious contaminant, although pure nitrogen will apparently not count.

In a recent paper[29] Davidson and Larsh have given a detailed account of alpha particle experiments with liquid argon which support the conclusion that electron trapping in pure liquid argon is small. The pulse size is, however, limited according to the authors, by recombination of the secondary electrons with the column of positive ions surrounding the track of the alpha particle. This conclusion results from the fact that the pulse size depends on the electric field and not on the dimension (d) of the counter. The electron trapping mechanism gives, as shown by (5), a dependence of pulse size on d.

The results obtained by Davidson and Larsh (Fig. 22) with radium gamma rays indicate that columnar ionization is less prevalent in this case. The gamma pulses are therefore larger than Polonium alpha particle pulses. The situation is confusing however because more large pulses are observed with wider electrode spacings and therefore smaller fields than in the case of smaller electrode spacing and higher field. Undoubtedly one contribution arises from the fact that the maximum range (and hence energy loss) is larger than the small counter's dimensions. The variations of observed pulse size with field strength at fixed electrode spacing appears to be understandable if electron trapping occurs. However it is not clear whether the authors believe any electron trapping occurs in pure argon. When nitrogen and oxygen are dissolved in liquid argon electron trapping definitely occurs.

Hutchinson has found that the largest pulses in liquid argon correspond to an energy loss by beta particles of 25 ev per ion pair. In solid argon he reports that with suitably large fields (13,000 volts/cm) the energy per ion pair drops to an apparent value of about 2 ev. He attributes the low value to multiplication in the crystal. Although this appears to be a reasonable explanation, it would seem that the simple exaplanation of a low energy gap is also possible. This point has not been discussed by Hutchinson.

Although polarization effects are not to be expected in the liquid, such effects have been noticed by Hutchinson in solid argon. In this case the pulses have the same sign after the field has been switched off as in the case when the field was on. It is possible to obtain this result from the simple theory outlined in the literature.[3] However, no further experiments have been reported on this subject so that this explanation is untested.

7. *Germanium*

McKay[31] has reported a new type of solid counter using a crystal of germanium. He has detected polonium alpha particles with this counter with the results shown in Fig. 23. This counter is quite a bit different from the type we have discussed so far for germanium is a semiconductor. However, under suitable conditions an ionization pulse may be observed by applying a bias to the crystal which is large enough to cut off the current flow.

A phosphor bronze point contact was made on the face of an N type high-back voltage germanium crystal. The opposite face of the germanium crystal was connected with a broad area contact of low ohmic resistance. By applying a negative voltage to the point with respect to the other face, the current could be made small through the so-called barrier layer. The back resistance appears to be of the order of 10^5 ohms. The point contact was connected to a fast amplifier of pass band 100 kilocycles to 15 megacycles. The amplifier input

had a capacitance of 17 $\mu\mu$f and the crystal contact less than 1 $\mu\mu$f. McKay states that the point showed a typical rectifier current voltage characteristic. The area of the contact was photosensitive.

The pulses observed were as shown in Fig. 23 for the various bias voltages indicated there. It will be noticed that the signal-to-noise ratio is quite large (difference in scale factors). The pulse rise time was less than 0.05 microsecond and appeared to be limited only by the amplifier. From the maximum pulse observed (12 millivolts) and the combined capacitance one computes a collected charge of 2×10^{-13} coulombs or the equivalent of 1.2×10^{6} electrons. One therefore finds a value of ϵ of about 5 ev per free electron. The sensitive area of the counter has a diameter of between 10^{-3} and 10^{-2} cm.

Since this counter has high speed, no polarization difficulties and gives large pulses only for heavy particles, it should be useful for fast counting and discrimination against beta particles and gamma rays. However, the small size restricts its present usefulness. The lifetime between rejuvenations, appears to be 10^{13} alphas/cm^2 which is a quite reasonable number. Orman[31] *et al* have detected RaE beta particles with a similar germanium P-N counter arrangement.

V. Miscellaneous

1. *Efficiency of Conduction Counters*

It might be expected that when counting alpha particles or beta particles every particle entering the crystal would be counted. This does not appear to be the case, at least in diamond counters.[65] We must remember that in all (integral bias) counting work we always count above a certain bias level. If the pulse is above the level, it is counted, if below it is not counted. Thus, even though each alpha particle could have produced a pulse, some of these pulses might have been below the bias setting for that experiment. Thus Ahearn's result indicates that certain alpha pulses were very small and below the noise level of his amplifier, but not necessarily zero. Ahearn reports that the efficiency for counting alpha particles increases rapidly with voltage gradient and approaches saturation at about 4,000 volts/cm. At or near saturation the best efficiency was 60 per cent. In view of Ahearn's observation that there are great local variations in the counting property on a single face of a diamond, this result may not appear unusual. It may be expected, however, with production of synthetic counting materials like CdS, that the efficiency of counting alpha particles will be 100 per cent.

Van Heerden[2] also reported that alpha particles in AgCl produced pulses smaller than their energy would indicate. This is an unexpected result which however may be due to imperfections or unusual conditions on the surface of the crystal. If a condensed film covered the surface and abstracted energy from the alpha particles without yielding conduction electrons this result would be explained. In any case Yamakawa[43] has found a smaller difference than van Heerden in energy per ion pair between alpha particles and beta particles when the former were produced by neutrons internally within an AgBr crystal. This point requires further study.

Efficiencies for the counting of beta particles have not been reported. It may be presumed from Fig. 21, due to van Heerden, that the efficiency is 100 per cent for 400 kev electrons in AgCl.

In the case of gamma rays the efficiency cannot be higher than the percentage of gamma radiation stopped by the crystal. Accurate measurements of efficiency are unavailable. However a figure of 13 per cent for radium gamma rays in a crystal of AgCl 4 mm thick has been reported.[66] Until plateaus in counting rate are observed the efficiency figures are not very meaningful.

It is to be noted that in counting beta particles and gamma rays, the range of the fast electrons in the crystal specimen may easily be equal to or larger than the thickness of the specimen. This is particularly true for thin diamond slices. It may therefore occur that only a fraction of the beta particle's energy is absorbed by the crystal. The pulse obtained may be close to the noise level and therefore not observed.

2. *Neutron Counting*

By using a mixture of LiBr and AgBr Yamakawa[43] succeeded in counting slow neutrons by conduction methods. The crystal was grown by the Bridgman technique and had a ratio of four silver atoms to one of lithium. The neutrons, as well as gamma rays, from the radium-beryllium (paraffin) source produced pulses of all sizes. Hence to find the neutron count, differential bias curves were taken with and without a cadmium absorber, and by subtraction the neutron contribution could be measured. It was observed that the pulses obtained from the neutrons extended well above the largest pulse for Ra gamma rays. The maximum energy of Ra gamma rays is about 2.4 Mev while the energy release in neutron capture by Li^6 is 4.7 Mev. Therefore one ought to observe pulse sizes due to neutrons of the order of twice those due to radium if alpha particles or H^3 particles yield as many free electrons as a beta particle of the same energy. From the observed pulse height distribution Yamakawa concludes that the energy/ion pair for the heavier particles (H^4 and H^3) is not more than twice, and perhaps equal to, the corresponding value for beta particles. As we have noticed previously, van Heerden found that alpha particles produced a smaller yield by a factor of four to six than beta particles. Since the alpha particles in Yamakawa's experiment were produced inside the crystal while van Heerden's alpha particles entered through the surface, the discrepancy may possibly be accounted for by surface losses.

The crystal used by Yamakawa had dimensions of 0.75 cm thick and 1.2 cm^2 area and had an over-all efficiency for slow neutrons of 5 per cent. By using lithium enriched in Li^6, a crystal two centimeters thick is estimated to have an efficiency of 70 per cent for slow neutrons.

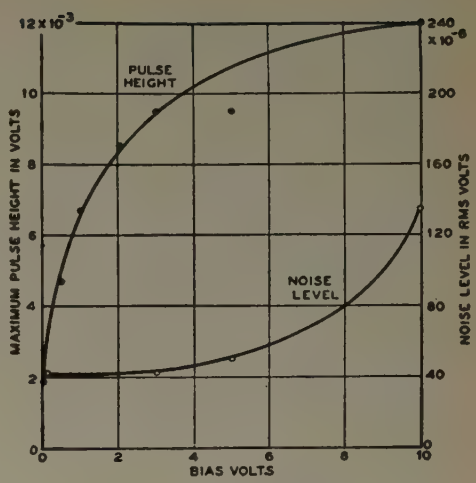

Fig. 23—Alpha particle pulses in a germanium semiconductor counter. The noise level is also shown plotted on a different vertical scale (McKay).

3. *Search for Counting Materials*

Many workers have searched among crystals and minerals for specimens which will count single ionizing particles. The unexpectedly small number of successful finds may probably be traced to the many difficulties involved in a trial. For example, a crystal specimen of AgCl will usually not count. Only when annealed properly will it count. Very few specimens of diamond will count gamma rays. Unfortunately, little or no description is usually given of unsuccessful attempts to find conduction counting crystals. Some noncounting materials have been mentioned only by Ahearn,[25] Jentschke[67] and the writer,[3] but it is hazardous to describe a crystal in such a manner. It is quite possible that one of the following conditions may be responsible for reporting a crystal to be a noncounter: (1) the material may be built of very small crystals so that the maximum length of travel of an electron is small—the pulse will be small accordingly; (2) trapping impurities may be present; (3) noise in the amplifier may be too high because an unnecessarily large pass band was employed; (4) particular conditions, e.g., annealing, low temperature, good electrode contact, good surfaces, freedom from space charge, etc., might not have been attainable with the specific arrangements of the experiment; (5) crystal imperfections and frozen-in trapping centers may be present without being visible; (6) beta particles may have been used with small crystals so that the energy loss is small; and (7) other unknown causes, such as those which are responsible for making some diamonds noncounters for gamma rays.

[65] A. J. Ahearn, "Conductivity pulses induced in diamond by alpha particles," Brookhaven Conference of High Speed Counters, August 14, 15, 1947.

[66] R. Hofstadter, "Use of silver chloride at low temperatures as counters," Brookhaven Conference Report on High Speed Counters, August 14, 15, 1947.

[67] W. Jentschke, "The crystal counter," *Phys. Rev.*, vol. 73, p. 77; January, 1948.

VI. Conclusions

Many of the results obtained at the present time with crystal conduction counters are easily explained in terms of presently accepted views concerning the solid state. There are other questions such as "Why does a material count?" and specifically, "Why do very few diamonds count gamma rays?" which must go without answer until further experiments are performed. Perhaps a good deal of the puzzle lies in the structure of the actual interior of microscopic bits of solids. This structure has not received an attentive study, at least in the case of insulators. The new probe which the conduction counter offers for this investigation will probably be used intensely by future investigators of the solid state. We must be satisfied now that part of the subject has yielded to known facts.

We may summarize our present knowledge and possible applications of conduction counters by concisely itemizing the following points:

A. Useful materials—AgCl, AgBr, S, diamond, CdS

B. Useful for γ rays and X rays—AgCl, AgBr, perhaps diamond, CdS
Useful for β particles—AgCl, AgBr, perhaps diamond, CdS and sulphur

C. Do counters give pulses proportional to energy? for:
alpha particles—yes, S
beta particles—yes, AgCl, AgBr, TlBr-TlI
γ rays—yes, under proper conditions in AgCl, AgBr, TiBr-TlI

D. Efficiency for γ rays and other penetrating particles:
Very high because of high density of silver and thallium halides, probably approaching 100 per cent
For slow neutrons—reasonably high (5 per cent)

E. Resolving time:
Depends on applied field and other conditions; for about 5,000 volts /cm the approximate values are as follows:
AgCl, AgBr $=0.2\times10^{-6}$ sec
Diamond $=0.04\times10^{-6}$ sec
CdS $=0.2\times10^{-6}$ sec

F. Lifetime—indefinite when space charges are removed (diamond); if not removed, about 10^6 1.0 Mev γ counts per cm^3 of material. About 10^8 5.0 Mev α counts per cm^3 of material

G. Lowest detectable energy—a few kiloelectronvolts (0.2 kev. in principle)

H. Energy per ion pair
AgBr—5.8 ev, AgCl—7.6 ev, Diamond 10 ev, CdS—10.0 ev: S—5.0 ev

I. East of handling
Convenient—Diamond, S, CdS
Inconvenient—AgCl, AgBr, TiBr-TlI

The crystal conduction counter offers to one interested in the solid state a new fascinating opportunity for study of the interior of insulating solids and perhaps semiconductors. To the nuclear physicist it does not yet offer a mature tool. The reason may, however, lie in the lack of attention such counters have recently received. It appears reasonable to expect in the near future the discovery of an important conduction counter material which will restore the balance of interest in the direction of conduction materials.

Acknowledgments

The preparation of this report was aided in part by a contract with the U. S. Army Signal Corps. The author acknowledges with pleasure permission of the editors of the McGraw-Hill publication, *Nucleonics*, to reproduce Figs. 1, 2, 3, 4, 6, 7, 8, 9, 11, 13, 17, 18, 20 from an earlier article.[3]

The Recording Storage Tube*

R. C. HERGENROTHER†, Associate, IRE, and B. C. GARDNER‡

Summary—**The recording tube is a cathode-ray type of storage tube embodying a new operating principle which enables reading to be accomplished without disturbing the information written into the tube. An output signal comprising a full modulation of several microamperes can be read out of the tube for 20,000 complete scannings of the storage surface with no appreciable deterioration in the signal quality and only a few per cent decrease in signal level. The output signal may be observed on a monitor tube which is scanned in synchronism with the reading beam and it may also be observed directly on a fluorescent screen within the recording tube.**

The theory underlying the operation of the recording tube is developed in detail.

Introduction

THE IDEAL STORAGE TUBE would be capable of (1) internally recording an input electrical signal of variable frequency and amplitude, which process is called "writing," (2) retaining the written information as long as desired, which process is called "memory," (3) repeating the written information in the form of an output electrical signal which process is called "reading," and (4) deleting the written information when it is no longer needed to make way for new information, which process is called "erasing." When the information is in the form of a picture, as for example a PPI radar display or a facsimile or television picture, it is also desirable that the picture can be displayed in the storage tube directly in addition to being displayed in any desired number of monitor tubes.

A storage tube having all these ideal properties would have many applications in instrumentation and communication. For example, such a tube could be used in an oscilloscope for recording transient currents or voltages which then could be displayed as long as desired for study or photographic recording. Another application would be for PPI radar display which would have the advantage of displaying a uniform brightness picture and of accumulating information so that moving targets would leave trails in the picture and random noise signals would be integrated out. Such a tube makes it possible to introduce a long time delay in an electrical

* Decimal classification: R138.31. Original manuscript received by the Institute, October 3, 1949; revised manuscript received, March 21, 1950. This work was conducted under U. S. Navy Bureau of Ships Contract NObsr-39350.

† Raytheon Manufacturing Company, Waltham, Mass.
‡ Varian Associates, San Carlos, Calif.

signal or to compress the time scale of the signal to effect a high-speed transmission or to expand the time scale to effect decoding of a received high-speed transmission. Another field of application for such tubes is number storage in electronic digital computers. Storage tubes having some of the properties of the ideal tube described above have appeared in the literature.[1–3] These storage tubes make use of an electron beam striking the storage surface in both the reading and writing operations. This means that during reading, the stored signal is used up in producing an output signal. The Haeff memory tube overcomes this effect by replenishing such signal loss by means of a holding gun; but, in so doing, the stored signal is limited to one of two equilibrium levels and the tube is incapable of writing intermediate or half-tone signal levels.

The "recording tube" which is the subject of this article effects reading by means of an electron beam *which does not come in contact with the stored charge.* This overcomes the difficulties encountered in other types of storage tubes mentioned above and enables the tube to write half tones and to read an almost unlimited number of times without disturbing the stored written charge. Another feature of the recording tube is that it uses a single electron gun and deflecting system for reading, writing, and erasing, which results in a simplified tube structure and permits tracking or point-by-point retrace of the same scanning paths during reading and writing. An additional feature of the tube is that the pattern of stored charge can be made visible in the tube itself, thus providing the possibility of direct viewing.

Description of the Recording Tube

An outline drawing of the recording tube is shown in Fig. 1. The electron gun which forms the beam used for reading and writing is magnetically focused and magnetically deflected. The tube could also be constructed with electric focus and electric deflection but experience shows that higher resolving power can be obtained with the magnetic focus and deflection system. The structure at the left of the first screen is that of a cathode-ray tube whose electron spot is focused and scanned over the area of the first screen. The first screen comprises a conducting mesh which has a high percentage opening and whose mesh size is sufficiently small that the focused electron spot covers four or more openings. This can be constructed of a woven wire mesh or can be a thin perforated metal sheet such as can be produced by electrodeposition.[4] To the right of the first screen and in close parallel spacing to it is the storage screen. The storage screen is operated at a voltage of the order of several hundred volts and must operate at different voltages for read and write as will be explained below. The electron gun anode and the first screen are operated at as high a voltage as possible to obtain the smallest possible electron spot size. The electron beam is then decelerated between the first screen and the storage screen with little disturbance of the electron spot size. The storage screen comprises a thin, perforated metal sheet similar to that used for the first screen. The storage material is in the form of a coating on the side of the metal screen facing away from the electron gun. This coating is applied to the metal screen by evaporation of the storage material in a vacuum bell jar and is made as thick as possible without unduly closing the metal screen perforations. That portion of the storage material which coats the inside edges of the holes would be exposed to the direct electron beam during reading and writing if it were not protected in some way. This protection is supplied by a thin metal coating which is evaporated on the uncoated side of the metal screen after the storage surface coating has been applied. Fig. 2 shows a photomicrograph of a 500-mesh storage screen before and after coating. To the right of the storage screen in Fig. 1 is a metal target which serves as an electron mirror during writing and as an electron collector for the output signal during reading.

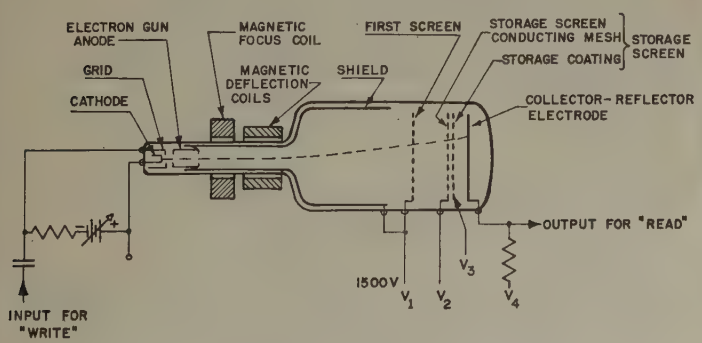

Fig. 1—Outline drawing of the recording tube.

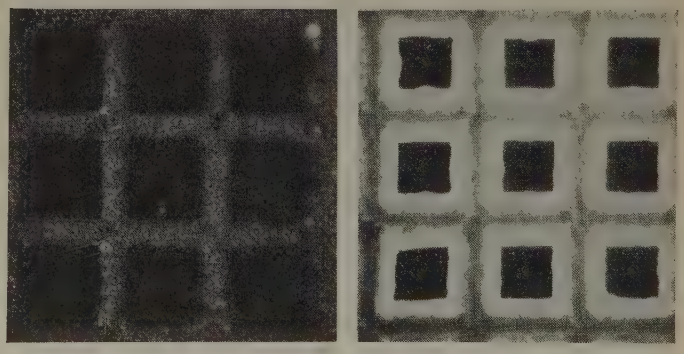

(a) (b)

Fig. 2—Photomicrograph of a 500-mesh storage screen: (a) before coating; (b) after coating on one face with storage material.

[1] A. V. Haeff, "A memory tube," *Electronics*, vol. 9, pp. 80–83; September, 1947.
[2] A. S. Jensen, J. P. Smith, M. H. Mesner, and L. E. Flory, "Barrier grid tube and its operation," *RCA Rev.*, vol. 9, pp. 112–135; March, 1948.
[3] L. Pensak, "The graphechon—a picture storage tube," *RCA Rev.*, vol. 10, pp. 59–73; March, 1949.
[4] H. B. Law, "A technique for the making and mounting of fine mesh screens," *Rev. Sci. Instr.*, vol. 19, pp. 879–881; December, 1948.

Operation of the Recording Tube

A. Erasing and Writing

When it is desired to write on the storage screen, the collector-reflector electrode potential V_4 is made negative relative to the electron gun cathode. The retarding field between the storage screen and the collector-reflector causes the beam passing through the storage screen holes to be reflected back so that it will fall on the storage coating of the storage screen as shown in Fig. 3. It should be noted that this reflection will occur in a region where the electric field is very uniform so the reflection is not disturbed by the field irregularities which

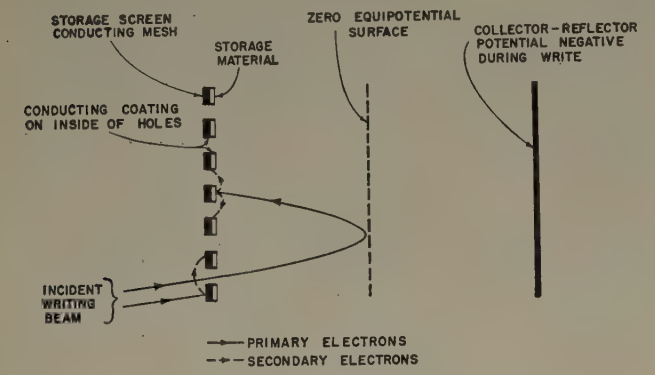

Fig. 3—Electron beam action during "write."

occur near the storage screen holes. The reflected writing beam will strike the storage surface with a velocity depending on the potential of this surface. If the storage surface potential is below the critical V_c characteristic of the storage surface, the storage surface will charge negative until it reaches cathode potential. On the other hand, if the storage surface potential is greater than V_c, the storage surface will charge to a potential near V_2, that of the storage-screen conducting mesh which acts as a collector for the secondary electrons. The details of these processes are described in Appendix A. By this means it is possible to cover the storage surface with a uniform charge, either at electron gun cathode potential or positive, which constitutes the erasing operation. Writing is then performed by adjusting the storage screen conducting mesh voltage V_2 in such a way that the beam writes a charge of sign opposite that used for erasing. During writing, the beam is scanned and its current is modulated with the input signal which deposits a varying charge on the storage surface at successive points according to the input signal amplitude. The amount of voltage change produced on a storage surface element during the writing operation depends on the scanning speed, the beam current, the geometry of the screens, and the storage material. The relation between these factors and the writing speed are discussed in detail in Appendix B. Since the writing speed for positive charge is an order of magnitude greater than the writing speed for negative charge, the preferred method of operation is to erase negative, that is, to charge the storage surface to cathode or zero potential and then to write positive on this. During erasing the spot size is not critical and the electron gun may be operated at much higher current levels than during writing when a sharply focused electron spot is required.

B. Reading

When it is desired to read the stored information out of the tube, the collector-reflector electrode potential V_4 is made more positive than the storage screen mesh potential V_2. The accelerating field between the storage screen and the collector electrode causes the beam passing through the storage screen holes to be collected as shown in Fig. 4. It should be noted that the current picked up by the collector electrode will be exactly equal to the current which has penetrated the storage screen. The field between the storage screen and the collector screen which accelerates electrons to the col-

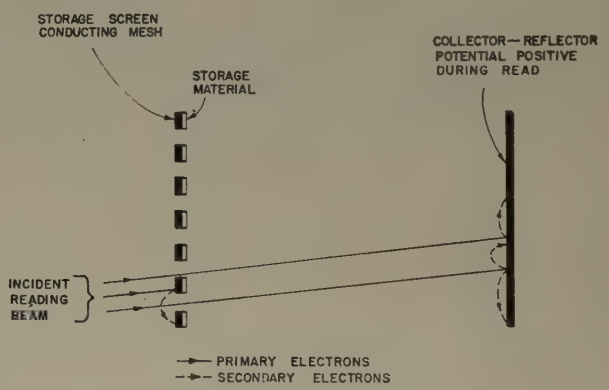

Fig. 4—Electron beam action during "read."

lector will prevent secondaries escaping from the collector. This not only preserves the storage screen charge but avoids any output signal modulation from nonuniformity in secondary-emission characteristics of any surfaces struck by the beam. During the reading, the beam current is kept constant and the reading beam is scanned over the storage screen, usually in a television-like line raster. The fraction of the incident beam which passes through the storage screen depends on the potential of the storage surface in the electron spot area. If the storage surface potential is more positive than the electron gun cathode potential, all of the beams striking the holes will pass through the screen giving a condition of saturation. As the storage surface potential is made equal to or more negative than the cathode potential, the effective hole size is decreased, which will cut down the amount of current passing through. The decrease in effective hole size with increased negative storage surface potentials was studied by means of an electrolytic trough. Fig. 5 shows a cross section of the storage screen with the location of the zero equipotential surfaces for various negative storage surface potential levels. The effective hole size for electrons starting from the cathode at zero velocity is given by this zero equipotential surface. At a sufficiently high negative

surface potential this hole closes up and the beam is cut off. This characteristic of storage screen transmission

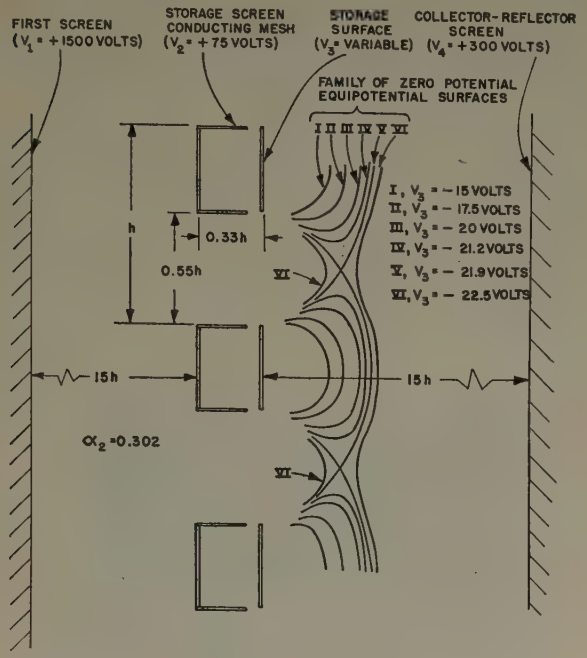

Fig. 5—Results of storage screen electric-field studies made with an electrolytic trough. The model represent a cross section of the storage screen through the center of a row of holes. The shape of the zero equipotentials for various storage surface potentials are shown. Note that cutoff occurs when the storage surface potential is −21.9 volts.

as measured on a typical recording tube is shown in Fig. 6. The method by which this characteristic was measured is described in Appendix C. The maximum voltage

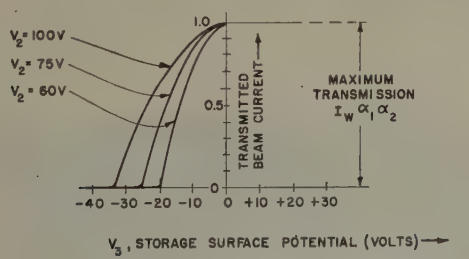

Fig. 6—Storage screen transmission characteristic of a typical recording tube.

range of the written charge pattern must be kept within the voltage range of the transmission characteristic if distortion in the input-to-output characteristic is to be avoided.

C. Circuitry

A schematic circuit diagram of a recording tube used in conjunction with a cathode-ray-tube viewing monitor is shown in Fig. 7. The scan in this case is a television-type raster for both writing and reading. The input signal modulates the recording tube beam current which in turn determines the amount of charge written on the storage surface from point to point during the scan.

Other modes of scanning and writing may be used with appropriate circuits. Some examples are radial or

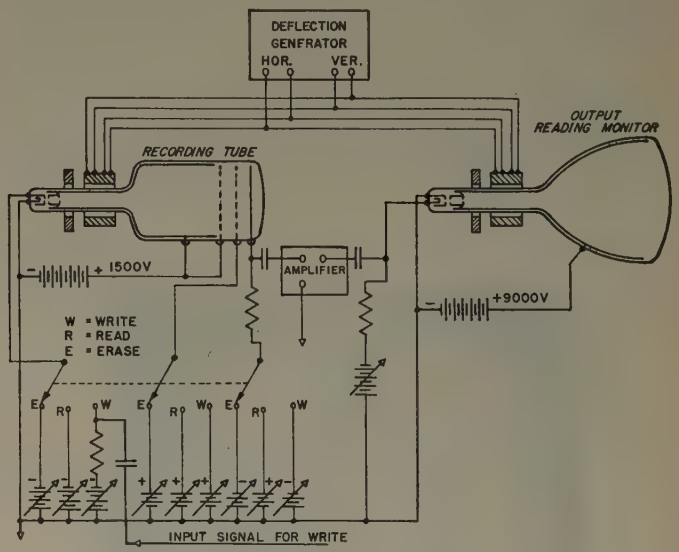

Fig. 7—Circuit diagram of recording tube using a monitor tube for reading.

PPI type of deflection for writing and oscilloscope type of writing, in which the writing beam current is kept constant and a beam trace is produced by signals applied to the deflection system. The mode of reading is independent of the writing mode used, but for many uses a raster scan is convenient for reading.

Recording Tube Performance

A. Writing Speed

The amount of storage surface voltage change produced by a given writing beam current depends on the scanning velocity and other factors described in Appendix B. When the storage surface voltage change during writing is such as to reach saturation on the storage screen transmission characteristic shown in Fig. 6, the writing is referred to as saturated writing. The linear speed of the writing beam electron spot on the storage surface producing saturated writing depends on the beam current and its referred to as the saturation writing speed.

Saturation writing speed of the recording tube is measured by writing a trace of known deflection speed and known beam current on the previously erased storage surface. The trace is then read on the viewing monitor and it is found that, as the writing deflection speed is decreased, a stronger reading signal is obtained until a lower limiting deflection speed is reached when a maximum output signal is obtained, indicating saturation.

Saturation writing speeds of 8,000 cm per second for writing positive on negative and 800 cm per second for writing negative on positive have been measured using a 10-microampere writing beam.

B. Resolving Power

The recording tube resolving power is measured by means of a standard television test pattern. This test pattern is written into the recording tube and is then read out on a monitor tube. Fig. 8 shows a photograph of the monitor tube reading the stored test pattern. Resolving powers of 400 lines across the storage screen diameter have been consistently obtainable. The resolving power is limited by the writing-beam electron spot diameter.

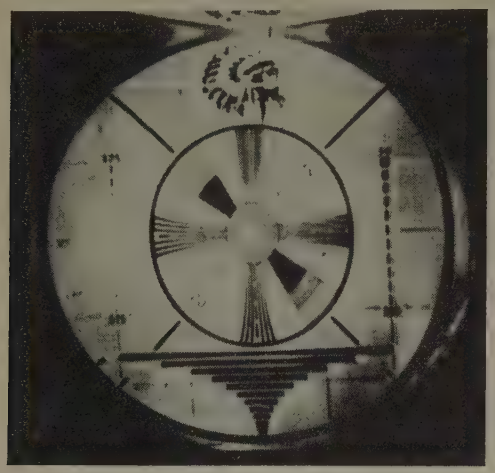

Fig. 8—Stored test pattern read out on monitor tube.

C. Holding Time

The recording tube has the unique property that its stored charge is completely shielded from the reading beam so that no loss of charge is produced by the reading beam directly. The stored charge can, however, be lost by two other processes.

1. *Charge Loss by Electrical Leakage through Storage Material:* The electrical resistivity of the storage material is finite and therefore the charge is eventually lost by electrical leakage through it. The time constant of this discharge depends only on the resistivity and the dielectric constant of the storage material as given by the relation

$$\tau = 8.84 \times 10^{-14}\, k\rho \text{ (seconds)} \qquad (1)$$

where τ = time required for storage surface potential to drop to $1/\epsilon$ of its original value
k = dielectric constant of storage material
ρ = resistivity of storage material (ohm cm).

This loss of the stored charge from electrical conduction can be measured by writing a pattern into the tube and then turning the tube off for a waiting period before reading out. It is found that the holding times measured in this way are in satisfactory agreement with (1). Some storage materials such as BaF_2 have a time constant of the order of 0.1 second whereas other materials such as CaF_2 have time constants of the order of 50 hours.

2. *Charge Loss by Positive Ions:* During reading, the electric field between the storage surface and the electron collector electrode is such as to accelerate electrons away from the storage surface. This field will therefore accelerate toward the storage surface any positive ions which are formed in this region by the reading beam. The amount of this ion current is very small but it will produce a very slow erasure of the stored charge under prolonged reading. The ratio of this ion current to the electron current producing it will be approximately the ratio of the ion erasing speed to the electron writing speed. Taking the ionizing coefficient of air as 8 ions per centimeter at a pressure of 1 mm of mercury for 300-volt electrons, we compute the ionization in the 0.075-cm space between the storage surface and the collector electrode at a pressure of 10^{-6} of mercury to be $8 \times .075 \times 10^{-6} = 0.6 \times 10^{-6}$ ions per electron. The ratio of ion erasing speed to writing speed is thus approximately 0.6×10^{-6} or it would take 1.6×10^{6} readings to completely erase a saturated writing by positive ions. Actual measurements show that 25,000 readings can usually be made from a written pattern in the recording tube before any loss of output signal can be detected. This number of readings would produce a $1\frac{1}{2}$ per cent erasure of the stored charge by ions if the pressure were 10^{-6} mm of mercury and a 15 per cent erasure if the pressure were 10^{-5} mm of mercury. The measured signal loss produced by reading therefore agrees in order of magnitude with the effect to be expected from positive ion discharge. In general, 10,000 readings are ample for most recording tube applications.

D. Other Recording Tube Performance Tests

An illustration of the use of different scanning methods for read and write is shown in Fig. 9 in which a radial

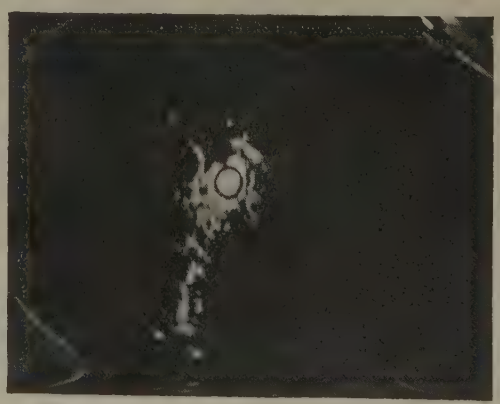

Fig. 9—Stored PPI display read out on a monitor tube.

scan was used for writing and a raster scan was used for reading. A radar PPI signal was written into the recording tube by putting this tube in place of the PPI cathode-ray tube in a radar set. The recorded signal was subsequently read out and photographed on a monitor tube using a raster scan.

Modifications of Recording Tube Design

Modifications of the basic recording tube described above have been designed and constructed and have given satisfactory performance. One such modification replaces the solid metal collector-reflector electrode of Fig. 1 with an open meshed metallic screen followed by a fluorescent screen. During reading, the major part of the reading beam passes through the mesh screen and strikes the fluorescent screen making the stored charge pattern directly visible in the tube. A photograph of such a pattern made directly visible on a fluorescent screen in the recording tube is shown in Fig. 10. This does not interfere with the output signal which can be

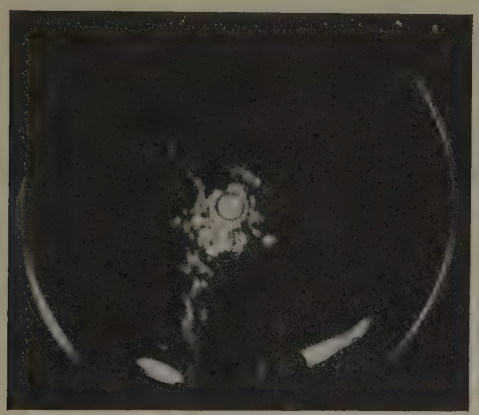

Fig. 10—Stored PPI display read out on the recording-tube fluorescent screen.

taken from the collector-reflector screen and displayed on other monitors. If the output electrical signal is not required, there is no need for focusing the reading beam which can be made as large as desired. If the reading beam can be defocused or overfocused enough to cover the whole storage screen, the fluorescent screen image can be made visible without scanning since the effect of the stored charge on the storage screen is merely to cast a shadow on the fluorescent screen.

Another modification of the basic recording tube of Fig. 1 divides the internal shield coating into two sections, forming an electrostatic lens between the anode potential section and the other section which is brought near or equal to the first screen potential. By proper design of the lens, the center of scanning can be located at a focal point of the lens and the first screen can be located at the corresponding principal plane so that all electron rays will strike the first screen at perpendicular incidence independent of scanning deflections.

Acknowledgments

The authors wish to express their indebtedness to Philo T. Farnsworth who invented the concept of the storage screen.[5] The assistance of John Buckbee, who developed the reading- and writing-test circuits and that of Walter Brady, Harold Sleeper, and others in the construction of the tubes is gratefully acknowledged.

[5] P. T. Farnsworth, "The image amplifier tube." Presented, IRE Rochester Fall Meeting, Rochester, N. Y., November 14, 1938.

Appendix A

Effect of Electron Bombardment on Storage Surface Charge

The behavior of the storage surface under electron bombardment is determined by the secondary electron-emission characteristic of the storage material. This characteristic, which differs in detail for different storage materials has the general shape shown in Fig. 11. The abscissa of Fig. 11 is the potential of the storage surface relative to the electron gun cathode, which is taken as zero reference voltage. The ordinate of Fig. 11

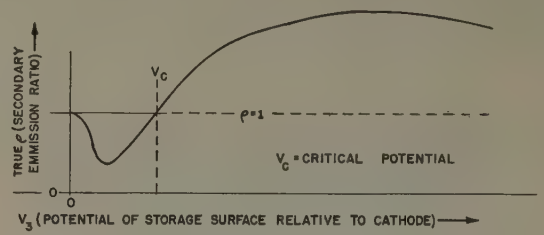

Fig. 11—Secondary-emission characteristic of storage material.

is the true secondary emission ratio ρ which is defined as the average number of secondary electrons released from the surface by one incident primary electron. These released secondaries, may be collected by another electrode or may be partly or entirely driven back to the storage surface either to the place of origin or to some other location on the storage surface, depending on the electric field near the storage surface. In order to measure the curve of Fig. 11, the electric field at the secondary emitting surface must be such as to draw away all the secondary electrons produced. The potential at which $\rho = 1$ on the positive slope part of this characteristic is called the critical potential V_c.

During writing, the conducting mesh of the storage screen can collect the secondary electrons produced by the writing-beam bombardment of the storage surface

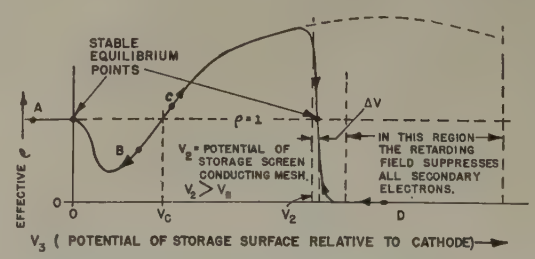

Fig. 12—Charging effect of writing beam when storage screen potential is above critical potential of storage material.

because these electrons are repelled by the reflector electrode field and can escape through the storage screen openings to the conducting mesh.

Fig. 12 illustrates the dynamic behavior of the storage surface charge under electron bombardment when

the storage screen conducting mesh potential V_2 is above the storage material critical potential V_c. A storage surface charge at point A would not be reached by the bombarding electrons and would be unaffected. A storage surface charge below critical voltage as at point B would become more negative until it reaches cathode potential zero where it will maintain equilibrium. A storage surface charge above critical voltage but below V_2, as at point C, will become positively charged until it reaches an equilibrium potential at $(V_2+\Delta V)$. Here ΔV, which is of the order of several volts, is the retarding potential required to suppress the excess of secondary electrons over primary electrons. A storage surface charge above V_2, such as at point D, will be in a retarding field which will force it to charge negatively until the equilibrium potential $(V_2+\Delta V)$ is reached.

Fig. 13 illustrates the case where the storage screen conducting mesh potential V_2' is below the critical potential V_c. Here again storage surface charges below cathode potential such as point A are unaffected, but all other charge conditions such as B, C, and D cause the storage surface charge to become more negative until the equilibrium zero, or cathode potential, is reached.

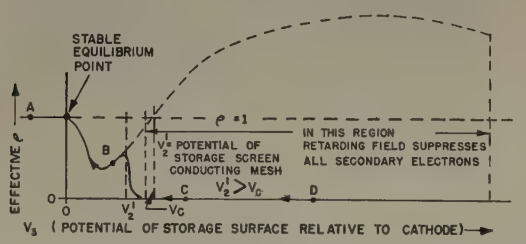

Fig. 13—Charging effect of writing beam when storage screen potential is below critical potential of storage material.

The electrical capacity between the storage surface and the storage screen conducting mesh is much greater than its capacity to other surrounding electrodes. For this reason, any changes in storage screen conducting mesh potential induce a nearly equal potential change on the storage surface.

The process of erasing or writing negative is performed by making the potential of the storage screen conductor mesh some value less than V_c such as V_2' in Fig. 13, and scanning the entire storage surface area until all points reach cathode potential. (The trapping of charges at points such as A does not normally occur in the read-write cycle but it is possible to produce such charges and also remove them by additional manipulation of conductor mesh voltages.) After the whole storage surface is at cathode potential, the electron beam is turned off and the potential of the storage screen conducting mesh is raised to a higher positive potential. This potential increase must exceed the critical V_c so that the storage surface potential becomes greater than V_c. This brings the storage surface to the condition represented by the point C in Fig. 12. The beam is now turned on and will write positive. A saturation condition is obtained when the storage surface potential reaches the level $(V_2+\Delta V)$. The writing range should be kept below this saturation condition.

When the recording tube is switched to reading, the electron beam cannot reach the storage surface and the storage screen conducting mesh potential may be switched to any desired value. In practice it is found advantageous to lower the conducting mesh potential to about 20 volts below the potential used during erasing. This potential lowering is affected before the reading beam is turned on and the storage surface potential pattern which was written on the storage screen is carried to a negative level by electrostatic induction.

Appendix B

The Writing-Speed Equation

The writing process comprises electrical charging of the storage surface by the incident writing beam. In this process the storage material is the dielectric of a condenser whose plates are respectively the storage screen conducting mesh and the electron spot area. We shall make the simplifying assumption that the electron spot is square in shape and has a uniform current density. The effect of various screen parameters on the charging speed will be developed below.

Let i = beam current (amp)
i_w = writing current (amp)
i_0 = average charging current (amp)
α_1 = fractional opening of first screen
α_2 = fractional opening of storage screen
d = thickness of storage coating (cm)
k = dielectric constant of storage coating
S = electron spot width (cm)
ΔV_s = potential change of storage surface during "write" (volts)
K = a charging factor which depends on details of charging mechanism
v = scanning speed of electron spot (cm per second)
c = capacity of electron spot area on storage surface (farads).

The writing current is that part of the electron beam current which falls on the storage surface area. This given by the relation

$$i_w = i\alpha_1\alpha_2(1 - \alpha_2) \text{ (amp)}. \tag{2}$$

The charging current depends on the secondary emission ratio ρ which, however, varies during the charging process as is illustrated in Figs. 12 and 13. The average charging current can be expressed as

$$i_0 = \frac{i_w}{S/2}\int_0^{S/v} (\rho - 1)dt = i_w K \text{ (amp)}. \tag{3}$$

The electron spot charging action will produce voltage change ΔV_s which can be expressed as

$$\Delta V_3 = \frac{1}{c}\frac{S}{v} i_0 \text{ (volts)}. \quad (4)$$

The capacity of the electron spot c can be expressed as

$$c = 8.85 \times 10^{-10} \frac{kS^2}{d}(1 - \alpha_2) \text{ (farads)}. \quad (5)$$

Substituting (2), (3) and (5) in (4)

$$v\Delta V_3 = 11.3 \times 10^{12} \frac{i\alpha_1\alpha_2 dK}{kS} \text{ (volts)}. \quad (6)$$

We shall call $v\Delta V_3$ the charging speed which can be conveniently defined as the electron spot scanning speed required to produce a voltage change of one volt on the storage surface. Equation (6) shows that the charging speed $v\Delta V_3$ increases with increasing beam current, fractional opening of first screen, fractional opening of the storage screen, storage material thickness and charging factor K, whereas $v\Delta V_3$ decreases with increased dielectric constant of storage material and spot width.

The charging factor K is found to increase as the storage conducting mesh voltage is increased above the storage material critical voltage and values of the order of $\frac{1}{2}$ have been measured. When the storage screen conducting mesh voltage is decreased below the storage material critical voltage as in erasing or negative writing, the charging factor K drops to the order of a tenth or a twentieth of the values observed with positive writing.

Appendix C

Measurement of Storage Screen Transmission Characteristic

To measure the storage screen transmission characteristic shown in Fig. 6, the writing beam is caused to write negative while being scanned back and forth along a single-line trace across the storage screen and, at the same time, the storage screen conducting mesh is modulated by a voltage which is proportional to the scan deflection. The writing is allowed to go to saturation so that at each point on the trace the storage surface reaches the potential of the electron gun cathode. When the beam is turned off and the modulation voltage is removed from the storage screen conducting mesh, the storage surface charge trace will have electrostatically induced on it a potential distribution corresponding to the removal of the modulation. At the center or zero deflection point on the trace, the storage surface potential will be cathode potential or zero and, at the maximum deflection corresponding to positive peak of the modulation voltage during the writing operation, the potential of the storage surface will be below cathode potential by an amount equal to the positive peak modulation voltage; conversely, at the other extreme deflection corresponding to the negative peak of the modulation voltage during the write operation, the storage surface will be above the cathode potential by an amount equal to the negative peak modulation. The tube is now switched to "read" and the output current from the collector electrode is displayed on an oscilloscope which is scanned in synchronism with the reading beam. The oscilloscope trace will display the storage screen transmission-characteristic curve and the calibration will be known if the peak modulation voltages during write are known. In order to establish a zero base line in the oscilloscope display, the writing beam was modulated to cut off at a frequency of several thousand cycles per second. Fig. 14 shows a photograph of a storage screen transmission-characteristic curve measured in this way.

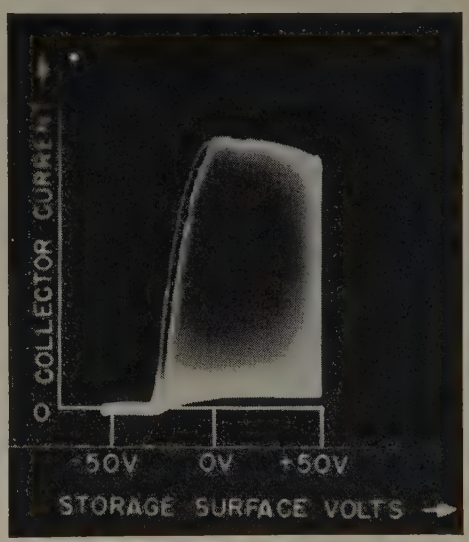

Fig. 14—Storage screen transmission characteristic displayed on oscilloscope.

The above-described method can be used for measuring the critical potential of the storage material by allowing the modulation voltage during write to exceed the critical voltage at some point. This will produce a discontinuity in the storage surface charge trace since those points on the trace corresponding to voltages greater than critical voltage will charge positive, whereas those below critical voltage will write negative as described above. When the oscilloscope display is now observed during the reading operation, the location of the discontinuity on the voltage scale can be measured and the modulation voltage corresponding to this point during writing can be determined.

Distributed Amplifiers: Practical Considerations and Experimental Results*

WILLIAM H. HORTON†, ASSOCIATE, IRE, JOHN H. JASBERG†, ASSOCIATE, IRE, AND JERRE D. NOE‡, MEMBER, IRE

Summary—**The principle of distributed amplification has recently been proposed as a means for obtaining amplification with conventional vacuum tubes over very great bandwidths. Unlike conventional circuits, distributed amplifiers have an attainable gain-bandwidth product which is not limited by shunt capacitance associated with the vacuum tubes and circuit wiring.**

This paper cites experimental results which essentially corroborate the predictions based on first-order theory. It is pointed out that when extreme bandwidths are sought, these predicted characteristics are modified by several factors which are difficult to control in actual practice. Corrective methods are available, however, which permit a limited control over these modifying effects. These methods are discussed and their applications are illustrated by measurements on actual amplifiers with pass-bands on the order of 200 to 300 Mc.

I. Introduction

A RECENT ADDITION to the field of wide-band amplification has been the development of the principles of distributed amplification.[1] The present paper has grown out of the experience of several people who have built and studied various types of distributed amplifiers. It is concerned primarily with the amplitude characteristics of the basic circuits as predicted from the original work, the factors which modify the predicted characteristics, and corrective methods which may be used to eliminate or counteract these modifying effects.

It will be assumed that the reader is familiar with the principles of distributed amplification as outlined in the above reference. The same notation will be employed in this present paper.

It was originally predicted that the effects of reflections from the transmission-line terminations could be controlled without too much difficulty, by using standard m-derived terminating sections. This has been borne out in practice and hence the effects of reflections are not discussed in the present paper.

II. Modifying Effects

The primary analyses were based upon idealized circuits. The derived relationships must, of course, be tempered by considerations of modifying factors which are difficult to control in a physical amplifier. The principal sources of deviation from the idealized case may be enumerated as follows: (1) attenuation due to coil losses; (2) attenuation due to grid losses; (3) grid and plate lead inductance; (4) capacitance distributed throughout the transmission-line coil windings.

The attenuation due to resistive losses in a transmission line is given approximately by

$$a \cong \frac{1}{\omega_c}\left[\frac{G}{2C}+\frac{R}{2L}\right]\frac{\partial\phi}{\partial x_k} \text{ nepers per section} \qquad (1)$$

where

G = conductance shunting C

R = resistance in series with L

ϕ = phase function of transmission line.

The effect of coil losses may be predicted directly from this expression. This is not worthy of a great deal of consideration, however, since grid losses are much more important in a high-frequency amplifier.

The effect of grid losses may be predicted through evaluation of the factor G in (1). This shunt conductance expresses the sum of the effects of transit time and of cathode-lead inductance combined with cathode-to-grid capacitance. If it is assumed that there is no capacitance in parallel with the inductance in the cathode lead, the input conductance becomes approximately

$$G \cong \omega^2 G_m(L_c C_g + KT^2) \text{ mhos} \qquad (2)$$

where

L_c = cathode-lead inductance

C_g = grid-cathode capacity

T = transit time

K = a constant depending on tube.

If there is appreciable cathode-to-screen and cathode-to-filament capacity shunting the cathode-lead inductance, (2) will be modified to give the following expression, which is given without proof:

$$G \cong \omega^2 G_m\left[\frac{L_c C_g}{1-p^2 x_k^2}+KT^2\right] \text{ mhos} \qquad (3)$$

where

$$p = \frac{\text{cutoff frequency}}{\text{cathode antiresonant frequency}}.$$

As stated above, grid loading is ordinarily the only source of attenuation worthy of consideration. On this assumption, the gain of an n-section distributed amplifier with losses may be obtained from the expression for the lossless case by means of the following expression:

$$A = A_0 e^{-n\alpha/2}\frac{\sinh\left(\frac{n\alpha}{2}\right)}{\sinh\left(\frac{\alpha}{2}\right)}. \qquad (4)$$

* Decimal classification: R363.4. Original manuscript received by the Institute, May 16, 1949; revised manuscript received, February 20, 1950. The work described herein was performed under a program sponsored jointly by the Hewlett-Packard Company, Palo Alto, Calif., and by the Microwave Laboratory, Stanford University, Stanford, Calif.

† Microwave Laboratory, Stanford University, Stanford, Calif.

‡ Stanford Research Institute, Palo Alto, Calif.

[1] E. L. Ginzton, W. R. Hewlett, J. H. Jasberg, and J. D. Noe, "Distributed amplification," PROC. I.R.E., vol. 36, pp. 956–969; August, 1948.

A_0 is the gain of the lossless circuit, and the frequency dependence of A_0 and α is a function of the circuit type being considered. In the derivation of (4), it is assumed that the input half section offers the same attenuation as the transmission line half section.

As an illustration, consider the effect of grid loading on the amplitude response of a distributed amplifier employing constant-K transmission lines. If the input conductance is assumed to have the frequency variation in (2), the attenuation factor becomes

$$\alpha = \frac{G_0\omega^2}{\omega_c C}\frac{1}{\sqrt{1-x_k^2}} = \alpha_0\frac{x_k^2}{\sqrt{1-x_k^2}}. \qquad (5)$$

Using this in conjunction with (4), normalized curves of gain for various values of $n\alpha_0/2$ may be plotted as a function of frequency. These curves are shown in Fig. 1.

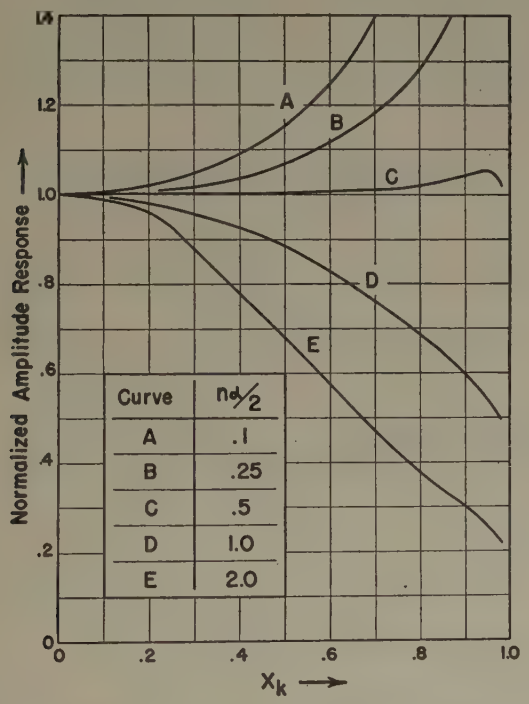

Fig. 1—Amplitude response of constant-K amplifier as a function of $n\alpha_0/2$.

The modifications caused by the presence of shunting capacitance in the cathode circuit can be shown by a similar family of curves. If it is assumed that the transit-time effects are small compared to the effect of the impedance in the cathode circuit, the attenuation factor may be written

$$\alpha = \alpha_0'\frac{x_k^2}{1-p^2x_k^2}\frac{1}{\sqrt{1-x_k^2}} \qquad (5a)$$

where α_0' is distinguished from α_0 since transit-time losses are not included in this equation. Using this relation, (4) may again be used to plot normalized gain curves. The resultant curves are shown in Figs. 2, 3, and 4, as a function of the parameters p and $n\alpha/2$. In Fig. 5 is shown the measured amplitude response curves of constant-K circuits[2] having 16 and 8 identical sections. These correspond to $n\alpha_0/2=1$ (curve A) and $n\alpha_0/2=0.5$ (curve B) where $p=0.5$.

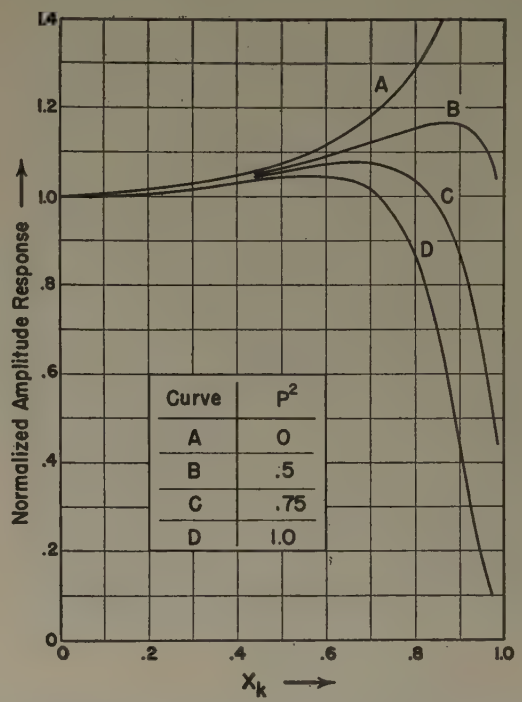

Fig. 2—Amplitude response of constant-K network as modified by antiresonant circuit in each cathode circuit. $n\alpha_0'/2=0.25$.

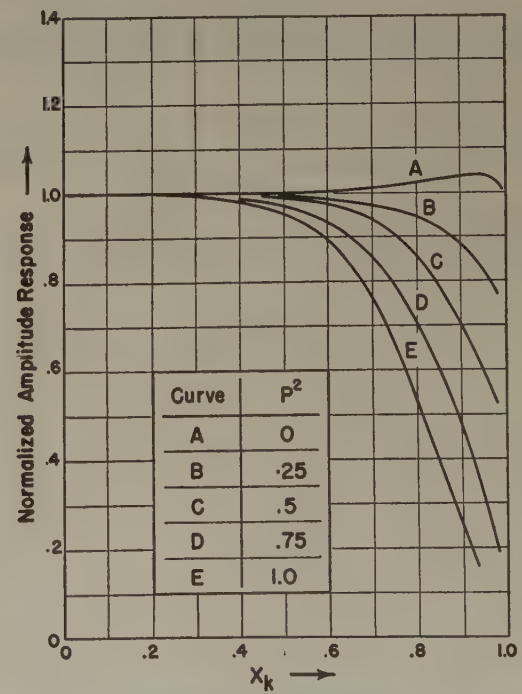

Fig. 3—Amplitude response of constant-K network as modified by antiresonant circuit in each cathode circuit. $n\alpha_0'/2=0.5$.

As another example of the effect of grid losses on the predicted response of a distributed amplifier, consider

[2] This amplifier employed sixteen 954's with no additional capacitive loading. The design cutoff frequency was 340 Mc. The nominal gain was 2.7.

the negative mutual circuit. If the effect of cathode-to-ground capacity is neglected, the attenuation due to cathode-lead inductance and transit time becomes

$$\alpha = \alpha_0 \frac{x_k^2 m^3}{[m^2 - (1 - m^2)x_k^2]\sqrt{m^2 - x_k^2}}. \qquad (6)$$

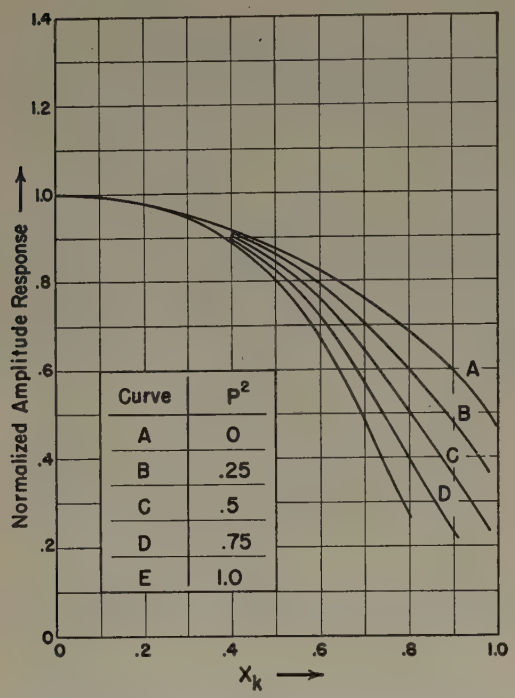

Fig. 4—Amplitude response of constant-K network as modified by antiresonant circuit in each cathode circuit. $n\alpha_0'/2 = 1$.

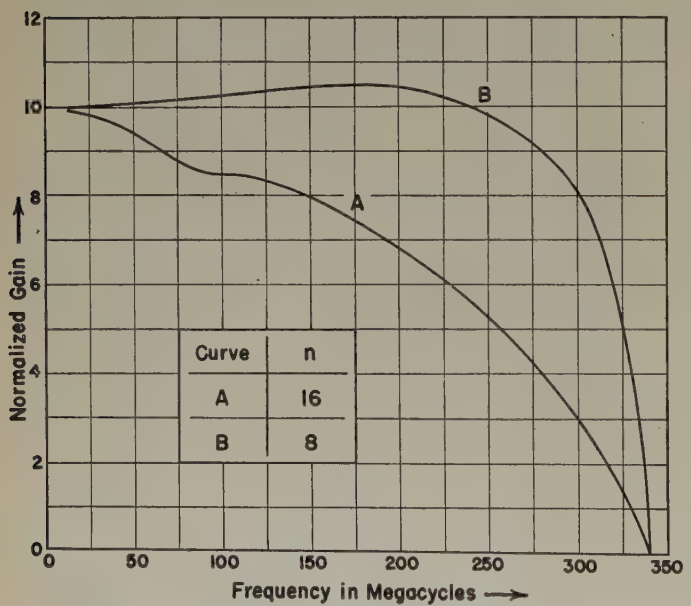

Fig. 5—Measured amplitude response constant-K circuit for $n\alpha_0/2 = 0.5$ and $n\alpha_0/2 = 1$ and for $p = 0.5$.

The curves plotted in Figs. 6, 7, and 8 show the amplitude response of a negative-mutual circuit for various values of m and $n\alpha_0/2$. These curves are again calculated from (4), using (6) as the value of α.

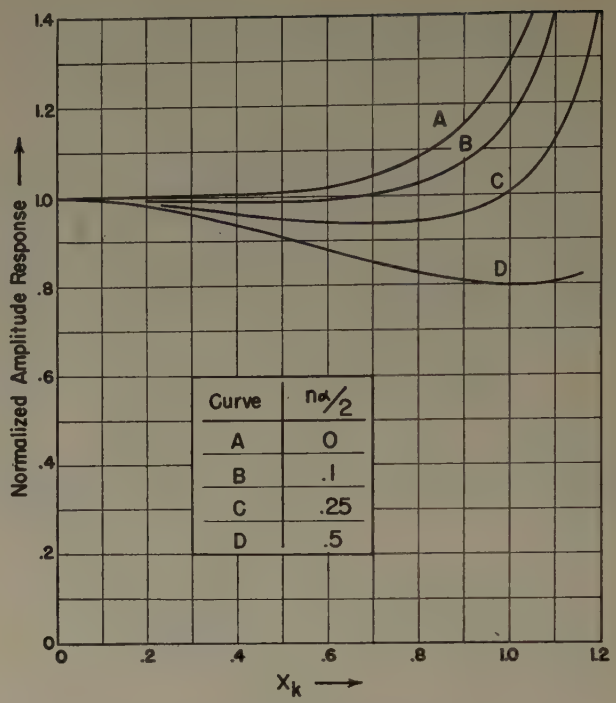

Fig. 6—Amplitude response of negative-mutual circuit as function of $n\alpha_0'/2$, $m = 1.225$.

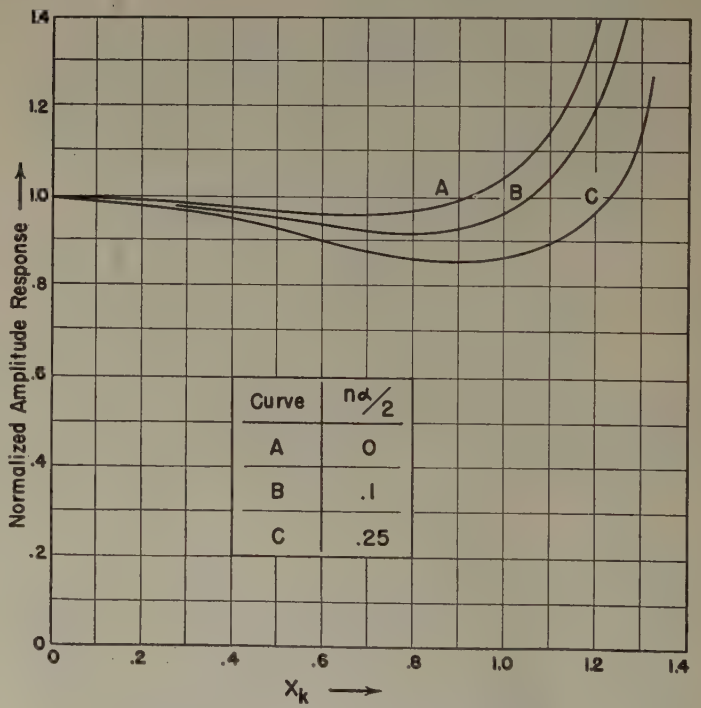

Fig. 7—Amplitude response of negative-mutual circuit as a function of $n\alpha_0'/2$, $m = 1.34$.

The effects of inductance in grid and plate leads can be evaluated in each of the circuit types under consideration. In the case of the constant-K structure, lead inductance causes the circuit to take on the configuration of a series-derived section with consequent lowering of cutoff frequency and nominal impedance.

The effect of grid and plate lead inductance on the bridged-T and negative-mutual circuits can be predicted

in a straightforward manner. In both circuits, the mutual inductance between coil halves results in placing an effective negative inductance in the center-tap lead which goes to plate, or grid, as the case may be.

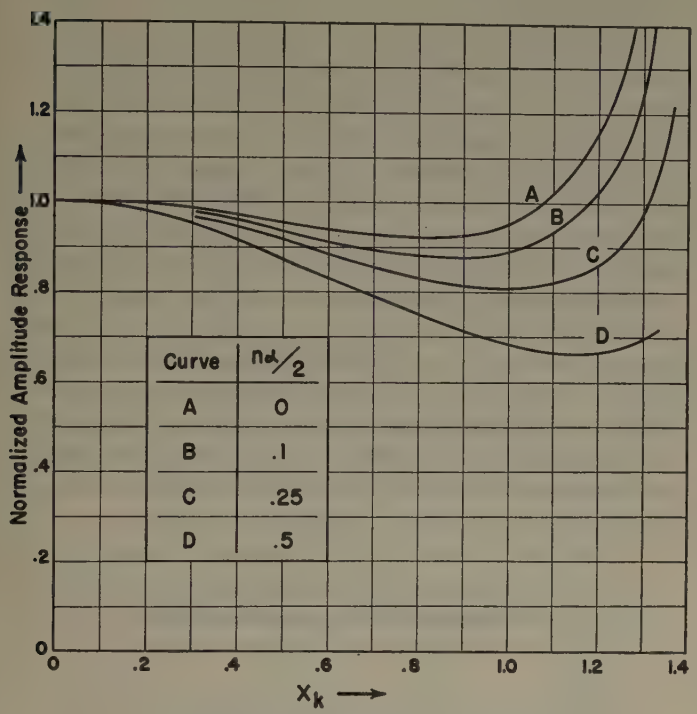

Fig. 8—Amplitude response of negative-mutual circuit as a function of $n\alpha_0'/2$, $m=1.4$.

Any positive inductance in this lead will annul an equivalent amount of negative inductance. The net result, then, is to decrease the effective coupling coefficient and to decrease the parameter m. As indicated in the previous paper, the design equations can be modified to take account of this factor.

The presence of distributed capacitance results in lowering the amplifier cutoff frequency and in altering the impedance of the transmission lines, thus making it difficult to terminate properly. The constant-K and paired-plate circuits with distributed capacitance are subject to an approximate analysis. If the distributed capacity in each coil can be considered as equivalent to a lumped capacity connecting the ends of the coil, the transmission-line sections take on the configuration of shunt-derived sections in an m-derived structure and the circuit may be analyzed as such.

The negative-mutual circuit does not yield readily to analysis when distributed capacitance is included. It has been found experimentally, however, that the negative-mutual circuit suffers from the effects mentioned above. This was determined from studies of a low-frequency model of the circuit in which the ratio of coil self-resonant frequency to amplifier cutoff frequency could be easily controlled. The transmission lines in this amplifier were terminated directly in R_0, with no intervening m-derived sections. The results are illustrated in Fig. 9. If the ratio of coil self-resonance frequency to amplifier cutoff frequency is greater than five or six, the response is quite close to what one would expect from the normal circuit with no m-derived terminations. As the coil self-resonant frequency approaches the amplifier cutoff frequency, the resistive termination becomes better, although marked attenuation appears at the high end of the pass band and the effective cutoff frequency becomes lower.

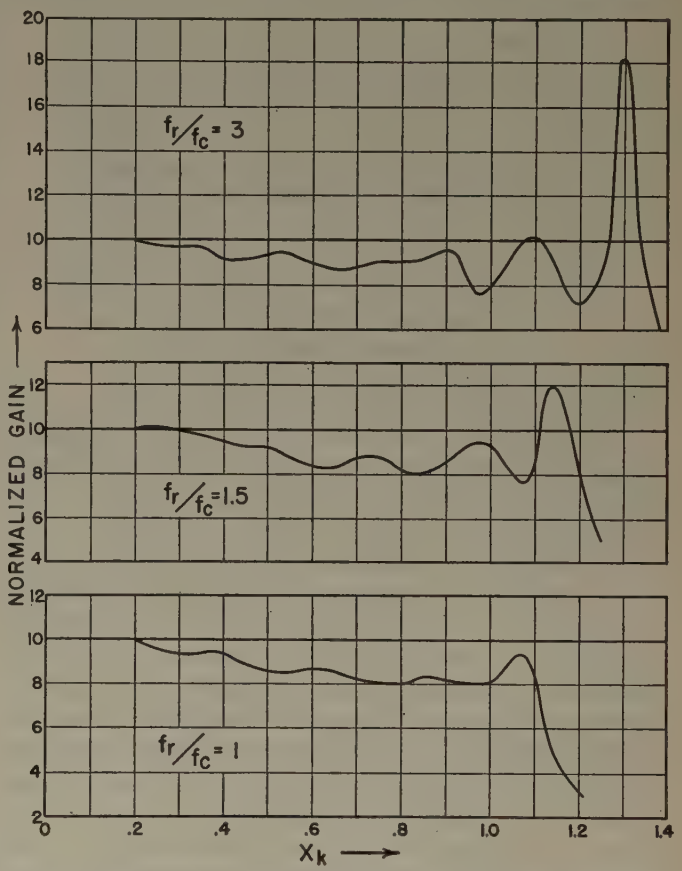

Fig. 9—Measured amplitude response of low-frequency model of negative-mutual circuit, showing effect of distributed capacitance in coils.

III. Corrective Methods

The discussion thus far has dealt with factors which modify the characteristics of distributed amplifiers. In each case the over-all effect has been to limit the frequency range over which distributed amplifiers may be made useful. Let us now consider various means for counteracting this effect to a limited extent.

Consider first the attenuation due to grid loading. In the case of the paired-plate circuit, which for zero losses has an absolutely uniform amplitude response up to the cutoff frequency, grid loading may cause a decided drop in gain in the upper portion of the band pass. Since the paired-plate circuit was developed to eliminate the sharp rise in gain near cutoff which is characteristic of the amplifier employing the constant-K connection, it seems probable that one could "unpair" a few of the plate connections in a paired-plate circuit and use the

resultant rising gain characteristic to counteract the attenuation due to grid loading. This approach is feasible and has been used in practice. Fig. 10 shows the over-all response of two cascaded 200-Mc amplifiers. Each amplifier consisted of seven sections, with four sections connected as a normal paired-plate circuit and three sections with the vacuum-tube plates tied to separate junctions.[3]

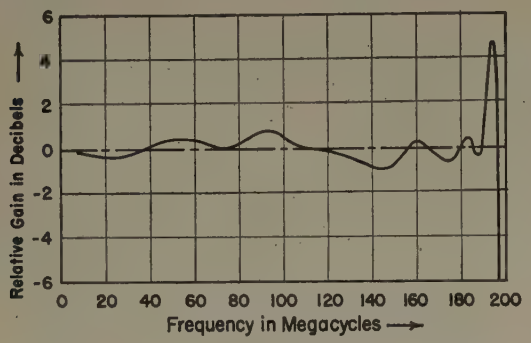

Fig. 10—Gain of two cascaded paired-plate stages.

In making use of the above method, one could build paired-plate amplifiers with higher and higher cutoff frequencies, in each case leaving more of the sections "unpaired" to counteract the increasing effects of grid losses. Finally, the paired-plate circuit would consist of an amplifier in which all plates were tied to separate junctions and the rise in gain due to the constant-K configuration would be completely counteracted by attenuation. Attempts to build an amplifier with an even higher cutoff frequency (using the same tubes, of course) would result in a drooping amplitude characteristic as the effects of attenuation increased. This leads to the concept of a gain-bandwidth product which is developed in the Appendix. There it is shown that if one chooses a given shape of the amplitude response curve and demands a certain gain, the cutoff frequency is automatically specified. If the designer seeks a flat amplitude response, he must choose a value of $n\alpha_0/2$ near 0.5, giving a response curve approximated by curve C of Fig. 1. If he chooses a nominal gain of e (the Naperian base, approximately 2.72) the cutoff frequency for which the circuits must be designed is given by

$$f_c = 0.607(f)\sqrt{\frac{G_m}{G}} \qquad (7)$$

where G is the tube input conductance at a given frequency f.

In the case of the negative-mutual circuit it would be of less significance to seek a similar gain-bandwidth factor based on grid losses. The primary purpose of the introduction of negative mutual inductance is to give a more linear phase shift throughout the pass band. It would be more to the point, then, to choose the circuit parameters on the basis of the desired phase characteristics and to examine the effect of grid losses on the resulting amplitude response, making the assumption that the attenuation has only a second-order effect on the time delay.

The foregoing discussions have dealt with a method of *counteracting* the effects of grid loading. Another way of achieving the same end would be to eliminate or decrease the grid loading itself. This can be done over a limited frequency range by using a small inductance placed in the screen lead of each vacuum tube. The combined effect of the control grid-to-screen grid capacitance and the screen lead inductance is equivalent to placing a negative resistance across the vacuum-tube input terminals. This may be proportioned to cancel the positive loading of the grid circuit. This system may be used up to frequencies where the capacitance from screen grid to ground begins to resonate with the total inductance in the screen lead. In Fig. 11 is shown the response curve of a bridged-T amplifier with and without this type of compensation.

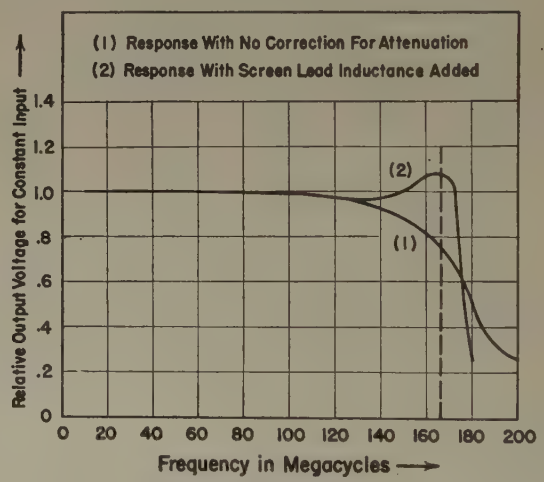

Fig. 11—Amplitude response of bridged-T circuit, showing effect of screen lead inductance.

The difficulties arising from distributed capacitance in the transmission-line coils may be overcome to a certain extent by using coils of small diameter.[4] This can be done even in the case of the negative-mutual circuit, where the greatest number of design parameters must be considered. In the design of a negative-mutual circuit, choice of cutoff frequency and nominal line impedance, in combination with the shunt capacitance imposed by the tube type, determines the value of total inductance of each coil. Choice of a coil self-resonant frequency several times higher than cutoff frequency then determines the coil diameter. The design value of the factor m, combined with the lead inductance which must be cancelled, fixes the coupling coefficient between coil halves and, hence, the ratio of length to diameter. The number of turns must then be chosen to give the

[3] This amplifier employed 6AK5's with the tube input capacity and output capacity each loaded to a value of 10 micromicrofarads. The over-all gain was 18 db. The ±1 db variation in gain may be due to misalignment. Reflections from the terminations probably contribute to the peak near cutoff.

[4] A. J. Palermo, "Distributed capacity of single-layer coils," PROC. I.R.E., vol. 22, pp. 897–905; July, 1934.

correct total inductance. All factors are thus fixed. If the resultant physical size of the coil is such that it can be built, and if the coil Q is satisfactorily high, then the design is practical. If the resultant coil is unsatisfactory in either of these respects, one must compromise by redesigning the coil on the basis of a lower value of the ratio of coil self-resonant frequency to amplifier cutoff frequency.

IV. Conclusions

The predictions on the performance of distributed amplifiers which were made in the previous paper were based upon certain assumptions pertaining to losses and extraneous effects due to lead inductance and distributed capacitance. Over the range for which these assumptions are valid, the predictions have been found to be correct. In the region where these assumptions are no longer valid, considerable progress has been made in determining the modification of characteristics which occur. These modifications are important because they determine the maximum bandwidth over which a distributed amplifier may be made useful. Some progress has been made in extending the useful range beyond the limits normally imposed. It has been found that it is possible, even with vacuum tubes not specifically designed for the purpose, to build distributed amplifiers with bandwidths greater than those attainable with more conventional circuits.

Where only amplitude response is of importance, the paired-plate circuit will find the greatest application. It is relatively easy to construct and it offers a simple method for correcting the effects of attenuation.

The negative-mutual circuit offers the advantage of a nearly linear phase characteristic. The initial design of this circuit is more complex, and it is more susceptible to difficulties arising from distributed capacitance in the coils. When a linear phase shift is important however, these added complexities are justified.

The bridged-T circuit suffers from the disadvantage of having twice the number of tuned circuits which require aligning. This is offset, however, by the ease with which the bridged-T transmission lines may be terminated, i.e., by a resistor, with no intervening matching sections. Reasonably uniform amplitude response and delay time may be obtained by use of this circuit.

Acknowledgment

The authors wish to express their appreciation to W. R. Hewlett, of Hewlett-Packard Company, Palo Alto, Calif., and to E. L. Ginzton, Director of the Microwave Laboratory, Stanford University. Their discernment resulted in the development of the principles of distributed amplification. Their continued interest has made this present study possible.

Appendix

The gain of a distributed amplifier stage using constant-K lines and with a half section on the input is, normalized to unity,

$$A = \frac{1}{n}\frac{e^{-\alpha/2}}{\sqrt{1-x_k^2}}\left[\frac{1-e^{-n\alpha}}{1-e^{-\alpha}}\right] = \frac{1}{n}\frac{e^{-n\alpha/2}}{\sqrt{1-x_k^2}}\frac{\sinh n\alpha/2}{\sinh \alpha/2} \tag{8}$$

where

$$\alpha = \frac{G}{2\omega_c C}\frac{d\phi}{dx_k} \text{ nepers per section}$$

G = total shunt conductance at grid of tube
C = shunt capacity of constant-K line
$\omega_c = 2\pi f_c$
ϕ = phase shift per section
x_k = normalized frequency parameter
n = number of sections per stage.

Using the following expression for α:

$$\alpha = \frac{G}{2\omega_c C}\frac{d\phi}{dx_k} = \frac{G}{\omega_c C}\frac{1}{\sqrt{1-x_k^2}} \tag{9}$$

and assuming that $G = G_0\omega^2$, where G_0 is a constant depending upon the tube used

$$\frac{n\alpha}{2} = n\frac{G_0\omega_c}{2c}\frac{x_k^2}{\sqrt{1-x_k^2}} = \frac{n\alpha_0}{2}\frac{x_k^2}{\sqrt{1-x_k^2}}. \tag{10}$$

Considering the relation

$$A_0 = \sqrt{\frac{L}{C}}\frac{nG_m}{2},$$

where A_0 is the value of stage gain at low frequencies, the factor $n\alpha/2$ may be written

$$\frac{n\alpha_0}{2} = \frac{nG_0\omega_c}{2C} = \frac{A_0}{2}\frac{G_0}{G_m}\omega_c^2. \tag{11}$$

Since the choice of $n\alpha_0/2$ determines the shape of the amplitude response, one may say that for a given response and a given tube type (which fixes G_0/G_m) the product $A_0\omega_c^2$ is fixed. So this leads essentially to a gain-bandwidth factor dependent upon grid losses. If amplitude response variation, nominal gain, and a tube type are determined, cutoff frequency is given by

$$f_c = \frac{1}{2\pi}\sqrt{\frac{n\alpha_0}{A_0}}\sqrt{\frac{G_m}{G_0}} \tag{12}$$

and L and C must be chosen to give this cutoff frequency if the desired gain curve is to be realized. If nearly uniform gain versus frequency is desired, $n\alpha_0/2$ is nearly equal to 0.5. Hence

$$f_c = \frac{1}{2\pi}\sqrt{\frac{G_m}{AG_0}} = .607f\sqrt{\frac{G_m}{G}}, \quad \text{for} \quad A = 2.72 \tag{13}$$

where f = frequency at which the tube input conductance is equal to G.

The Design of Wide-Band Phase Splitting Networks*

W. SARAGA†, SENIOR MEMBER, IRE

Summary—**A number of articles and patents dealing with the properties and design of phase splitting networks, particularly in conjunction with single sideband modulators, have been published in the last few years. However, all of them have been restricted either to particular methods of design or to a particular number of design parameters. The present paper gives the results of a general investigation of phase splitting networks, dealing separately with network analysis, network synthesis and performance curve approximation problems. For the most important types of curve approximation, Taylor and Tchebycheff approximations, explicit formulas for any number of design parameters and for any required closeness of approximation are stated. Alternatives to the classical all-pass lattice network are given, and dissipation compensated phase shift networks are developed. In this way, clear and comparatively simple design instructions for simple as well as for difficult specifications for phase splitting networks are obtained. Furthermore, it is believed that some of the theoretical results obtained and methods developed, e.g., the Taylor and Tchebycheff approximations, the method of obtaining dissipation compensation, one of the methods of network synthesis, and the representation of approximating curves as iterated functions of two variables, with fractional index of iteration, are novel and of general theoretical interest.**

I. Introduction

THE DESIGN of phase splitting circuits to produce constant phase differences over wide frequency bands has frequently been discussed during the last decade. Such circuits have chiefly been used for single sideband modulators for carrier telephony, for polyphase radio systems, for frequency-shift keying, and for wide-band circular time bases for cathode-ray oscillographs.

It is interesting to note that in three early references to phase splitting of a signal band no wide-band network for direct phase splitting is provided, but an auxiliary two-phase single frequency carrier supply with suitable modulator and demodulator stages is used instead,[1] (Wirkler,[2] Vilbig[3]). Hartley,[4] as early as 1925, described a wide-band phase splitting network consisting of two filters with different cutoff frequencies and different numbers of sections. Very simple wide-band phase splitting circuits which do not provide a constant amplitude output have been described by Honnell[5] and Lenehan.[6] Wide-band phase splitting circuits consisting of two phase shifting networks with constant output amplitudes have been described by Byrne,[7] Loyet,[8] Hodgson,[9] Dome,[10] Norgaard,[11] and Luck.[12]

Byrne and Loyet give the theoretical and measured performance of various phase splitting circuits, but they do not give any design information. Hodgson, on the other hand, discusses design methods in detail. His main recommendation is to design each phase shift network separately so that its phase shift β over the frequency band in question varies linearly with the logarithm of the frequency, say $\beta = A + A_0 \log f$ where A and A_0 are constants. If A_0 is made the same for both networks but A is different for each network, say A_1 and A_2, then the difference of the two phase shifts β_1 and β_2 is $\beta_1 - \beta_2 = A_1 - A_2$, i.e., a constant, as required. Dome follows the same general idea, but whereas Hodgson's discussion is chiefly in terms of lattice and bridged-T phase shift networks, Dome describes a number of interesting alternatives to the classical lattice network. In Hodgson's patent the individual performances of the two phase shift networks are specified separately; Luck discusses the design and performance of a phase splitting circuit as a whole. This constitutes an important step forward. However Luck considers networks with four design parameters only.

It is the purpose of this paper to investigate phase splitting networks with any number of design parameters, for any desired bandwidth and for any desired closeness to the desired ideal performance.[13] This will be done in the following order: (1) network analysis, (2) performance curve approximation, (3) network synthesis. It will be found that it is comparatively easy to obtain results of general validity and applicability. In many respects the problems to be solved are similar to or identical with those encountered in the development of a comprehensive method and theory of filter design. However, in the case of phase splitting circuits consisting of constant resistance phase shift circuits the solution of these problems is easier than in the case of filter design, because complications due to mismatching do not arise. Furthermore, it so happens that in the theory

* Decimal classification: R246.2×R143. Original manuscript received by the Institute, August 1, 1949.

† Research Laboratories, Telephone Manufacturing Co. Ltd., London, England.

[1] British Patent No. 301,362, dated August 27, 1927.

[2] Walter H. Wirkler, U. S. Patent No. 2,173,145, dated November 26, 1937.

[3] F. Vilbig, "Experimentelle Untersuchung der Verschiebung eines theoretisch beliebig grossen Frequenzbandes um einen bestimmten Phasenwinkel," *Telegraphen- Fernsprech- und Funktech.*, vol. 27, pp. 560–561; December, 1938.

[4] Ralph V. L. Hartley, U. S. Patent No. 1,666,206, dated January 15, 1925.

[5] M. A. Honnell, "Single-sideband generator," *Electronics*, vol. 18, pp. 166–168; November, 1945.

[6] B. E. Lenehan, "A new single sideband carrier system," *Elec. Eng.*, vol. 66, pp. 549–552; June, 1947.

[7] John F. Byrne, "Polyphase broadcasting," *Trans. Elec. Eng.*, vol. 58, pp. 347–350; July, 1939.

[8] Paul Loyet, "Experimental polyphase broadcasting," PROC. I.R.E., vol. 30, pp. 213–222; May, 1942.

[9] K. G. Hodgson, British Patent No. 547,601, dated January 31, 1941.

[10] R. B. Dome, "Wide-band phase shift networks," *Electronics*, vol. 19, pp. 112–115; December, 1946.

[11] Donald E. Norgaard, "A new approach to single sideband," *QST*, vol. 32, pp. 36–43; June, 1948.

[12] David G. C. Luck, "Properties of some wide-band phase splitting networks," PROC. I.R.E., vol. 37, pp. 147–151; February, 1949.

[13] Some of the networks obtained as a result of this investigation form the subject of British Patent Application No. 16698/49.

of the transformation of elliptic functions, which is applicable to filter as well as to phase splitting circuit design, the particular transformations applicable to phase splitting circuit design are simpler than those applicable to filter design.

II. The Basic Circuit

Fig. 1 shows schematically a phase splitting circuit consisting of two phase shift networks which are paralleled at their inputs. At this initial stage of our investigation the phase shift networks are assumed to be conventional all-pass constant resistance single lattice section networks with series arm reactances X_1 and X_2 and lattice arm reactances $-R_0^2/X_1$ and $-R_0^2/X_2$, respectively.

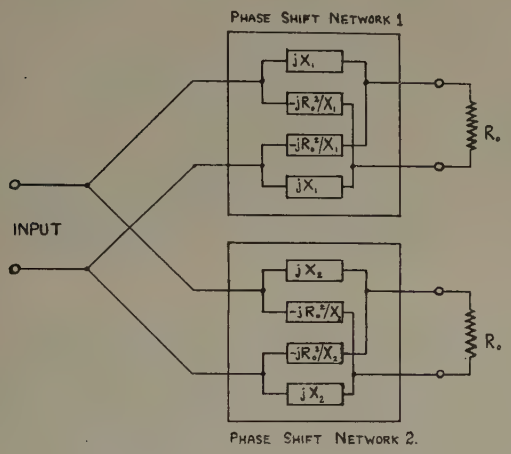

Fig. 1—Basic phase-splitting circuit.

Then the phase shifts β_1 and β_2 produced by the networks separately are given by

$$\tan \tfrac{1}{2}\beta_1 = X_1/R_0 \quad \text{and} \quad \tan \tfrac{1}{2}\beta_2 = X_2/R_0 \tag{1}$$

so that the phase shift difference $\psi = \beta_1 - \beta_2$ is given by

$$y = \tan \tfrac{1}{2}\psi = \tan \tfrac{1}{2}(\beta_1 - \beta_2) = \frac{X_1/R_0 - X_2/R_0}{1 + (X_1/R_0)(X_2/R_0)}. \tag{2}$$

If $\beta_1 - \beta_2 = 90°$, $y = 1$. Thus in an ideal 90° phase splitting circuit, y should be unity, over a specified frequency range, or $|\log y| = 0$.

The significance of deviations of y from unity can only be discussed with reference to a particular application of the phase splitting circuit. It is interesting to consider a single sideband modulator using a phase splitting network. If it is assumed that all amplitude and phase relations are exactly as required (see Fig. 2), with the one exception that y is not exactly unity, it can be shown that the amplitude A_1 of the wanted sideband and the amplitude A_2 of the unwanted sideband, are given by

$$(L_1)_{db} = 20 \log_{10} |A_{10}/A_1| = 20 \log_{10} \sec \tfrac{1}{2}\delta$$
$$= 10 \log_{10} (1 + \tan^2 \tfrac{1}{2}\delta) \tag{3a}$$

$$(L_2)_{db} = 20 \log_{10} |A_{10}/A_2| = 20 \log_{10} \operatorname{cosec} \tfrac{1}{2}\delta$$
$$= 10 \log_{10} (1 + \cot^2 \tfrac{1}{2}\delta) \tag{3b}$$

where δ is the deviation of the phase difference $\beta_1 - \beta_2$ from 90°, i.e.,

$$\delta = \beta_1 - \beta_2 - \frac{\pi}{2} \tag{4}$$

and A_{10} is the value of A_1, for $\delta = 0$. If y is given, we can obtain δ directly from y, by means of

$$\tan \tfrac{1}{2}\delta = \frac{y-1}{y+1} \quad \text{or} \quad \sec^2 \tfrac{1}{2}\delta = \frac{2(y^2+1)}{(y+1)^2} \quad \text{or}$$
$$\operatorname{cosec}^2 \tfrac{1}{2}\delta = \frac{2(y^2+1)}{(y-1)^2}. \tag{5}$$

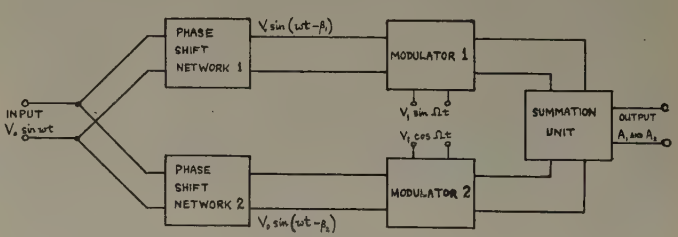

Fig. 2—Single sideband modulator using phase-splitting circuit.

Combining (3a) and (3b) with (5), we can obtain L_1 and L_2 as functions of y. The result has been plotted in Fig. 3. It is important to note that the transformation $y \to (1/y)$ leaves L_1 and L_2 unchanged and transforms δ into $-\delta$.

Equation (2) is very similar to an expression occurring in the evaluation of the insertion loss L of a lattice section filter between a source resistance R_0 and a load resistance R_0, with series arm reactances X_A and lattice arm reactances X_B. We find

$$L_{db} = 10 \log_{10} (1 + E^2) \tag{6a}$$

$$E = \frac{1 + (X_A/R_0)(X_B/R_0)}{(X_A/R_0) - (X_B/R_0)}. \tag{6b}$$

It is seen by comparing (6b) and (2) that $1/E$ and y are formed in the same way from reactances X_A, X_B and X_1, X_2, respectively. This similarity has important consequences for the analysis and synthesis of phase splitting networks, and will be made use of in subsequent sections.

III. Network Analysis

The object of this section is to find, as a necessary preparation for network design and synthesis, the general characteristics of the function y defined by (2), if y is obtained from physical networks. Since

$$y = \tan \tfrac{1}{2}(\beta_1 - \beta_2) = \frac{\tan \tfrac{1}{2}\beta_1 - \tan \tfrac{1}{2}\beta_2}{1 + \tan \tfrac{1}{2}\beta_1 \tan \tfrac{1}{2}\beta_2}, \qquad (7)$$

we start with a discussion of the characteristics of $\tan \frac{1}{2}\beta_1$ and $\tan \frac{1}{2}\beta_2$. From (1) it follows that $\tan \frac{1}{2}\beta_1$ and $\tan \frac{1}{2}\beta_2$ as functions of the normalized frequency x have to satisfy Foster's reactance theorem; for instance, they have to be odd rational functions of x; all poles and zeros are simple and occur at real frequencies; zeros and poles are alternating; at $x=0$ and $x=\infty$ no other values than 0 or ∞ are permitted. The degrees of denominator and numerator of each expression differ by one.

$y=\tan \frac{1}{2}(\beta_1-\beta_2)$ is a function of a less restricted character. Like $\tan \frac{1}{2}\beta_1$ and $\tan \frac{1}{2}\beta_2$ it is an odd rational function of x which is zero or infinity at zero and infinite frequency. But its zeros and poles need not alternate or occur at real frequencies, and the degree of denominator and numerator can differ widely.

This follows directly from (7) and is, because of (6b), equally valid for y and $1/E$. Dealing now with y only, since it is required that y is approximately equal to unity over a band from, say, $x=\sqrt{k}$ to $x=1/\sqrt{k}$, it is obviously not permissible to have any poles or zeros of y within this band. On the other hand, we have seen that at $x=0$ and $x=\infty$, y will be 0 or ∞, and therefore y will tend to deviate more and more from unity for very large and very small values of x. It seems plausible, therefore, to recommend (see, e.g., Hodgson[9]) that no poles or zeros should occur at real x values except at 0 and ∞, as such poles or zeros would tend to increase the deviation of y from unity; the poles or zeros at 0 and ∞ should be of the first degree. Then the degrees of numerator and denominator must differ by one. We shall see in the next section that Taylor and Tchebycheff approximations lead to expressions which are in agreement with this recommendation.

In what follows we shall assume that at $x=0$ we have $y=0$.[14] Then y will be of the form

$$y = Hx \frac{(x^2 + c_1^2)(x^2 + c_2^2) \cdots (x^2 + c_a^2)}{(x^2 + d_1^2)(x^2 + d_2^2) \cdots (x^2 + d_b^2)} \qquad (8a)$$

where $b-a=0$ or 1, and where the constants c_1^2, $c_2^2 \cdots$ and d_1^2, $d_2^2 \cdots$ and H are real and positive. We shall denote by n the highest degree of x occurring in y, and

[14] This assumption entails no loss of generality as the only other possible choice is $y=\infty$ at $x=0$. However, in this case we would have $1/y=0$ at $x=0$, and then we could apply the results of the following discussion to $1/y$ which approximates unity as closely as y does.

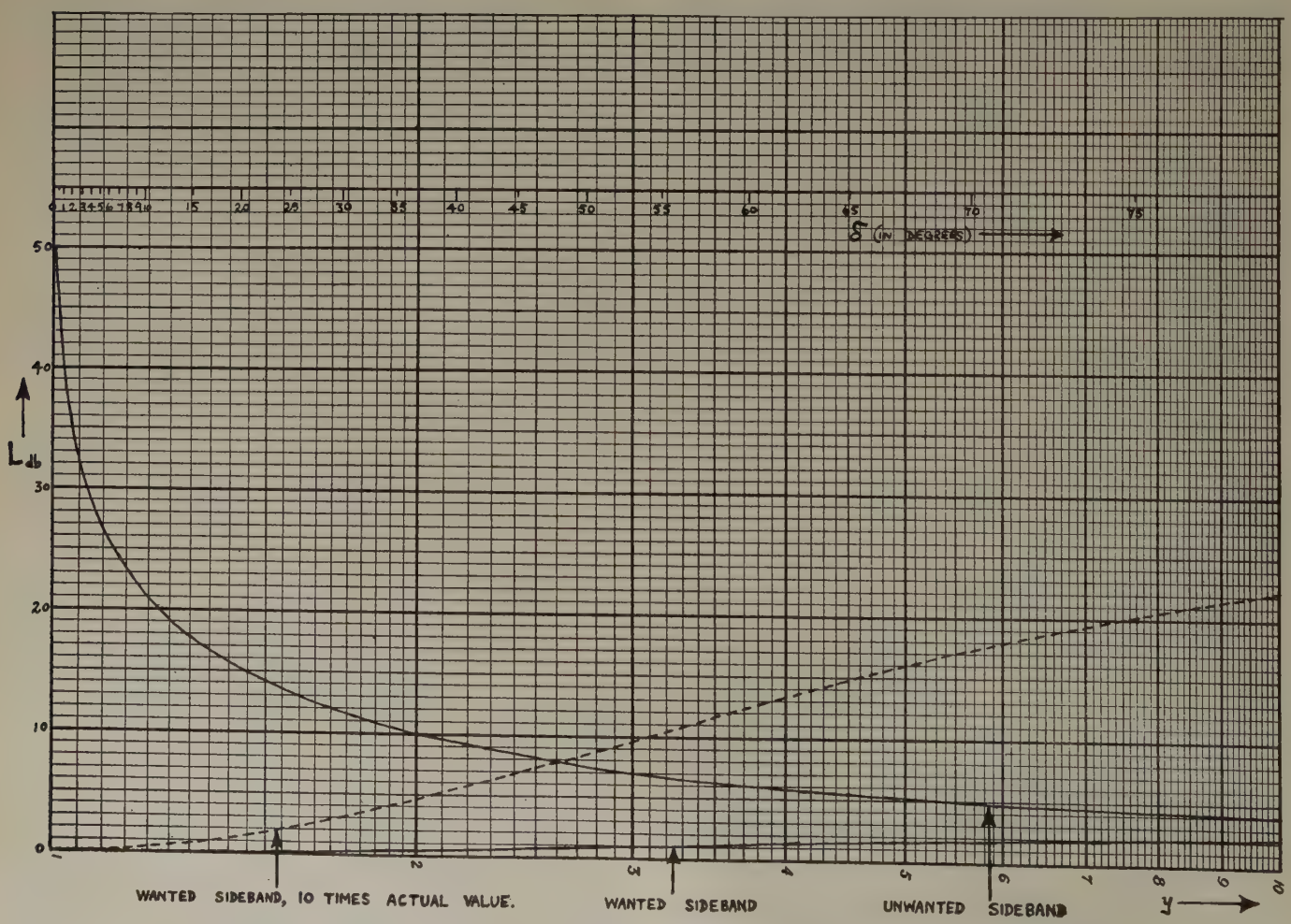

Fig. 3—Output (wanted and unwanted sideband) as function of deviation from 90° phase difference.

we shall see later that the order of approximation can be denoted by the same number n. Equation (8a) can also be written in the form

$$y = x\frac{A_0 + A_2x^2 + \cdots + A_{2a}x^{2a}}{1 + B_2x^2 + \cdots + B_{2b}x^{2b}} \tag{8b}$$

where all A's and B's are real. An important case arises when y as a function of log x is symmetrical about $x=1$, i.e., log $x=0$. Then the transformation $x\rightarrow(1/x)$ leads to $y\rightarrow(1/y)$ if n is odd, but it leaves y unchanged if n is even. Expressions for y_n when y_n is symmetrical are listed below for n-values from 1 to 6.

$$\left.\begin{aligned} &y_1 = x; \quad y_2 = \frac{Hx}{1+x^2}; \quad y_3 = x\frac{a+x^2}{1+ax^2};\\ &y_4 = \frac{Hx(1+x^2)}{(1+ax^2)\left(1+\frac{1}{a}x^2\right)}\\ &y_5 = x\frac{(a+x^2)(b+x^2)}{(1+ax^2)(1+bx^2)};\\ &y_6 = \frac{Hx(1+ax^2)\left(1+\frac{1}{a}x^2\right)}{(1+x^2)(1+bx^2)\left(1+\frac{1}{b}x^2\right)} \end{aligned}\right\}. \tag{8c}$$

IV. Approximation of the Required Performance Curve

In this section we shall discuss methods for finding such values for the constants in the expressions for y ((8a), (8b), or (8c)) that y becomes a good approximation to unity in the range $x=\sqrt{k}$ to $x=1/\sqrt{k}$. If another value for y, say $y=y_0$, is required, y has to be replaced in the discussion that follows by y/y_0. We shall start with Taylor and Tchebycheff approximations, for there it is possible to go beyond a recommendation of methods of approximation to a statement of explicit formulas which give the constants in terms of k, i.e., of the range of x.

1. *Taylor Approximations*

A Taylor approximation of the nth order is characterized by the fact that there are n design parameters which have been so chosen that for a specified value of x, say $x=x_0$, y itself and the first $(n-1)$ differential coefficients d^ry/dx^r for $r=1, 2 \cdots (n-1)$ are the same for the required curve and the approximating curve. Thus the higher n is, the more closely the approximating curve approximates the required one.

If we assume that $x_0=1$, then the Taylor approximation of the nth order is given by

$$y_n = \tanh\,[n \tanh^{-1} x] \tag{9a}$$

By writing (9a) in the form

$$y_n = \frac{(1+x)^n - (1-x)^n}{(1+x)^n + (1-x)^n} \tag{9b}$$

we see that the highest degree of x occurring in y_n is n and that y_n is an odd rational function of x, symmetrical about $x=1$ against a logarithmic frequency scale.

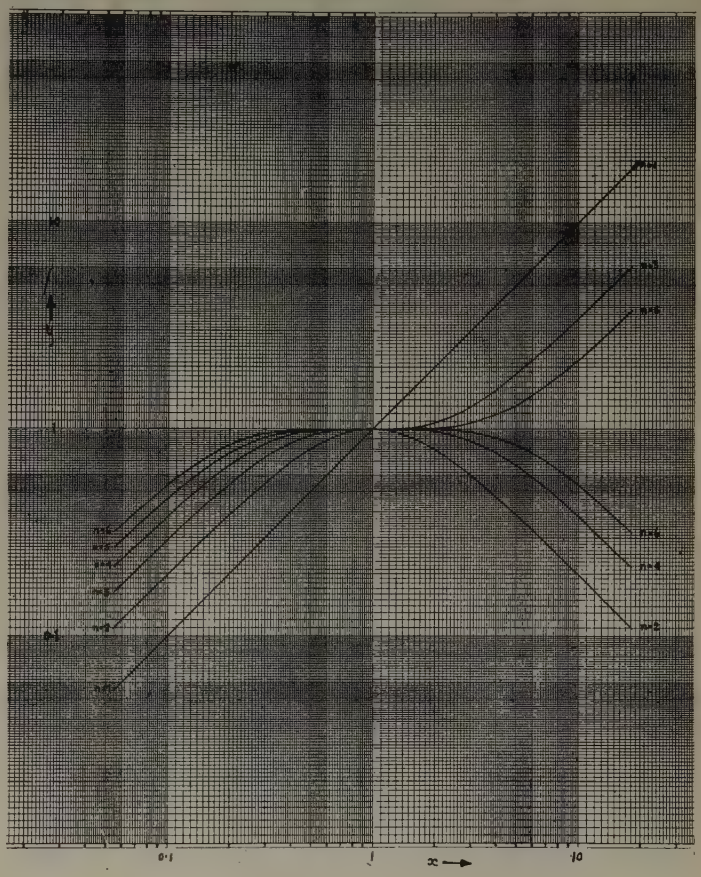

Fig. 4 (a)—Taylor approximations.

By writing it in the form

$$\frac{1-y_n}{1+y_n} = \left(\frac{1-x}{1+x}\right)^n \tag{9c}$$

we can easily prove (putting $y_n=1+\epsilon$ and $x=1+\Delta$) that the first $n-1$ differential coefficients at $x=1$ are zero, as required for a Taylor approximation to $y=1$. It may be convenient to list y_n for $n=1, 2 \cdots 6$.

$$\left.\begin{aligned} &y_1 = x; \quad y_2 = \frac{2x}{1+x^2}; \quad y_3 = \frac{x(3+x^2)}{1+3x^2};\\ &y_4 = \frac{4x(1+x^2)}{1+6x^2+x^4}; \quad y_5 = \frac{x(5+10x^2+x^4)}{1+10x^2+5x^4};\\ &y_6 = \frac{2x(3+10x^2+3x^4)}{1+15x^2+15x^4+x^6} \end{aligned}\right\}. \tag{9d}$$

These curves are plotted in Fig. 4(a) on log-log paper, for an x range from $x=\sqrt{k}=\sqrt{0.003}$ to $x=1/\sqrt{k}$, i.e.,

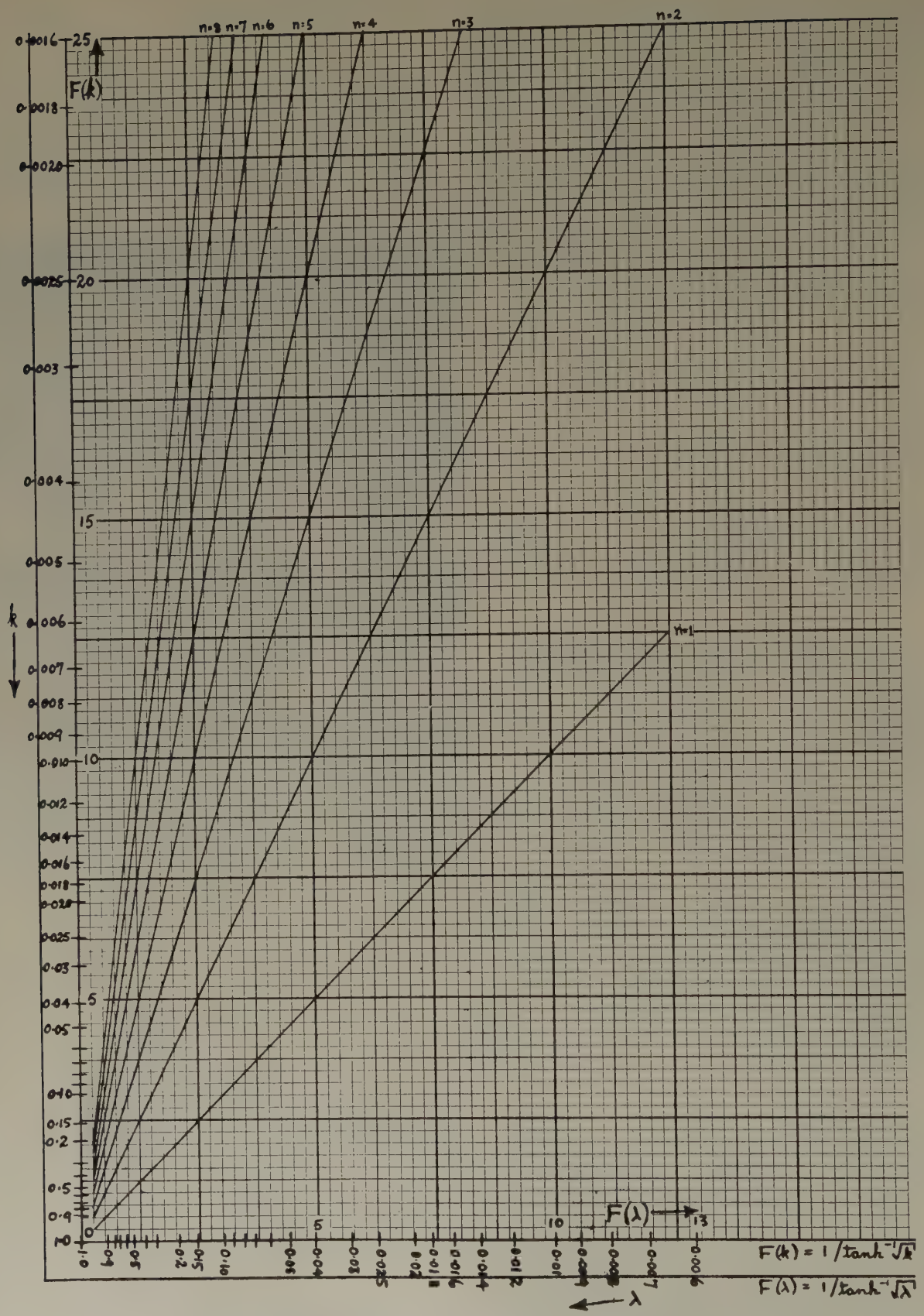

Fig. 4 (b)—Deviation of Taylor approximations from required performance.

for $k=0.003$. This corresponds, for instance, to a frequency range from 30 cps to 10 kc.

It will be see from (9b) that if x is replaced by $1/x$ y_n remains unchanged for even n values, and is replaced

by $1/y_n$ for odd values of n. The deviation of $|\log y_n|$ from 0 increases with $|\log x|$. If the limits of the x range are denoted as $\sqrt{k}$ and $1/\sqrt{k}$ and the limits of the y range as $\sqrt{\lambda}$ and $1/\sqrt{\lambda}$, then λ as a function of k is given by

$$\sqrt{\lambda} = \tanh [n \tanh^{-1} \sqrt{k}], \tag{9e}$$

which, as far as the functional relation is concerned, is similar to (9a). If we write (9e) in the form

$$1/\tanh^{-1} \sqrt{\lambda} = \frac{1}{n} (1/\tanh^{-1} \sqrt{k}) \tag{9f}$$

we see that λ as a function of k can be represented as a straight line with slope $1/n$ through the origin of the co-ordinate system, for any n value, if we use functional scales defined by the $1/\tanh^{-1}\sqrt{\ }$ function for λ and k. This has been done in Fig. 4(b). In view of the functional similarity between (9f) and (9a), Fig. 4(b) also represents y_n as a function of x, in other words, Fig. 4(b) can be looked upon as showing the same curves as Fig. 4(a). It will be seen that if k is given, $|\log \lambda|$ decreases with increasing n, i.e., the range of y becomes smaller.

For synthesizing networks which have the performance described by (9a) we must find—as will be explained in Section V—the values of x at which $y = +j$. They are given by

$$x = j \tan \left[\frac{\pi}{n}\left(\frac{1}{4} + m\right)\right] \tag{9g}$$

where $m = 0, 1, 2, \cdots, (n-1)$.

2. *Tchebycheff Approximations*

A Tchebycheff approximation is characterized by the fact that the maximum deviation occurring is a minimum. The theory of the transformation of elliptic functions very conveniently describes odd rational functions of x, symmetrical against a logarithmic x scale about $x=1$, which over the range $x=\sqrt{k}$ to $x=1/\sqrt{k}$ approximate $y=1$, within the limits $\sqrt{\lambda}$ and $1/\sqrt{\lambda}$, in the Tchebycheff manner. As stated above, such limits for y are equivalent to limits δ_{max} and $\delta_{min} = -\delta_{max}$ for the deviation δ of the phase difference ψ from the required value 90°, and $\tan \frac{1}{2}\delta_{max} = (1-\sqrt{\lambda})/(1+\sqrt{\lambda})$. Using Cayley's[15] symbols, it can easily be shown that the Tchebycheff approximation of the nth order is given by

$$y_n/\sqrt{\lambda} = sn(u/M, \lambda) \tag{10a}$$

$$x/\sqrt{k} = sn(u, k). \tag{10b}$$

The highest degree of x occurring in the rational function defined by (10a) and (10b) is n. Cayley uses the suffix '1' for λ and M to indicate that a "second transformation" from a modulus k to a larger modulus λ is meant. However, in the following discussion it is convenient to use in many cases the suffix n to denote the order of the transformation. Therefore, in order to avoid confusion, Cayley's suffix '1' will not be used. For the purposes of this discussion it is also convenient to denote λ sometimes as k_n. In equations (10a) and (10b) u is an auxiliary variable which is defined by (10b), and y_n is defined in terms of u by (10a). k has been defined above. λ and M can be derived from k as follows: K'/K is a function of k, say $K'/K = F(k)$ known in the theory of elliptic functions (tabulated for instance by Hayashi[16]). Λ'/Λ denotes the same function of λ so that $\Lambda'/\Lambda = F(\lambda)$. λ can be obtained from k by means of the relation

$$\Lambda'/\Lambda = F(\lambda) = \frac{1}{n} K'/K = \frac{1}{n} F(k). \tag{10c}$$

It will be shown that if k is given, $|\log \lambda|$ decreases with increasing n, i.e., the range of y becomes smaller. Furthermore, K can be found as a function of k, and Λ as the same function of λ, in Hayashi's tables. Then M is given by

$$M = K/\Lambda. \tag{10d}$$

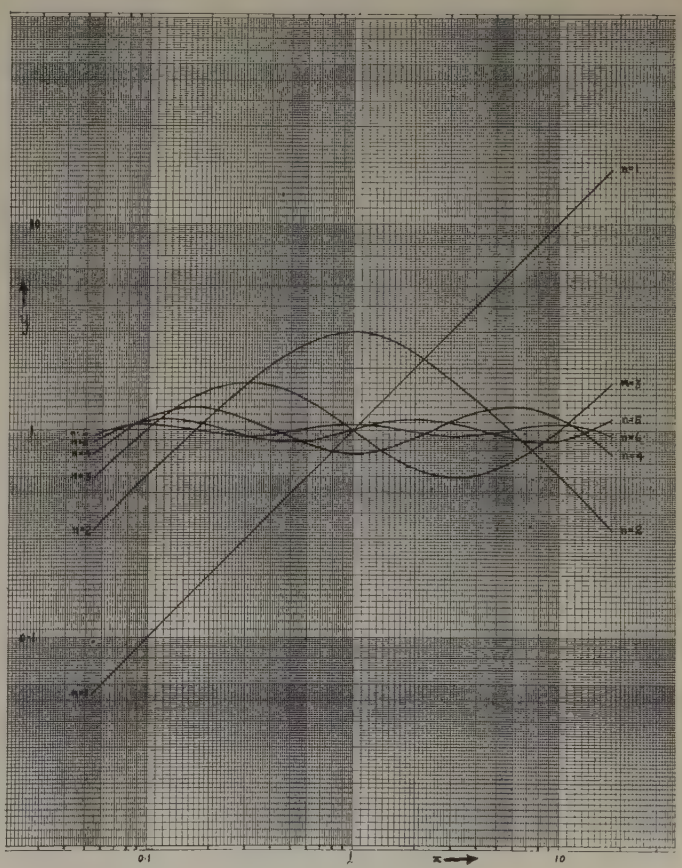

Fig. 5 (a)—Tchebycheff approximations.

[15] A. Cayley, "Elliptic Functions," 2nd ed., George Bell & Sons, London; 1895.

[16] K. Hayashi, "Tafeln der Besselschen, Theta, Kugel- und anderer Funktionen," Berlin; 1930.

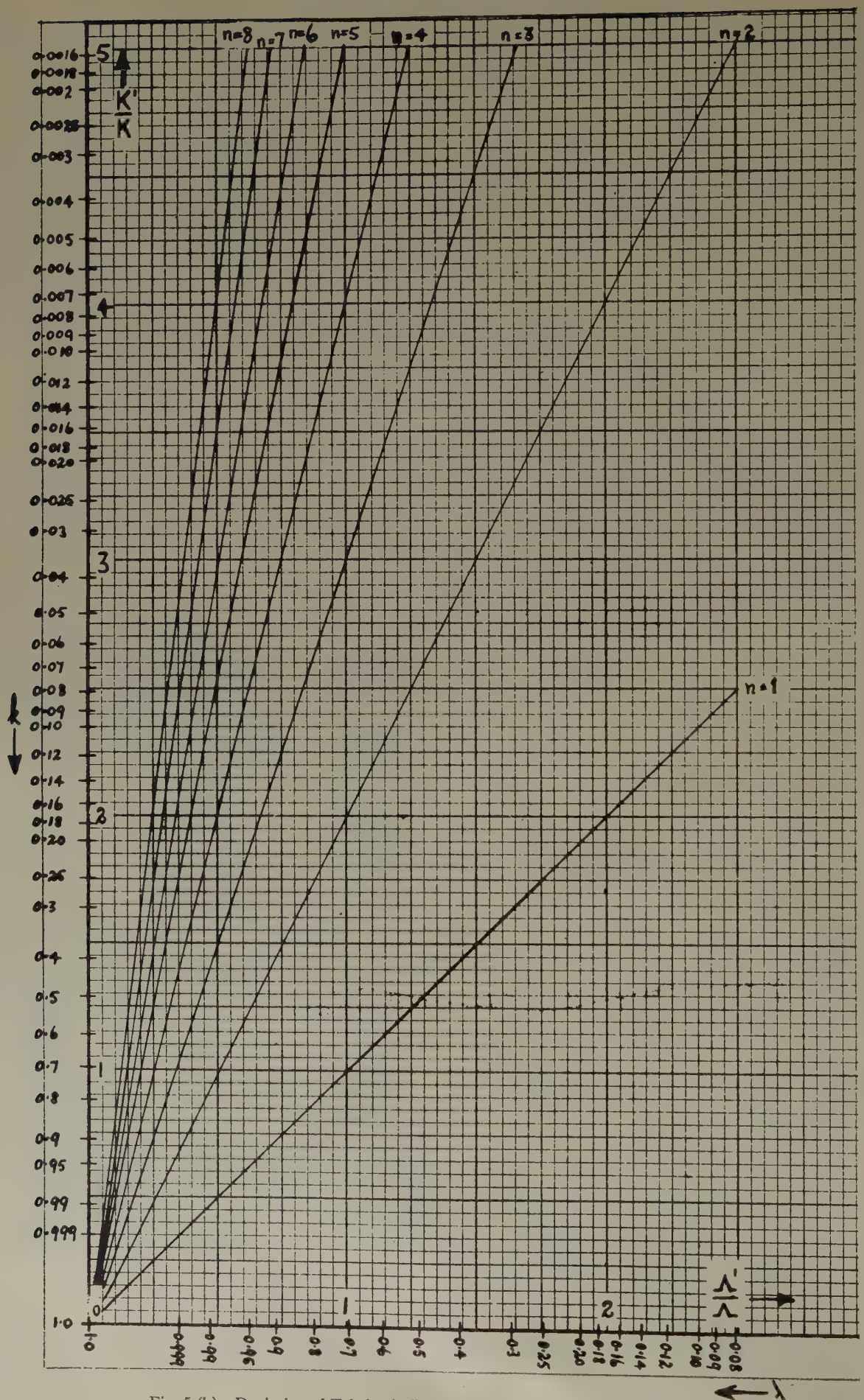

Fig. 5 (b)—Deviation of Tchebycheff approximations from required performance.

TABLE Ia

TCHEBYCHEFF APPROXIMATIONS; y AND u AS FUNCTIONS OF x.

$$\frac{y_n}{\sqrt{\lambda}} = sn\left(\frac{u}{M_n}, \lambda\right) \tag{10a}$$

$$\frac{x}{\sqrt{k}} = sn(u, k) \tag{10b}$$

$$M_n = \frac{K}{\Lambda} = \frac{K'}{n\Lambda'}$$

x as a function of $u = u_1 + ju_2$ is described by the following table and diagram

x	$0 \cdots \sqrt{k}$	$\sqrt{k} \cdots 1$	$1 \cdots 1/\sqrt{k}$	$1/\sqrt{k} \cdots \infty$
u_1	$0 \cdots K$	K	K	$K \cdots 0$
u_2	0	$0 \cdots \frac{1}{2}K'$	$\frac{1}{2}K' \cdots K'$	K'

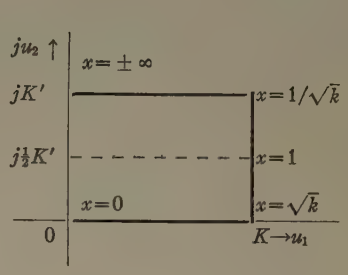

Best form of (10b)

for $x = 0 \cdots \sqrt{k}$ $\quad x/\sqrt{k} = sn(u_1, k), \quad u_2 = 0$

for $x = \sqrt{k} \cdots 1/\sqrt{k}$ $\quad x/\sqrt{k} = 1/dn(u_2, k'), \quad u_1 = K, \quad k' = \sqrt{1 - k^2}$

for $x = 1/\sqrt{k} \cdots \infty$ $\quad x/\sqrt{k} = 1/[k\, sn(u_1, k)], \quad u_2 = K'$

Best form of expression giving y as a function of x if $x = \sqrt{k} \cdots 1/\sqrt{k}$

$$\frac{y}{\sqrt{\lambda}} = \frac{1}{dn\left[\frac{1}{M_n} dn^{-1}\left(\frac{\sqrt{k}}{x}, k'\right), \lambda'\right]}, \qquad \lambda' = \sqrt{1 - \lambda^2}$$

Thus $\lambda = k_n$ can be obtained for any k and n, and, k being specified, n can be so chosen as to make $\log \sqrt{\lambda}$, which denotes the maximum deviation of $|\log y|$ from 0, as small as required. λ as a function of k and n is represented in Fig. 5(b). Since (10c) is of the same form as (9f) it is again possible to draw the λ curves as straight lines with slope $1/n$ if linear scales for K'/K and Λ'/Λ are used. It should be noted that in the case of Tchebycheff approximations the curves relating λ to k (Fig. 5b) do not at the same time relate y_n to x. It will be seen that for any given k- and n-values the values of λ obtained from Fig. 5(b) i.e., for Tchebycheff approximations are much nearer to 1 than those obtained from Fig. 4(b), i.e., for Taylor approximations.

y_n as a function of x can be evaluated directly from (10a) and (10b) by means of tables of elliptic functions, e.g., Milne-Thomson's[17] tables together with Hayashi's tables. For this purpose, equations (10a) and (10b) can be modified as shown in Table I(a). The Tchebycheff approximations for $n = 1, 2 \cdots 6$ for an x-range from $\sqrt{k}$ to $1/\sqrt{k}$ where $k = 0.003$ are shown diagrammatically in Fig. 5(a). For these diagrams the formulas given in Table I(a) have not been used. Only the x values at which maxima or minima of y occur and those at which $y = 1$ have been evaluated numerically, and the curves have been so drawn as to go through these points. However, for $n = 4$ (see Section VI) a numerical check for a great number of points has shown very good agreement with the drawn curve. The curves have an oscillatory behavior, all maxima and minima occur at the y-values $1/\sqrt{\lambda}$ and $\sqrt{\lambda}$ respectively, the value of λ depending on the n value and the k value under consideration. For even n values there are $\frac{1}{2}n$ maxima, $\frac{1}{2}(n-2)$ minima, two intersections with the line $y = \sqrt{\lambda}$ and n intersections with the line $y = 1$. For odd n values there are $\frac{1}{2}(n-1)$ minima and $\frac{1}{2}(n-1)$ maxima, one intersection with the line $y = \sqrt{\lambda}$, one intersection with the line $y = 1/\sqrt{\lambda}$ and n intersections with the line $y = 1$.[18]

In order to be able to plot these characteristic points of y we must know the values of x at which $y_n = \sqrt{\lambda}$, 1 and $1/\sqrt{\lambda}$. On the other hand, in order to be able to write y_n as a rational function of x in the form of equation (8c) we must know the values of x at which $y_n = 0$ and $y_n = \infty$ and the value of H in the case of even n values (see below). Lastly, in order to synthesize a net-

[17] L. M. Milne-Thomson, "Die elliptischen Funktionen von Jacobi," Julius Springer, Berlin; 1931.

[18] It is interesting to note that in the case of filter design a "first transformation" from a modulus k to a smaller modulus λ has to be used. This transformation, though similar in many respects to the one used in our problem, differs from the one defined by equations (10a) and (10b) in so far as it leads to a rational function of x only for odd n values. For even n values, in order to obtain y as a rational function of x, x has, as Darlington has shown, to be defined by a more complicated relation between x and u (see reference in footnote 27).

TABLE Ib

TCHEBYCHEFF APPROXIMATIONS; x AS A FUNCTION OF y.

$$\frac{y_n}{\sqrt{\lambda}} = sn\left(\frac{u}{M_n},\ \lambda\right) \qquad \frac{x}{\sqrt{k}} = sn(u,\ k)$$

$$x = \sqrt{k}\ sn\left\{\left[M_n\, sn^{-1}\left(\frac{y_n}{\sqrt{\lambda}},\ \lambda\right) + j2q\frac{K'}{n}\right],\ k\right\}, \qquad q = 0, 1, 2, 3, \cdots, (n-1).$$

Let $M_n sn^{-1}\left(\frac{y_n}{\sqrt{\lambda}},\ \lambda\right) = T$, then

y_n	T	x
0	0	$j\sqrt{k}\ sc\left[2q\frac{K'}{n},\ k'\right]$
j	$j\frac{1}{2}\frac{K'}{n}$	$j\sqrt{k}\ sc\left[\left(\frac{1}{2}+2q\right)\frac{K'}{n},\ k'\right]$
∞	$j\frac{K'}{n}$	$j\sqrt{k}\ sc\left[(1+2q)\frac{K'}{n},\ k'\right]$
$-j$	$j\frac{3}{2}\frac{K'}{n}$	$j\sqrt{k}\ sc\left[\left(\frac{3}{2}+2q\right)\frac{K'}{n},\ k'\right]$
$\sqrt{\lambda}$	K	$\sqrt{k}\ nd\left[2q\frac{K'}{n},\ k'\right]$
1	$K+j\frac{K'}{n}\left(\frac{1}{2}\text{ or }\frac{3}{2}\right)$	$\sqrt{k}\ nd\left[\left(\frac{1}{2}+q\right)\frac{K'}{n},\ k'\right]$
$1/\sqrt{\lambda}$	$K+j\frac{K'}{n}$	$\sqrt{k}\ nd\left[(1+2q)\frac{K'}{n},\ k'\right]$

$$sc(u,\ k) = \frac{sn(u,\ k)}{cn(u,\ k)}, \qquad nd(u,\ k) = \frac{1}{dn(u,\ k)}$$

This table is given in greater detail in Tables II and III.

work having a performance curve in accordance with y, we have to find the values of x at which $y = +j$. All these values of x can be found from (10a) and (10b) by first inverting (10a) to find u as a function of y and then substituting this expression for u in (10b). However, to simplify the engineering application of Tchebycheff approximations, the x values at which y becomes 0, j, ∞, $-j$ and $\sqrt{\lambda}$, 1, $1/\sqrt{\lambda}$, are listed in Tables I, II, and III. The expressions tabulated are so regular in form that it is easy, if required, to extend by analogy the Table to any n value. The value H mentioned above is given by

$$H = \sqrt{\lambda/k}/M_n. \tag{11}$$

When dealing with Tchebycheff approximations it is often convenient to make use of the "index law" which is valid for these approximations. Let $y_n(x, k)$ denote the nth order approximation to $y_n = 1$ over the x range $\sqrt{k}$ to $1/\sqrt{k}$, and let k_n denote the range of variation of $y_n(x, k)$, i.e., y_n varies between $\sqrt{k_n}$ and $1/\sqrt{k_n}$. Furthermore, let $y_m(y_n, k_n)$ denote the mth order approximation to $y_m = 1$ over the y_n range $\sqrt{k_n}$ to $1/\sqrt{k_n}$, and let $(k_n)_m$ denote the range of variation of y_m, i.e., y_m varies between $\sqrt{(k_n)_m}$ and $1/\sqrt{(k_n)_m}$. Then $y_m(y_n, k_n)$ considered as a function of x when x varies from $\sqrt{k}$ to $1/\sqrt{k}$ is identical with $y_p(x, k)$, the pth order approximation to $y_p = 1$, over the x range $\sqrt{k}$ to $1/\sqrt{k}$, if $p = mn$. This can be expressed formally by

$$\left.\begin{aligned} y_m(y_n, k_n) &= y_p(x, k), & p &= mn \\ (k_n)_m &= k_p, & p &= mn \end{aligned}\right\}. \tag{12}$$

By virtue of the index law we can, if we have explored the case of $n = 2$, apply all results obtained to $n = 4 = 2\times 2$ and $n = 8 = 2\times 4$. If we have explored $n = 2$ and $n = 3$, we can combine the results to obtain the cases $n = 6 = 2\times 3$ and $n = 9 = 3\times 3$. A generalizing interpretation of the index law will be given in the Appendix.

3. *Alternative Theory of Tchebycheff Approximations*

So far, the theory of Tchebycheff approximations has been discussed in terms of elliptic functions. This leads to the most concise and general type of expressions. At the same time it must be realized that many engineers are unfamiliar with elliptic functions and that it is sometimes difficult to obtain good tables of elliptic functions. It is therefore important to note that it is possible to formulate the approximations purely algebraically, without the use of elliptic functions. In practice, a combination of the two methods of attack, appropriate to the particular case under consideration, is sometimes the best choice.

The algebraic theory for $n=2$, 4, 8 is very simple indeed. Starting with $n=2$, $y_2=d_2x/(1+x^2)$ leads to the following relations:

for $x=\sqrt{k}$ and $x=1/\sqrt{k}$, $y_2=y_{2\min}=d_2\sqrt{k}/(1+k)$;

and for $x=1$, $y_2=y_{2\max}=\frac{1}{2}d_2$.

The condition $y_{2\min}y_{2\max}=1$ leads to $k_2=2\sqrt{k}/(1+k)$ and $d_2=2/\sqrt{k_2}$. With this value for d_2, y_2 is the Tchebycheff approximation of the second order for the range k. The cases $n=4$ and $n=8$ can be discussed by applying the index law. The results are tabulated in Table IV.

TABLE II

TCHEBYCHEFF APPROXIMATIONS; x FOR $y=0, +j, \infty, -j$.

$n=1$	
x	y_1
0	0
$+j$	$+j$
$\pm\infty$	$\pm\infty$
$-j$	$-j$
0	0

$n=2$	
x	y_2
$j\sqrt{k}\,sc(0) \quad =0$	0
$j\sqrt{k}\,sc\left(\frac{K'}{4}, k'\right)$	$+j$
$j\sqrt{k}\,sc\left(\frac{K'}{2}, k'\right)=+j$	$\pm\infty$
$j\sqrt{k}\,sc\left(\frac{3}{4}K', k'\right)$	$-j$
$j\sqrt{k}\,sc(K', k') \quad =\infty$	0
$j\sqrt{k}\,sc\left(\frac{5}{4}K', k'\right)$	$+j$
$j\sqrt{k}\,sc\left(\frac{3}{2}K', k'\right)=-j$	$\pm\infty$
$j\sqrt{k}\,sc\left(\frac{7}{4}K', k'\right)$	$-j$
$j\sqrt{k}\,sc(0) \quad =0$	0

$n=3$	
x	y_3
$j\sqrt{k}\,sc(0) \quad =0$	0
$j\sqrt{k}\,sc\left(\frac{K'}{6}, k'\right)$	$+j$
$j\sqrt{k}\,sc\left(\frac{K'}{3}, k'\right)$	$\pm\infty$
$j\sqrt{k}\,sc\left(\frac{K'}{2}, k'\right)=+j$	$-j$
$j\sqrt{k}\,sc\left(\frac{2}{3}K', k'\right)$	0
$j\sqrt{k}\,sc\left(\frac{5}{6}K', k'\right)$	$+j$
$j\sqrt{k}\,sc(K', k') \quad =\infty$	$\pm\infty$
$j\sqrt{k}\,sc\left(\frac{7}{6}K', k'\right)$	$-j$
$j\sqrt{k}\,sc\left(\frac{4}{3}K', k'\right)$	0
$j\sqrt{k}\,sc\left(\frac{3}{2}K', k'\right)=-j$	$+j$
$j\sqrt{k}\,sc\left(\frac{5}{3}K', k'\right)$	$\pm\infty$
$j\sqrt{k}\,sc\left(\frac{11}{6}K', k'\right)$	$-j$
$j\sqrt{k}\,sc(0) \quad =0$	0

In the General Case	
x	y_n
$j\sqrt{k}\,sc(0) \quad =0$	0
$j\sqrt{k}\,sc\left(\frac{1}{2n}K', k'\right)$	$+j$
$j\sqrt{k}\,sc\left(\frac{2}{2n}K', k'\right)$	$\pm\infty$
$j\sqrt{k}\,sc\left(\frac{3}{2n}K', k'\right)$	$-j$

$$sc(u, k)=\frac{sn(u, k)}{cn(u, k)}=sc(u+2K, k)$$

$$sc(2K-u, k)=sc(-u, k)=-sc\,(u, k)$$

TABLE III

TCHEBYCHEFF APPROXIMATIONS; x FOR $y=\sqrt{\lambda}, 1, 1/\sqrt{\lambda}$.

$n=1$	
x	y_1
$\sqrt{k}$	min
1	1
$1/\sqrt{k}$	max

$n=2$		
x		y_2
$x_1=\sqrt{k}\,nd(0)$	$=\sqrt{k}$	min
$x_2=\sqrt{k}\,nd\left(\frac{1}{4}K', k'\right)$		1
$x_3=\sqrt{k}\,nd\left(\frac{2}{4}K', k'\right)$	$=1$	max
$1/x_2=\sqrt{k}\,nd\left(\frac{3}{4}K', k'\right)$		1
$1/x_1=\sqrt{k}\,nd\left(\frac{4}{4}K', k'\right)$	$=1/\sqrt{k}$	min

$n=3$		
x		y_3
$x_1=\sqrt{k}\,nd(0)$	$=\sqrt{k}$	min
$x_2=\sqrt{k}\,nd\left(\frac{1}{6}K', k'\right)$		1
$x_3=\sqrt{k}\,nd\left(\frac{2}{6}K', k'\right)$		max
$x_4=\sqrt{k}\,nd\left(\frac{3}{6}K', k'\right)$	$=1$	1
$1/x_3=\sqrt{k}\,nd\left(\frac{4}{6}K', k'\right)$		min
$1/x_2=\sqrt{k}\,nd\left(\frac{5}{6}K', k'\right)$		1
$1/x_1=\sqrt{k}\,nd\left(\frac{6}{6}K', k'\right)$	$=1/\sqrt{k}$	max

In the General Case	
x	y_n
$x_1=\sqrt{k}\,nd(0)$ $=\sqrt{k}$	min
$x_2=\sqrt{k}\,nd\left(\frac{1}{2n}K', k'\right)$	1
$x_3=\sqrt{k}\,nd\left(\frac{2}{2n}K', k'\right)$	max
$x_4=\sqrt{k}\,nd\left(\frac{3}{2n}K', k'\right)$	1

$$nd(u, k)=1/dn(u, k)=nd(-u, k)$$
$$nd(u+2K, k)=nd(u, k)$$
$$nd(K'\pm u, k')=1/[k\,nd(u, k')]$$

For $n=3$ the derivation of an expression for y_3 is less simple. We start with an expression of the form $y_3=Hx(A_0+x^2)/(B_0+x^2)$, which, in order to be symmetrical about $x=1$, simplifies to $y=x(a+x^2)/(1+ax^2)$. Then we have to determine a so that, for a given range k, y behaves in a Tchebycheff manner. y is required to be equal to $\sqrt{\lambda}$ if $x=\sqrt{k}$; furthermore, y has also the value $\sqrt{\lambda}$ as a minimum value at an unknown x value, say $x=b$. Therefore

$$y-\sqrt{\lambda}=[x(a+x^2)-\sqrt{\lambda}(1+ax^2)]/(1+ax^2)$$

must be equal to $(x-\sqrt{k})(x-b)^2/(1+ax^2)$. Comparing coefficients we obtain three equations:

$$a\sqrt{\lambda}=\sqrt{k}+2b,\quad a=b^2+2b\sqrt{k}\quad\text{and}\quad\sqrt{\lambda}=b^2\sqrt{k}.$$

If we introduce α, a term used by Cayley, by means of

$$b=\sqrt{k}/\alpha$$

we find

$$a=k/\alpha^2+2k/\alpha \tag{13a}$$

and

$$k^2=\alpha^3\frac{2+\alpha}{1+2\alpha},\qquad \lambda^2=\alpha\left(\frac{2+\alpha}{1+2\alpha}\right)^3. \tag{13b}$$

Equations (13a) and (13b) determine α, a and λ in terms of k (λ can also be determined by means of tables of elliptic functions, or by means of a graph like that in Fig. 5(b)). Then we can find $b^2=\sqrt{\lambda/k}$. Thus we know y as a function of x and the following details:

$y=\sqrt{\lambda}$ at $x=\sqrt{k}$ and $x=b$

$y=1/\sqrt{\lambda}$ at $x=1/\sqrt{k}$ and $x=1/b$

$y=1$ at $x=1$ and $x=\frac{1}{2}(a-1)\pm\sqrt{\frac{1}{4}(a-1)^2-1}$.

TABLE IV

TCHEBYCHEFF APPROXIMATIONS FOR $n=2, 4, 8$; ALGEBRAIC RELATIONS

$x=[F(d_2/y_2)]^{\pm 1}$	$y_2=\dfrac{d_2x}{1+x^2}=[F(d_4/y_4)]^{\pm 1}$	$y_4=\dfrac{d_4y_2}{1+y_2^2}=[F(d_8/y_8)]^{\pm 1}$	$y_8=\dfrac{d_8y_4}{1+y_4^2}$
$\sqrt{k}$	min	min	min
$F\{d_2/F[d_4/F(d_8)]\}$	$F[d_4/F(d_8)]$	$F(d_8)$	1
$F[d_2/F(d_4)]$	$F(d_4)$	1	max
$F\{d_2/F[d_4F(d_8)]\}$	$F[d_4F(d_8)]$	$1/F(d_8)$	1
$F(d_2)$	1	max	min
$F\{d_2F[d_4F(d_8)]\}$	$1/F[d_4F(d_8)]$	$1/F(d_8)$	1
$F[d_2F(d_4)]$	$1/F(d_4)$	1	max
$F\{d_2F[d_4/F(d_8)]\}$	$1/F[d_4/F(d_8)]$	$F(d_8)$	1
1	max	min	min
$1/F\{d_2F[d_4/F(d_8)]\}$	$1/F[d_4/F(d_8)]$	$F(d_8)$	1
$1/F[d_2F(d_4)]$	$1/F(d_4)$	1	max
$1/F\{d_2F[d_4F(d_8)]\}$	$1/F[d_4F(d_8)]$	$1/F(d_8)$	1
$1/F(d_2)$	1	max	min
$1/F\{d_2/F[d_4F(d_8)]\}$	$F[d_4F(d_8)]$	$1/F(d_8)$	1
$1/F[d_2/F(d_4)]$	$F(d_4)$	1	max
$1/F\{d_2/F[d_4/F(d_8)]\}$	$F[d_4/F(d_8)]$	$F(d_8)$	1
$1/\sqrt{k}$	min	min	min
	min: $y_2=\sqrt{k_2}$, max: $y_2=\dfrac{1}{\sqrt{k_2}}$	min: $y_4=\sqrt{k_4}$, max: $y_4=\dfrac{1}{\sqrt{k_4}}$	min: $y_8=\sqrt{k_8}$, max: $y_8=\dfrac{1}{\sqrt{k_8}}$

$y_2=+j$ if $x=[F(d_2/j)]^{\pm 1}$

$y_4=+j$ if $y_2=[F(d_4/j)]^{\pm 1}$, $x=[F(d_2/y_2)]^{\pm 1}$

$y_8=+j$ if $y_4=[F(d_8/j)]^{\pm 1}$, $y_2=[F(d_4/y_4)]^{\pm 1}$, $x=[F(d_2/y_2)]^{\pm 1}$

$$k_2=\frac{2\sqrt{k}}{1+k}, \qquad k_4=\frac{2\sqrt{k_2}}{1+k_2}, \qquad k_8=\frac{2\sqrt{k_4}}{1+k_4}$$

$$d_2=2/\sqrt{k_2}, \qquad d_4=2/\sqrt{k_4}, \qquad d_8=2/\sqrt{k_8}$$

$$F(z)=\tfrac{1}{2}z-\sqrt{(\tfrac{1}{2}z)^2-1} \qquad 1/F(z)=\tfrac{1}{2}z+\sqrt{(\tfrac{1}{2}z)^2-1}$$

If we replace in the discussion of the case $n=3$ the independent variable x by the second-order approximation y_2 and k by k_2, we obtain a sixth-order approximation, and by repeating this process we obtain a twelfth-order approximation. If in the discussion of the case $n=3$ we replace x by y_3 and k by k_3 we obtain the

ninth-order approximation. For the prime numbers $n=5, 7, 11, \cdots$ etc., however, the algebraic theory becomes progressively more difficult (see Cayley).

4. *Approximation by Other Methods*

In most cases the requirements concerning the performance of phase splitting networks can probably be satisfied by means of Tchebycheff or Taylor approximations which have been discussed in the preceding section. Sometimes, however, requirements may be stipulated for which these types of approximations are not the best possible solutions. Then other types of approximations have to be obtained.

If it is required to have an exact phase difference of 90° at n specified values of x, then the parameters of the function y which satisfies these requirements can be obtained by solving n linear simultaneous equations. Zobel[19] has discussed this method in great detail with reference to the design of attenuation equalizers and phase shift networks. The application to the design of phase splitting networks does not raise any new problems.

Zobel recommends the use of this method not only in cases where the performance at a number of points is specified, but also where a good approximation over a whole range of x values is required. However, in such cases Zobel's method often leads to disappointments (see e.g., comments by Saraga[20] and Baum[21]) and graphical methods of curve fitting are to be preferred.

A survey of graphical curve fitting methods shows that they can conveniently be classified as curve summation or curve shifting and shaping methods (see Saraga[20]). It is usually necessary to transform the coordinate system in which the required performance curve and its tolerance band are specified in order to make the application of these graphical methods possible. In the summation method, a curve which fits the tolerance band is obtained by adding a number of standard curves in different positions. From these positions the parameters of the approximating curve can be obtained (for examples, see Laurent,[22] Rumpelt,[23] Saraga,[20] Scowen,[24] Baum[21]). In the shifting and shaping method which can be used for a limited number (not more than 4 to 5) of parameters only, one single standard curve is shifted and shaped by scale changes and shearing until it fits the required tolerance band (see Pyrah,[25] Truscott,[26] Saraga[20]). The application of these methods to the specific problems of phase splitting networks will not be discussed here.

V. Network Synthesis

At this stage we shall assume that in one way or another a suitable performance function $y(x)$ has been determined. The next step is the determination of two phase shift networks which will produce this function y. The problem to be solved is to find X_1/R_0 and X_2/R_0 when

$$y = \frac{(X_1/R_0) - (X_2/R_0)}{1 + (X_1/R_0)(X_2/R_0)}$$

is known. As this problem occurs also in the design of symmetrical filters where (see equation (6b))

$$\frac{1 + (X_A/R_0)(X_B/R_0)}{(X_A/R_0) - (X_B/R_0)}$$

is given and X_A/R_0 and X_B/R_0 have to be found as physically possible reactances, we can apply its solution to our problem. Darlington[27] gives the following instructions for determining the reactances (modified here in accordance with the symbols used in this paper):— Write y in the form $y=xB'/P$ where B' and P are polynomials in x^2. Then express $P+pB'$ in the form $(P_1+pB_1)(P_2-pB_2)$ where P_1, B_1, P_2, B_2, are even polynomials in $p=jx$, such that the roots of $P_1+pB_1=0$ are the roots of $P+pB'=0$ (i.e. $y=+j$) which have negative real parts. Then $jX_1/R_0=pB_1/P_1$ and $jX_2/R_0=pB_2/P_2$.

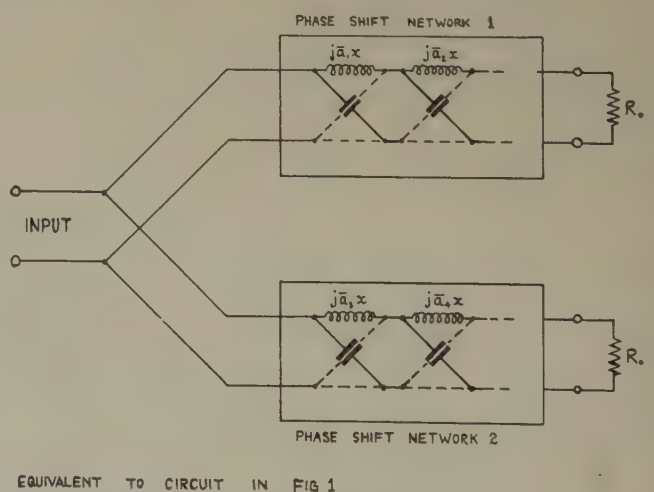

Fig. 6—Basic phase-splitting circuit, decomposed into elementary phase shift sections.

[19] O. J. Zobel, "Distortion correction in electrical circuits with constant resistance recurrent networks," *Bell Sys. Tech. Jour.*, vol. 7, pp. 438–534; July, 1928.
[20] W. Saraga, "Attenuation and phase shift equalisers," *Wireless Eng.*, vol. 20, pp. 163–181; April, 1943.
[21] R. F. Baum, "A contribution to the approximation problem," Proc. I.R.E., vol. 36, pp. 863–869; July, 1948.
[22] T. Laurent, "New principles for practical computation of filter attenuation by means of frequency transformation," *Ericsson Technics*, vol. 3, pp. 57–72; 1939.
[23] E. Rumpelt, "Schablonenverfahren fuer den Entwurf elektrischer Wellenfilter auf der Grundlage der Wellenparameter," *Telegraphen Fernsprech. Funk und Fernsch-und Technik*, vol. 31, pp. 203–210; August, 1942.
[24] F. Scowen, "Electric Wave Filters," Chapman & Hall Ltd., London, pp. 72–74; 1945.
[25] F. Pyrah, "Constant impedance equalisers: Simplified method of design and standardisation," *British P.O. Elec. Eng.'s Jour.*, vol. 92, pp. 204–211; October, 1939.
[26] D. N. Truscott, "Logarithmic charts and circuit performance," *Electronic Eng.*, vol. 14, pp. 745–748; May, 1942.
[27] S. Darlington, "Synthesis of reactance 4-poles which produce prescribed insertion loss characteristics," *Jour. Math. Phys.*, vol. 13, pp. 257–353; September, 1939.

Darlington's instructions, given without explicit proof, can be modified in a way which includes the proof. For this purpose we consider those values of x at which $y=\tan\frac{1}{2}(\beta_1-\beta_2)=j$; at these values, say $x=x_j$, the phase-shift difference $\frac{1}{2}(\beta_1-\beta_2)$ approaches $+j\infty$ which must be due to $\frac{1}{2}\beta_1$ tending towards $+j\infty$ or $\frac{1}{2}\beta_2$ tending towards $-j\infty$. Let us now assume that the two basic phase shift networks with series reactances X_1 and X_2 (see Fig. 1) consist of "elementary" phase shift sections in tandem, each section being characterized by its phase shift β and its normalized series arm reactance $\bar{a}x=\tan\frac{1}{2}\beta$ or its normalized series arm inductance $\bar{a}$ (see Fig. 6).[28] Then at each x_j one of these elementary phase angles $\frac{1}{2}\beta$ must tend to $+j\infty$ and $\tan\frac{1}{2}\beta=j$, if β is a constituent of β_1, or to $-j\infty$ and $\tan\frac{1}{2}\beta=-j$, if β is a constituent of β_2. Since $\tan\frac{1}{2}\beta=\bar{a}x$, we find $\bar{a}=\pm j/x_j$. We take that sign which makes $\bar{a}$, the normalized inductance, positive. If, in order to obtain a positive $\bar{a}$ we have to take the positive sign, the corresponding β is a constituent of β_1, whereas in the other case we obtain a constituent of β_2. In this way we not only find X_1 and X_2, but also, at the same time, the constituent elementary sections forming the two basic phase shift networks. It can be shown that forming the expressions for X_1 and X_2 from the inductances of the elementary phase shift sections in accordance with the addition theorem of the tan-function leads to the expressions given by Darlington.

It will be seen that n elementary sections lead to an expression for y in which the highest degree of x is n, and vice versa. Thus the number of network elements increases with the highest degree of x occurring.

VI. Two Practical Design Examples

It is felt that in selecting practical examples for discussion in this article it is best to take very simple ones, as then the method of obtaining the networks can be shown most clearly. As a first example we shall discuss a case in which a Taylor approximation is required, and we select a simple case, namely $n=3$. Then the best approximation is given by

$$y_3=\frac{3x+x^3}{1+3x^2} \tag{14}$$

(see equations (9d)). Since n is odd, the number of sections of the two phase shifting networks must differ by one. Let us assume that the network with X_1, consists of two sections, say with series arm inductances $\bar{a}_1$ and $\bar{a}_2$, respectively. Then the network with X_2 has one single section, say with series arm inductance $\bar{a}_3$. Thus we obtain

$$\tan\tfrac{1}{2}\beta_1=\frac{(\bar{a}_1+\bar{a}_2)x}{1-\bar{a}_1\bar{a}_2x^2},\qquad \tan\tfrac{1}{2}\beta_2=\bar{a}_3x$$

and

$$y=\tan\tfrac{1}{2}(\beta_1-\beta_2)=\frac{(\bar{a}_1+\bar{a}_2-\bar{a}_3)x+\bar{a}_1\bar{a}_2\bar{a}_3x^3}{1+(\bar{a}_2\bar{a}_3+\bar{a}_3\bar{a}_1-\bar{a}_1\bar{a}_2)x^2}. \tag{15}$$

In this simple case we can obtain $\bar{a}_1$, $\bar{a}_2$, $\bar{a}_3$ by comparing coefficients in (14) and (15). Then $\bar{a}_1+\bar{a}_2-\bar{a}_3=3$;

$$\bar{a}_1\bar{a}_2\bar{a}_3=1;\qquad \bar{a}_2\bar{a}_3+\bar{a}_3\bar{a}_1-\bar{a}_1\bar{a}_2=3.$$

By substituting we obtain a cubic equation for $\bar{a}_3$ with one positive root: $\bar{a}_3=+1$. Then $\bar{a}_1=2+\sqrt{3}$, $\bar{a}_2=2-\sqrt{3}$ and $X_1/R_0=4x/(1-x^2)$, $X_2/R_0=x$. X_1 and X_2 can be interchanged. In a more complicated case we would solve the equation $y=+j$ and would obtain the three roots $x=-j$, $x=+j(2+\sqrt{3})$ and $x=+j(2-\sqrt{3})$ either by means of equation (9g) or algebraically. In view of the signs of the roots, the first one must correspond to X_2 and the other two must correspond to X_1. Thus we obtain $\bar{a}_1=2+\sqrt{3}$, $\bar{a}_2=2-\sqrt{3}$ and $\bar{a}_3=+1$ as before.

As a second example we shall discuss a case in which a Tchebycheff approximation is required. We shall take $n=4$ so that we can use an algebraic method as well as the transformation of elliptic functions for obtaining the network elements. The specified x range is assumed to be from $x=\sqrt{k}$ to $x=1/\sqrt{k}$ where $k=0.003$. This corresponds to a frequency range from 30 cps to 10 kc. Then by means of Hayashi's tables $k_4=\lambda$ is found to be 0.5959. The y curve is shown in Fig. 5(a). Table II gives the expressions for the four x values at which $y=+j$. Then using Milne-Thomson's tables, we find $x=+j2.469$, $x=-j/2.469$, $x=+j0.05618$, $x=-j/0.05618$. Then for one phase-shift network $\bar{a}_1=2.469$, $\bar{a}_2=0.05618$ and for the other network $\bar{a}_3=1/\bar{a}_2=17.80$, $\bar{a}_4=1/\bar{a}_1=0.4049$. From these values of $\bar{a}_1$, $\bar{a}_2$, $\bar{a}_3$, $\bar{a}_4$ we find

$$X_1/R_0=2.526x/(1-0.1387x^2),$$
$$X_2/R_0=18.20x/(1-7.208x^2)$$

and $y_4=15.68x(1+x^2)/[1+38.62x^2+x^4]$. X_1 and X_2 can be interchanged. Applying the algebraic theory we obtain from Table IV

$$d_2=6.052,\qquad d_4=2.591,\qquad k_4=\lambda=0.5959$$

and

$$y_4=d_4d_2x(1+x^2)/[1+(2+d_2^2)x^2+x^4]$$
$$=15.68x(1+x^2)/[1+38.62x^2+x^4]$$

as before.

VII. Alternative Phase Shift Networks

The preceding discussion has been based on conventional constant resistance phase shift networks with

[28] In the general case of such a decomposition of a phase shift network the individual a values obtained are not necessarily real but may occur in conjugate complex pairs. Then the two corresponding elementary sections can be combined to one physical section with normalized series arm reactance $ax/(1-bx^2)$ where $a^2<4b$. However, in the case of phase-splitting networks, complex $\bar{a}$ values do not occur if a Taylor or Tchebycheff approximation is used for the performance curve, and they do not seem to occur in other good approximations. On the other hand, their occurrence is the rule in filter design.

series arm reactances X and lattice arm reactances $-R_0^2/X$, inserted between equal resistances R_0. Then the phase shift is $\beta = 2 \tan^{-1} X$. It is possible to alter one of these resistances without altering the phase shift; then a basic flat loss occurs. This is indicated in Fig. 7. Marrison[29] has shown that it is possible to replace the two lattice arm reactances by resistances R_0 without altering the phase shift (see Fig. 8). Then, if the

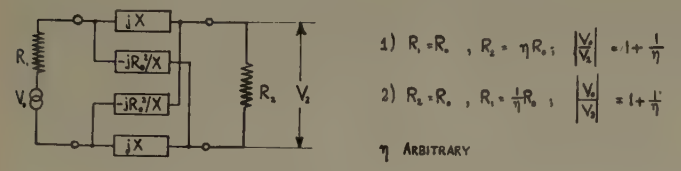

Fig. 7—Classical phase shift lattice network.

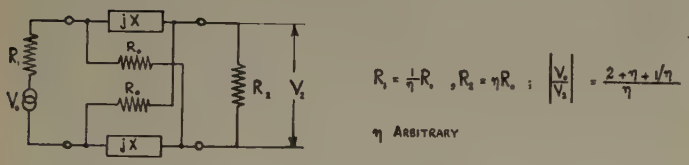

Fig. 8—Alternative to network in Fig. 7.

source and load resistance are both equal to R_0, a flat loss of 6 db is produced. It is possible to make the source resistance $(1/\eta)R_0$ and the load resistance ηR_0. Then an additional flat loss depending on η is produced, but the phase shift is still unaltered. Saraga[30] has shown that it is possible to replace one of the two remaining reactive arms by a resistance R_0 (see Fig. 9) without

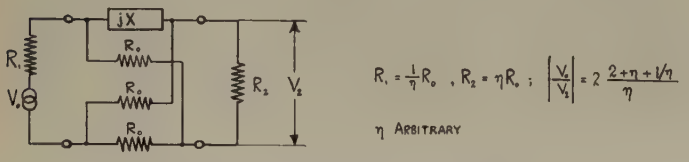

Fig. 9—Alternative to network in Fig. 7.

altering the phase shift. Then, if $\eta = 1$, the basic loss is 12 db instead of 6 db. Two other types of phase shift networks, one due to Nyquist and described by Sandeman[31] (see Fig. 10) and the other described by Wald[32] (see Fig. 11) can be shown to be special cases of the network in Fig. 9, but with more reactive elements than necessary for producing the phase shift actually produced. The circuit in Fig. 9 can be replaced by a hybrid circuit (see Sandeman). Dome[10] and Luck[12] have described a number of so-called half-lattice networks which are driven from a balanced source.

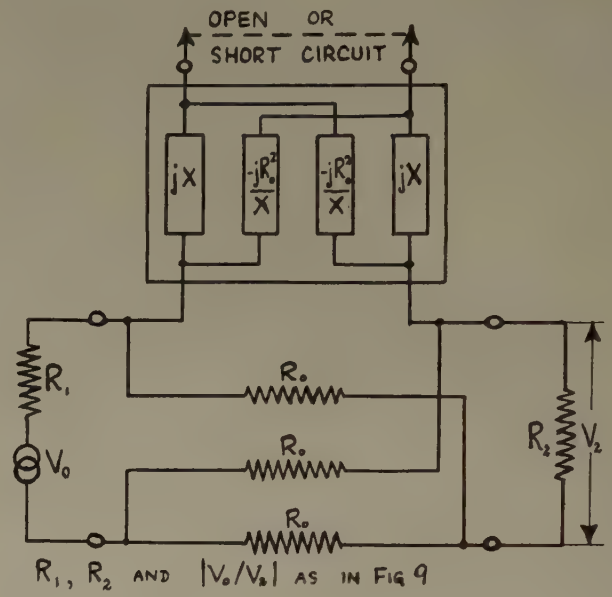

Fig. 10—Alternative to network in Fig. 7.

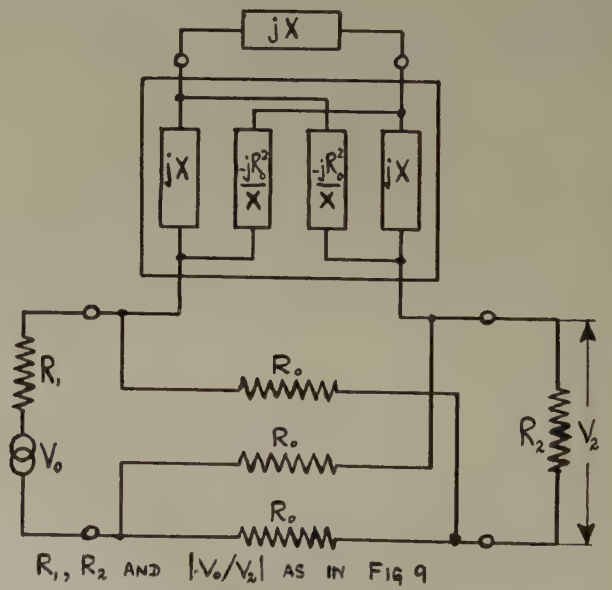

Fig. 11—Alternative to network in Fig. 7.

VIII. Dissipation-Compensated Phase Shift Networks

The effect of dissipation in the elements of a phase shift network is to distort the phase characteristic and

[29] W. A. Marrison, United States Patent No. 1,926,877, dated September 12, 1933.
[30] W. Saraga, British Patent No. 594,431, dated May 29, 1945, and U.S. Patent Application No. 670,264.
[31] E. K. Sandeman, "Phase compensation," *Elec. Commun.*, vol. 7, pp. 309–315; April, 1929.
[32] M. Wald, "Eine Kunstschaltung zur Verdreifachung des Winkelmasses eines Kreuzgliedes und ihre Anwendung zum Phasenausgleich in Pupinleitungen," *Elekt. Nach.* vol. 19, pp. 196–199; October, 1942.

to produce an attenuation varying with frequency. If the Q-values of the different components are not the same, the impedance is also affected. Starr[33] has described methods for approximate compensation of these effects of dissipation. Darlington[27] and Bode[34] have described methods for perfect compensation of the effects of dissipation. The networks are designed to meet predistorted specifications which are obtained from the original ones by assuming the occurrence of negative dissipation; then positive dissipation produces the required performance. A different method of obtaining dissipation-compensated phase shift networks will be described here.

Since any phase shift network can be built as a tandem combination of one- and two-parameter phase shift networks, it is sufficient to consider the dissipation compensation of such networks. The basic idea of the method is to consider only networks which contain a resistance in series with each inductance and a resistance in parallel with each capacitance so that these resistances can take up the dissipation resistances of reactive elements, and to design these networks so that they have the required phase characteristic β and a flat loss α_0. For the lattice network in Fig. 12 the transfer constant $\theta=\alpha+j\beta$ is given by $\tan h\frac{1}{2}\theta=Z/R_0$.

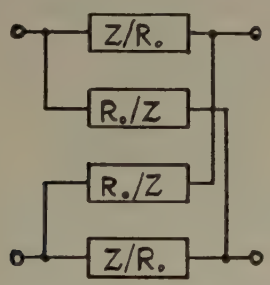

Fig. 12—Lattice network, shown for reference purposes in conjunction with Figs. 13 and 14.

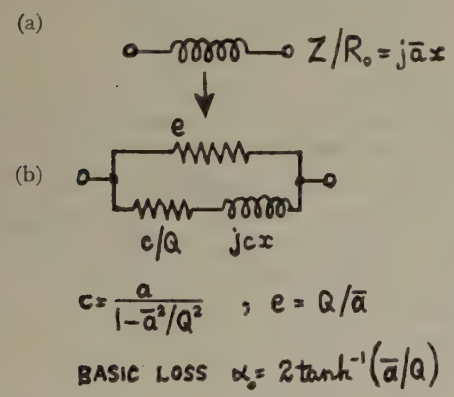

Fig. 13—Dissipation compensation of one-parameter phase shift network.

[33] A. T. Starr, British Patent No. 342,407, dated October 30, 1929.
[34] H. W. Bode, "Network Analysis and Feedback Amplifier Design," D. Van Nostrand Company, Inc., New York, N. Y., pp. 216–218; 1945.

For the one-parameter type of phase shifting network without dissipation $Z/R_0=j\bar{a}x$ (see Fig. 13(a)), and $\tan\frac{1}{2}\beta=\bar{a}x$, $\alpha=0$. Our aim is to find an impedance Z with resistances as stated above so that $Z/R_0=(C+j\bar{a}x)/(1+jC\bar{a}x)$ where $C=\tanh\frac{1}{2}\alpha_0$ and α_0 is the basic loss of the network. It can easily be shown that the network in Fig. 13(b) represents an impedance Z of this form. Its elements will be positive if Q is not too small.

We now consider the two-parameter phase shift network (without dissipation) in which Z/R_0 is as shown in Fig. 14(a). Then

$$Z/R_0=jax/(1-bx^2) \quad \text{and} \quad \alpha=0, \quad \tan\tfrac{1}{2}\beta=ax/(1-bx^2).$$

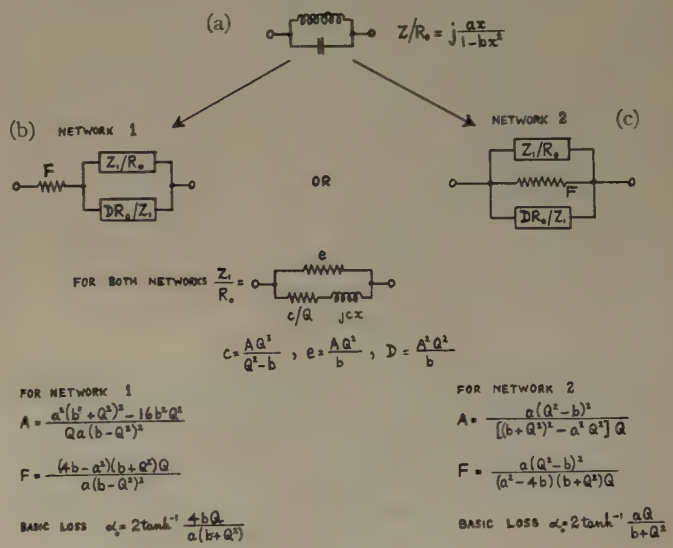

Fig. 14—Dissipation compensation of two-parameter phase shift network.

We have to find an impedance Z with resistances as stated above so that

$$Z/R_0=[C+jax/(1-bx^2)]/[1+jCax/(1-bx^2)].$$

It can be shown that the two networks shown in Figs. 14(b) and (c) have this impedance if the relations stated in these figures are satisfied. In Fig. 14(c) it is, of course, possible to absorb the resistance FR_0 in Z_1/R_0 DR_0^2/Z_1. It will be seen that the resistance FR_0 is negative in Fig. 14(b) if $a^2>4b$, and negative in Fig. 14(c) if $a^2<4b$. In Fig. 14(c) $F<0$ does not make the network necessarily nonphysical.

If $a^2\geqq 4b$ the phase shift network defined by the series arm reactance in Fig. 14(a) can be replaced by two simpler networks of the type defined by the series impedance in Fig. 13(a). As stated in Section V, footnote reference 28, only the case $a^2\geqq 4b$ seems to occur in phase-splitting problems, but the other case has been treated here too because the three transformations, described by Figs. 13 and 14, together make it possible to transform any given phase shift network into a dissipation compensated one.

Note: Since writing this manuscript the author has seen the papers by Dagnall and Rounds[35] and Farkas, Hallenbeck and Stehlick[36] in which various other methods for dissipation compensation of phase shift networks are discussed.

APPENDIX

Curve Approximation

Both equations (9e) and (10c) which give the deviation of y from unity for a given range of x and a given order n for Taylor and Tchebycheff approximations, can be written in the form

$$h(\lambda) = m + h(k), \quad \text{where} \quad m = \log_2 n,$$

and

$$h(\lambda) = \log_2 \tanh^{-1} \sqrt{\lambda}, \qquad h(k) = \log_2 \tanh^{-1} \sqrt{k}$$

in the case of (9e) and

$$h(\lambda) = \log_2 \frac{1}{[F(\lambda)]}, \qquad h(k) = \log_2 \frac{1}{[F(k)]}$$

in the case of (10c). This means that in both cases $\lambda = k_n$ as a function of k can be written in the form

$$k_n = k_2{}^m(k)$$

where $k_2{}^m(k)$ means the mth iteration of the function $k_2(k)$. Here "mth iteration" refers not only to integral values but also to fractional values of m, since $m = \log_2 n$ is only integral if n is an integral power of 2. Some discussions of the concept of non-integral iteration of functions have been given by Haldane,[37] Silberstein,[38] Hadamard.[39]

It is not possible to interpret in the same way the approximating function y as an iterated function of k because y is a function not only of k, but of x and k. However, if we generalize the concept of iteration so as to apply to functions of two variables (see Boole[40]), then y_n can be regarded as the mth iteration of $y_2(x, k)$ where $m = \log_2 n$. This will now be shown.

Since $y_2(x, k)$ leads from two independent to one dependent variable, an iteration is only possible if we introduce a second dependent variable, say, an arbitrary function $z_2(x, k)$. Then we shall define as $(y_2)^2$ and $(z_2)^2$ the functions $(y_2)^2 = y_2(y_2, z_2)$ and $(z_2)^2 = z_2(y_2, z_2)$. Furthermore, we can define iterated functions $y_2{}^m$ and $z_2{}^m$, for integral as well as non-integral values of m, as functions $y_2{}^m = F(x, k, m)$ and $z_2{}^m = G(x, k, m)$ of three variables which satisfy the following relations.

$$\left.\begin{aligned} &F(x, k, 1) = y_2(x, k), \qquad G(x, k, 1) = z_2(x, k) \\ &F[F(x, k, m_1), G(x, k, m_1), m_2] = F[x, k, (m_1 + m_2)] \\ &G[F(x, k, m_1), G(x, k, m_1), m_2] = G[x, k, (m_1 + m_2)] \end{aligned}\right\}. \qquad (16)$$

Now if we choose as arbitrary function $z_2(x, k)$ the function $k_2(k)$—which happens to be independent of x—we see that the index law (equations (12)) can be expressed in the form of equations (16) if $m = \log_2 n$ as before. In other words:—y_n and k_n can be interpreted as the mth iteration of y_2 and k_2 when regarded as a pair of functions of x and k.

It is interesting to note that such an interpretation is also possible if, instead of an approximation by a rational function, the approximation by a polynomial is under consideration. If $y = 0$ is to be approximated by the polynomial $y_n = A_0 + A_1 x + A_2 x^2 + \cdots + x^n$ in the range $x = -\eta$ to $x = +\eta$, the nth order Tchebycheff approximation is

$$y_n = (\eta^n / 2^{n-1}) \cos [n \cos^{-1} (x/\eta)],$$

and the nth order deviation $\eta_n = 2^{1-n}\eta^n$. It is easy to show that $y_n = y_2{}^m(x, \eta)$ and $\eta_n = \eta_2{}^m(x, \eta) = \eta_2{}^m(\eta)$. These and other questions connected with non-integral functional iteration are treated in a mathematical paper by the author which is being prepared for publication.

Acknowledgment

Thanks are due to J. G. Flint, Chief Engineer of the Telephone Manufacturing Co., for permission to publish this paper. The author also wishes to thank Miss L. Fosgate for producing the drawings, and Miss L. Fosgate and Miss J. Freeman for carrying out and checking a number of calculations. The loan of the elliptic function tables by Milne-Thomson and Hayashi, by Scientific Computing Service Ltd., London, is gratefully acknowledged.

[35] C. H. Dagnall and P. W. Rounds, "Delay equalization of eight-kilocycle carrier programme circuits," *Bell Sys. Tech. Jour.*, vol. 28, pp. 181–195; April, 1949.

[36] F. S. Farkas, F. J. Hallenbeck, and F. E. Stehlick, "Band pass filter, band elimination filter and phase simulating network for carrier programme systems," *Bell Sys. Tech. Jour.*, vol. 28, pp. 196–220; April, 1949.

[37] J. B. S. Haldane, "On the non-linear difference equation $\Delta x_n = k\phi(x_n)$," *Proc. Cambridge Phil. Soc.*, vol. 28, part II, pp. 234–243; 1932.

[38] L. Silberstein, "Construction of groups of commutative functions," *Phil. Mag.*, pp. 43–54; January, 1945.

[39] J. Hadamard, "Two works on iteration and related questions," *Bull. Amer. Math. Soc.*, vol. 50, pp. 67–75; February, 1944.

[40] G. Boole, "A Treatise on the Calculus of Finite Differences," Macmillan and Co., London, 3rd Ed., p. 17; 1880.

Detection of a Pulse Superimposed on Fluctuation Noise*

BERNARD M. DWORK†, ASSOCIATE, IRE

Summary—**Given a known pulse superimposed on fluctuation noise having a known spectrum, we determine the frequency response of that linear device which would give the maximum value for the ratio between peak amplitude of the signal and the root-mean-square of the noise at the output. This result is applied to the case in which the fluctuation noise has a flat spectrum, and it is shown that in that case the optimal network is physically realizable if the pulse differs from zero for only a finite interval of time. The noise-suppressing efficiency of a conventional *RC* circuit is computed for pulse shapes of practical interest.**

Introduction

WE ASSUME a given signal pulse superimposed on a given noise background. We inquire as to the frequency response of a linear device such that the peak amplitude of the signal output shall be as large as possible, as compared to the rms of the noise output.

The solution of this problem could, for example, be applied to the construction of equipment used in the determination of the number of signal pulses occurring during some rather long interval of time (i.e., the precise time of occurrence of each pulse is not of interest) provided that: (1) the pulses are all of the same general shape; (2) the time interval between successive pulses is comparatively long; and (3) the number of spurious counts caused by noise is a function of the ratio of peak amplitude of signal to root mean square of noise at the output, and is independent of *all* other factors.

Symbols

$e(t)$ = signal at input terminals
$H(w) = |H(w)| \exp [j\phi(w)]$ = frequency response of the device
$F(w)$ = Fourier transform of $e(t)$
$E(t)$ = signal at output terminals
$S = \max_t |E(t)|$
F^* = complex conjugate of F
N = rms of noise at output
Max $\{x, y\}$ = the larger of the two numbers x, y
$w = 2\pi f$ = radian frequency
$\sigma(w)$ = frequency distribution of noise (voltage or current, not power) at input terminals (Thus, if input noise voltage is due to a resistor R then $\sigma(w) = \sqrt{2KTR}$. The familiar Nyquist formula is divided by $\sqrt{2}$ as we shall integrate w from $-\infty$ to $+\infty$)
$E_0(t)$ = instantaneous response to unit impulse applied at $t = 0$ of a network having frequency response: $F^*(w) \exp(-jwT)$.

* Decimal classification: R143×R148.6. Original manuscript received by the Institute, October 15, 1949.
† U. S. Atomic Energy Commission, New York, N. Y.

As the linear device can with little loss in generality be assumed to have no internal sources of noise, we can write[1]

$$N^2 = \frac{1}{2\pi}\int_{-\infty}^{\infty} |H(w)\sigma(w)|^2 dw.$$

We also note that

$$F(w) = \int_{-\infty}^{\infty} \exp(-jwt)e(t)dt$$

$$(1/2)[E(t^+) + E(t^-)] = (1/2\pi)\int_{-\infty}^{\infty} \exp(jwt)F(w)H(w)dw.$$

We now consider the problem: Given $e(t)$ and $\sigma(w)$, to pick $H(w)$ so that S/N is a maximum. The solution is contained in the following result.

Theorem

If a signal pulse (whose Fourier[1] transform is $F(w)$) is superimposed on fluctuation noise (frequency distribution $\sigma(w)$), then the maximum possible value for S/N at the output will be obtained if, and only if, we set

$$H(w) = F^*(w) \exp(-jwT)/[\sigma(w)]^2 \quad (T \text{ any real number})$$

and the value of S/N so obtained is[2]

$$M = \sqrt{(1/2\pi)\int_{-\infty}^{\infty} |F(w)/\sigma(w)|^2 dw}.$$

Proof

The method of proof is to show that for any $H(w)$ the value of S/N is at most M. We then show that if $H(w)$ is of the stated form, then $S/N \geqq M$. Hence, $S/N = M$, if $H(w)$ is of the stated form. We now give the details:

(We assume that the output signal $E(t)$ has no discontinuities except for a finite set of isolated finite jumps. Little is lost in the way of generality as usually discontinuities play a role only in the approximation of continuous phenomena.)

By definition of S, $(S/N)^2 = [\max_t |E(t)|/N]^2$; but for all t

$$|E(t)| \leqq \max\{|E(t^+)|, |E(t^-)|\}$$

$$\leqq (1/2\pi)\int_{-\infty}^{\infty} |F(w)H(w)|\, dw.$$

[1] G. A. Campbell and R. M. Foster, "Fourier Integrals for Practical Application," Bell Telephone System Monograph B584, p. 39, 1942.

[2] A similar result for the case in which $\sigma(w)$ is constant, appears on p. 964 of J. Van Vleck and David Middleton, "A theoretical comparison of the visual, aural, and meter reception of pulsed signals in the presence of noise," *Jour. Appl. Phys.*, vol. 17, pp. 940–971; November, 1946.

U OF I
LIBRARY

Hence, for all t

$$2\pi |E(t)/N|^2 \leqq \left[\int_{-\infty}^{\infty} |F(w)H(w)|\,dw\right]^2 \Big/ \int_{-\infty}^{\infty} |H(w)\sigma(w)|^2 dw \leqq \int_{-\infty}^{\infty} |F(w)/\sigma(w)|^2 dw.$$

This last inequality is obtained by applying Schwartz's inequality in function space to the functions[3] $|F/\sigma|$ and $|H\sigma|$. Hence,

$$S/N \leqq \sqrt{(1/2\pi)\int_{-\infty}^{\infty} |F(w)/\sigma(w)|^2 dw} = M.$$

This completes the first part of the proof.

We must now show that $S/N = M$ if $H = F^* \exp(-jwT)/\sigma^2$. We observe that $S \geqq E(t)$ for all t, hence in particular

$$S \geqq \max\{|E(T^+)|, |E(T^-)|\} \geqq (1/2)[E(T^+) + E(T^-)] = (1/2\pi)\int_{-\infty}^{\infty} F(w)H(w)\exp(jwT)dw.$$

Hence, if H has the suggested form, we obtain by substitution

$$S \geqq M^2$$

while by substitution in the general expression for N we obtain

$$N = M.$$

Hence $H = F^* \exp(-jwT)/\sigma^2$ implies that $S/N \geqq M$. But, from the previous paragraph, $S/N \leqq M$. Hence, if H has the indicated form, $S/N = M$.

We now prove the converse: If $S/N = M$, then $H(w)$ must have the indicated form.

Given any $H(w)$ such that $S/N = M$, and if $E(t)$ attains the value S, when $t = T'$, then the argument (i.e., phase angle) of $F(w)\ H(w) \exp(jwT')$ must be independent of w (otherwise, by changing the phase characteristic of $H(w)$ we could get a larger S without changing N so that S/N would exceed M, but this is impossible). As the argument of the integrand is a constant, the absolute value of the integral is the integral of the absolute value, i.e.,

$$S = (1/2\pi)\left|\int_{-\infty}^{\infty} FH \exp(jwT')dw\right| = (1/2\pi)\int_{-\infty}^{\infty} |FH|\,dw,$$

but by hypothesis

$M^2 = (S/N)^2$, hence

$$\int_{-\infty}^{\infty} |F/\sigma|^2 dw = \left[\int_{-\infty}^{\infty} |FH|\,dw\right]^2 \Big/ \int_{-\infty}^{\infty} |H\sigma|^2 dw.$$

Applying the equality condition of Schwartz's inequality in function space[3] we obtain: $|H\sigma| = c|F/\sigma|$, where c is any constant.

Hence, $S/N = M$ implies that $|H| = c|F|/\sigma^2$. But, argument $F(w)H(w) \exp(jwT') =$ constant implies argument $H(w) =$ constant $-$ argument $F(w) - jwT'$.

Hence

$$H(w) = c'F^* \exp(-jwT')/\sigma^2,$$

where c' is the result of changing c so as to include the constant in the above expression for the argument of $H(w)$. This completes the proof.

This theorem reduces to a particularly simple form when $\sigma(w) = \sigma(0)$ for all frequencies (or in practice at all frequencies of interest).

Corollary

If $\sigma(w) = \sigma(0)$ for all w, then the optimum value of S/N is

$$\frac{1}{\sigma(0)}\sqrt{\int_{-\infty}^{\infty} [e(t)]^2 dt}.$$

Proof

If $\sigma(w) = \sigma(0)$ for all w, then the expression for the optimum value of S/N reduces to[1]

$$M = \sqrt{(1/2\pi)\int_{-\infty}^{\infty} |F(w)/\sigma(0)|^2 dw} = \frac{1}{\sigma(0)}\sqrt{\int_{-\infty}^{\infty} [e(t)]^2 dt}.$$

Hence, M reduces to the indicated value.

This corollary will simplify the computation of the optimum performance. In general, it will not be economical to construct networks having the response indicated in the theorem. The value of the result lies in that it gives a basis for the determination of the performance of any suggested, more easily constructed, network. The criterion discussed here (i.e., the ratio between peak signal and rms of noise) differs from Norbert Wiener's rms error criterion,[4] which involves the minimization of the rms value of the difference between input signal and output signal plus noise. The criterion to be used in designing equipment obviously will depend upon the equipment's function.

Physical Realizability

The final topic to be treated is the question of the physical realizability of any network capable of giving the optimal results obtainable with given shape signal pulse and a given noise spectrum. This question can be

[3] Courant-Hilbert, "Methoden Der Mathematischen Physik," vol. I, Interscience Publishers, Inc., New York, N. Y., p. 40.

[4] Norbert Wiener, "The Extrapolation, Interpolation, and Smoothing of Stationary Time Series," John Wiley & Sons, Inc., New York, N. Y., p. 129; 1949.

completely answered for the case in which the noise spectrum is flat. The criterion for physical realizability of any linear response function $H(w)$ is that

1. The response of $H(w)$ to unit impulse at $t=0$ be zero for all $t<0$.
2. $|H(w)|$ is an even function of frequency and argument of $H(w)$ is a real odd function of frequency.[5]

We can now state the solution to the problem just proposed.

Theorem 2

If the noise spectrum is flat (i.e., if $\sigma(w)=1$), then the maximal network for the detection of a pulse $e(t)$ is physically realizable if, and only if, there exists a T_0 such that $e(t)$ vanishes for all $t>T_0$.

Proof

From previous results the optimal network has the frequency response $H(w)=F^*(w)\exp(-jwT)$, where T can be set at any desired value. Now

$$F(w)=\int_{-\infty}^{\infty}e(t)\exp(-jwt)dt$$

so that

$$F^*(w)=\int_{-\infty}^{\infty}e(t)\exp(jwt)dt$$

$$=\int_{-\infty}^{\infty}e(t)\cos wt\,dt+j\int_{-\infty}^{\infty}e(t)\sin wt\,dt.$$

It is readily ascertained that

$$|F^*(w)\exp(-jwT)|$$

is an even function of w, while the phase angle of $F^*(w)\exp(-jwT)$ is an odd function of w. We note for later use that the phase angle, $\phi(w)$, of $F(w)$ is an odd function of frequency. The only remaining criterion involves the response to unit impulse applied at $t=0$. This is given by

$$E_0(t)=(1/2\pi)\int_{-\infty}^{\infty}F^*(w)\exp(-jwT)\exp(jwt)dw.$$

But

$$e(t)=(1/2\pi)\int_{-\infty}^{\infty}F(w)\exp(jwt)dw$$

$$=(1/2\pi)\int_{-\infty}^{\infty}|F(w)|\exp[j\phi(w)]\exp(jwt)dw,$$

substituting $-w$ for w and $-(t-T)$ for t, we obtain

$$e[-(t-T)]$$

$$=(1/2\pi)\int_{-\infty}^{\infty}|F(w)|\exp[-j\phi(w)]\exp[+jw(t-T)]dw$$

$$=(1/2\pi)\int_{-\infty}^{\infty}F^*(w)\exp(-jwT)\exp(jwt)dw$$

but the right-hand side is precisely the previous expression for $E_0(t)$, the response of the maximal network to unit impulse applied at $t=0$. Hence

$$E_0(t)=e[-(t-T)].$$

The condition for realizability thus becomes: Is it possible to choose T so that $e(-t+T)=0$ for all $t<0$? This will be true if, and only if, T can be chosen so that $e(t)=0$ for all $t>T$. This concludes the proof.

Application

We shall apply the above results to the computation of the noise suppressing efficiency of a double RC circuit (Fig. 1) for the case in which the superimposed thermal noise has a flat frequency distribution. We define the noise suppressing efficiency of a given network in the detection of a given pulse superimposed on a given distribution of fluctuation noise as the ratio: actual (S/N)/optimal (S/N).

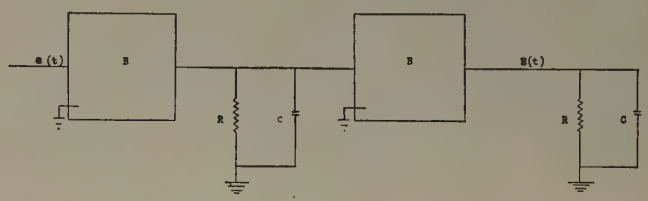

Fig. 1—Double RC circuit. B is an infinite input impedance device whose output current is directly proportional to the input voltage.

Case 1: Rectangular Pulse

We compute the efficiency of the circuit of Fig. 1 in the detection of rectangular pulses. We can write

$$e(t)=1,\ 0\leqq t\leqq T$$

$$0,\ t<0,\ T<t \quad \text{i.e.,}\quad e(t)=S_{-1}(t)-S_{-1}(t-T)$$

$$\sigma(w)=1$$

$$H(w)=[a/(a+jw)]^2 \text{ (for } a=1/RC \text{ this is the response of Fig. 1).}$$

From the Corollary: Optimum $(S/N)=\sqrt{T}$. We compute the actual S/N:

Laplace transform of input signal is

$$F(p)=[1-\exp(-pT)]/p.$$

Hence

$$E(t)=\frac{a^2}{2\pi j}\int_{-j\infty}^{j\infty}[1-\exp(-pT)]\exp(pt)dp/[p(a+p)^2].$$

Integrating in the complex plane, maximizing with respect to t and dividing by

$$N=\sqrt{(1/2\pi)\int_{-\infty}^{\infty}|H(w)|^2dw}=\sqrt{a}/2,$$

[5] G. E. Valley and H. Wallman, "Vacuum Tube Amplifiers," McGraw-Hill Book Co., Inc., New York, N. Y., pp. 721–727; 1948.

we obtain

$$S/N = 2\sqrt{T}\, g(aT)$$

where

$$g(x) = \frac{(\exp x) - 1}{\sqrt{x}} \exp\left[-\frac{x \exp x}{(\exp x) - 1}\right],$$

hence

$$\text{efficiency} = (S/N)/\text{optimum}\,(S/N) = 2g(aT) = 2g(T/RC).$$

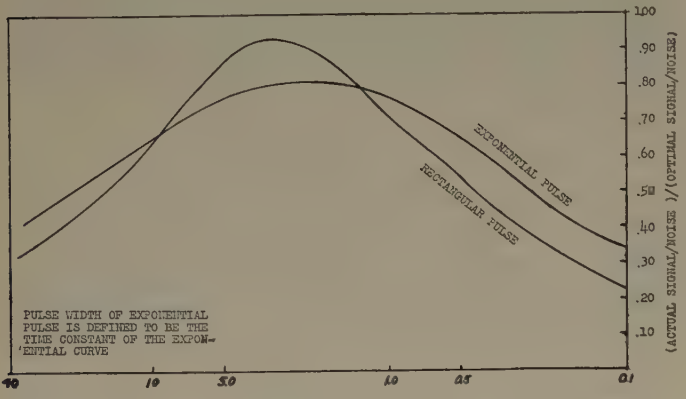

Fig. 2—Noise suppressing efficiency of double *RC* circuit in the detection of a pulse superimposed on fluctuation noise having a flat frequency distribution.

The functional relationship between efficiency and T/RC is shown in Fig. 2. Maximum efficiency is 93 per cent and occurs for pulse width $= 2.98\ RC$ (2.98 is an approximation to double the root of

$$\frac{\sinh z}{z} = \sqrt{2}).$$

Case 2: Exponentially Decaying Pulse

The problem is precisely that of Case 1, except that now

$$e(t) = \exp(-bt)S_{-1}(t).$$

Using Corollary: Optimum $S/N = 1/\sqrt{2b}$. Computing the actual S/N, the output is given by

$$E(t) = \frac{1}{2\pi j}\int_{-j\infty}^{j\infty} a^2 \exp(pt)dp/[(p+b)(p+a)^2];$$

evaluating the integral, maximizing with respect to time and dividing by N we obtain

$$S/N = 2\psi(a/b)/\sqrt{b}$$

where

$$\psi(y) = \frac{y^{3/2}}{y-1}\, x \exp\left[-x\frac{y}{y-1}\right]$$

and where x is the solution of

$$y = (\exp x - 1)/x.$$

Hence, efficiency $= (S/N)/\text{optimum}\,(S/N) = 2\sqrt{2}\,\psi(a/b)$. The relationship is shown in Fig. 2. Maximum efficiency in this case is 81 per cent and occurs when pulse width/$RC = 2.18$ (taking pulse width to be time constant of the exponential decay).

The Measurement of Contact Difference in Potential on Certain Oxide-Coated Cathode Diodes*

I. E. LEVY†

Summary—**Contact difference in potential for a conventional-type oxide-coated cathode diode is defined in terms of voltage required to establish zero field between the anode and cathode. Contact difference in potential has been found to be relatively unaffected by a wide fange of impurities added to the coating. Tests have shown that the E_{ct} measurement is a sensitive technique for observing changes which take place on an initially clean anode.**

THE PURPOSE of this study was to determine the effect on contact difference in potential of (1) various impurities added to the conventional radio-tube cathode coating and (2) the anode deposit from the cathode due to tube processing techniques.

I. Conventional Diodes

The diode structure chosen for the first part of this work is a diode of conventional receiving tube design, utilizing a cylindrical cathode and anode.

* Decimal classification: R331×R262.9. Original manuscript received by the Institute, October 21, 1949; revised manuscript received February 27, 1950.

This work was sponsored by the Office of Naval Research as part of contract N7 ONR-389.

† Raytheon Manufacturing Co., Newton, Mass.

Definition of Contact Difference in Potential

Contact difference in potential for a diode of this kind will be defined as the applied voltage required to establish an average of zero electric field in the space halfway between the cathode and anode in the absence of space charge. The contact difference in potential as defined in this manner depends on the difference between the average work function of the anode and the average work function of the cathode. Changes in work function resulting from impurity migrations and parts and processing changes would enable one to determine qualitatively to what extent the surface of the anode has been affected.

Measurement of Contact Difference in Potential

The measurement of contact difference in potential described below is based upon a so-called "low-field" temperature-limited emission test. The conditions for this low-field test are $E_f = 1.75$ v, $E_p = 4$. Since our test diode has a 6.3-v heater, this test gives a means of observing temperature-limited direct-current emission

and still keeps the anode voltage below the point where poisoning might occur due to breakdown of oxide and chlorides on the anode surface.

Fig. 1 shows E_p-I_p plots of three tubes, widely different for low-field emission, but having essentially the same contact difference in potential. Curve *abcd* in Fig. 1, for example, shows that the true zero field is located somewhere between points *b* and *c*. True zero field for the other curves will be located also somewhere in the vicinity of the bend of the E_p-I_p curve. On these E_p-I_p curves, the electron emission is noted under the low-field test, namely 4 v applied potential and cathode

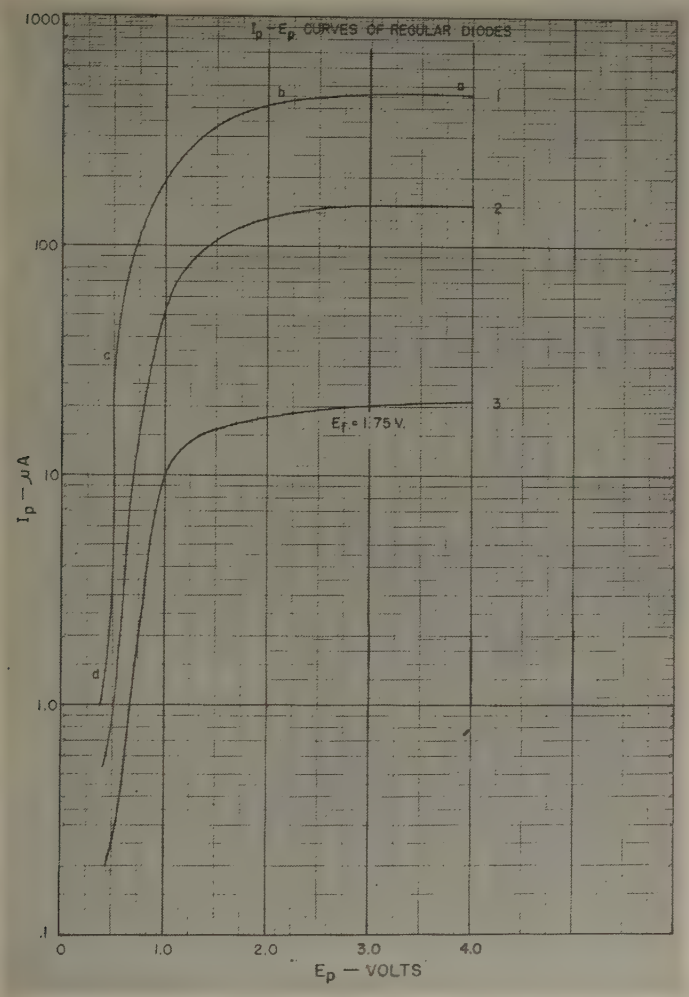

Fig. 1—Curves of 3 diodes with widely varying low-field emission, but essentially identical contact difference in potential.

temperature of 643°K (E_f 1.75). Then the applied voltage necessary to give 1 per cent of this low-field emission current is determined. At this voltage which will be defined as $E_{.01}$, this great reduction in current has resulted from the fact that only high-energy electrons are able to cross the space in such a retarding field. In the life history of this particular diode, it is anticipated that changes in $E_{.01}$ brought about by the condensation of impurities on the anode, and other changes in the anode and cathode surface will be a reasonably accurate measure of the *changes* of true contact difference in potential as previously defined. In the absence of the effects due to surface inhomogeneity (anode and cathode) and space charge, zero field current should be observed at $E_{.01}$ plus 0.25 v. This added term represents

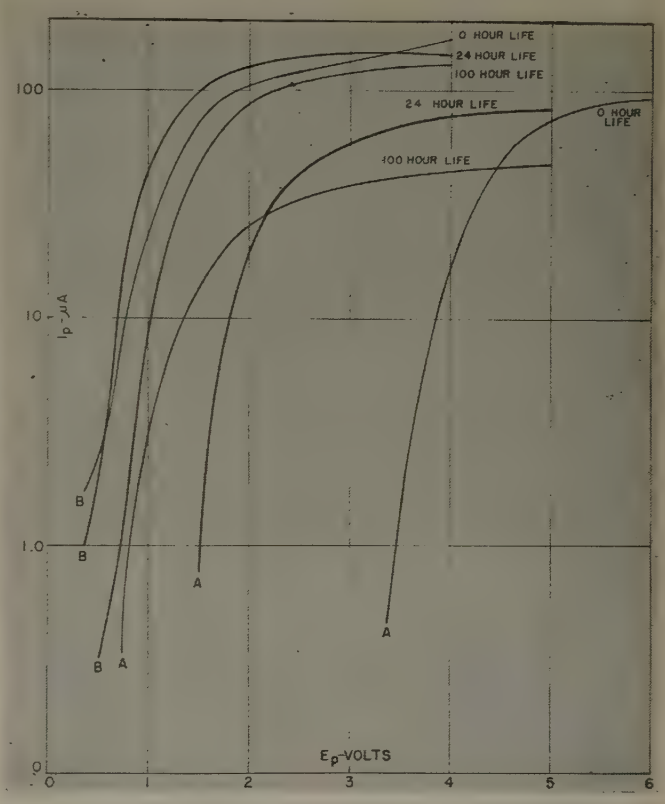

Fig. 2—E_p-I_p curves for special diodes with sliding sleeve and control after various time intervals on life.

Note: *A* lots are special diodes with sliding sleeve. *B* lots are control, sleeve omitted. All during activation processing of *A* lots, the sleeve protected the anode. Tubes were then put on life so that the sleeve no longer protected the anode from any deposit.

the change in voltage required at a temperature of 643°K to change the emission by a factor of 100.[1] An inspection of all curves in Fig. 1 shows that the observed change in current for this range of voltage is far less than that predicted. This discrepancy is undoubtedly the result of the cathode and anode inhomogeneity and space charge enumerated above. A reasonable guess as to the influence of these factors brings us to the conclusion that the true contact difference in potential is, on the average, approximately equal to $E_{.01}+0.7$; this will be referred to as E_{ct}. Thus, $E_{ct}=E_{.01}+.7$.

Correlation of Contact Difference in Potential with Cathode Coating Impurities

Seven lots of diodes, consisting of various impurities added to the conventional double carbonate coating, "Radio Mixture #3," were checked for E_{ct}. The results summarized in Table I show no significant difference in E_{ct} between these lots both initially and after life.

[1] Computed by

$$\frac{1}{100} = e^{-\epsilon V/KT}.$$

where

ϵ = electron charge 1.6×10^{-19} coulombs
K = Boltzman constant 1.38×10^{-23} joules per degree
T = absolute temperature 643°K.

TABLE I

CONTACT DIFFERENCE IN POTENTIAL ON LOTS WITH VARIOUS IMPURITIES ADDED TO THE CATHODE COATING

Lot	Average E_{ct} Volts Zero Hours	Average E_{ct} Volts After 500 Hours Life
#735—Melt *E* (high Cu & Mg)	1.1	1.2
#737—Melt *I* (high per cent S & Si)	1.1	1.3
#783—.35 per cent Ta	1.2	
#785—Control for .35 per cent Ta	1.2	
#747—Metallic chromium .15 per cent	1.2	1.3
#745—Metallic chromium .05 per cent	1.2	1.3
#749—Control for metallic chromium	1.1	1.3

II. Diodes Made with Sliding Sleeve over the Cathode

In order to determine the effect of plate deposit due to tube processing on contact difference in potential, a diode was developed with a sliding sleeve between the cathode and anode in such a way that the sleeve could protect the anode from any deposit, while the tube was in the conventional upright position. When the tube was inverted, the sliding sleeve would fall away and leave the anode exposed to any deposit from the cathode.

Constructional Features of Special Diode

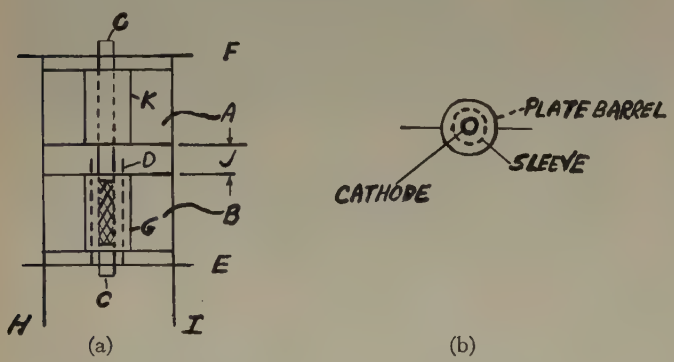

Fig. 3—(a) Constructional features of special diode. (b) Top view.

In Fig. 3, two half-diode plates *A* and *B* with cylindrical barrels *K* and *G* are mounted on regular stem-plate supports *H* and *I*. The cathode *C* is only coated on the lower end as indicated by the shaded portion. The sliding sleeve *D* in the normal upright position of the tube rests on the bottom mica *E* and completely protects the inside of the barrel *G* from any cathode deposit. The sleeve is large enough so that it can never touch the cathode. During processing and activation of the cathode any deposit from the cathode will land on the sleeve *D* and leave the plate barrel *G* clean. Then when the tube is to be tested, or a current is to be drawn to anode *B* the entire structure is inverted. The sliding sleeve *D* will then slide into plate barrel *K* and rest against the top mica *F*.

Experiments Conducted on Special Diode

Six special diodes made with sliding sleeves and six of a control lot were made with standard processing procedures. The control-lot tubes were identical to the special diodes, except that the sleeve was omitted. On the special tubes the sleeve protected the anode from any deposit all during exhaust processing. After activation was completed, the special diodes were inverted so that the sliding sleeve no longer protected the anode. In this position average $E_p = I_p$ curves for the six tubes from each lot were drawn at $E_f = 1.75$ for 0, 24, and 100 hours on life. The life-test conditions were $E_f = 6.3$, $E_b = 100$ v dc, and $R_L = 1{,}000$ ohms.

I_p was about 80 ma per square centimeter.

Test Results

The life data for the special diode with sliding sleeve and control are plotted in Fig. 2.

It is seen that tubes made with the sliding sleeve have considerably higher contact difference in potential (E_{ct}) than the control at zero hours life. The reason for this is probably due to the fact that diodes made with the sliding sleeve have a much higher anode work function because of the clean anode. As life progressed, the contact difference in potential (E_{ct}) of the diodes made with the sliding sleeve decreased, until at the end of 100 hours, tubes made with the sliding sleeve had lower E_{ct} than the control. This can be explained by the fact that on life, the anode was not protected from the cathode and picks up considerable Ba, Sr, and other impurities which lowered the work function and decreased E_{ct}. When E_{ct} was computed for these curves by the technique already discussed, it was seen that, whereas the control had an insignificant E_{ct} change on life, the tubes with the sliding sleeve showed a decrease in E_{ct} of about 87 per cent after 100 hours.

Conclusions

It is evident that this E_{ct} test is a sensitive technique for observing changes which take place on the surface of an initially clean anode. Since with the conventional diode structure, it seems impossible to prevent the deposition of Ba, Sr, and other impurities onto the anode during normal processing, the low readings of E_{ct} which were obtained on the diodes which served as a control for the sliding sleeve tubes (see Fig. 2) must be largely due to this deposition and subsequent lowering of the anode work function. While it is true that the E_{ct} measurements do not offer much information concerning the cathode, they are valuable in supplying information concerning the condition of the anode.

Acknowledgments

The author is greatly indebted to W. B. Nottingham of Massachusetts Institute of Technology for his help in formulating the E_{ct} testing technique; to J. Cardell of Raytheon Manufacturing Company who was responsible for supplying many of the test lots; and to R. L. McCormack of Raytheon for his over-all supervision and guidance.

Microwave Attenuators for Powers up to 1,000 Watts*

H. J. CARLIN†, MEMBER, IRE, AND E. N. TORGOW†, ASSOCIATE MEMBER, IRE

Summary—**A new type of high-power, broad-band probe attenuator is described which operates on a capacitance-divider principle. A typical design reduces input powers up to 1,000 watts, by a fixed ratio, to a low level which can be conveniently measured by bolometric means. The prototype consists of a probe, a buffer-equalizer attenuator, and a lossy tapered matched load. Two designs are required to cover the frequency band 1,000 to 10,000 Mc with relatively constant attenuation and voltage standing-wave ratio below 1.30.**

I. Microwave Measurements at High Power Levels

THE TESTING of microwave equipment at high power levels is most conveniently done by the use of conventional test equipment which is designed to operate at nominal power magnitudes. The type of device described here accepts powers up to 1,000 watts average at its input terminals, and at its output terminals provides a level which is down a fixed multiple of the input power. It has been possible to do this with an input voltage standing-wave ratio less than 1.30, over a broad band, and an attenuation swing which is quite nominal. Such a device is very useful, since it may be calibrated as an attenuator at low power levels.

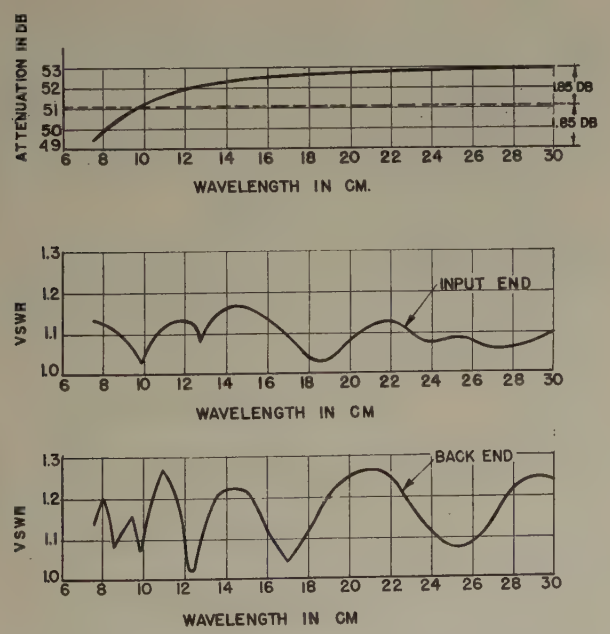

Fig. 1—Voltage standing-wave ratio and attenuation characteristics of the high-power 50-db probe-type $\frac{7}{8}$-inch line attenuator: frequency range, 1,000–4,000 Mc.

It is then applied to the high-power measurement by terminating the device in a low-level power meter head, which may be a bolometer designed to operate up to, say, 1 mw. Accepting this latter figure as representative, a 100-watt attenuator should produce a power level reduction of 50 db, and a 1,000-watt unit an attenuation of 60 db. Fig. 1 shows the performance characteristics of a 50-db unit for the frequency band 1,000 to 4,000 Mc. It will be noted that maximum voltage standing-wave ratio (either looking in at the input terminals or in at the output terminals) is less than 1.30, and the attenuation variation is ± 1.85 db in 50 from 1,000 to 4,000 Mc, or ± 1.00 db in 50 from 1,000 to 3,000 Mc. Characteristics of other units up to 60 db, and covering frequencies up to 10,000 Mc are shown in Figs. 2, 3, and 4.

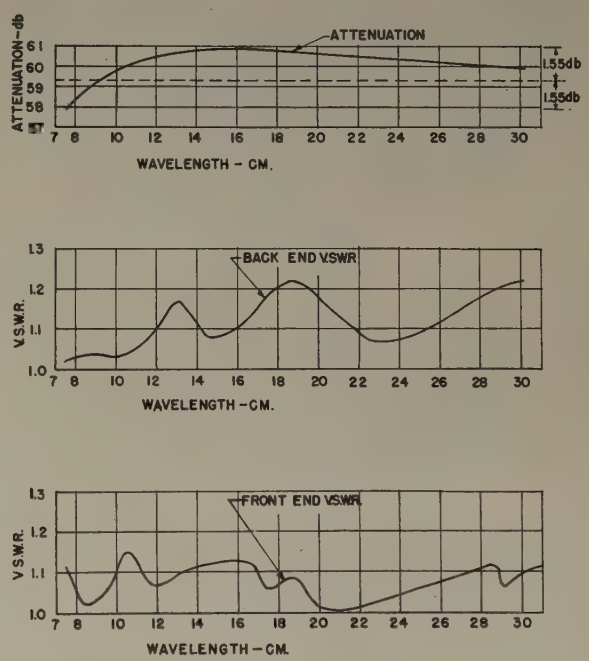

Fig. 2—Voltage standing-wave ratio and attenuation characteristics of the high-power 60-db probe-type $\frac{7}{8}$-inch line attenuator: frequency range, 1,000–4,000 Mc.

II. Design of the High-Power Attenuator

A. General Description

The high-power attenuator is essentially a combination of three components. Fig. 5 shows a schematic diagram of the device. The first component is a broad-band probe. This, as will be seen subsequently, operates as a capacitive voltage divider and effects the major portion of the attenuation. The second component is a metallized film attenuator which is connected in tandem with the output of the probe. This device buffs out the

* Decimal classification: R396.9×R310. Original manuscript received by the Institute, October 11, 1949; revised manuscript received, February 6, 1950. Presented at the 1949 IRE National Convention, March 7, 1949, New York, N. Y. This paper was prepared in connection with Watson Laboratories Contract W33-038-ac-13848 and Navy Bureau of Ships Contract NObs-28376 with the Polytechnic Institute of Brooklyn.

† Microwave Research Institute of the Polytechnic Institute of Brooklyn, Brooklyn, N. Y.

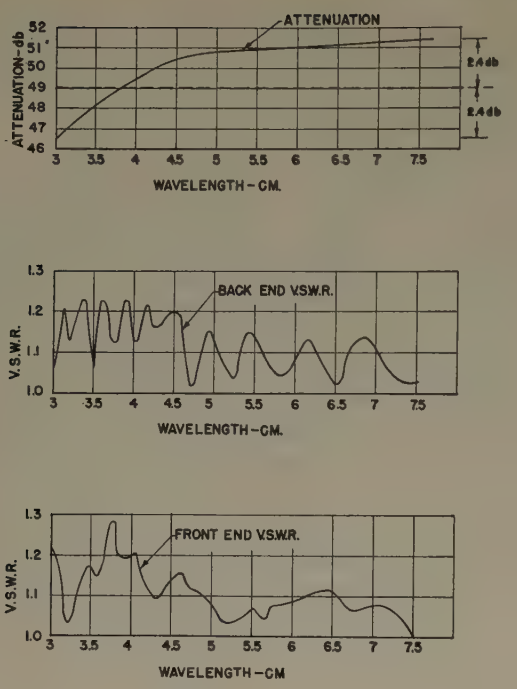

Fig. 3—Voltage standing-wave ratio and attenuation characteristics of the high-power 50-db probe-type $\frac{3}{8}$-inch line attenuator; frequency range, 4,000–10,000 Mc.

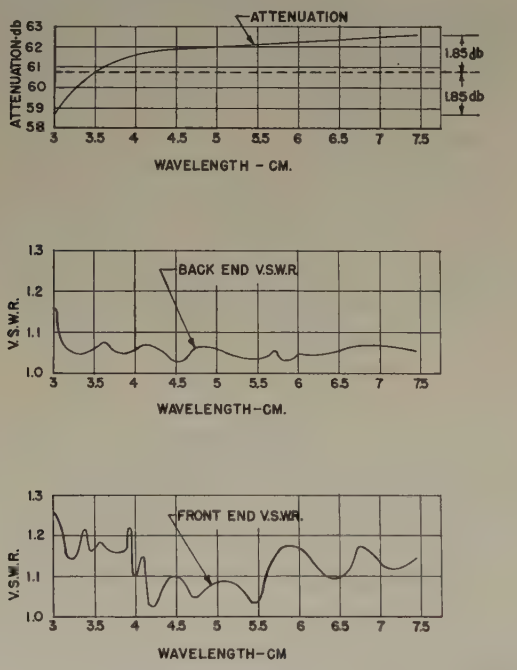

Fig. 4—Voltage standing-wave ratio and attenuation characteristics of the high-power 60-db probe-type $\frac{3}{8}$-inch line attenuator: frequency range, 4,000–10,000 Mc.

high impedance mismatch which exists at the output of the proble. In addition, this attenuator has an attenuation variation with frequency which is in the opposite sense to that of the probe; thus partial attenuation equalization results. The third component of the attenuator is a broad-band load which absorbs most of the power. As shown in Fig. 5, this load is permanently connected in the main line. The operation of the high-power attenuator depends on the characteristics of each of these components.

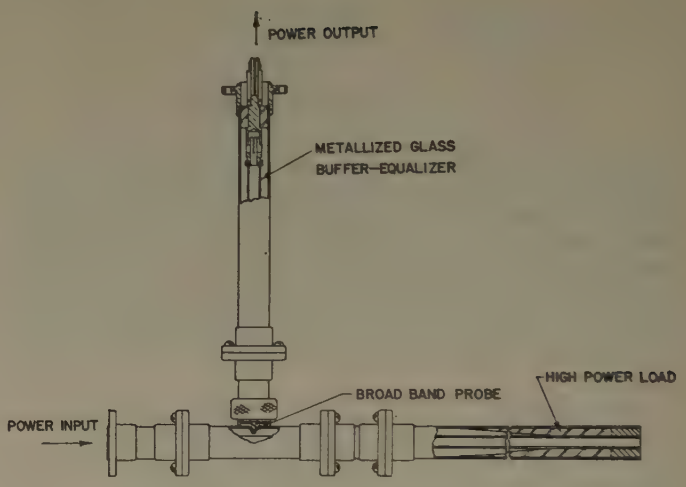

Fig. 5—Schematic diagram of broad-band high-power attenuator.

Fig. 9 is a photograph of three high-power attenuators for different power and frequency ranges. The illustration shows these attenuators terminated in broad-band bolometer powermeters for use in the measurement of high radio-frequency power levels.

B. The Attenuating Probe

Fig. 6(a) is a schematic diagram of the probe construction, and Fig. 6(b) shows an approximate equivalent circuit. If the probe inductance is neglected, it can be seen that the device functions as a capacitive voltage divider. The probe-to-center-conductor capacitance is

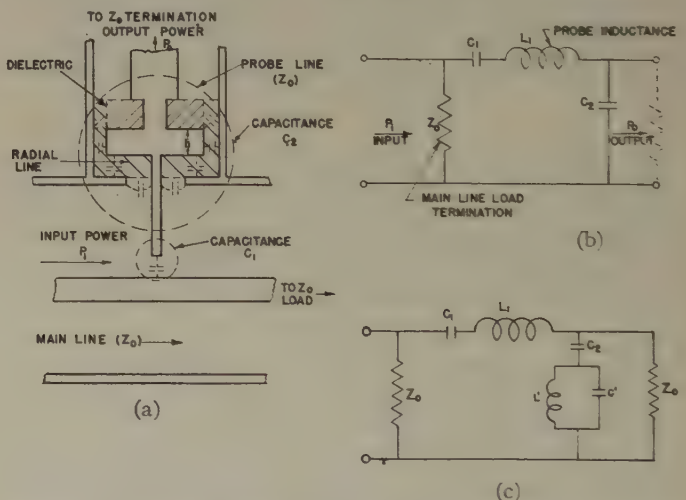

Fig. 6—(a) Schematic diagram of probe. (b) Approximate equivalent circuit of probe. (c) Derived equivalent circuit.

small and is represented by C_1. The shunt capacitance consists of discontinuity capacitance, and the capacity that exists between the face of the probe line disk and the milled flat surface of the outer conductor which surrounds the hole through which the probe enters the main line. The length "h" is small compared to wavelength, so that all the capacities may be considered lumped together. The end of the probe line is surrounded by dielectric to increase the shunt capacity, and this si-

multaneously acts as a mechanical bead support. In the initial calculations of C_1 and C_2, the discontinuity capacitance formulas of Whinnery and Jamieson[1] were used in addition to the simple parallel-plane capacitance equation. Final attenuation values were obtained experimentally by adjusting the probe length. Even though simplifying assumptions were made for calculating the capacitances and the mechanical dimensions of the probe line, comparatively little redesign was required. To check the assumed form of the circuit shown in Fig. 6(b), an equivalent lossless four-pole was determined from the measured insertion loss characteristics of the probe. To do this, a rational approximating function was determined by interpolation to characteristic curves of the probe, such as that shown in Fig. 7. A network was then realized by the Darlington[2] reactance four-pole synthesis procedure. The form of the result is shown in Fig. 6(c) and this essentially agrees with the circuit of Fig. 6(b). The antiresonance in the shunt branch occurs well outside the frequency range of operation and may be related to a resonance of the radial line section shown in Fig. 6(a).

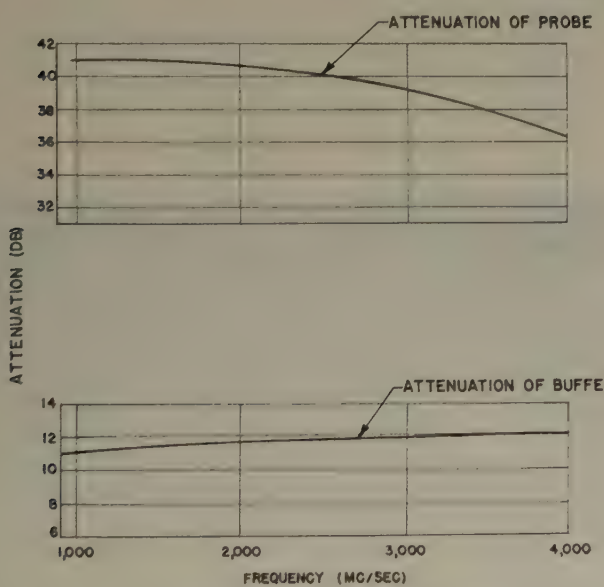

Fig. 7—Attenuation characteristics of probe and metallized buffer, (1–4 kMc).

Referring to Fig. 6(b) and neglecting the inductance L_1, the ratio of input to output power is given by

$$\alpha = 10 \log \frac{P_i}{P_0}$$

$$= 10 \log \left[\frac{1}{(\omega C_1 Z_0)^2} + \left(\frac{C_2}{C_1} + 1 \right)^2 \right] \text{db}. \qquad (1)$$

If the normalized probe reactance, $1/\omega\, C_1 Z_0$, is small with respect to the ratio C_2/C_1, then the attenuation is approximated by

$$\alpha = 10 \log \frac{P_i}{P_0} = 20 \log \left(\frac{C_2}{C_1} \right) \text{db}. \qquad (2)$$

Thus for 40 db of probe attenuation, the design parameters at the high-frequency end of the band (4,000 Mc) may be chosen as

$$\frac{C_2}{C_1} = 100$$

$$\frac{1}{\omega C_1} = 10 Z_0, \qquad (3a)$$

where the probe impedance is made large with respect to the characteristic impedance of the main line to prevent the introduction of excessive reflection. Then

$$\alpha_{4,000} = 40.14 \text{ db}$$

$$\alpha_{1,000} = 40.72 \text{ db}. \qquad (3b)$$

This ideal performance was actually not realized as seen in Fig. 7, which shows attenuation versus frequency for the probe alone. The attenuation drops sharply at the high-frequency end of the band. This is essentially due to the probe inductance, which reduces the effective capacitive reactance of the probe, $[1/\omega C_1 - \omega L_1]$, markedly at the high-frequency end of the band. The buffer attenuator discussed in the next section, partially compensates for this.

C. The Buffer Attenuator

The back end of the probe attenuator presents an impedance which is badly mismatched to the characteristic impedance of the probe line. If the probe is terminated in a slightly mismatched load, a reflection factor results which fluctuates with frequency (as the reflection magnitude and phase of the load vary) and which is not easily corrected for.

If the load has a voltage standing-wave ratio of ρ_L, and the probe a back-end voltage standing-wave ratio of ρ_g, the maximum variation of output level (due to the possible phasings of the load and probe impedances) is given by

$$\Delta D = 10 \log \frac{\text{max power level}}{\text{min power level}}$$

$$= 20 \log \frac{1}{\rho_L} \frac{\rho_g \rho_L + 1}{(\rho_g/\rho_L) + 1} \text{db}. \qquad (4)$$

To see the order of magnitude of this effect, observe that if ρ_g becomes very large,

$$\Delta D \doteq 20 \log \rho_L \text{ db}$$

$$\rho_g \gg 1. \qquad (5)$$

Thus a load of arbitrary phase and of maximum voltage standing-wave ratio equal to 1.30, may introduce a fluctuation in power level of as much as 2.28 db.

[1] J. R. Whinnery, H. W. Jamieson, and T. H. Robbins, "Coaxial line discontinuities," Proc. I.R.E., vol. 32, pp. 695–710; November, 1944.

[2] S. Darlington "Synthesis of reactance four-poles," *Jour. Math. & Phys.*, vol. 28; September, 1939.

In order to reduce this, a metallized glass attenuator, matched at both ends and designed according to methods described by Carlin and Griemsmann[3], is placed in tandem with the probe output. An attenuator nominally valued at 13 db, gives a resultant maximum back end voltage standing-wave ratio of 1.30. In this case the variation in attenuation, due to the junction reflection where the buffer joins the probe line, is calibrated into the over-all performance of the probe-buffer combination. The maximum uncertainty in output level for a load with a voltage standing-wave ratio of 1.30 terminating the buffer may now be calculated by letting $\rho_g = 1.30$ and $\rho_L = 1.30$ in (4). The resultant maximum swing is 0.28 db. Since voltage standing-wave ratio of load and buffer do not reach 1.30 simultaneously, the reflection error in practice is actually considerably less than the above figure.

In addition the attenuation loss of the buffer varies in a direction opposite to that of the probe.[3] Fig. 7 shows the attenuation curve of the buffer alone. The result of adding the buffer to the probe gives the overall attenuation curve shown in Fig. 1, and the total attenuation is close to 50 db over the band. The buffer introduces approximately 0.9 db of equalization.

D. The High-Power Load and Power Ratings

It is desirable that the coaxial load which is placed at the termination of the main line be very well matched over the frequency band. If the voltage standing-wave ratio of this load is $\rho_T = 1.30$, then the maximum possible variation in probe voltage is 1.30. Of course, the load is permanently fixed to the line as an integral portion of the attenuator, so that the effect of this probe voltage variation is included in the attenuator calibration. However, a large voltage standing-wave ratio gives rise to to an erratic calibration curve of attenuation versus frequency. The actual load used has a maximum voltage standing-wave ratio of 1.08 over the band from 1,000–4,000 Mc, and a performance curve is shown in Fig. 8.

To achieve this design, a tapered lossy dielectric is used, as shown in Fig. 8. The dielectric material is a mixture of carbon and X-pandotite which is capable of absorbing large powers. The design is based on a report by Carlin and Blass[4] which considers the solution of a lossy tapered transmission line.[5] From a thermal point of view it was found that this type of coaxial load could be rated at an average power capacity of 1,000 watts if suitably supplied with cooling fins and a blower. Since high voltage tests on the probes indicated breakdown powers of 324 kw peak for the $\frac{7}{8}$-inch line unit, and 86 kw peak for the $\frac{3}{8}$-inch line unit, the load becomes the deciding factor for average ratings, and the probe breakdown determines the peak power rating of the entire attenuator assembly.

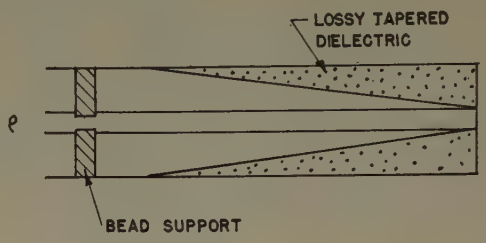

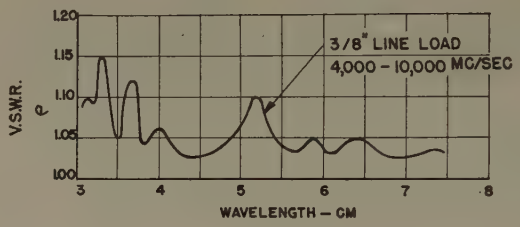

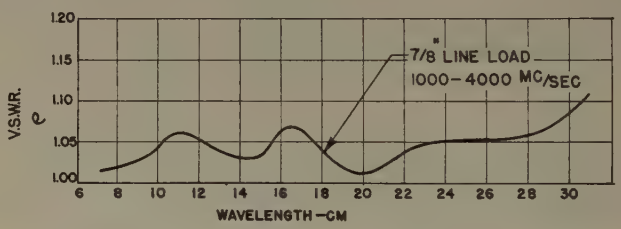

Fig. 8—Characteristics of coaxial high-power loads.

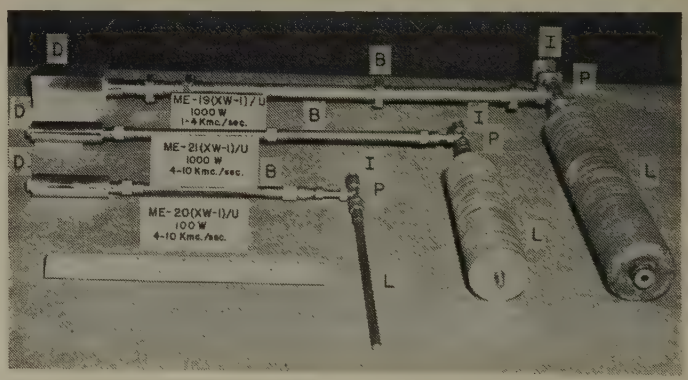

Fig. 9—Photograph of high-power probe attenuators; *B*—Buffer-Equalizer, *D*—Bolometer Powermeter, *I*—Input to Attenuator, *L*—High Power Load, *P*—Probe.

Conclusion

The units described in this paper have proven extremely useful as high-power attenuators, presenting small variation in attenuation over large frequency bands, and having input voltage standing-wave ratios less than 1.30 at all frequencies. As can be seen from Figs. 1, 2, 3, and 4, the 50-db unit has an attenuation variation of 51.1 ± 1.85 db from 1,000 to 4,000 Mc and the 60-db unit 59.35 ± 1.55 db over this band. The $\frac{3}{8}$-inch line units show swings of 49.0 ± 2.4 db and 60.75 ± 1.85 db from 4,000 to 10,000 Mc. This constitutes excellent performance for attenuators in the microwave region.

[3] H. J. Carlin, and J. W. E. Griemsmann, "A Bead Supported Coaxial Attenuator," 1947 *Proc. Natl. Electronics Conf.*, pp. 79–89.

[4] H. J. Carlin, and J. Blass, Report R-167-48, "Theoretical Attenuation Characteristics of a Tapered Dielectric Coaxial Attenuator," October 15, 1948. Prepared under Contract NObs-28376, sponsored by Bureau of Ships.

[5] Detailed test procedures on the loads are given in Polytechnic Institute of Brooklyn Report R-198-49, PIB-142, dated April 1949, Contract No. W33-038-ac-13848, by M. Tanenbaum.

Microwave Attenuation Statistics Estimated from Rainfall and Water Vapor Statistics*

HOWARD E. BUSSEY†

Summary—**Annual distribution curves are obtained for values of total atmospheric attenuation over a 50-km path and a 1-km path at Washington, D. C. These results are obtained by analyzing the available meteorological data, though these are usually ill-suited to the purpose; theoretical coefficients are used for converting into radio attenuation values. The problem of obtaining rainfall rates on the longer path is solved empirically using data from a network of rain gauges; these data, together with additional inference, indicate that annual statistics for hourly point depths may be interpreted as equivalent to instantaneous rates on a path about 50 km long. Extensions of the results to other portions of the country are discussed.**

Introduction

MICROWAVES are attenuated by oxygen, water vapor and precipitation in the atmosphere.[1,2] This attenuation increases rather sharply for frequencies above 10,000 Mc, and a quantitative knowledge of its occurrence should prove useful in the selection or allocation of microwave frequencies.

The present paper estimates the expected number of hours per year that a fixed transmission path will experience various values of total atmospheric attenuation. The attenuation statistics are obtained from existing meteorological data, using accepted theoretical or experimental coefficients for converting the various meteorological concentrations into radio attenuation values. The estimates are obtained for a 50-km path and for a short path, about 1-km long. The attenuation statistics are computed specifically for the locality of Washington, D. C.; however, the analysis is quite general and high rainfall rates are discussed for the whole United States.

The main problem which had to be solved in order to obtain attenuation statistics was that of obtaining path rainfall rates. (A path rainfall rate is defined as the space average of the point rates along a path.) Path rates, as such, have never been observed, and in fact techniques have not been available for observing them; they must be inferred from point data and it is not obvious how rainfall statistics for a long path are related to those from a point; it is not expected that a point rate will extend uniformly over a large area.

The statistical meteorological approach which was employed has the advantage that results are obtained with much less expense and effort than would be required in an experimental microwave approach. It would, of course, be desirable to obtain experimental confirmation of the predictions made here; however, the experiment would be very difficult since it would involve year around recording of the signal level over a long path, and changes in signal level due to refractive bending would have to be separated from the results. It is also true that an experiment might need to run for several years in order to get a stable climatological average.

It should be noted that the theoretical coefficients for rain attenuation[3] have been used in the present report, and these are so far not entirely confirmed by the limited experimental evidence. An attenuation coefficient as used here states the loss of power of a radiation in decibels per kilometer due to absorption and scattering. Free-space attenuation or other attenuation associated with the geometry of the transmission is not included.

Water Vapor Statistics

For a given path it is assumed that the attenuation due to oxygen is constant. This is reasonable since daily or seasonal changes in pressure or temperature alter the oxygen concentration negligibly; then only the concentration of rainfall and water vapor occurring over a path are subject to important variations.

Water vapor statistics for a point may be obtained from ordinary meteorological observations. The absolute humidity is most directly related to the attenuation. Using Weather Bureau Form 1030 the absolute humidity was obtained for 7:30 P.M. each day during one year at Washington, D. C. This single observation at a point gave annual statistics representative of the total time on a long path. Such a meager sampling is sufficient because of the horizontal homogeneity of air masses and the comparative slowness of the changes.

Fig. 1 shows cumulative distributions for the attenuation statistics at Washington, D. C., based upon the humidity data for one year, 1946, which was a normal year. The lower intercept of each curve is the value of gaseous absorption which is exceeded all of the time, due to the ever-present oxygen plus 1 g/m³ water vapor. Going from 100 per cent to 0 per cent, the water vapor concentration increases from 1 to 21 g/m³ in a fairly linear manner and the attenuation increases as shown.

* Decimal classification: R113.501. Original manuscript received by the Institute, September 20, 1949; revised manuscript received, February 8, 1950. Presented, URSI-IRE Joint Meeting, Washington, D. C., May, 1947; also, San Diego Symposium on Tropospheric Wave Propagation, San Diego, Calif., July, 1949.

† Central Radio Propagation Laboratory, National Bureau of Standards, Washington, D. C.

[1] Regarding rain attenuation, see L. Goldstein, "Radio Wave Propagation Experiments" Summary Technical Report of the Committee on Propagation, NDRC, vol. 2, chap. 10, pp. 148–174; 1946. (Reprinted, 1949, by the Academic Press, New York, N. Y.)

[2] Regarding gaseous absorption, see J. H. Van Vleck, "The absorption of microwaves by uncondensed water vapor," *Phys. Rev.*, vol. 71, pp. 425–433; April, 1947, and references there on oxygen absorption.

[3] The theoretical coefficients used were obtained from three papers; (1) J. W. Ryde and D. Ryde, "Attenuation of centimeter waves by rain, hail, fog and cloud," General Electric Company, Ltd., Wembley, England, May 1945. (2) F. Haddock, "Scattering and attenuation of microwave radiation through rain," paper given at URSI Meeting, May, 1947, Washington, D. C.; (3) L. Goldstein, footnote reference 1.

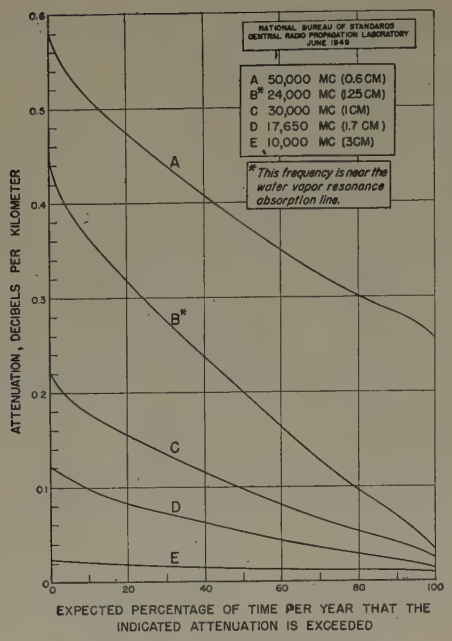
NATIONAL BUREAU OF STANDARDS
CENTRAL RADIO PROPAGATION LABORATORY
JUNE 1949
A 50,000 MC (0.6 CM)
B* 24,000 MC (1.25 CM)
C 30,000 MC (1 CM)
D 17,650 MC (1.7 CM)
E 10,000 MC (3 CM)
* This frequency is near the water vapor resonance absorption line.
ATTENUATION, DECIBELS PER KILOMETER
EXPECTED PERCENTAGE OF TIME PER YEAR THAT THE INDICATED ATTENUATION IS EXCEEDED

Fig. 1—Cumulative distributions for gaseous attenuation values at Washington, D. C. The oxygen attenuation is assumed constant; the distribution arises entirely from variations of the water vapor.

In the final results these statistics of gaseous absorption are correlated with and added to the occasional precipitation attenuation which occurs.

Rainfall Rates Investigation

Point rainfall data, i.e., rates from a rain gage, have been presented occasionally as being of interest in radio-climatology, but generally there has been little or no discussion of what path rates might be expected, given these point rates; the present investigation attempts to remedy this. Successive 1-hour depths (or mean hourly rates) are the precipitation data widely available. We constantly attempt to relate other rainfall data to these available 1-hour point rates data. It is noteworthy in the investigation that the cumulative distribution curve as a whole is the only parameter of rainfall rates which is studied. By observing the whole distribution curve, without peering into its individual parts, one is able to solve approximately a problem which would be very complicated from most other viewpoints.

Rates for a Short Path

First of all it will be assumed that point rates are identical with path rates if the path is short enough; a path 1 km long will be assumed to be short enough. The available rainfall data, namely 1-hour rates, are then interpreted as being directly, mean, 1-hour, 1-km path rates. It is desirable to have instantaneous path rates instead of hourly means, and for this purpose approximately instantaneous point rates are needed.

A general analysis of instantaneous point rates has not yet been published; however, approximately instantaneous rate statistics have been tabulated by the Soil Conservation Service, U. S. Department of Agriculture. Some of these data were graciously lent to the author by Krimgold of the Soil Conservation Service. These tabulations give the rates in successive intervals, each interval being so chosen that the rate is uniform during the interval. These data are instantaneous, to the extent that each chosen interval has a truly uniform rate; the judgment of the coders is accepted in this respect. The shortest interval used was 1 minute, but nevertheless these will henceforth be called instantaneous data.

From these tabulations, distributions were obtained showing how the instantaneous rate distributed itself about the mean rate each hour. Briefly, it was found that on the average, about 20 per cent of the time during an hour was really time of zero rate or of the very low rate known as a "trace"; about 35 per cent of the time, the mean hourly rate was exceeded and to exceed it by five or six times for a few minutes was a fairly common occurrence. These instantaneous distribution curves were used to break down all of the mean 1-hour rates[4] at Washington into shorter "instantaneous" segments. These segments were compounded into a cumulative distribution curve; thus instantaneous point rates, assumed to be also instantaneous 1-km path rates, were obtained.

The annual cumulative distribution curves for the mean 1-hour rates and the computed instantaneous rates are shown in Fig. 2. In addition, Fig. 2 shows distribution curves for mean 2-hour rates and mean 30-minute rates. These curves were obtained by making a percentage comparison of 2-, 1-, and $\frac{1}{2}$-hour data for one year or more, and then applying these same percentage comparisons to the long-time distribution of 1-hour means in Fig. 2.

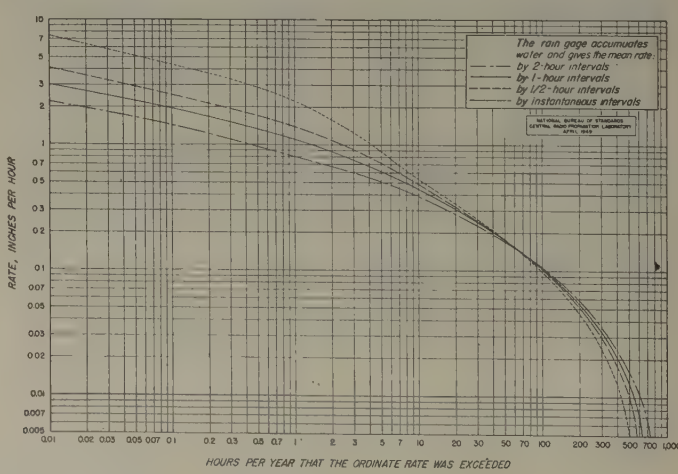
The rain gage accumulates water and gives the mean rate:
by 2-hour intervals
by 1-hour intervals
by 1/2-hour intervals
by instantaneous intervals
RATE, INCHES PER HOUR
HOURS PER YEAR THAT THE ORDINATE RATE WAS EXCEEDED

Fig. 2—Cumulative distributions for point rates at Washington, D. C. The 1-hour curve is based upon observed long-time data. The other 3 curves are not actually observed but are computed or derived from the 1-hour curve.

The four curves show good regularity, except for a slight dip in the instantaneous curve, the cause of which is not known. The indicated total duration of measurable rainfall is seen to increase as the observing period grows longer, since more and more time of zero rate gets

[4] Long-time statistics for mean 1-hour rates at Washington were obtained mostly from R. T. Zock, "Climatic Handbook for Washington, D. C.," U. S. Government Printing Office, pp 109–123; 1949.

included in the successive means. The apparent annual duration of rain increases about 16 per cent with half-hourly means, 25 per cent with 1-hourly means and 50 per cent with 2-hourly means.

By an integration process, the annual depth of water expected at Washington, D. C., namely 42.2 inches, can be calculated from each of these curves. Since the annual depth of water must remain constant, regardless of the observing interval used, the curves naturally cross over. Rather unexpectedly they seem to intersect at about the same point; no particular reason for this is apparent.

The information in Fig. 2 is useful not only for a short (1-km) path, but also for interpreting certain aspects of the investigation below, of rates on a 50-km path.

Rates on a 50-Km Path

For rates on a longer path, one desires data from a widespread, fine, synchronized network of rain gages. The best of such data have been published by the Soil Conservation Service for the Muskingum area of Ohio.[5] These are successive half-hourly maps showing the precipitation depths at some 450 rain gauges in an area roughly 90 miles in diameter. To obtain statistics from these maps it is necessary to select a definite path for study. Almost any length of path could have been studied; a 50-km length was chosen as being appropriate to microwave communications problems.

Two 50-km paths at right angles to each other intersecting approximately as a "T," were selected in the vicinity of Mt. Vernon, Ohio. Using a transparent overlay to locate these paths, the 30-minute mean 50-km path rates were estimated for each path during the year 1938. At the same time, mean 1-hour point rates for one point in each path were obtained by adding successive half-hourly depths. The points used here were at such ends of the paths as to be separated.

Cumulative distribution curves for the 30-minute path rates and their associated 1-hour point rates are shown in Fig. 3. One curve averages the data of the two paths and the other curve averages the data from the two selected points. In order to indicate the good agreement of the data from the two paths and the two points, the cumulative frequency points have been plotted side by side, and in several instances they superpose. At high rates the statistics become somewhat unstable because so few occasions are present.

To be sure, a longer period of comparison than one year would be desirable. Lacking this, however, Fig. 3 will be assumed to show the relation which exists between 1-hour point statistics and 30-minute 50-km path statistics. The duration of the path rates exceeds that of the point rates by about 12 per cent at the 0.01 inch per hour level. Here, as in Fig. 2, the curves must then be expected to cross over, since the average annual depth of precipitation on a path ought to be the same

[5] U. S. Dept. of Agriculture, Soil Conservation Service. "Precipitation on the Muskingum River watershed, by 30-minute intervals," 1938.

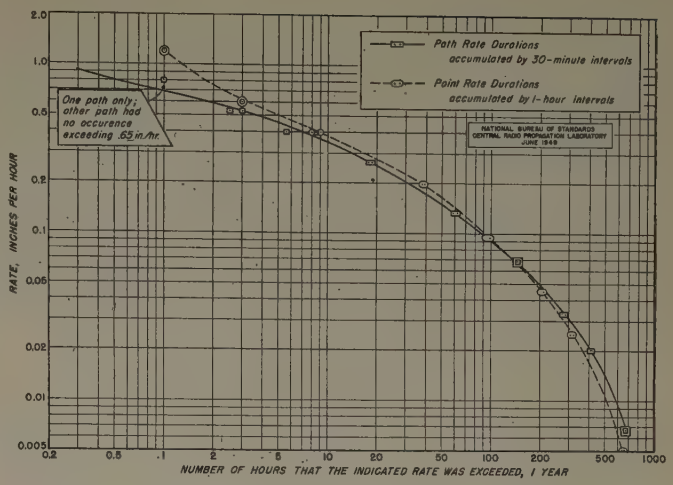

Fig. 3—Cumulative distributions for 30-minute 50-km path rates and 1-hour point rates of rainfall. Data for two paths and two points (one point in each path) are shown, and an average curve is constructed in each case. The paths were located near Mt. Vernon, Ohio; the statistics are based upon one year of record, 1938.

as the depth at a representative point in the path. The curves do cross over and, since many hours of data are represented in the lower portions of the curves being compared, it seems certain that the crossing over and increasing separation of the curves at high rates is a real effect.

Instantaneous Rates for a 50-Km Path

One might be satisfied with the work of Fig. 3, having found statistics for a long path by 30-minute intervals as compared with the available 1-hour point statistics. However, it is not difficult to make an estimate of instantaneous statistics for this 50-km path. This estimate is made using the previous experience with instantaneous rates for a short path, i.e., from the analysis in Fig. 2. Since instantaneous rates on a long path have never been observed, it is only by analogy that we may obtain any information concerning them.

There can be no doubt that the instantaneous rate on our long path varies about the mean and goes to zero occasionally within some of the 30-minute means. It is easy to predict then, how the instantaneous distribution must look for the 50-km path. It must be separated from the means curve in approximately the same way as the instantaneous curve is separated from the 30-minute means curve in Fig. 2. From this approximation it is estimated in Fig. 3 that the desired instantaneous curve would, if it could be obtained, approximately coincide with the dashed curve there which represents the associated 1-hour point rates.

In the above paragraph, the approximation has just been made that an annual distribution of 1-hour point rates is identical with an annual distribution of instantaneous 50-km path rates in Ohio. If this approximation extends to other locations outside of Ohio, then it is indeed a convenient one, for 1-hour point data have been observed for many years all over the world. An hypothesis is suggested later to explain why 1-hour point rates should thus appear to represent instantaneous statistics

for a 50-km path. On very general grounds it would seem that point rates must be related to path rates through such characteristics of storms as their size, shape, persistence, and velocity of translation. Since these storm characteristics change rather slowly with climate, we will now assume an extension of the Ohio finding (that 1-hour point rates give instantaneous 50-km path rates) to other areas at middle latitudes, e.g., all over the United States except in very rough mountainous terrain.

Attenuation Results

As an example of how to use the above work, complete atmospheric attenuation statistics are obtained for Washington, D. C. for a 1-km and a 50-km transmission path. Presumably we can make similar computations for most other locations in the middle latitudes if 1-hour and 1-minute point rates can be obtained. Though 1-hour point rates are available in principle, they are actually collected and published for only a few stations;[6] 1-minute point rates have never been published; however, they might be roughly inferred from 1-hour rates by assuming that Fig. 2 portrays a general relation between these rates.

Fig. 4 shows for Washington, D. C., for several radio frequencies, the expected annual distribution curves for the total atmospheric attenuation coefficient, where losses due to oxygen plus water vapor and precipitation correlated have been added together. The 100-per cent intercept in each case in Fig. 4 is the same as in Fig. 1 and it shows only the gaseous absorption value exceeded all of the time. From 100 per cent down to 5 per cent in frequency, water vapor is the controlling factor. Since water vapor statistics are not functions of the path length, the 1-km and 50-km statistics coincide down to 5 per cent. Below 5 per cent in frequency, precipitation attenuation is the controlling factor; the curves separate there and subsequently cross over, reflecting the shapes of the 1-hour and the instantaneous distributions in Fig. 2; it must be remembered that the 1-hour statistics are now identified as 50-km path statistics.

It will be noted that the left intercept of the graph breaks off the predictions at 0.01 per cent, or at about 1 hour per year. The remaining 1 hour is controlled by "excessive" rainfall rates, and the Ohio analysis has not given a direct comparison of path and point durations at these rates.

A diurnal or seasonal frequency breakdown of when attenuation takes place would probably be of commercial interest. Alexander[6] gives a good bibliography on diurnal rainfall variations. A good diurnal and seasonal analysis for Washington, D. C. is given by Zock.[7]

[6] Two distributions are available as follows: W. F. MacDonald, "Hourly frequency and intensity of rainfall at New Orleans," *Monthly Weather Rev.*, vol. 57, pp. 1–8; January, 1929. Also H. F. Alexander, "Study of hourly precipitation at Oklahoma City," *Monthly Weather Rev.*, vol. 66, pp. 126–130; May, 1938.

[7] See page 144 of footnote reference 4.

Predictions for Other Path Lengths; Use of Excessive Rainfall Data

Excessive rainfall occurrences may be of special interest; fortunately excessive statistics are widely available having been compounded for civil engineering use. Predictions for any interval from 5 minutes to 24 hours are available; however, we have so far seen how to use either 1-minute or 1-hour data; methods of using intermediate interval data ought to be developed. Path lengths in between 1 and 50 km are probably the most common; there ought to be a method of interpolating in between the 1- and 50-km results, wherever the separation is significant. In order to accomplish either of these extensions easily, a theory is needed for relating point rates data to path rates data. We now suggest a rather natural hypothesis which may explain how mean point rates are related to instantaneous path rates; it is concerned with the translational motion of storms. In Ohio or at Washington this speed of translation aloft is 45 or 50 kilometers per hour on the average. A rain gauge on the ground may be considered to observe a slice out of a storm during any interval, the length of the slice being proportional to the interval and the speed. If the translating rainfall pattern on the ground were constant with time, then the catch of water from any slice would give the instantaneous path rate exactly. Of course the rain intensity pattern does not remain constant, but it has a probability of changing in either a positive or a negative sense; it is possible that, over a period of a year, the rates from these slices approach toward instantaneous path rates statistics. From the speeds mentioned above, it is consistent with this hypothesis that 1-minute data have been identified as instantaneous 1-km rates and that 1-hour data have been identified as instantaneous 50-km rates, in the foregoing.

Assuming now that this hypothesis is true (it has not been proved) additional predictions may be made. We have the immediate extension, that the $\frac{1}{2}$-hour and the 2-hour curves of Fig. 2 should be interpreted as instantaneous rates respectively on 25- and 100-km paths. In addition, the separations of the curves in Fig. 2 may be used as a guide for interpolating to other path lengths. At an abscissa of 1 hour (for example) in Fig. 2 one finds the rates to be expected on paths 1, 25, 50 and 100 km long. By putting these four rates and lengths on another set of co-ordinates and drawing a smooth curve, an approximate interpolation can be made for all paths from 1 to 100 km long. In Fig. 4, attenuation may be interpolated for paths between 1 and 50 km using this same smooth curve. For example, a 10-km path is estimated to be about 40 per cent of the way down from the 1- to 50-km values at the 1-hour level.

It will be of interest to know the most extreme 50-km rate which occurred anywhere in the Muskingum maps. Other locations occasionally had higher rates than the two paths being studied. Scanning all of the maps entirely, (some 12,000 maps comprised the two years of

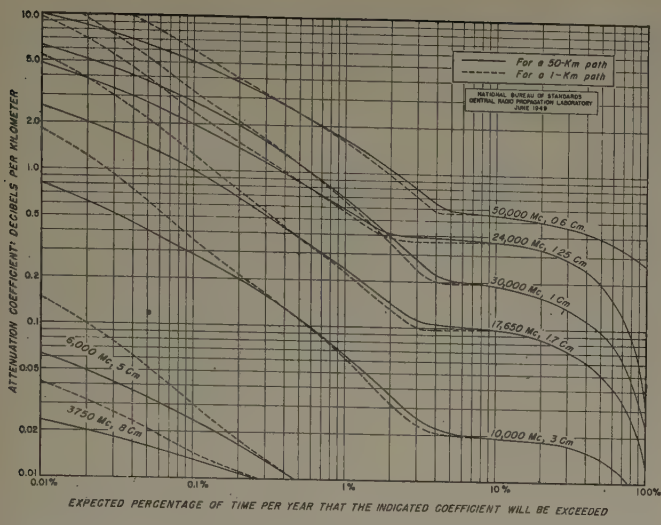
For a 50-Km path
For a 1-Km path
NATIONAL BUREAU OF STANDARDS
CENTRAL RADIO PROPAGATION LABORATORY
JUNE 1949
50,000 Mc, 0.6 Cm
24,000 Mc, 1.25 Cm
30,000 Mc, 1 Cm
17,650 Mc, 1.7 Cm
6,000 Mc, 5 Cm
3750 Mc, 8 Cm
10,000 Mc, 3 Cm
ATTENUATION COEFFICIENT: DECIBELS PER KILOMETER
EXPECTED PERCENTAGE OF TIME PER YEAR THAT THE INDICATED COEFFICIENT WILL BE EXCEEDED

Fig. 4—Cumulative distributions for the total atmospheric attenuation per kilometer to be expected on 1- and 50-km paths at Washington, D. C. Rain, water vapor, and oxygen attenuations have been combined.

record) it was noted that the highest 30-minute 50-km path rate was 3.2 inches per hour. This occurred in an oblong rain area moving with a cold front. In scanning the maps as a whole, one examines nearly an infinite number of paths; it is impossible to predict the amount of time that one fixed path will experience this rate, but it will be noted that Fig. 2 predicts that 3 inches per hour on 50 km should persist 0.01 hour per year on the average. Frequencies such as this from the extremes of a distribution must always be used with caution. Also it

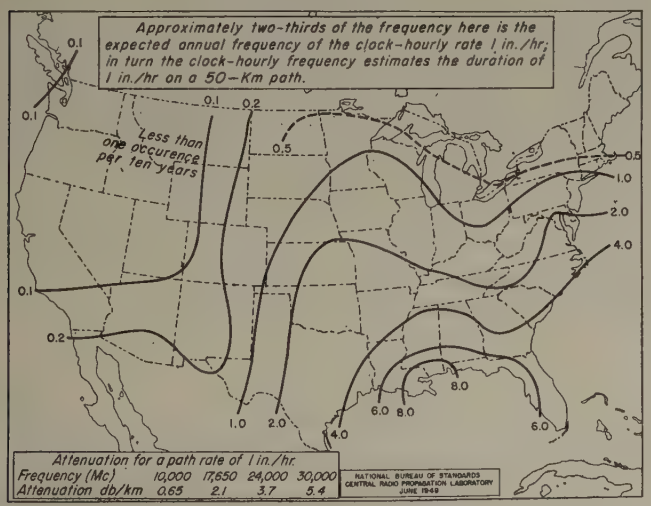
Approximately two-thirds of the frequency here is the expected annual frequency of the clock-hourly rate 1 in./hr; in turn the clock-hourly frequency estimates the duration of 1 in./hr on a 50-Km path.
Less than one occurence per ten years
Attenuation for a path rate of 1 in./hr.
Frequency (Mc) 10,000 17,650 24,000 30,000
Attenuation db/km 0.65 2.1 3.7 5.4
NATIONAL BUREAU OF STANDARDS
CENTRAL RADIO PROPAGATION LABORATORY
JUNE 1949

Fig. 5—The expected annual frequency of a point rate of 1 inch or more per 60 minutes; the 60 minutes is especially selected and does not usually correspond to a clock hour.

must be apparent that no accurate relation between extreme point rates and 50-km path rates has been obtained, since the highest rates on the two paths studied were in the range 0.8 to 1.0 inch per hour.

Examples of the available excessive rainfall data for the whole United States will now be considered: Fig. 5, drawn from Dyck and Mattice,[8] shows the expected annual frequency of a point rate greater than 1 inch per selected 60 minutes; the interval is selected to include the maximum 60-minute depth. A brief study was made to compare the annual frequencies of ordinary clock-hourly data and these selected hourly data, at 1 inch per hour. The clock-hourly frequency was approximately 0.7 of the selected hourly frequency for the places where comparative data were available. Then Fig. 5 adjusted by a factor of 0.7 indicates the expected annual duration, in hours, of the 50-km path rate 1 inch per hour, using the approximation from Ohio to connect point rates to path rates.

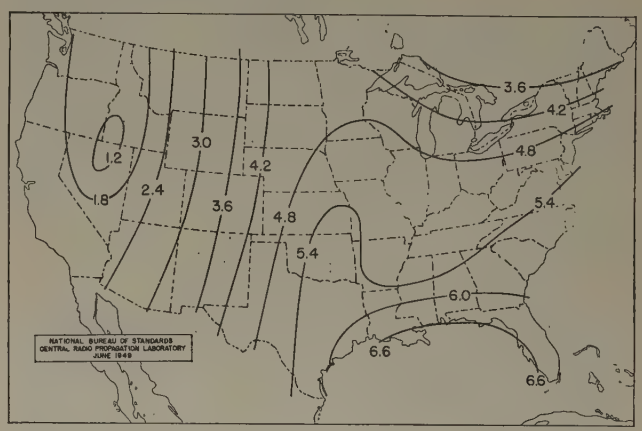

Fig. 6—Smoothed contours of the 5-minute rainfall rate (in./hr) to be expected once per two years on the average (Yarnell). A short path (3-km) is likewise expected to experience the rate shown about 2½ minutes per year on the average.

As another example of the available extreme statistics Fig. 6, based upon Yarnell[9] is given, which shows the 5-minute rate of rainfall for a point expected to occur once per two years on the average. Since the time interval is short, it is assumed that these data are related to only a short path, say 2 or 3 kilometers in length. Thus, Fig. 6 indicates the short path rate to be expected during the worst 2½ minutes per year, on the average.

Yarnell gives excessive data for other intervals and for recurrence frequencies as rare as once per hundred years. The tenative hypothesis about storm translation would suggest that 10-minute data apply to an 8-kilometer path, 30-minute data to a 25-kilometer path, etc.; then, for example, a "5-year" 10-minute rate would indicate the instantaneous 8-km path rate to be exceeded 2 minutes per year on the average. All of these excessive data are based upon selected intervals, not successive clock intervals and an overestimate of a path duration should always be obtained, as for example the overestimate in the ratio 1 to 0.7 which was described in connection with Fig. 5.

Acknowledgment

The author is indebted to T. J. Carroll for his guidance in this work and for suggesting the problem, and to C. T. Zahn, for his helpful suggestions.

[8] H. D. Dyck and W. A. Mattice, "A study of excessive rainfall," *Monthly Weather Rev.*, vol. 69, pp. 293–301; October, 1941.

[9] D. L. Yarnell, "Rainfall Intensity-Frequency Data," U. S. Dept. of Agriculture, Misc. Pub. No. 204; August, 1935.

The Permittivity of Air at a Wavelength of 10 Centimeters*

W. ERIC PHILLIPS†, SENIOR MEMBER, IRE

Summary—**This paper reports measurements of the permittivity of moist air under different conditions of pressure, temperature, and water-vapor content taken at a frequency of 3,036 Mc. The method and apparatus used are described. Results of observations made are given, and their probable accuracy is discussed.**

I. Introduction

THEORETICAL TREATISES[1–3] have indicated quite clearly that the propagation of very-high-frequency radio energy is intimately connected with the permittivity of the earth's atmosphere, and with the variations in the value of the permittivity with height above the earth's surface. It has been quantitatively demonstrated[4] that propagation over land is by a mechanism other than diffraction under both standard[5] and nonstandard meteorological conditions. Experimental evidence[6–10] indicates that very short radio waves are propagated close to the surface of the earth over distances greatly in excess of the optical distances. There is further evidence[11] that energy thus propagated is in the nature of a ground wave as opposed to a sky wave, and that the Kennelly-Heaviside layer of the upper atmosphere plays no part in such propagation. This apparent bending of the radio beam around the curvature of the earth is attributed partly to diffraction, but mainly to refraction in a lower atmosphere whose refractive index gradient is influenced by its water-vapor content. As a preliminary to a long-term investigation of the anomalous propagation of ultra-short radio energy over sea paths, it was considered advisable to make accurate determinations of the permittivity of air under different conditions of pressure, temperature and water-vapor content at, at least, one frequency in the ultra-high-frequency band. The frequency chosen was of the order of 3,000 megacycles per second.

Published results of permittivity measurements[12,13] are confined to frequencies of the order of 50 Mc for dry air at N.T.P., and for water vapor at a temperature of 100° C; Saxton,[14] however, has published measured values of the permittivity of water vapor at temperatures in the range 100° C to 215° C, and taken at wavelengths of 9.0, 3.2 and 1.6 cm.

II. Measurement of the Permittivity of Air

A. General

The two principal methods available for the measurement of permittivity at radio frequencies are the heterodyne and the standing-wave methods. The former is more suitable at low frequencies, and was used by Tregigda.[12] The latter method, which has been used in the present work and which was adopted by Kerr[13] in his determinations, only becomes practicable at high frequencies. Kerr used a length of short-circuited concentric transmission line, coupled to an oscillator, on which standing waves were set up when its electrical length was equal to an integral number of half-wavelengths of the exciting frequency. The permittivity of the gas k_e is given by $k_e=(v/c)^2$, where c is the phase velocity in a vacuum, and v the phase velocity in the gas forming the dielectric. For a given frequency,

$$k_e = \left(\frac{\lambda_g}{\lambda_v}\right)^2, \tag{1}$$

where λ_v is the wavelength in a vacuum, and λ_g, the wavelength in the gas. Thus the permittivity is obtainable from a comparison of the lengths of standing waves set up in the resonant line in a vacuum with their lengths in the gas.

In the present work, where measurements are taken with centimeter waves, it was found more expedient to

* Decimal classification: R216.3. Original manuscript received by the Institute, August 15, 1949; revised manuscript received, December 22, 1949.

† University of Natal, Durban, South Africa.

[1] T. L. Eckersley, "Ultra-short-wave refraction and diffraction," *Jour. IEE*, vol. 80, pp. 286–304; March, 1937.

[2] H. G. Booker, and W. Walkinshaw, "The mode theory of tropospheric refraction and its relation to wave-guides and diffraction," Meteorological Factors in Radio-Wave Propagation, The Physical Society of London. pp. 80–127; April 8, 1946.

[3] B. J. Starnecki, "A study of some of the factors influencing microwave propagation," *Jour. IEE*, Part IIIa, vol. 93, p. 106; 1946.

[4] M. D. Rocco, and J. B. Smyth, "Diffraction of high-frequency radio waves around the earth," Proc. I.R.E., vol. 37, pp. 1195–1203; October, 1949.

[5] The refracting property of the atmosphere is defined as standard if the index of refraction near the earth is a linear function of elevation and is decreasing at the rate of 1.18×10^{-8} per foot.

[6] Marchesse Marconi, "Radio microwaves," *Electrician*, vol. 110, p. 3; January, 1933. And *Proc. Roy. Inst.*, vol. 27, p. 509; 1933.

[7] A. G. Clavier, "Production and utilisation of micro-rays," *Elec. Comm.*, vol. 12, p. 3; 1933. And A. G. Clavier and L. C. Gallant, *Elec. Comm.*, vol. 12, p. 222; 1934.

[8] C. R. Englund, A. B. Crawford, and W. W. Mumford, "Further results of a study of ultra-short-wave transmission phenomena," *Bell Sys. Tech. Jour.*, vol. 14, p. 369; 1935.

[9] E. C. S. Megaw, "Experimental studies of the propagation of very short radio waves," *Jour. I.E.E.*, Part IIIa, vol. 93, p. 79; 1946.

[10] R. L. Smith-Rose, "A preliminary investigation of radio transmission conditions over land and sea on centimetre wavelengths," *Jour. IEE*, Part IIIa, vol. 93, p. 98; 1946.

[11] H. G. Booker, "Elements of radio meteorology," *Jour. IEE*, Part IIIa, vol. 93, p. 69; 1946.

[12] A. C. Tregigda, *Phys. Rev.*, vol. 57, p. 294; 1940.

[13] F. J. Kerr, "Refractive indices of gases at high radio frequencies," *Proc. Phys. Soc.*, vol. 55, p. 92; 1943.

[14] J. A. Saxton, "The dielectric properties of water vapour at very high radio frequencies," Meteorological Factors in Radio-Wave Propagation, The Physical Society of London, pp. 215–237; April 8, 1946.

use a cylindrical cavity resonator. The cavity resonator is superior to the concentric line in that it is mechanically simpler, and the effect of the detector on the position of standing-wave maxima may be eliminated by detecting the existence of standing waves externally to the cavity. The existence of standing waves may be detected by observation of the current magnitude in the transfer circuit between the oscillator and resonator. From a measurement of the resonant wavelengths, at a given exciting frequency and for a given mode of propagation, it was possible to estimate the permittivity of the gas dielectric.

B. Method

From the well-known theory of propagation in circular section waveguides it can be shown that for a waveguide filled with a dielectric of permittivity k_e, the wavelength in the tube, on the assumption that the permeability is unity, is given by

$$\lambda_{tube_{mn}} = \frac{1}{\sqrt{\frac{k_e}{\lambda^2} - \left(\frac{r_{mn}}{2\pi a}\right)^2}} \text{ cm}, \qquad (2)$$

where λ is the free-space wavelength, a is the radius of the waveguide and r_{mn} is the m^{th} root of $J_n(r)=0$, J_n being the Bessel function of the first kind and m and n defining the rank of the root and the order of the Bessel function, and hence defining the mode of the transmission of the E or TM wave. For the H or TE wave corresponding roots of $(d/dr)J_n(r)=0$ must be used.

If λ and $\lambda_{tube_{mn}}$ are measured, k_e can be determined from (2). Further, if the tube wavelength in vacuum λ_{t_v} is known, as well as the tube wavelength in the dielectric λ_{t_a}, then λ may be eliminated, and the expression for the permittivity becomes

$$k_e = \frac{\frac{1}{\lambda_{t_a}^2} + \left(\frac{r_{mn}}{2\pi a}\right)^2}{\frac{1}{\lambda_{t_v}^2} + \left(\frac{r_{mn}}{2\pi a}\right)^2}, \qquad (3)$$

since $k_e=1$ for a vacuum.

The tube wavelengths may be obtained by adjusting the length of the cavity until resonance occurs; the length of the cavity will then be an integral number of half-tube wavelengths. The values of λ_{t_a} and λ_{t_v} must be obtained for the same exciting frequency, but the value of this frequency does not occur in (3); therefore, it is not necessary to make an accurate determination of the frequency. The technique employed was to evacuate the cavity and from a plot of the resonance curve to obtain the tube wavelength in vacuum; air was then admitted into the cavity and a resonance curve again obtained, giving the tube-wavelength in air.

From these two measurements together with a knowledge of r_{mn} and the radius of the waveguide it was possible from (3) to compute the permittivity of the air in the cavity.

C. Equipment

The experimental setup of the equipment is shown in Fig. 1.

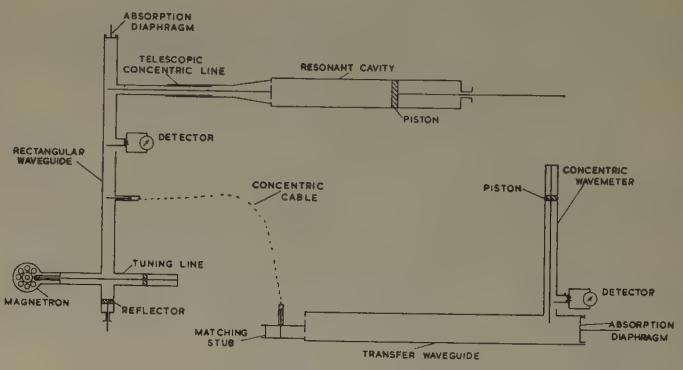

Fig. 1—Circuit diagram.

1. Wavemeter. The wavemeter used was of the coaxial cavity type as illustrated in Fig. 2. The central conductor, which extends slightly into the guide, abstracts sufficient energy to set up standing waves; these may be detected by a second pickup connected to a crystal and galvanometer.

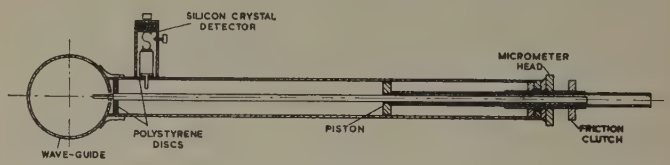

Fig. 2—Wavemeter.

2. Resonant Cavity. The resonant cavity was constructed from a length of circular cross-section copper tubing of 4 inches internal diameter with walls $\frac{1}{8}$ inch thick. To one end of the tube was attached a copper ring, and a copper disk concentric with this was held in position by a polystyrene insulating disk. Such an arrangement forms a suitable means of exciting the E_0 type of wave inside the tube. Inserted in the other end of the tube is a movable copper piston attached to a rod sliding in a bush fitted with an airtight gland made integral with the end-plate. The piston is a disk of diameter slightly less than the internal diameter of the tube. Contact with the walls of the tube, is maintained by twenty-four phosphor bronze springs arranged around the periphery of the piston. The end plate carries a micrometer head which may engage with the piston rod through a friction clutch, thus enabling accurate adjustments to be made. Piston displacements were measured by means of a traveling microscope. The whole was rendered airtight by soldering all metallic joints and by applying "dope" to polystyrene-metal joints. Provision was made for exhausting the cavity. Details of construction are given in

Fig. 3 and the general appearance is shown in Fig. 4.

D. Experimental Technique

1. General Procedure. After warming up the rectifier and generating tubes, the high-tension dc supply was

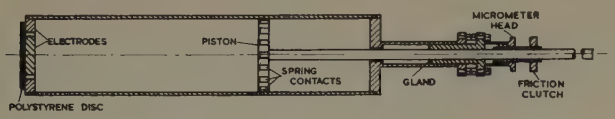

Fig. 3—Resonant cavity (interior)

switched on and the output of the magnetron adjusted to the desired value. No measurements were taken until the generator had been in operation for about an hour, after which period it had usually settled down to stable conditions of operation. It was found essential to em-

Fig. 4—Resonant cavity (exterior).

ploy a voltage stabilizing device, of the carbon-pile type, operating in conjunction with the motor-alternator set supplying power to the magnetron through the associated equipment.

Three sets of frequency measurements were taken at intervals of ten minutes, and if they proved stability of frequency, resonant cavity measurements were taken. Although the frequency does not enter directly into the permittivity relation, frequency measurements were taken periodically throughout a day's run to check maintenance of frequency stability.

The resonant cavity was then exhausted and standing-wave measurements taken. Dry air was admitted through a chemical drying system of activated alumina and phosphorus pentoxide, and standing-wave measurements again taken. The cavity was again evacuated and a second vacuum run taken, and so on. On each occasion three vacuum and three air runs were taken, each run taking about 15 to 20 minutes. In this way frequency and temperature drift were practically eliminated.

2. Frequency Measurements. The frequency was ascertained by determining the positions of successive standing-wave maxima in the concentric line wavemeter which was excited from the magnetron output waveguide. Although the standing wavelength in air is not a true measure of the frequency of the generated energy (the phase velocity in air being different from that in vacuum), it suffices to check the constancy of frequency, and also indicates, within very close limits, the actual frequency being used. No absolute measurement of frequency is necessary.

Readings of the standing-wave detector were taken for different settings of the wavemeter piston, and resonance curves plotted for four consecutive maxima.

3. Resonant Cavity Measurements. The cavity was evacuated to a pressure of 0.01 mm of Hg, and a resonance curve along the complete length of the cavity taken by reading detector deflections for different settings of the piston. This was done to ascertain whether there were any propagation anomalies in the cavity, and to determine the number of complete standing waves in the cavity when adjusted to its maximum length.

Detailed resonance curves in the regions of the fifth and sixth maxima were then taken, and from a mathematical examination of these curves it was possible to estimate the standing-wavelength to an accuracy better than 0.001 cm. Three vacuum-air runs were taken in succession, and detailed resonance curves at the sixth maximum taken for both vacuum and air. Portions of three of the resonance curves obtained are shown in Fig. 5. The shift in the maximum positions of two consecutive vacuum-air resonance curves divided by the number of

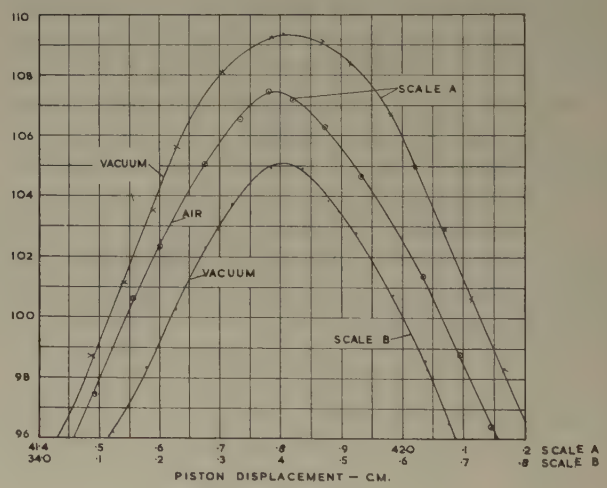

Fig. 5—Resonance curve.

complete standing-waves between the piston and the input end of the cavity, is the change in standing wavelength due to a change of dielectric from vacuum to air. The permittivity of the enclosed air is given from (3) by

$$k_e = \frac{\dfrac{1}{\lambda_{t_a}^2} + 0.00567695}{\dfrac{1}{\lambda_{t_v}^2} + 0.00567695},$$

for the E_{01} mode of propagation, and for $a = 5.08$ cm.

Dry Air: Air was admitted slowly, into the previously evacuated cavity, through a chemical drying system.

Dry Air at Reduced Pressure: Air was admitted slowly,

into previously evacuated cavity through a chemical drying system, until the required pressure was obtained.

Saturated Air: Air was admitted slowly, into the previously evacuated cavity, after bubbling through pure water at room temperature. To ensure complete saturation of the air, the air in the cavity was in communication with a water surface during the resonance measurements.

Moist Air: Undried room air was admitted into the cavity, and wet and dry bulb thermometer readings taken near the point of admission. The velocity of the air passing into the cavity was kept as low as possible so as to preclude the possibility of any change in the water-vapor content of the air on its passage into the cavity.

Water Vapor: A small quantity of pure water was admitted into the evacuated cavity.

E. Experimental Results

1. Frequency Measurement. Resonance measurements in the vicinity of four consecutive maxima gave $\lambda = 9.882 \pm 0.002$ cm.

2. Preliminary Exploration of Resonant Cavity. The cavity was exhausted to a pressure of 0.01 mm of Hg and standing-wave measurements taken along its entire length.

Average value of $\frac{1}{2}\lambda_{t_g} = 7.40$ cm
Average value of $\lambda_{t_g} = 14.80$ cm.

Value of λ_{t_g} calculated from (2) for $r_{01} = 2.405$, $a = 5.08$ cm and $\lambda = 9.882$ cm is 14.805 cm. This value of λ_{t_g} compares favorably with the measured value, and confirms the E_{01} mode of propagation.

3. Permittivity of Dry Air. A typical series of results is given in Table I. The mean of nine determinations is $k_e = 1.0005548$ at a pressure of 759.09 mm of Hg, and a temperature of 25.5° C.

4. Permittivity of Dry Air at Reduced Pressure. Mean of three determinations in each case are shown in Table II.

TABLE II

k_e	*Pressure (mm Hg)*	*Temperature (° C)*
1.000393_4	555.48	22.0
1.000278_9	384.00	23.0
1.000129_8	180.08	22.0

5. Permittivity of Air Saturated with Water Vapor. Mean of three determinations

$$k_e = 1.0008060,$$

at a pressure of 752.45 mm Hg and a temperature of 22° C.

6. Permittivity of Moist Air. Mean of three determinations in each case are shown in Table III.

TABLE III

k_e	*Pressure (mm Hg)*	*Temperature (° C)*	*Relative Humidity (Per cent)*
1.000735	752.40	21.3	88.1
1.000728	752.30	22.0	83.3
1.000687	755.30	19.5	63.1
1.000668	756.45	19.0	55.7

7. Permittivity of Water Vapor. Mean of three determinations

$$k_e = 1.000257_7$$

at a pressure of 21.10 mm Hg and a temperature of 23° C. Assuming the Clausius-Mosotti relation this is equivalent to a value at 100° C and 760 mm Hg of $k_e = 1.005920$.

F. Discussion of Results

Individual determinations obtained in subsection 3 showed a maximum variation of 0.002 per cent from the mean. This figure has no real meaning. A better conception of the accuracy of the determinations is given by a consideration of the last four significant figures of the individual permittivity values. The maximum variation

TABLE I

Series	*Run*	*Time (hrs.)*	*Temp. ° C and Pressure (mm Hg)*	*Tube Wavelength (cm)*		*Shift from Vacuum Mean (cm)*	k_e
				Vacuum	*Air*		
11a	Vacuum, 1	10.22 to 10.42	25° C 0.013	14.8040			
11b	Air, 1	11.03 to 11.23	25° C 759.54		14.7952	0.0095	1.000573_0
11c	Vacuum, 2	11.38 to 11.53	25° C 0.012	14.8051			
11d	Air, 2	12.03 to 12.24	25° C 759.88		14.7955	0.0092	1.000554_1
11e	Vacuum, 3	12.36 to 12.54	25° C 0.011	14.8050			
11f	Air, 3	13.00 to 13.14	25° C 759.90	Mean 14.8047	14.7953	0.0094	1.000566_0

from the mean is 3.45 per cent. It is considered that a considerable part of this variation is due not to errors in measurement, but to distortion of the wave by slight deformations of the tube and to wave distortions in the proximity of the launching electrodes. The probable error calculated on external consistency is ± 0.000021, giving for the permittivity of dry air at a frequency of 3036.43 Mc/sec, 25.2° C and 759.1 mm Hg a value of

$$k_s = 1.00055_5 \pm 0.00002_1.$$

On the assumption of the Clausius-Mosotti relation this is equivalent to a value at 0° C and 760 mm Hg of

$$k_s = 1.00060_6 \pm 0.00002_3.$$

From subsection 4 the values of the permittivity of dry air at 0° C and at different pressures, together with the probable error are—

at 555.8 mm Hg, $k_s = 1.00042_5 \pm 0.00001_0$;
at 384.0 mm Hg, $k_s = 1.00030_2 \pm 0.00000_2$;
at 180.8 mm Hg, $k_s = 1.00014_{02} \pm 0.00000_{02}$.

From subsection 5, for air saturated with water vapor at a temperature at 22° C and at a total pressure of 752.5 mm Hg, the value of the permittivity is

$$k_s = 1.00080_6 \pm 0.00002_0.$$

In subsection 6 results are given for air containing different amounts of water vapor. The water vapor content is given in terms of relative humidity. The relative humidity was computed from readings of wet and dry bulb thermometers and a correction made for atmospheric pressure. At best, relative humidity values arrived at in this way are very approximate, and any corresponding permittivity measurements, although in themselves comparatively accurate, must be regarded as approximations.

The value of the permittivity of saturated water vapor given in subsection 7 has a probable error of ± 0.0000014, and the value at 100° C and 760 mm Hg is

$$k_s = 1.00592_0 \pm 0.00003_5.$$

Applying the linear theorem and adopting methods employed by Englund, Crawford, and Mumford[8] the following expression for the permittivity of moist air may be obtained:

$$k_s - 1 = \frac{2\pi}{T}\left(P + \frac{48P_s}{T}H\right)10^{-6}, \qquad (4)$$

where P is the barometric pressure of moist air in mm of mercury, P_s is the pressure of saturated water vapor at absolute temperature $T°K$, and H is the percentage relative humidity. This formula is expected to hold only for frequencies far below all microwave absorption lines and for pressures sufficiently low that interactions between molecules are negligible. Near a resonant frequency, in general, k_s becomes complex, as it does also at high pressures, and additivity is expected to break down. In fact, on the resonance peak the absorption coefficient is independent of pressure, until pressure is so low that saturation phenomena are appreciable. In the case of ammonia vapor these phenomena are well known and pronounced. In water vapor, however, Van Vleck[15,16] has shown that although absorption due to the 1.3-cm line is appreciable, there is no appreciable contribution to the real refractive index. He has, in fact, shown that for frequencies even as high as 30,000 Mc the value of k_s is not expected to differ from the static value. In the work described in this paper no attempt has been made to measure absorption coefficients.

III. Conclusion

Measurements have been made of the permittivity of moist air under various conditions of temperature, water vapor content, and pressure. The observed values are consistent with the static values as given by equation (4). The experimental results of the paper confirm previous beliefs regarding the importance of water vapor in the atmosphere on refraction. It would appear, then, that an important factor in anomalous propagation with centimeter-wave radio transmission is the variation of the moisture content of the lower atmosphere with height. The work described in this paper was done as a preliminary investigation to the undertaking of a long-term research project on the correlation of microwave propagation phenomena with meteorological conditions off the coast of Natal.

IV. Acknowledgment

The work described was carried out with the assistance of an equipment grant from the South African Council for Scientific and Industrial Research.

[15] J. H. Van Vleck, MIT Rad. Lab. Rep., Nos. 43–2, 1942; and 664, 1945.
[16] J. H. Van Vleck and V. Weisskopf, *Rev. Mod. Phys.*, vol. 17, p. 227; 1945.

The Beacon Technique as Applied to Oblique Incidence Ionosphere Propagation*

J. T. DEBETTENCOURT†, AND H. KLEMPERER‡, ASSOCIATE, IRE

Summary—**A method is shown for determining transmission time for each mode of transmission via the ionosphere and obliquely incident thereupon. The method makes use of an interrogator-responsor at the transmitting site and a beacon transpondor at the receiving site. Limitations of the method are discussed and preliminary results are shown for a 1,500-mile, north-south path.**

I. Introduction

A TRANSMITTED single pulse signal, reaching the ionosphere at an oblique angle, is propagated with different transmission modes or paths. These require different times of travel so that the signal reaching a remote receiver generally comprises a train of pulses.[1]

Studies of the characteristics of ionosphere transmission require the identity of the mode of transmission of a given component of the received pulse train. This can be accomplished by a measurement at the receiving location of the times of arrival, or of the angles of arrival of the various components of the received train of pulses. This paper is concerned with the first of these two methods.

When several pulses are arriving with different transmission times, a measurement of relative transmission times at the receiver can assist mode identification, even though certain ambiguities arise. In the analysis of fixed-distance transmission, several charts are useful. Based upon simple spherical-earth geometry, these charts give the computed transmission times or relative transmission times as a function of effective height of the layer for various modes of transmission. When ambiguities arise in using these charts, they can be reduced if one has knowledge of the variation of heights and maximum limiting frequencies as a function of time of day.[2] Also helpful are charts of computed angle-of-arrival and antenna patterns of interrogator and transpondor. The angle-of-arrival charts are most useful when using highly directive antennas.

The method which depends upon the measurements of relative delay time fails when only one pulse is being received. Moreover, if two pulses are being received, there are still ambiguities in transmission mode identity. These difficulties can be overcome if one can measure the one-way transmission time of the received pulse (or pulses).

* Decimal classification: R112.43. Original manuscript received by the Institute, January 24, 1949; abstract received, February 27, 1950. Presented, Joint URSI-IRE Meeting, Washington, D.C., October 8, 1948.

† Raytheon Manufacturing Company, Waltham, Mass.

‡ Formerly, Raytheon Manufacturing Company; now, Massachusetts Institute of Technology, Cambridge, Mass.

[1] A more complete discussion of the modes of transmission may be found in the literature, such as "Ionospheric Radio Propagation," U. S. Department of Commerce, National Bureau of Standards, Circular 462, June 25, 1948; prepared by the Central Radio Propagation Laboratory.

[2] These data were obtained from CRPL vertical incidence sounding at Baton Rouge (same latitude as midpoint) and Washington (same latitude as northern point of 2-hop transmission).

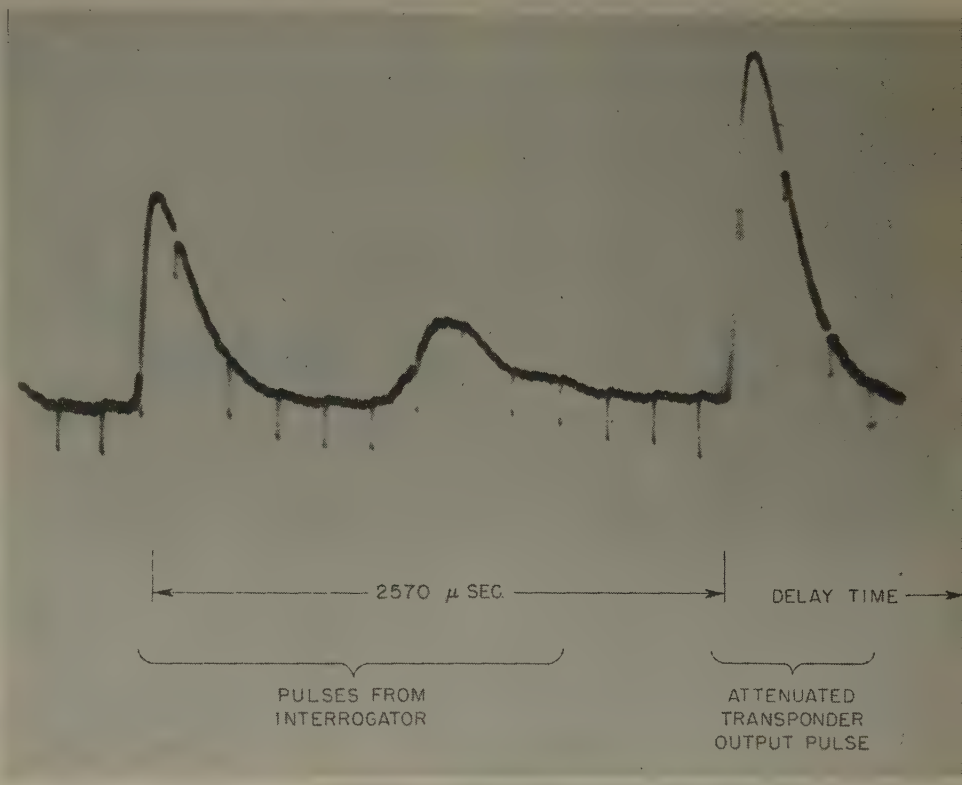

Fig. 1—Expanded-sweep, A-scope photograph of pulses recorded at output of transpondor beacc receiver (1510 EST, 8/19/48). Shown are F_2 pulses from interrogator and delayed tran pondor output pulse.

II. The Ionosphere Beacon Technique

In determining the transmission time of a given transmission mode, use is made of a beacon transpondor at the receiving site. The technique is similar to that used in microwave beaconry. The two-way transmission time between outgoing interrogating pulse and beacon reply pulse is measured. Since frequency affects transmission time, the beacon and interrogator are operated on the same frequency rather than operating cross band.

It is assumed that reciprocity holds for the two directions of transmission. That is, the transmission time T_1 from interrogator to transpondor is assumed the same as the transmission time T_2 for the reverse direction. Consequently, the one-way transmission time, t, $(t = T_1 = T_2)$ is given by

$$t = 1/2(T - D), \qquad (1)$$

where T is the two-way transmission or delay time from outgoing to reply pulse measured at the interrogator, and D is the known inserted system delay time, measured in the same units as t and T.

Knowing the one-way transmission time from equation (1), and referring to plots of computed transmission time for various layer heights and angle of arrival, one can identify the mode of transmission, the effective layer height and the computed angle of arrival.

III. Description of Experimental Apparatus

For the experiments, the interrogator was located near Boston and transpondor in the Caribbean area, 2,615 km distant. The equipment was practically identical at each location, consisting of horizontal rhombic antennas and 20-kw peak-power pulsed transmitters operating at 16.08 Mc per second. The pulse width was 100 microseconds and repetition rate of 20 per second. The rhombics were duplexed for transmission and reception. The repetition rates were crystal-controlled, monitored, and manually adjusted for synchronism, as with loran operation.

Data were of two kinds, both photographic. One record comprises a sequence of photographs of an A scope, showing pulse amplitudes versus delay time. The other record is a continuous strip photograph of an oscilloscope, intensity-modulated by received echo pulses and shows delay time versus time of day.

IV. Experimental Results

Some of the experimental results are shown below as A-scope photographs taken on August 19, 1948.

Fig. 1 taken at 1510 EST shows an expanded sweep photograph of the pulse amplitudes versus delay time of echoes received at the beacon transpondor. The time markers are 200 microseconds apart. The first two pulses are those received from the interrogator corresponding to two transmission modes. The third pulse at the extreme right is an attenuated transpondor pulse, delayed 2,570 microseconds from the first received pulse.

Fig. 2 taken at 1505 EST is a full sweep photograph of all echoes received at the interrogator, with 1,000- and 5,000-microsecond time marks. At the extreme left is a portion of the main "bang" of the interrogator. At a delay of 10.5 milliseconds, and extending to 16.0 milliseconds, is a group of pulses known as long "back-scatter."[3] At 18.0 milliseconds is a "phantom" pulse, marking the position of an expanded sweep strobe. At a delay of 21.0 to 23.5 milliseconds are the reply pulses from the southern transpondor beacon. These were checked as due to the beacon by turning the beacon on or off.

Fig. 3 is a photograph, taken at 1510 EST at the interrogator, of an expanded sweep of the beacon reply pulses, with 200- and 1,000-microsecond markers.

The system delays are 2,570 microseconds inserted at the beacon (Fig. 1) plus 100 microseconds at the interrogator (delay between the transmitted pulse and start of indicator sweeps), a total of 2,670 microseconds. The measured total delay is 18,000 plus 3,400 or 21,400 microseconds, giving a one-way transmission time of 9,365 microseconds for the first pulse.

Use of the charts and data referred to above reveals that the transmission time of the first pulse corresponds to a 1-hop F_2 mode, with a 10.6° arrival angle and an effective oblique incidence layer height of 400 km (effective vertical incidence height was 380 km at Baton Rouge at the same time).

On the basis of the transmission mode identified for the first pulse, the second pulse was identified as resulting from a 2-hop F_2 transmission mode.

V. Conclusions

The beacon technique is useful in identifying the mode of travel of pulsed transmissions over oblique incidence ionosphere paths. It is most useful in measurement of one-way transmission time when single pulses are received. The assumption of reciprocity must be studied further. When two or more pulses are received having the same transmission time, the method cannot be used, but must be supplemented by other measurements such as those of angle of arrival. The technique is also useful for identifying sources of "back-scatter."

VI. Acknowledgment

This work was carried out as part of an Air Force program under Contract W28-099ac173 with Watson Laboratories. The interest and assistance of R. I. Cole and P. Sharki of those laboratories are gratefully acknowledged, as well as that of N. Smith, of CRPL, who furnished the referenced vertical incidence data.

[3] The beacon technique is being used to identify sources of "back scatter," i.e., whether from the ground or from the *E* region. Results are to be published later.

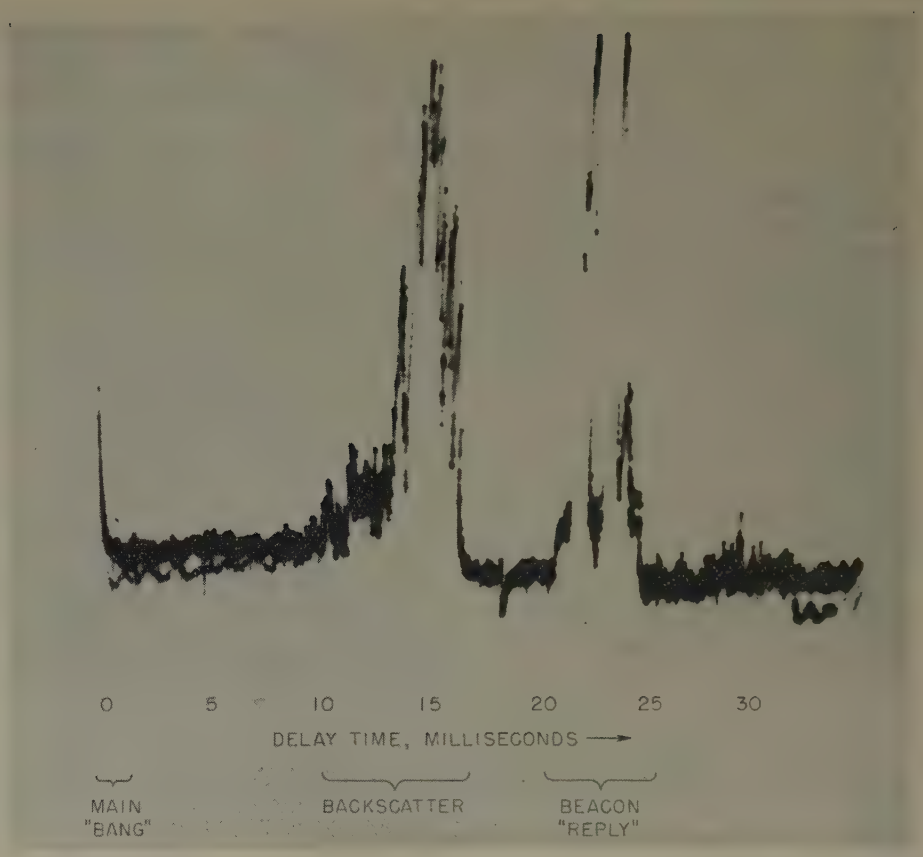

Fig. 2—Full-sweep, A-scope photograph of pulses recorded at output of interrogator receiver (1505 EST, 8/19/48). Shown are backscatter and pulses from transpondor.

Fig. 3—Expanded-sweep, A-scope photograph of transpondor beacon pulses recorded at output of interrogator receiver (1510 EST, 8/19/48.)

Low-Q Microwave Filters*

JOHN REED†, ASSOCIATE, IRE

Summary—**Waveguide bandpass transmission filters, each stage of which is composed of two similar irises spaced a distance s apart, are considered. The distance between stages for effectively quarter-wave coupling is shown to be $s \pm 1/4\lambda_g$. The loaded Q of one stage is computed, and the frequency consciousness of the iris susceptance is shown to have no effect on the spacing condition, but to have a substantial effect upon the loaded Q, especially for low values of Q.**

Introduction

THIS PAPER WILL treat waveguide filters, each stage of which is composed of two identical inductive irises spaced so as to give match (zero reflection coefficient) at the resonant frequency. The spacing between two such stages is computed so that the first derivative of the voltage reflection coefficient with respect to frequency of the two stages in cascade is zero at the design frequency (effectively quarter-wave or critical coupling). The loaded Q is also computed, and experimental procedure and results are discussed. Pritchard[1] and Fano and Lawson[2,3] in their analyses of this problem have assumed that the iris susceptance is large and constant with frequency. Then the spacing between stages is a quarter wavelength, and the formula for loaded Q is fairly good for high values of iris susceptance, but rather poor for low values. Mumford[4] assumes for computing the value of loaded Q of a stage that the susceptance of the iris is constant with changing frequency. It will be shown in this paper that the frequency consciousness of the iris susceptance which has been previously neglected makes no difference in the spacing between stages, but it may be responsible for as much as one-sixth of the total Q of a single stage.

General Theory of Critical Coupling

Consider a two-stage filter in waveguide made from four identical inductive irises spaced along the guide distances of s, m, and s, respectively. A transmission-line equivalent circuit of this is shown in Fig. 1. The admittance at point a looking to the right into a matched load is

$$Y_a = 1 + jB, \tag{1}$$

where B is the normalized susceptance of the iris. The normalized admittance Y_i a distance s toward the generator from a point where the admittance is Y is given by

$$Y_i = \frac{Y + jt}{1 + jYt} \qquad t = \tan \frac{2\pi s}{\lambda_g}$$

$$\lambda_g = \text{guide wavelength.} \tag{2}$$

Using this to transform the admittance Y_a to point b and adding the admittance jB there and rationalizing, we get

$$Y_b = \frac{1 + t^2 + j(B^3t^2 - 3B^2t + 2B)}{1 - 2Bt + B^2t^2 + t^2}. \tag{3}$$

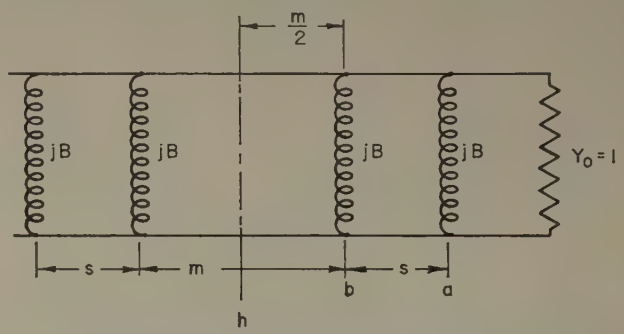

Fig. 1—Equivalent circuit of two-stage filter.

At resonance $t = 2/B$; then Y_b is equal to $1 + j0$, and complete transmission takes place for one stage.

To determine the behavior of a stage near resonance, equation (3) is differentiated with respect to λ_g, remembering that both B and t are dependent on λ_g and then t inserted as $2/B$

$$\left(\frac{dY_b}{d\lambda_g}\right)_{Y_b=1} = \frac{\left(B^3 \frac{dt}{d\lambda_g} + 2B \frac{dB}{d\lambda_g}\right)(-2 + jB)}{B^2 + 4}. \tag{4}$$

To achieve critical coupling as defined in the introduction, consideration is given to frequencies very near resonance. For match here, the admittance at any point between the two stages looking toward a matched load must be the complex conjugate of that looking toward a matched generator. In particular, at the center h the admittance looking toward the load must be purely real. If we write the admittance Y_b in terms of a Maclaurin series taking only the first two terms, we obtain from (4) $Y_b = 1 + \delta(-2 + jB)$, where δ is a real number proportional to the deviation from resonance. Inserting this admittance into the transmission line (2) and solving

* Decimal classification: R143.2×R118. Original manuscript received by the Institute, May, 11, 1949; revised manuscript received, January 12, 1950.

† Raytheon Manufacturing Company, Newton, Mass.

[1] W. L. Pritchard, "Quarter-wave coupled wave-guide filters," *Jour. Appl. Phys.*, vol. 18, pp. 862–872; October, 1947.

[2] R. M. Fano and A. W. Lawson, "Microwave filters using quarter wave couplings," PROC. I.R.E., vol. 35, pp. 1318–1323; November, 1947.

[3] G. L. Ragan, "Microwave Transmission Circuits," McGraw-Hill Book Co., Inc., New York, N. Y., pp. 677–715 (also p. 160); 1948.

[4] W. W. Mumford, "Maximally-flat filters in wave guide," *Bell Sys. Tech. Jour.* vol. 27, pp. 684–713; October, 1948.

for m so that the imaginary part of Y_h is zero (neglecting terms of order δ^2), we obtain

$$m = s \pm \frac{\lambda_g}{4}. \tag{5}$$

From consideration of (4) we see that (5) is correct, no matter what variation of B with frequency is assumed.

If the complex admittance looking to the right at the center of a dissipationless symmetrical network such as Fig. 1 with a matched load is expressed as $Y_h = G_h + jB_h$, then the insertion loss L of the network, the ratio of input to transmitted power, is given by

$$L = 1 + \left(\frac{B_h}{G_h}\right)^2. \tag{6}$$

Analysis of a Single Stage

Most obstacles such as inductive posts or irises used in the construction of waveguide filters[4] introduce a negative susceptance proportional to the guide wavelength. Computing the magnitude of the admittance change with frequency

$$\left|\left(\frac{dY_b}{df}\right)\right|_{Y_b=1} = \frac{1}{f}\left(\frac{\lambda_g}{\lambda_a}\right)^2\left[-B\sqrt{B^2+4}\,\tan^{-1}\frac{2}{B} + \frac{2B^2}{\sqrt{B^2+4}}\right] \tag{7}$$

f = frequency λ_a = free space (air) wavelength.

A single stage can be represented near resonance by a resonant shunt susceptance and interconnecting lines as proposed by Mumford.[4] The value of this susceptance

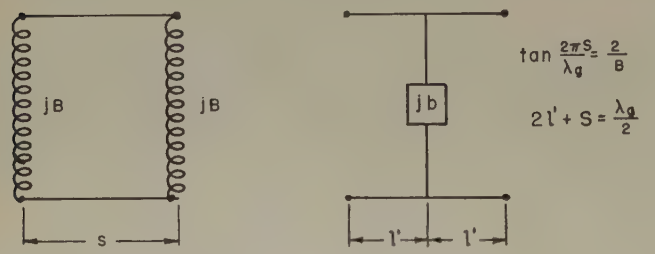

Fig. 2—Equivalent circuit of single stage.

b is assumed to vary proportionally to the frequency difference from resonance. The insertion loss of a shunt susceptance is found by (6) to be $L = 1 + (b^2/4)$, and thus the load power will drop to half when the value of b is equal to $+2$ or -2. Consequently, $b = 4Q_L(\Delta f/f)$, and equating $|dY_b|$ and b, we obtain

$$Q_L = \frac{1}{4}\left(\frac{\lambda_g}{\lambda_a}\right)^2\left[-B\sqrt{B^2+4}\,\tan^{-1}\frac{2}{B} + \frac{2B^2}{\sqrt{B^2+4}}\right] \tag{8}$$

Table I shows the values of Q computed for stages made of inductive susceptances in $0.9'' \times 0.4''$ inner dimension waveguide operating at 9,090 megacycles per second. The first column gives the iris susceptance B. The second column gives the value of Q as computed by the formula of Pritchard[1] and Fano and Lawson[2,3]

$$Q_L = \frac{1+B^2}{4}\left(\frac{\lambda_g}{\lambda_a}\right)^2 \tan^{-1}\frac{2B}{B^2-1}. \tag{9}$$

The third column gives the value of Q as computed from the formula

$$Q_L = \frac{\pi B^2}{4}\left(\frac{\lambda_g}{\lambda_a}\right)^2. \tag{10}$$

TABLE I

Q_L of Waveguide Stages Resonant at 9,090 Megacycles per Second ($\lambda_a = 4.77$ cm, $\lambda_a = 3.30$ cm) as Computed by Various Formulas

B	Q_L (old) (9)	Q_L (approximate) (10)	Q_L (exact) (8)	Per Cent Contribution of Iris B to Exact Q (8)
− 2*	5.79	6.56	8.44	17.4
− 4	22.9	26.2	28.8	12.9
− 6	54.5	59.0	61.8	9.6
− 8	98.1	105.	108.	7.5
−10	154.	164.	166.	6.2
−12	226.	236.	240.	5.2

* Experimental value = 8.5.

Both (8) and (9) lead to this result for very high values of Q, and its simplicity and closeness to the exact formula make it very useful. The fourth column shows the value of Q using the exact formula (8), while the fifth column shows the per cent contribution to the total Q of the frequency consciousness of iris susceptance. This is the second term in brackets in (8) and is neglected in Mumford's paper.

Experimentally, the value of Q_L for a low-Q stage can be determined from the slope of a graph of standing-wave ratio in decibels as a function of frequency. With a matched termination a susceptance b will cause a voltage standing-wave ratio r of

$$r = 1 + \frac{|b|}{2}\left[|b| + \sqrt{b^2+4}\right]$$

or

$$|b| = \frac{r-1}{\sqrt{r}}.$$

For b small this reduces to $r = 1 + b$ or r in decibels $= 8.686b$.

A useful formula for the tolerances on iris location can be derived from (4). Multiplying both sides of this equation by $d\lambda_g$ and using the above-mentioned formulas, there results

$$VSWR = 1 + 2\pi\frac{r^2-1}{r}\Delta\left(\frac{d}{\lambda_g}\right), \tag{11}$$

which relates the voltage standing-wave ratio caused by a stage in terms of r, the standing-wave ratio introduced by each iris, and $\Delta(d/\lambda_g)$, the fraction of a wavelength

which one iris is moved along the guide from the resonant length. This formula is valid for any use of irises as matching devices.

An equivalent circuit of an infinitely thin iris is a purely imaginary shunt admittance when the reference planes are taken at the center of the iris. For a thick iris this circuit is still valid, provided care is taken to choose the reference planes properly. Thus, for a filter using thick irises, it is necessary to lengthen the distance between irises to correct for this thickness and the distance between stages by the same amount.

Effect of Connecting Line between Stages

An equivalent network for the two-stage critically coupled filter of Fig. 1 is shown in Fig. 3. In this equivalent circuit the spacing between the two stages will be regarded as a quarter wavelength at all frequencies near resonance. Thus the effect of spacing m between stages in Fig. 1 will have to be considered. The insertion loss of the circuit of Fig. 3 is found by (6) to be $L=1+(b_e^4/4)$.

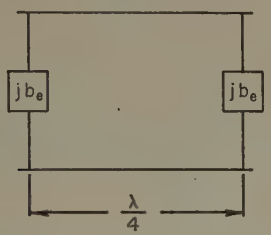

Fig. 3—Equivalent circuit for Fig. 1.

For a single stage the admittance at point b at resonance is $1+j0$, and if plotted on a Smith Chart, it will vary with frequency along some curve, its rate being determined by (4). This curve will be an arc of a circle if the change of susceptance B is neglected, and the resulting reflection from one stage will be a maximum when the length between susceptances becomes a quarter guide wavelength different from the resonant length. Then $t=-(B/2)$, and the admittance Y_b will be

$$Y_b = \frac{1 + j(B^3 + 2B)}{1 + B^2}$$

so that on a Smith-type impedance chart the curve of admittance Y_b for various frequencies will lie on a circle, a diameter of which is a line drawn from the center of the chart to the point where the admittance has this value. (See Fig. 4.) It is interesting to note that this diameter passes through the point where the admittance is $1+jB$. The diameter D of this circle is the magnitude of the reflection coefficient at this point; namely,

$$\frac{B\sqrt{B^2+4}}{B^2+2}.$$

The reflection coefficient at point b, Γ_b, near resonance varies as $D \sin \theta$; this is the equation in polar coordinates for the circle on the Smith Chart which describes the admittance Y_b when θ is the angle between the tangent to the circle at resonance and the reflection vector. The admittance at the center of the two stages will vary along the $B/Y_0=0$ line on the circle diagram near resonance, and for small deviations from resonance this curve will be an arc of a circle of diameter A. On matching the magnitudes of reflection coefficient near resonance, there results $A\phi=D\theta$. The angle on a Smith Chart which the points on the Y_b circle must be rotated to bring them to the Y_h circle is $2\pi m/\lambda_g$. The difference between ϕ and θ is equal to the derivative of this with respect to frequency times the frequency deviation from resonance.

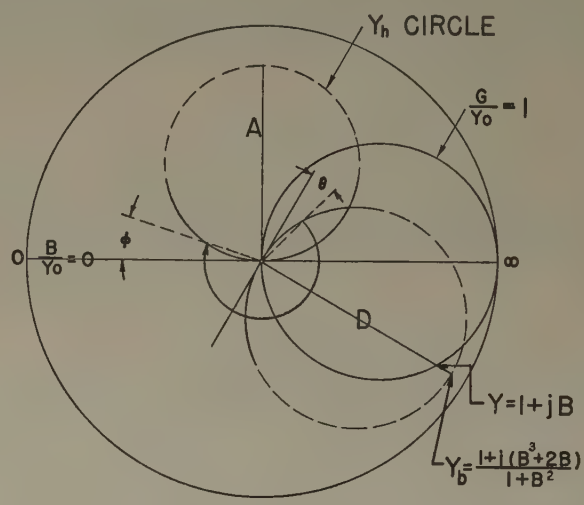

Fig. 4—Smith Chart plot of admittance Y_b and Y_h of Fig. 1.

For Fig. 4 near resonance $G_h=1$ and $B_h=A\phi^2$, and since for small values of the reflection coefficient Γ_h, $Y_h=1+2\Gamma_h$, we get

$$Q_e = \sqrt{Q_L^2 \frac{B^2+2}{B\sqrt{B^2+4}} + \frac{\pi m}{\lambda_g}\left(\frac{\lambda_g}{\lambda_a}\right)^2 Q_L}, \qquad (12)$$

which represents the effective Q of each of the two stages where $b_e=4Q_e(\Delta f/f)$ as before. An experimental check of an actual filter with $B=-2$, $s=3/8\lambda_g$, and $m=5/8\lambda_g$ gave $Q_e=10.8$. The value computed from this formula was 10.3. The value of Q_L of a single stage is 8.5.

For resonant irises which are spaced $n\lambda_g/4$ apart or for large B and stages spaced $m=n\lambda_g/4$ apart, this formula reduces to Mumford's[4]; namely,

$$Q_e = Q_L + \frac{n\pi}{8}\left(\frac{\lambda_g}{\lambda_a}\right)^2.$$

Experimental Results

To check the theory developed in this paper, a series of low-Q filters was built. Symmetrically placed inductive posts were used rather than inductive irises; the posts were one-sixteenth inch brass rods mounted parallel to the narrow face of the waveguide. The susceptance of a pair of these posts was found experimentally in 0.4 by 0.9 inch inner dimension waveguide

at 9,090 megacycles to be given for susceptance between 0 and -6 by

$$B = -\frac{\lambda_g}{a}\cot^2\frac{\pi d}{2a}.$$

In this formula d is the distance between center lines of the posts decreased by 0.094 inch, and a is the inner width of the guide.

The center line spacing of a pair of posts to give a susceptance of -2.0 was found. Then a single stage was constructed of two pairs spaced three-eighths of wavelength apart, and its Q was measured as 8.5. (See Table I.) It was necessary to lengthen the spacing between pairs by about 0.010 inch to correct for the thickness of the posts.

In the computation of the spacing for critical coupling equation, only the lowest mode is assumed to be present. From (5) the spacing between stages should be either one-eighth or five-eighths of a guide wavelength, and two-stage filters were made to these specifications. When the spacing was the lesser of these values (0.233 inch), the plot of standing-wave ratio as a function of frequency showed a match on either side of resonance, but the standing-wave ratio at resonance was 2.3 decibels (in voltage 1.32). This high standing wave is presumably due to higher mode interaction, since when the spacing between stages was lengthened by a half wavelength; the standing-wave ratio at resonance dropped to 0.1 decibel (in voltage 1.02), and the curve was flat at this point. The measurement of Q's was mentioned earlier.

Continuously Adjustable Electronic Filter Networks*

GLENN E. TISDALE†, ASSOCIATE MEMBER, IRE

Summary—**Standard network theory is used to explain the advantages of *RC* networks in the design of filters with frequency response characteristics which are continuously adjustable over several decades. The theoretical discussion is followed by a review of some simple circuits from which most filter characteristics may be obtained. The shape of the response as a function of frequency is determined largely by passive networks. Tubes serve to isolate the passive networks and, in some cases, to invert their response by means of feedback amplification. An example of the method is demonstrated by the design of an adjustable low-pass high-pass filter.**

Review of Theory

THE DIMENSIONLESS complex ratio of the output voltage to the input voltage of any four-terminal network can be written[1] in terms of the complex frequency, $p=\sigma+j\omega$, as

$$F(p) = \frac{a_m p^m + a_{m-1}p^{m-1} + \cdots + a_1 p + a_0}{b_n p^n + b_{n-1}p^{n-1} + \cdots + b_1 p + b_0}. \quad (1)$$

This quotient of two polynomials in p can be called the transfer function of the network. The constants a and b are real in physical circuits, but are not necessarily positive. If (1) is factored to give zeros p' and poles p'', the result has the form

$$F(p) = \frac{a_m(p-p_1')(p-p_2')\cdots(p-p_m')}{b_n(p-p_1'')(p-p_2'')\cdots(p-p_n'')}. \quad (2)$$

Because the coefficients of p in (1) are real, any complex or imaginary zeros or poles of $F(p)$ must occur in conjugate pairs. In addition, the poles must have negative, nonzero real parts,[2] i.e., they fall in the left half of the p plane. Zeros may fall anywhere in the p plane.

Except for the output level, a_m/b_n in (1), any stable characteristic can be obtained with passive networks. This is stated as a theorem by Bode,[3] and it eliminates speculation about new filter characteristics possible with the use of tubes. Tube parameters, such as the amplification factor, cannot usually be specified closely, nor can they be varied widely without the appearance of nonlinear phenomena. The shape of the response characteristics as a function of frequency will therefore be derived from passive sections. Tubes will serve only to isolate sections, to raise the output level, or, as will be shown later, to invert certain transfer functions by means of feedback amplification.

The necessary conditions for a shift of the attenuation and phase characteristics of a transfer function intact along the logarithmic frequency scale can be obtained from (1) and (2). A response in the sum form of (1) is shifted by a factor s if each of its terms is multiplied by s raised to the power of p in that particular term. If s is greater than unity, the response is shifted to a lower frequency. The same shift in frequency is obtained by a division by s of the poles and zeros of the factored expression of (2). A dimensional analysis of $F(p)$ will now be used to realize this frequency shift by a variation of the circuit parameters of physical networks. It will be shown that RC networks are particularly suitable for this purpose at low frequencies.

Equation (1) may be factored to give

$$F(p) = \left(\frac{a_0}{b_0}\right)\frac{\alpha_m p^m + \alpha_{m-1}p^{m-1} + \cdots + \alpha_1 p + 1}{\beta_n p^n + \beta_{n-1}p^{n-1} + \cdots + \beta_1 p + 1}, \quad (3)$$

* Decimal classification: R143.2×R386. Original manuscript received by the Institute, October 14, 1949; revised manuscript received, January 30, 1950. This paper is an abstract of a dissertation presented for the degree of Doctor of Philosophy at Yale University, May, 1949.

† Formerly, Yale University, New Haven, Conn.; now, Servo Corporation of America, New Hyde Park, L. I., N. Y.

[1] H. W. Bode, "Network Analysis and Feedback Amplifier Design," D. Van Nostrand Co., New York, p. 25; 1945.

[2] See p. 111 of footnote reference 1.

[3] See p. 245 of footnote reference 1.

where $\alpha_k = a_k/a_0$ and $\beta_k = b_k/b_0$ can be considered as functions of passive elements with no loss in generality, as stated previously. It is seen that a_0/b_0 is dimensionless, since $F(p)$ is the ratio of two voltages. Likewise, all the terms of the quotient are dimensionless, since they form a series with unity. As p has the dimension of the reciprocal of time, or $1/[T]$, the dimensions of α_k and β_k are $[T]^k$.

By definition, the dimensions of the three circuit elements are

$$\begin{aligned} &\text{Resistance, } R \ \frac{\text{EMF}}{\text{Current}} \quad \text{or} \quad [R]; \\ &\text{Capacitance, } C \ \frac{\text{Current-Time}}{\text{EMF}} \quad \text{or} \quad \frac{[T]}{[R]}; \\ &\text{Inductance, } L \ \frac{\text{EMF-Time}}{\text{Current}} \quad \text{or} \quad [R][T]. \end{aligned} \tag{4}$$

For the purposes of this discussion the symbols $[R]$, $[L]$, and $[C]$ are defined as any mathematical combination of the corresponding circuit elements having the dimensions of a single element of that kind. Thus the expressions $C_1+C_2+C_3$ and C_1C_2/C_1+C_2 are both represented by $[C]$. In (3) for $F(p)$ the dimensions $[T]^k$ for α_k and β_k can be obtained by using relations (4) from the formulas

$$\left.\begin{matrix}[\alpha_k] \\ [\beta_k]\end{matrix}\right\} = [C]^{k-j}[L]^j[R]^{k-2j} = [T]^k. \tag{5}$$

Here j is an integer of either sign.

It was stated previously that the characteristic $F(p)$ may be shifted along the frequency scale by a factor s if each coefficient α_k and β_k of p^k is divided by s^k. This division can be associated with the terms of (5) as follows:

$$\frac{[C]^{k-j}}{s^{k-j}} \cdot \frac{[L]^j}{s^j} \cdot [R]^{k-2j}. \tag{6}$$

This result indicates that a sufficient condition for the frequency shift of a characteristic is the alteration of the values of all capacitances and inductances in the circuit by the reciprocal of the shifting factor. Resistances, being frequency insensitive, remain fixed. Unfortunately, this result is often impractical at low frequencies. An attempt to vary R and C instead of L and C is, in general, unsuccessful.

If no inductances are present, $j=0$, and

$$\left.\begin{matrix}[\alpha_k] \\ [\beta_k]\end{matrix}\right\} = [C]^k[R]^k. \tag{7}$$

If no capacitances are present, $j=k$, and

$$\left.\begin{matrix}[\alpha_k] \\ [\beta_k]\end{matrix}\right\} = [L]^k[R]^{-k}. \tag{8}$$

In either of these expressions the frequency shift can be made by a variation of all values of any single parameter. At low frequencies the RC function with variable resistors is usually most suitable. Because all resistors must be variable, circuit design should include a minimum of this type of element. It is therefore of importance to know the relation between the number of resistors and the degree of the numerator and denominator of $F(p)$; in other words, the number of available zeros and poles.

It can be shown by the methods of matrix algebra that the largest number of poles and zeros of $F(p)$ is less than or equal to the number of separate resistors in an RC network. This statement is also true for the number of separate capacitors. In general, therefore, RC networks having an equal number of resistors and capacitors will present a given number of poles and zeros most economically. An effect of extra capacitors is discussed later.

In establishing a method for the design of a general filter characteristic using RC networks, a difficulty arises due to the restriction on the location of the poles. While zeros may appear anywhere on the complex plane, the poles are always negative-real.[4] This restriction is removed by the introduction of vacuum tubes.

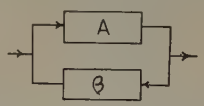

Fig. 1—Representation of feedback amplifier.

Complex poles are obtained if a network having equivalent complex zeros is used as the β circuit of a simple feedback loop. For the feedback amplifier of Fig. 1 it can be shown[5] that

$$F(p) = \frac{A}{1 + A\beta} \approx \frac{1}{\beta}, \tag{9}$$

if the gain A of the amplifier is sufficiently large that $A\beta \gg 1$. Then any zeros of the β circuit will become poles, and vice versa, within the validity of the approximation.

Design Procedure

The design of an electronic RC filter network can begin with the statement of the frequency characteristic in the form of a transfer function, factored to give poles and zeros. The function is then broken up into a number of separately realizable factors. The networks from which the factors are realized are joined by cathode followers or other isolating devices to give the original function.

A variety of more or less familiar circuits can be used to obtain particular configurations of poles and zeros. Simple ladder structures provide poles and zeros on the real axis and zeros at the origin. Zeros on the imaginary axis can be obtained from the parallel T and similar

[4] E. A. Guillemin, "Communications Networks," John Wiley and Sons, Inc., New York, N. Y., vol. II, p. 208; 1935.
[5] MIT Staff, "Applied Electronics," John Wiley and Sons, Inc., New York, N. Y., p. 526; 1943.

structures.[6] These same structures yield complex zeros, but as their transfer functions are cubic in form, the design problems are considerable. Complex zeros in the left-half plane are more readily obtained from the bridged T of Fig. 2 for which the polynomials in $F(p)$ are quadratic. If the transfer function for this network

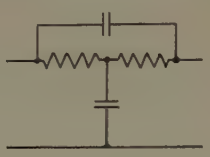

Fig. 2—Bridged-T network.

is inverted in a feedback loop, the complex zeros become a pair of complex poles. A capacitor shunted across the output of the bridged T shifts the poles without affecting the zeros. This example of the effect of extra elements of one kind in an RC network also provides information on the changes in the characteristic due to the loading of each network by the grid-to-ground capacities of the isolating stages.

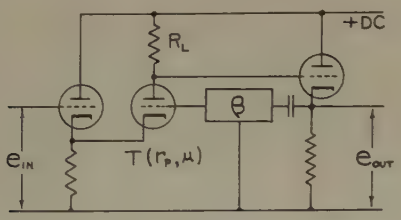

Fig. 3—Practical form of feedback amplifier for μ-circuit inversion.

A practical circuit[7] for the inversion of a β circuit is shown by Fig. 3. The transfer function of this circuit is

$$F(p) = \frac{1+\mu}{1+\dfrac{r_p + R_k(1+\mu)}{R_L} + \mu\beta} \approx \frac{1}{\beta}. \qquad (10)$$

if the amplification factor μ of amplifier T is many times greater than unity, and if the effective cathode impedance R_k presented to T is many times less than R_L. From the exact expression it is seen that the number of zeros cannot exceed the number of poles, regardless of the form of β.

Adjustable Low-Pass High-Pass Filter

An example of the method is the development of an adjustable electronic filter having the frequency characteristics of the prototype low-pass section of Fig. 4. This network has a flat response in the pass band and an attenuation rate of 18 db per octave well above the cutoff frequency. The transfer function is

$$F(p) = KF_1(p)F_2(p)$$

$$= \frac{K}{\left(1+\dfrac{p}{\omega_k}\right)\left(1+2\zeta\dfrac{p}{\omega_n}+\left(\dfrac{p}{\omega_n}\right)^2\right)}. \qquad (11)$$

The constants K, ω_k, ω_n, and ζ are real and positive, and $\zeta<1$, which implies a pair of complex poles. Reasonable design values for a flat pass band and sharp cutoff are $\zeta=0.35$ and $\omega_k/\omega_n=0.707$. Reduction of ζ sharpens the cutoff at the expense of flat pass response.

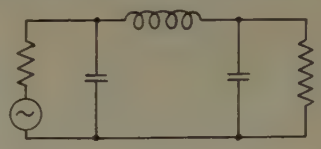

Fig. 4—Prototype low-pass section.

The real pole of $F_1(p)$ is obtained by a single RC section. Inversion of a bridged T yields the complex poles of $F_2(p)$, and in addition a pair of real zeros, which must be cancelled by a matching pair of real poles. The complete circuit is shown by Fig. 5. In the electronic network $K=1$, which implies essentially unity transmission for this section below cutoff. In the prototype section, $K<1$.

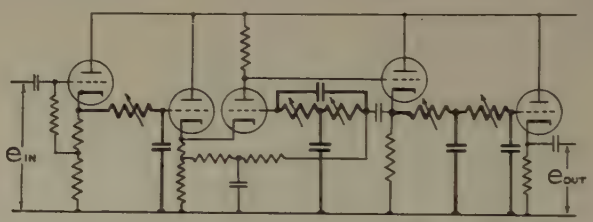

Fig. 5—Continuously adjustable low-pass filter. The RC networks which determine the frequency characteristics are drawn with heavy lines. The variable resistors are ordinarily gauged.

The high-pass equivalent of Fig. 4 is obtained by the substitution of ω_n/p for p/ω_n in (11). The result is

$$G(p) = \frac{K\dfrac{p^3}{\omega_n^3}}{\left(\dfrac{p}{\omega_n}+\dfrac{\omega_n}{\omega_k}\right)\left(1+2\zeta\dfrac{p}{\omega_n}+\left(\dfrac{p}{\omega_n}\right)^2\right)}. \qquad (12)$$

If $\omega_k=\omega_n$, $G(p)$ is obtained from the low-pass expression by the addition of three zeros at the origin. If $(\omega_k/\omega_n)\neq 1$, the shape of the high-pass and low-pass curves will be mirror images about ω_n if the two values for this ratio are reciprocal. The zeros are introduced by reversing the positions of R and C in the ladder sections of Fig. 5. The inverted β circuit is unchanged. A few switches permit the circuit to perform as a high-pass or a low-pass filter.

Acknowledgment

The author is indebted to W. J. Cunningham for helpful suggestions made during the course of this investigation.

[6] G. R. Harris, "Bridged reactance-resistance networks," Proc. I.R.E., vol. 37, pp. 882–887; August, 1949.

[7] G. E. Valley and H. Wallman, "Vacuum Tube Amplifiers," McGraw-Hill Book Co., New York, N. Y., p. 402; 1948.

Design Relations for the Wide-Band Waveguide Filter*

SEYMOUR B. COHN†, MEMBER, IRE

Summary—**Design formulas are derived and presented graphically for a wide-band waveguide filter structure analyzed in a previous paper. The design procedure is outlined and a brief example given. Experiments indicate that the design cutoff frequencies and the infinite-attenuation frequency may be relied upon within one or two per cent.**

THE WAVEGUIDE FILTER structure considered in this paper is shown in Fig. 1. This structure is most suitable for pass-band widths of the order of 1.5 to 1. The low-frequency cutoff f_c is provided by the natural cutoff of the waveguide, while the high-frequency cutoff f_1 is provided by the constrictions and cavities. The attenuation-versus-frequency response is sketched in Fig. 2. An accurate solution for this filter is given in a previous paper.[1] The formulas of that publication, however, are too unwieldly and contain too many parameters to enable simple application to a filter design problem. In this paper, it will be shown how the original equations may be simplified and represented graphically with very little loss of accuracy.

The Original Formulas

The following formulas for the image parameters are given in the paper on the analysis of this filter.[1]

$$y_I = \sqrt{y_{sc}y_{oc}} \tag{1}$$

$$\theta = \alpha + j\beta = 2 \tanh^{-1} \sqrt{\frac{y_{oc}}{y_{sc}}} \tag{2}$$

where y_I is the image admittance of the filter, y_{sc} and y_{oc} the short- and open-circuit admittances of a half section, θ the image transfer function of one section, α the image attenuation function in nepers, and β the image phase constant in radians. All admittances are normalized with respect to the characteristic admittance of the rectangular-waveguide portions of the filter which are of height b and width a (Fig. 1). If a is held constant, the characteristic admittance of the guide is inversely proportional to b. Hence, the normalized characteristic admittance of the terminating line is equal to b/b_T. The half-section admittances are given by

$$y_{oc} = \frac{j}{\delta} \tan\left[\frac{\pi l'}{\lambda_g} + \tan^{-1}\left(\frac{\delta y_{oc'}}{j}\right)\right] \tag{3}$$

$$y_{sc} = \frac{j}{\delta} \tan\left[\frac{\pi l'}{\lambda_g} + \tan^{-1}\left(\frac{\delta y_{sc'}}{j}\right)\right] \tag{4}$$

where

$$y_{oc'} = j \tan\frac{\pi l}{\lambda_g}$$

$$+j\frac{2b}{\lambda_g}\left\{\frac{S_0(\delta)}{\pi^2} + \sum_{n>0}\left[\frac{\tanh\dfrac{n\pi lF}{b}}{F} - 1\right]\frac{\sin^2 \pi n\delta}{n(\pi n\delta)^2}\right\} + j\epsilon_{oc} \tag{5}$$

$$y_{sc'} = -j \cot\frac{\pi l}{\lambda_g}$$

$$+j\frac{2b}{\lambda_g}\left\{\frac{S_0(\delta)}{\pi^2} + \sum_{n>0}\left[\frac{\coth\dfrac{n\pi lF}{b}}{F} - 1\right]\frac{\sin^2 \pi n\delta}{n(\pi n\delta)^2}\right\} + j\epsilon_{sc} \tag{6}$$

$$F = \sqrt{1 - \left(\frac{b}{n\lambda_g}\right)^2} \tag{7}$$

$$\epsilon_{oc} \approx \epsilon_{sc} \approx \epsilon \approx -0.09b/\lambda_g \tag{8}$$

where δ is the ratio b'/b, and b', l', and l are dimensions shown in Fig. 1. λ_g is the guide wavelength of a uniform rectangular guide of width a. $S_0(\delta)$ is the Hahn function of zero order, which is tabulated by Whinnery and Jamieson.[2] Their value for $\delta = 0.05$ is in error, however, and should be $S_0(0.05) = 26.23$. For $\delta \leqq 0.15$, the following formula for $S_0(\delta)$ is within 0.4 per cent.

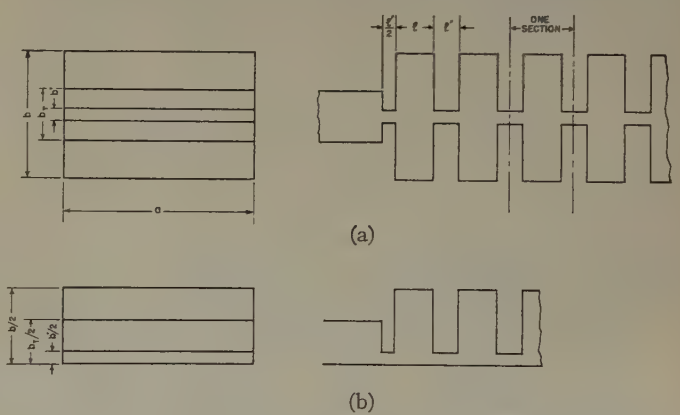

Fig. 1—The broad-band waveguide filter. The design information applies to both (a) and (b).

$$S_0(\delta) \approx \pi^2\left(\log_e\frac{1}{\delta} - 0.338\right). \tag{9}$$

The correction term of (8) is sufficiently accurate if δ is less than about 0.15, which is the case in the design of this type of filter. More accurate expressions for ϵ are given in (42) and (43) of footnote reference 1.

Formulas for the Filter Parameters

In the design of a filter, one must first decide where to place the cutoff and infinite-attenuation frequencies,

* Decimal classification: R386.1×R118. Original manuscript received by the Institute, September 20, 1949.

† Sperry Gyroscope Company, Great Neck, L. I., N. Y.

[1] S. B. Cohn, "Analysis of a wide-band waveguide filter," PROC. I.R.E., vol. 37, p. 651; June, 1949.

[2] J. R. Whinnery and H. W. Jamieson, "Equivalent circuits for discontinuities in transmission lines," PROC. I.R.E., vol. 32, pp. 98–115; February, 1944.

and what value of terminating resistance to use. For a waveguide filter section, these parameters are more conveniently expressed by the wavelengths λ_c, λ_{g1}, and $\lambda_{g\infty}$, and by the height b_T of the terminating guide. $\lambda_c(=2a)$ is the cutoff wavelength of a rectangular guide of width a, λ_{g1} the cutoff guide wavelength of the filter structure, and $\lambda_{g\infty}$ the infinite-rejection guide wavelength (Fig. 2). When a filter is being designed, it is necessary to obtain

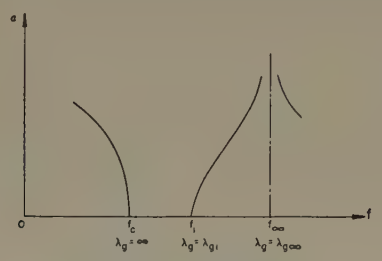

Fig. 2—Attenuation-versus-frequency response.

the filter dimensions which correspond to these given parameters. The difficulty of doing this by means of (1) through (8) is obvious. Hence it is necessary to change the form of these equations so that a straightforward design procedure will be possible. This is done below.

Let b_o be the terminating-guide height which would match the filter at f_c (i.e., for $\lambda_g \to \infty$). Then, by (1),

$$\lim_{\lambda_g \to \infty} (y_T)^2 = \left(\frac{b}{b_o}\right)^2 = [\lim y_{oc} \lim y_{sc}]_{\lambda_g \to \infty}.$$

When (3), (4), (5), and (6) are substituted and the limiting process carried out, one obtains[3]

$$\left(\frac{b}{b_o}\right)^2 = \left(\frac{l}{l+\delta l'}\right)\left\{1 + \frac{l'}{\delta l} + \frac{2b}{\pi^3 l} S_o(\delta) - \frac{2b}{\pi l}\sum_{n>0}\left[1 - \tanh\frac{n\pi l}{b}\right]\frac{\sin^2 \pi n\delta}{n(\pi n\delta)^2} + \frac{\lambda_g \epsilon}{\pi l}\right\}. \quad (10)$$

The actual height b_T of the terminating guide need not be equal to b_o. It will generally be chosen to give a perfect match at some point within the pass band, as explained later in the Design Procedure section.

Next, an implicit relation for the cutoff wavelength λ_{g1} will be obtained. This cutoff occurs when $y_{sc}=0$.[1] By means of (4) and (6), therefore, one obtains

$$\frac{\cot \pi \frac{l}{b}\frac{b}{\lambda_{g1}}}{\pi \frac{l}{b}\frac{b}{\lambda_{g1}}} = 2\frac{b}{l}\frac{S_o(\delta)}{\pi^3} + \frac{\tan \pi \frac{l'}{\lambda_{g1}}}{\pi\delta \frac{l}{b}\frac{b}{\lambda_{g1}}} + \frac{2b}{\pi l}\sum_{n>0}\left[\frac{\coth \frac{n\pi l}{b}\sqrt{1-(b/n\lambda_{g1})^2}}{\sqrt{1-(b/n\lambda_{g1})^2}} - 1\right]\frac{\sin^2 \pi n\delta}{n(\pi n\delta)^2}$$

$$+ \frac{\epsilon}{\pi \frac{l}{\lambda_{g1}}}. \quad (11)$$

The largest value of λ_{g1} which satisfies this equation yields the desired cutoff wavelength.

Lastly, an implicit relation for the infinite-attenuation wavelength will be derived. By (2), the attenuation α is infinite for $y_{oc}=y_{sc}$. When (3) and (4) are set equal, and (5) and (6) substituted, one obtains[3]

$$\csc\left(2\pi \frac{l}{b}\frac{b}{\lambda_{g\infty}}\right) = 2\frac{b}{\lambda_{g\infty}}\sum_{n>0}\frac{\operatorname{csch}\left[\frac{2\pi nl}{b}\sqrt{1-\left(\frac{b}{n\lambda_{g\infty}}\right)^2}\right]}{\sqrt{1-(b/n\lambda_{g\infty})^2}}\frac{\sin^2 \pi n\delta}{n(\pi n\delta)^2}. \quad (12)$$

Equations (10), (11), and (12) relate the critical wavelengths and the matching height to the filter dimensions, but they are still too complex for convenient use. It will now be shown how they may be put in graphical form with very little loss of accuracy.

The Design Graphs

Equation (12) contains three parameters, $b/\lambda_{g\infty}$, l/b, and δ. It is plotted in Fig. 3, where it is seen to be independent of δ for $l/b>0.2$. For $l/b<0.2$, linear interpolation between the curves for $\delta=0$ and 0.1 provides sufficient accuracy.

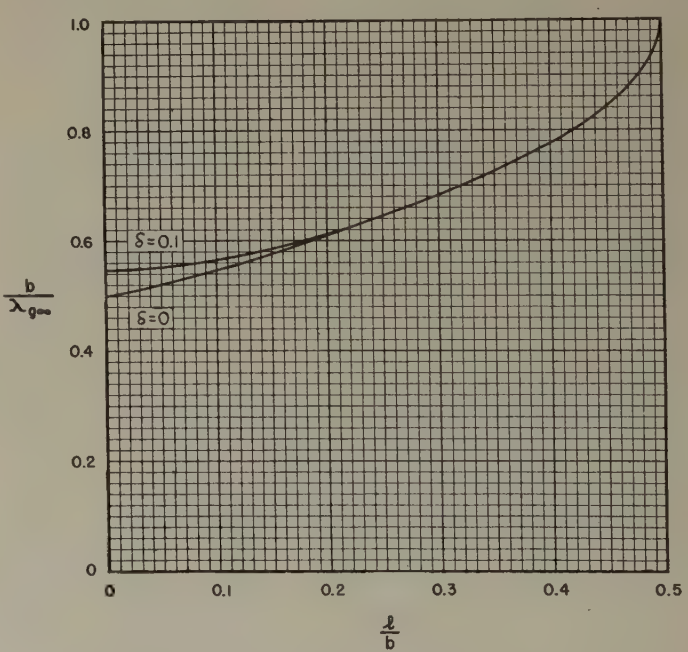

Fig. 3—Infinite-attenuation-wavelength curve.

Equation (10) has four parameters, b/b_o, l'/l, b/l, and δ. Fortunately, a greater error can be tolerated in b/b_o than in b/λ_{g1} or $b/\lambda_{g\infty}$, and hence several approximations may be made:

1. In practice, the product $\delta l'$ is generally less than one tenth as large as l. If the factor $l/(l+\delta l')$ is replaced

[3] These steps are performed in detail in "A Theoretical and Experimental Study of a Waveguide Filter Structure," by S. B. Cohn, Office of Naval Research, Cruft Laboratory, Harvard University, Report No. 39, April 25, 1948.

by unity, only a five per cent error in the image admittance match will result for $\delta l'$ as large as ten per cent of l. In any case where this error might be significant, the term $[1+\delta l'/l]^{1/2}$ may be used as a correction factor for the b_o value obtained from the simplified formula.

2. δ is usually equal to about one tenth or less. Because of this, and because the infinite series in (10) converges very quickly, the factor $(\sin \pi n\delta)^2/(\pi n\delta)^2$ may be set equal to unity with little error.

3. $\pi l'/\lambda_{g1}$ is usually small enough so that only a small error is introduced by setting $\tan \pi l'/\lambda_{g1}$ equal to $\pi l'/\lambda_{g1}$.

When these approximations are made in (10) and (11), and when the second resulting relation is subtracted from the first, one obtains

$$\frac{b/\lambda_{g1}}{b_o/\lambda_{g1}} = 1 + \frac{\cot \pi \dfrac{l}{b} \dfrac{b}{\lambda_{g1}}}{\pi \dfrac{l}{b} \dfrac{b}{\lambda_{g1}}} - \frac{2b}{\pi l} \sum_{n>0} \frac{1}{n} \left[\frac{\coth \dfrac{n\pi l}{b} \sqrt{1-(b/n\lambda_{g1})^2}}{\sqrt{1-(b/n\lambda_{g1})^2}} - \tan \frac{n\pi l}{b} \right]. \quad (13)$$

This has three parameters, b_o/λ_{g1}, b/λ_{g1}, and l/b. It is plotted in Fig. 4. The dashed curves are constant $\lambda_{g1}/\lambda_{g\infty}$ contours, which were calculated from Fig. 3 for $\delta = 0$.

Equation (11) has four parameters, b/λ_{g1}, l/b, l'/λ_{g1}, and δ. Since only three independent parameters can be displayed on a single two-dimensional graph, (11) will be divided into two separate relations, one of which may be directly calculated very simply, and the other of which may be reduced to three parameters and plotted. In (11) let

$$\frac{2S_o(\delta)}{\pi^3} + \frac{\tan \pi \dfrac{l'}{\lambda_{g1}}}{\pi\delta \dfrac{b}{\lambda_{g1}}} = G \quad (14)$$

where

$$G = \frac{\cot \pi \dfrac{l}{b} \dfrac{b}{\lambda_{g1}}}{\pi \dfrac{b}{\lambda_{g1}}} - \frac{2}{\pi} \sum_{n>0} \left\{ \frac{\coth \dfrac{n\pi l}{b} \sqrt{1-\left(\dfrac{b}{n\lambda_{g1}}\right)^2}}{\sqrt{1-\left(\dfrac{b}{n\lambda_{g1}}\right)^2}} - 1 \right\} \frac{\sin^2 \pi n\delta}{n(\pi n\delta)^2} + \frac{E}{\pi b/\lambda_{g1}}. \quad (15)$$

Equation (15) has four parameters—G, l/b, b/λ_{g1}, and δ—but δ may be eliminated as before by setting $(\sin \pi n\delta)^2/(\pi n\delta)^2$ equal to one. When this is done, only three parameters are left—G, l/b, and b/λ_{g1}. These are plotted in Fig. 5.

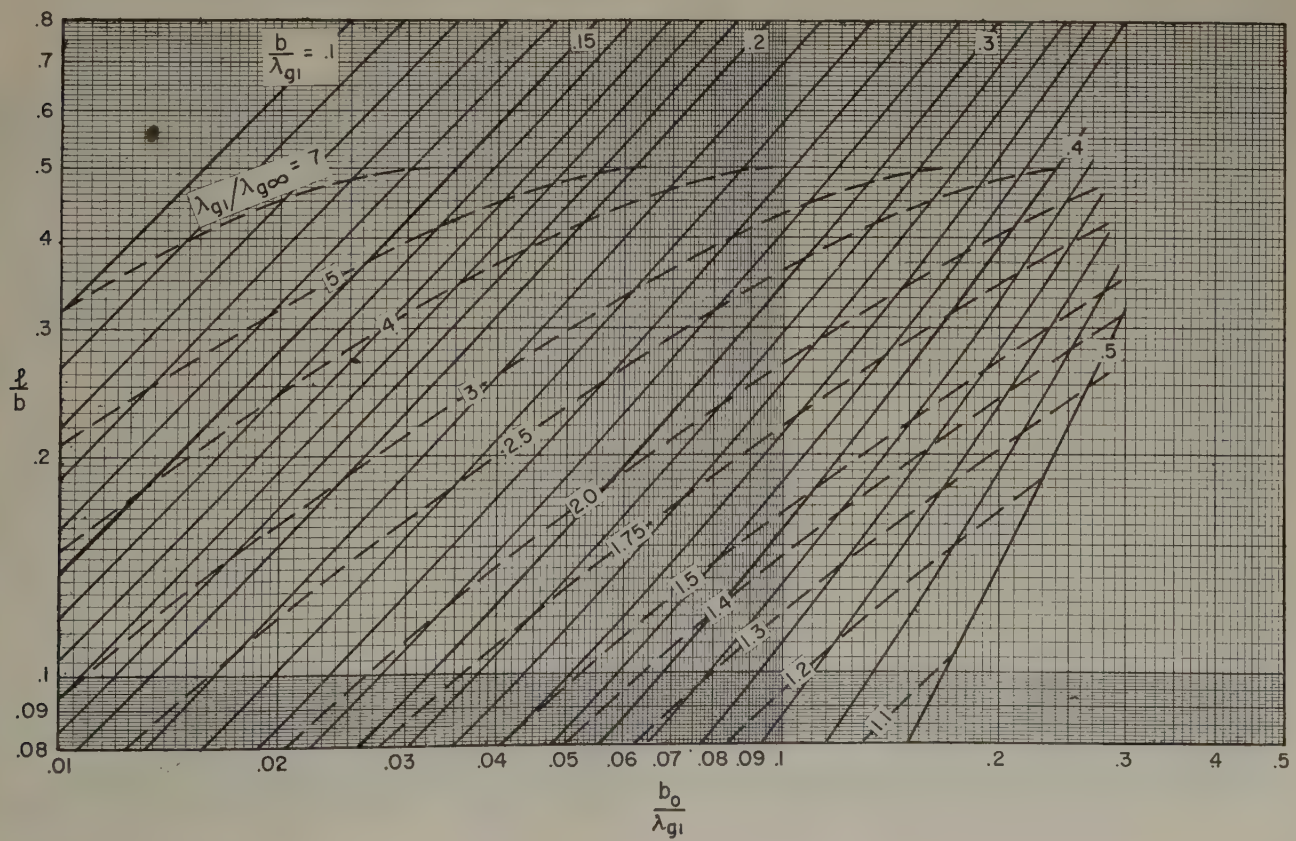

Fig. 4—Design graph giving the parameter b.

The parameters δ and l' are the last ones to be determined in carrying out a design. This may be conveniently done with (9) and (14) written in the following form

$$\tan \pi \frac{l'}{\lambda_{g1}} = \pi\delta \frac{b}{\lambda_{g1}}\left[G - \frac{2}{\pi}\log_e \frac{1}{\delta} + 0.215\right]. \quad (16)$$

After b/λ_{g1} and G have been found, a value of δ should be judiciously chosen, and then l' calculated by (16).

Design Procedure

The lower and upper cutoff frequencies and the infinite-attenuation frequencies are usually the given quantities in a filter-design problem. Corresponding to these three frequencies, the following wavelengths should be determined in the conventional manner: λ_c, λ_{g1}, and $\lambda_{g\infty}$. The width a of the structure is then given by $a=\lambda_c/2$. When the height b_T of the terminating guide has been chosen, a value of b_o may then be selected so that the image admittance of the filter will match the terminating impedance at some point in the pass band. In order to obtain such a match at λ_{g2}, the following approximate formula for b_o may be used:

$$b_o = b_T\sqrt{1 - (\lambda_{g1}/\lambda_{g2})^2}. \quad (17)$$

This follows from the approximate formula for the image admittance given in (24) of footnote reference 1. A fairly good over-all match occurs in the pass band if $b_o \approx 0.7\ b_T$. A much better match occurs if *transforming end sections* are used.[4]

[4] Radio Research Laboratory Staff, "Very High-Frequency Techniques," McGraw-Hill Book Co., New York, N. Y., Section 26–10; 1947.

Next, from Fig. 4, obtain l/b and b/λ_{g1} in terms of b_o/λ_{g1} and $\lambda_{g1}/\lambda_{g\infty}$. Then, from Fig. 5, obtain G in terms of l/b and b/λ_{g1}. Lastly, assume a value of δ and calculate l' from (16). If l'/b' is less than one half, or if l'/λ_{g1} is greater than $\lambda_{g1}/10$, a different value of δ should be tried.

Example: Let $a=2.750$ inches ($f_c=2145$ Mc), $b_T=b_o=0.375$ inch, $f_1=3{,}000$ Mc ($\lambda_{g1}=14.3$ cm $=5.63$ inches), and $f_\infty=3{,}500$ Mc ($\lambda_{g\infty}=10.8$ cm). Hence $b_o/\lambda_{g1}=0.0666$ and $\lambda_{g1}/\lambda_{g\infty}=1.32$, and by Fig. 4, $l/b=0.089$ and $b/\lambda_{g1}=0.410$. Therefore, $b=0.410\times5.63=2.31$ inches and $l=0.089\times2.31=0.206$ inch. By Fig. 5, $G=4.06$. Let $b'=0.125$ inch, so that $\delta=b'/b=0.125/2.31=0.0541$. By (16), $l'=0.302$ inch.

A large number of sections may be used in order to have a sharp cutoff and high attenuation in the stop band. The sections need not all have the same f_∞ value, since dissimilar sections have almost identical image-admittance functions, if their cutoff frequencies and b_o values are the same.[1] Fig. 6(a) shows three sections each having the values of b_o, b', λ_c, and λ_{g1} of the above example. The infinite-attenuation frequencies are, however, from left to right 3,500, 4,500, and 5,500 Mc. By having sections with different f_∞ values, the insertion loss may be kept high in the passband, and also the spurious response of each section near $b/\lambda_g=1$ will fall in the stop band of another section. A further discussion on the removal of spurious responses is given in the literature for a similar type of waveguide filter.[5]

[5] See pp. 734–736 of footnote reference 4.

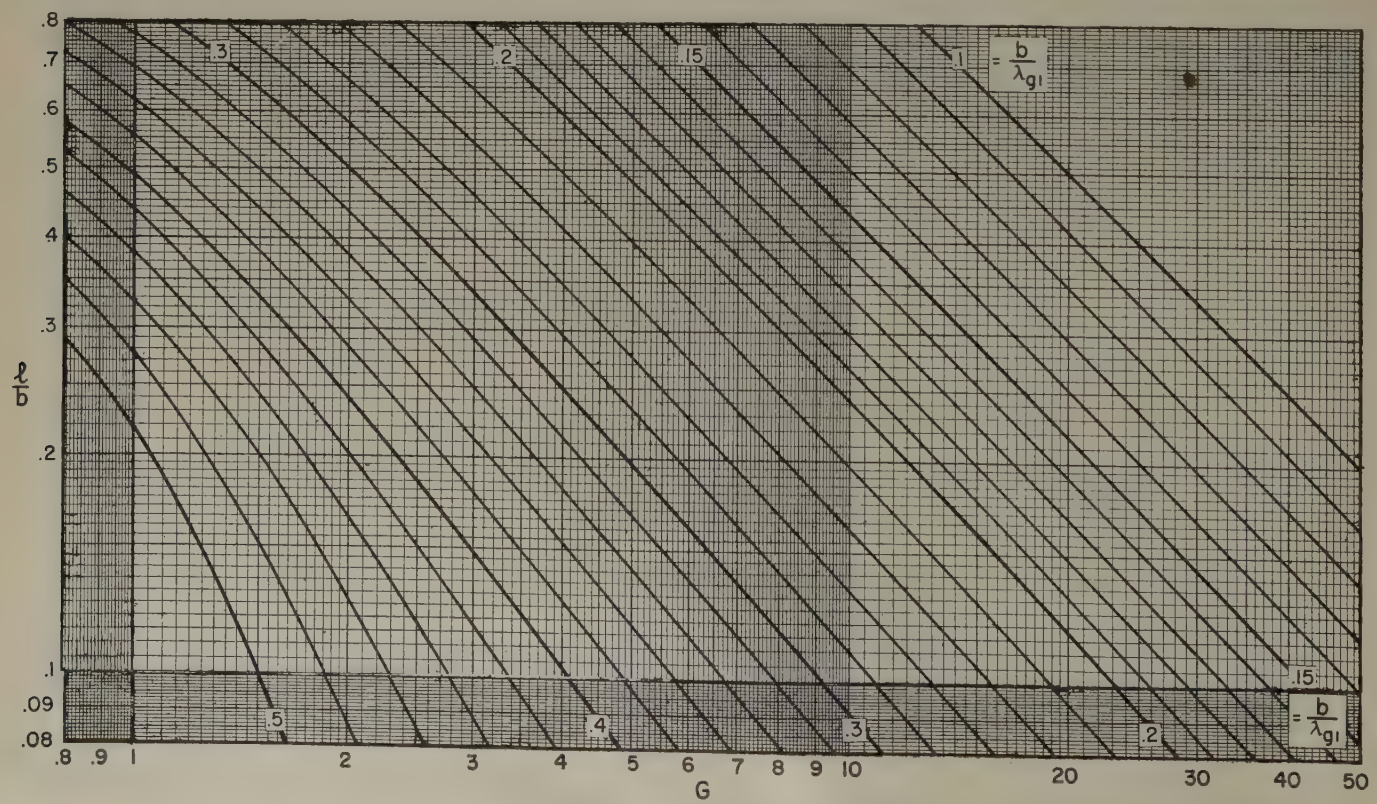

Fig. 5—Design graph giving the parameter G.

Before connecting the end sections to the terminating guide, the discontinuity capacitance due to the junction of heights b_T and b' must be compensated. This may be done to a close approximation by shortening the length of the constriction at each end of the filter from $l'/2$ to $l'/2-\Delta l'$, where $\Delta l'$ is given by[3]

$$\Delta l' = \frac{b'}{\pi}\left(\log_e \frac{b_T}{b'} - 0.386\right). \tag{18}$$

Fig. 6(b) shows the assembled filter, after correction of the end constrictions.

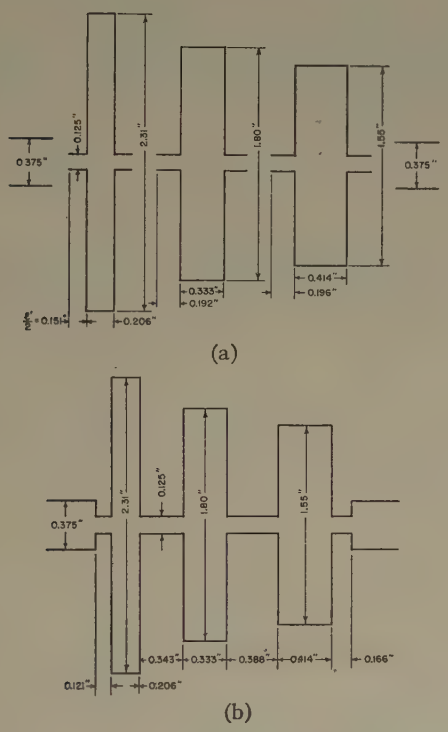

Fig. 6—A three-section waveguide filter, (a) before assembly and (b) after assembly. (f_1=3,000 Mc, a=2.75 inches.)

Verification of Accuracy

Six individual sections terminating in 2.75×0.375-inch guide were constructed with a wide range of physical parameters. The f_1 cutoff frequencies were calculated from (11), except for filter number 5, and also from the design graphs. They were measured by two different methods which checked each other within 0.3 per cent.[3] The various cutoff-frequency values are listed in Table I. The data in the "Tests" column are averages for the two tests.

TABLE I
Values of f_1

Filter No.	Equation (11)	Design Curves	Tests
1	2,993 Mc	3,000 Mc	2,980 Mc
2	3,003	3,000	2,991
3	2,834	2,843	2,822
4	3,000	3,016	3,001
5		3,000	3,024
6	2,995	3,000	2,991

In each case, the spread of f_1 values is less than one per cent. The f_∞ values were calculated by (12) and also measured, and these too agree within one per cent. Since f_c is the natural cutoff frequency of the waveguide, which is known exactly, it need not be checked.

The approximations used in obtaining (13) and Fig. 4 cause an error in the image admittance of up to 5 or 10 per cent, which is generally too small to be of consequence. If the correction factor $[1+\delta l'/l]^{1/2}$ mentioned above in the Design Graph section is used, this error can be greatly reduced.

Acknowledgment

The writer wishes to acknowledge the many helpful suggestions of R. W. P. King and L. Brillouin toward the preparation of this paper.

Slot Radiators*

NICHOLAS A. BEGOVICH†, Associate, IRE

Summary—**The electromagnetic fields throughout all of space produced by an excited finite length slot in an infinite extent perfectly conducting metallic sheet have been calculated by the double current sheet diffraction formula. The space dependence of the fields is the same as that of a thin wire antenna, but with the electric and magnetic fields interchanged. An integration of Poynting's vector over the surface of the slot gives an input resistance of 363 ohms for a center-driven half-wavelength slot. The mutual admittance between slots necessary in slot array calculations is also determined.**

* Decimal classification: R326.81. Original manuscript received by the Institute, July 21, 1949; revised manuscript received, February 13, 1950.

† Hughes Aircraft Company, Culver City, Calif.

I. Introduction

BY AN EXTENSION of Babinet's principle, Booker[1] has postulated that a resonant slot in an infinite extent perfectly conducting sheet should have the same field pattern as a thin wire resonant antenna, but with the electric and magnetic fields interchanged. In addition, the input resistance of a center-driven half-wavelength slot should be 485 ohms. Recent

[1] H. G. Booker, "Slot aerials and their relation to complementary wire aerials," *Jour. IEE*, vol. 93, part IIIA, pp. 620–626; 1946.

measurements by Putnam,[2] however, have shown an input impedance of 350 ohms. Measurements by Bailey[3] have also shown the same discrepancy between the predicted theoretical and the measured impedance. This disagreement has suggested the recalculation of the fields produced by a slot radiator and the input impedance of the slot.

II. Calculation of Fields

Smythe[4] has recently developed a diffraction formula which gives rigorously the fields throughout all of space produced by an excited aperture in an infinite perfectly conducting metallic sheet. The vector potential of the diffracted field in mks units is[5]

$$A = \frac{je^{j\omega t}}{2\pi\omega}\int_S\int \frac{1+j\beta r}{r^2}(\bar{n}\times\bar{E})\times\bar{r}_1 e^{-j\beta r}dS, \qquad (1)$$

where $\bar{r}_1$ is a unit vector in the direction of r (see Fig. 1) and $\bar{n}$ is a unit vector normal to the sheet.[6] The time

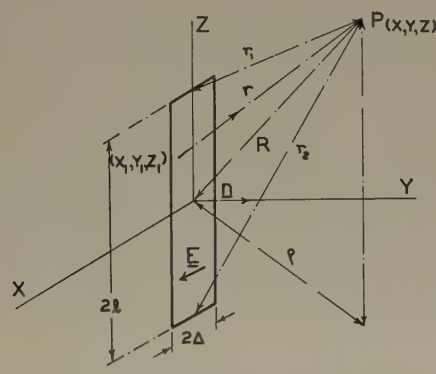

Fig. 1—Slot configuration.

dependence of the electric field in the aperture is $e^{j\omega t}$. The electric and magnetic field of the diffracted fields are given by

$$\bar{E} = -j\omega A, \quad \text{and} \quad \bar{H} = \frac{1}{\mu}\nabla\times A. \qquad (2)$$

The fields given by (1) are exact provided that the correct value of $\bar{E}$ in the aperture or slot is used.

The configuration and dimensions of the slot are shown in Fig. 1, where Δ is assumed infinitely small. The field distribution in the slot will be assumed to be

$$\bar{E} = \bar{\imath}\mathcal{E}\sin\beta(l\mp z_1)\delta(x_1), \qquad (3)$$

where the minus sign is used when $z_1>0$; and the positive sign when $z_1<0$. The transverse field dependence is given by the delta function which has the following properties:

$$\delta(x_1) = 0; \qquad x_1 \neq 0, \qquad (4a)$$

$$\int_{-\infty}^{\infty} f(x_1)\delta(x_1)dx_1 = f(0), \qquad (4b)$$

and

$$\int_{-\infty}^{\infty}\delta(x_1)dx_1 = 1. \qquad (4c)$$

The electromotance across the center of the slot is $+\mathcal{E}$ as shown by the use of (4c). Writing (3) in (1), and integrating with respect to x_1, we obtain

$$\bar{A} = -\frac{j\mathcal{E}e^{j\omega t}}{2\pi\omega}(\bar{\jmath}x-\bar{\imath}y)U = -\bar{e}_\phi\frac{j\mathcal{E}e^{j\omega t}}{2\pi\omega}\rho U, \qquad (5a)$$

where

$$U = \int_{-l}^{+l}\frac{1+j\beta R}{R^3}e^{-j\beta R}\sin\beta(l\mp z_1)dz_1, \qquad (5b)$$

and

$$R^2 = x^2+y^2+(z-z_1)^2 = \rho^2+(z-z_1)^2. \qquad (5c)$$

The Fourier transform of the integrand of (5b) exclusive of the sine term is[7]

$$\frac{1+j\beta R}{R^3}e^{-j\beta R} = \frac{1}{\pi\rho}\int_{-\infty}^{+\infty}(g^2-\beta^2)^{1/2}K_1[\rho(g^2-\beta^2)^{1/2}]e^{-j(z-z_1)g}dg, \quad (\rho>0) \qquad (6)$$

where K_1 is the modified Bessel function of the second kind. Writing (6) in (5b) and since interchanging the order of integration is permissible[8] the z_1 integration results in

$$U = \frac{\beta}{\pi\rho}[2\cos\beta l\, N_1 - N_2 - N_3], \qquad (7)$$

where

$$N_i = \int_{-\infty}^{+\infty}\frac{K_1[\rho(g^2-\beta^2)^{1/2}]}{(g^2-\beta^2)^{1/2}}e^{-jgt_i}dg, \qquad (7b)$$

and

$$t_1 = z, \quad t_2 = z-l; \quad \text{and} \quad t_3 = z+l. \qquad (7c)$$

In Appendix B, it is shown that

$$N_i = -\frac{j\pi}{\beta\rho}\{e^{-j\beta(\rho^2+t_i^2)^{1/2}} - \cos\beta t_i\}. \qquad (8)$$

[2] J. L. Putman, "Input impedance of centre-fed slot aerials near half-wave resonance," *Jour. IEE*, vol. 95, part III, pp. 290–294; July, 1948.

[3] C. E. G. Bailey, "Slot feeders and slot aerials," *Jour. IEE*, vol. 93, part IIIA, pp. 615–619; 1946.

[4] W. R. Smythe, "The double current sheet in diffraction," *Phys. Rev.*, vol. 72, pp. 1066–1070; December, 1947.

[5] See Appendix A for nomenclature.

[6] Note (1) differs by a minus sign from that given in footnote reference 4. The correctness of the sign in (1) can be seen by allowing $r\to 0$ where the diffracted and aperture fields must then be in the same direction and in time phase.

[7] G. A. Campbell and R. M. Foster, "Fourier Integrals for Practical Applications," Bell Telephone Monograph B-584, transform 867.5, p. 111; September, 1931.

[8] H. S. Carslaw, "Introduction to the Theory of Fourier's Series and Integrals," Dover Publications, Inc., New York, N. Y., pp. 191, 199, and 87; 1930.

Consequently, the use of (8), (7), and (5) results in

$$A = \bar{e}_\phi \frac{\mathcal{E}e^{j\omega t}}{2\pi\omega\rho}\left\{e^{-j\beta r_1} + e^{-j\beta r_2} - 2\cos\beta l e^{-j\beta r}\right\}, \quad (9)$$

where $r=(\rho^2+z^2)^{1/2}$ and $r_2^1=(\rho^2+[l\mp z]^2)^{1/2}$. The comparison of the electric and magnetic field components derived from (9) by the use of (2) for the slot and the field components of an infinitely thin wire antenna[9] of length $2l$ and current distribution.

$$I = I_0 \sin\beta(l \mp z_1) \quad (10)$$

(see (3) for sign convention) is given in Table I. The dipole fields are multiplied by two since (1) gives the fields only in the positive half space $x \geqq 0$. Note that the space dependence of electric and magnetic fields have interchanged with a sign reversal as postulated by Babinet's principle.[1]

TABLE I

EQUALITY OF FIELD COMPONENTS FOR A SLOT AND WIRE RADIATOR

Slot Radiator	*Wire Radiator*
$-\frac{E\phi}{\mathcal{E}}$	$\frac{2H\phi}{I_0}$
$\sqrt{\frac{\mu}{\epsilon}}\frac{H\rho}{\mathcal{E}}$	$\sqrt{\frac{\epsilon}{\mu}}\frac{2E\rho}{I_0}$
$\sqrt{\frac{\mu}{\epsilon}}\frac{Hz}{\mathcal{E}}$	$\sqrt{\frac{\epsilon}{\mu}}\frac{2Ez}{I_0}$

III. Half-Wave Slot Input Admittance

To calculate the input impedance of a half-wave slot, the y component of complex Poynting's vector will be integrated over the area of the slot.[10] The y component of the complex Poynting's vector is proportional to the product of E_x and the conjugate of H_z; namely,

$$P_y = -\frac{1}{2}E_x H_z^*$$

$$= -j\frac{\mathcal{E}^2}{4\pi}\sqrt{\frac{\epsilon}{\mu}}\left\{\frac{1}{r_1}e^{j\beta r_1} + \frac{1}{r_2}e^{j\beta r_2}\right\}\delta(x_1)\cos\beta z_1. \quad (11)$$

The complex rms power radiated by the slot is

$$p + jq = \int_{-l}^{+l}\int_{-\Delta}^{+\Delta} P_y dx_1 dz_1 = \tfrac{1}{2}\mathcal{E}^2 Y_i^s \text{ watts}, \quad (12)$$

where Y_i^s is the driving admittance across the center of the slot. By the use of (4b) the x_1 integration in (12) is immediately determined. The z_1 integration can be evaluated in terms of sine and cosine integrals. Comparing the results for the calculations with that given by Carter[11] for the resonant wire antenna, we find

$$Y_i^{2s} = 2Y_i^s = 4\frac{\epsilon}{\mu}Z_i^{w*}, \quad (13)$$

where Y_i^{2s} is the driving admittance when the slot is allowed to radiate on both sides of the sheet and Z_i^{w*} is the conjugate of the driving impedance of the half-wave wire antenna. Writing $Y_i^{2s}=1/Z_i^{2s}$, we can write (13) as[12]

$$Z_i^{2s}Z_i^{w*} = \frac{1}{4}\frac{\mu}{\epsilon} = 3{,}600\pi^2. \quad (14)$$

Using the value $73.2+j42.5$ given by Carter for Z_i^w, we obtain from (14) the driving impedance of the slot

$$Z_i^{2s} = R_i^{2s} + jX_i^{2s} = 362.5 + j210.5 \text{ ohms}. \quad (15)$$

R_i^{2s} is in excellent agreement with the measured value of 350 to 360 ohms given by Putnam.[2] However, X_i^{2s} disagrees with Putnam's measurements. This is to be expected, since the measured input reactance is a combination of the slot reactance and the reactance of the local waves produced by the discontinuity in the transmission line feeding the slot.

IV. Mutual Coupling

The mutual coupling between two slots can be determined by the integration of the cross product terms in Poynting's vector. Since the calculation is identical to the procedure used for wire antennas[13] only the results will be given. For two slots oriented as shown in Fig. 2,

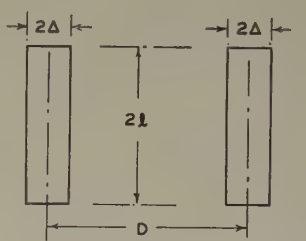

Fig. 2—Slot configuration for maximum mutual coupling.

the mutual impedance between the slots when they are allowed to radiate on both sides of the metallic sheet and the mutual impedance between two wire antennas is related by

$$Z_m^{2s}Z_m^{w*} = \frac{1}{4}\frac{\mu}{\epsilon}. \quad (16)$$

[9] J. A. Stratton, "Eectromagnetic Theory," McGraw-Hill Book Co., Inc., New York, N. Y., p. 457; 1941. Note j corresponds to $-i$ in Stratton's notation since he takes the time dependence as $e^{-i\omega t}$.

[10] For this method to be applicable to a nonresonant length slot, the slot must have a finite width. The similar situation occurs in wire antennas; compare J. Aharoni, "Antennae," Oxford University Press, London, p. 188; 1946.

[11] P. S. Carter, "Circuit relations in radiating systems and applications to antenna problems," PROC. I.R.E., vol. 20, pp. 1004–1041; June, 1932.

[12] This equation has been given by Booker, in footnote reference 1. However, in Booker's calculation of Z_i^{2s} he neglected the reactive part of Z_i^w, thus giving 485 for R_i^{2s} instead of the correct value given in (15).

[13] S. A. Schelkunoff, "Electromagnetic Waves," D. Van Nostrand Company, Inc., New York, N. Y., p. 372; 1943.

That (16) and (15) should be the same follows since Z_i^{2s} can be derived from Z_m^{2s} by letting the distance between the slots vanish. Equation (16) holds not only for the configuration shown in Fig. 2, but for any orientation between the slots confined to a single metallic sheet. Consequently, the formulas and tables given by Carter[11,14] for colinear, staggered, and other dipoles configurations can be immediately applied to similarly oriented slots by the use of (16).

V. Induced Currents

The currents induced in the metallic sheet containing the slot are given by the value of the magnetic field at the surface of the sheet. Measurements made by Putnam et al[15] of a slot at the center of a sheet nine wavelengths in diameter are in good agreement with the theoretical values.

VI. Conclusions

It has been rigorously demonstrated that the field pattern of a slot in an infinite metallic sheet and that of a wire antenna are identical, with, however, the electrical and magnetic fields interchanged. This result is in complete agreement with that derived from Babinet's principle. The relationship between the driving and mutual admittance of slots and wire dipoles has also been shown.

Appendix A

Nomenclature

$j = (-1)^{1/2}$
ω = angular frequency
β = wave number
ϵ = permittivity of free space $(1/36\pi)10^{-9}$ farads/meter
μ = permeability of free space $4\pi 10^{-7}$ henrys/meter
$\bar{n}$ = unit vector normal to sheet containing slot
$x_1\ y_1\ z_1$ = co-ordinates of point in slot
x, y, z = co-ordinates of observation point
$r = \{(x-x_1)^2+(y-y_1)^2+(z-z_1)^2\}^{1/2}$ in (1)
$r = (\rho^2+z^2)^{1/2}$ in (9)
$R = \{x^2+y^2+(z-z_1)^2\}^{1/2}$
$\rho = \{x^2+y^2\}^{1/2}$
$-\epsilon$ = impressed electromotance across center of slot
$\delta(x)$ = delta function
K_n = modified Bessel function of the second kind
$2l$ = length of slot
Y_i^s = driving admittance of slot when it radiates on one side of the metallic sheet
Y_i^{2s} = driving admittance of slot when it radiates on both sides of the metallic sheet
Z_i^{2s} = driving impedance of slot when it radiates on both sides of the metallic sheet
Z_i^w = driving impedance of wire antenna
Z_m^{2s} = mutual impedance of two slots
Z_m^w = mutual impedance of two wire antennas.

Appendix B

Consider the following integral[16]

$$\frac{\pi e^{-j\beta(t^2+\rho^2)^{1/2}}}{(\rho^2+t^2)^{1/2}} = \int_{-\infty}^{+\infty} K_0[\rho(\xi^2-\beta^2)^{1/2}]e^{-jt\xi}d\xi. \quad (17)$$

The path of integration of (17) is the real axis of the ξ plane indented at the branch points at $\xi = \pm\beta$ as shown in Fig. 3. The semicircles at $\xi = \pm\beta$ are infinitely small,

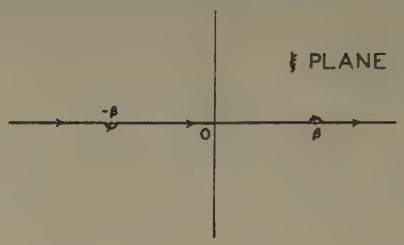

Fig. 3—Integration path for equation (17).

and their position above and below the real axis being chosen so that $0 \leqq \rho h(\xi^2-\beta^2)^{1/2} \leqq \pi/2$. The integral on the right side of (17) stands for

$$\lim_{\Delta\to 0}\left\{\int_{-\infty}^{-\beta-\Delta} + \int_{\xi=-\beta} + \int_{-\beta+\Delta}^{+\beta-\Delta} + \int_{\xi=+\beta} + \int_{\beta+\Delta}^{+\infty} K_0[\rho(\xi^2-\beta^2)]e^{-jt\xi}d\xi\right\}, \quad (18)$$

where Δ is the radius of the semicircles at $\xi = \pm\beta$. Since for each of the integrals in (18), the integrands and its partial derivative with respect to β is continuous in (ξ, β), both sides of (17) can be differentiated with respect to the parameter β.[17] The derivative of the left side of (17) with respect to β gives

$$-j\pi e^{-j\beta(\rho^2+t^2)^{1/2}}, \quad (19)$$

while the derivative of the right side (18) gives as $\Delta \to 0$[18]

$$\rho\beta\int_{-\infty}^{+\infty} \frac{K_1[\rho(\xi^2-\beta^2)^{1/2}]}{(\xi^2-\beta^2)^{1/2}} e^{-jt\xi}d\xi - \pi j\cos\beta t. \quad (20)$$

Combining (19) and (20) results in (8). The above results can also be obtained by using transforms 871.2 and 942 given in footnote reference 7. However, in using transform 942, it must be shown that it applies when the Bessel functions are of the first order.

[14] See also summary of a number of papers on wire antennas by F. E. Terman, "Radio Engineers Handbook," McGraw-Hill Book Company, Inc., New York, N. Y., pp. 797–804; 1945.

[15] J. L. Putman, B. Russell, and W. Walkinshaw, "Field distributions near a centre-fed half-wave radiating slot," *Jour. IEE*, vol. 95, part III, pp. 280–289; July 1948.

[16] See footnote reference 7, transform 868, p. 111. This transform has been called the modified Sommerfeld's integral. See S. A. Schelkunoff, "Modified Sommerfeld's integral and its applications," Proc. I.R.E., vol. 24, pp. 1388–1398; October, 1936.

[17] See footnote reference 8, pp. 200–202, and E. T. Whittaker and G. N. Watson, "A Course of Modern Analysis," Cambridge Press, New York, N. Y., p. 67, example 1; 1943.

[18] See footnote reference 13, p. 49 (3–16) and p. 51 (4–7) and (4–11).

On the Existence of a Surface Wave in Dipole Radiation over a Plane Earth*

T. KAHAN† AND G. ECKART‡

Summary—**In a paper published in 1909, Sommerfeld[1] stated the existence of a surface-type wave in the radiation of a vertical Hertzian dipole over a plane earth. Weyl,[2] in 1919, objected to this solution. Despite a great number of papers on this problem, it had not been definitively settled so far. Its solution is given in the present paper by proving in a quite general way that this surface wave cannot be included in the said dipole radiation and by pointing out a thus-far hidden error in Sommerfeld's computation.**

I. Discussions on the Surface Wave

A. Sommerfeld's Solution of the Problem

IN 1909, SOMMERFELD published an outstanding paper on the radiation of a Hertzian dipole over the plane earth. He states the problem as follows: Suppose $z=0$ is the separation plane of two media, one with the material constant k_1 (in $z>0$) and the other with constant k_2 ($z<0$). At the origin of the co-ordinate system lies a Hertzian dipole (see Fig. 1). The two Hertzian functions are sought for in the two media which have to meet the following conditions:

$$\Delta\pi_1 + k_1^2\pi_1 = 0, \quad z > 0$$
$$\Delta\pi_2 + k_2^2\pi_2 = 0, \quad z < 0 \tag{1a}$$

$$\pi_1 = \pi_2, \quad \frac{1}{k_1^2}\frac{\partial\pi_1}{\partial z} = \frac{1}{k_2^2}\frac{\partial\pi_2}{\partial z} \quad \text{at} \quad z = 0 \tag{1b}$$

$$\pi_1 = 0, \quad z > 0, \quad r = \infty, \quad \text{and} \quad z = +\infty$$
$$\pi_2 = 0, \quad z < 0, \quad r = \infty, \quad \text{and} \quad z = -\infty$$
$$(r = \text{cylinder radius}) \text{ (Fig. 1))} \tag{1c}$$

$$\left.\begin{aligned}\pi_1 &- \frac{\exp(ik_1R)}{R} \text{ for } z \geqq 0\\ \pi_2 &- \frac{\exp(ik_2R)}{R} \text{ for } z \leqq 0\end{aligned}\right\} \text{finite and continuous with first derivatives everywhere, } R = 0 \text{ included} \tag{1d}$$

where R is the distance of the point of reception P from the transmitter which lies at the origin ($z=0, r=0$). (See Fig. 1.)

Sommerfeld then obtains his well-known solution in the form of the following integral,

$$\pi_1 = \int_0^\infty \frac{J_0(\lambda r)(k_1^2 + k_2^2)e^{-z\sqrt{\lambda^2-k_1^2}}}{k_1^2\sqrt{\lambda^2-k_1^2} + k_2^2\sqrt{\lambda^2-k_2^2}}\lambda d\lambda \quad (z>0) \tag{2}$$

where the signs of the radicals have to be chosen in such a manner that for $\lambda\to+\infty$ the value of the roots tends towards $+\lambda$. He then treats the integral in the following manner. He splits $J_0(\lambda r)$ into $\frac{1}{2}H_0^{(1)}(\lambda r)$ and

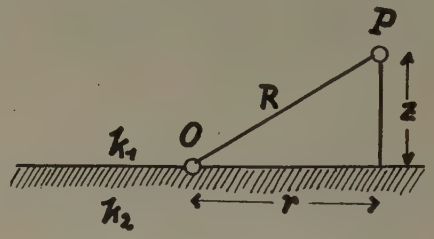

Fig. 1—Position of the dipole.

$\frac{1}{2}H_0^{(2)}(\lambda r)$, and displaces the path of integration over $H_0^{(1)}$ in the upper half-plane λ towards the positive imaginary half axis, and the integral over $H_0^{(2)}$ towards the negative imaginary axis. Then the integrals over the quarter circles infinitely distant nullify themselves and those taken along the imaginary axis cancel each other. The integrals over both branch cuts beginning at k_1 and k_2 remain, as well as the residue of the pole in accordance with Sommerfeld at a point marked on Fig. 2. We shall see later that it must actually lie in the point marked by a cross in Fig. 2. The integral taken over the branch cut of k_2 may be neglected. The integral over the cut of k_1 is developed asymptotically and yields the part of the solution which Sommerfeld calls the "space wave," and which, as we shall see, represents by itself the correct solution. The residue of the pole yields the "surface wave." It is, with an arbitrary factor C,

$$P = \pi C H_0^{(1)}(sr)e^{+z\sqrt{s^2-k^2}} \tag{3}$$

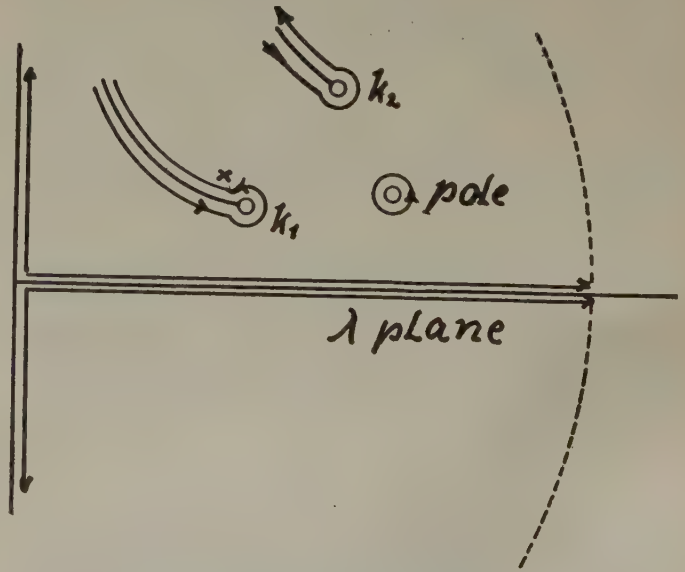

Fig. 2—Branch cuts and pole.

* Decimal classification: R120. Original manuscript received by the Institute, June 6, 1949.
† Institut Henri Poincaré, Paris, France.
‡ Office National d'Etudes et de Recherches Aéronautiques, Paris, France.
[1] A. Sommerfeld, "Über die Ausbreitung der Wellen in der drahtlosen Telegraphie," *Ann. der Phys.*, vol. 28, p. 665–736; 1909.
[2] H. Weyl, "Ausbreitung elektromagnetischer Wellen über einem ebenen Leiter," *Ann. der Phys.*, p. 481–500; 1919.

where s, the λ value of the pole is defined by

$$\lambda_{\text{pole}} = s = \sqrt{\frac{k_1^2 k_2^2}{k_1^2 + k_2^2}}. \tag{4}$$

We shall deal later with the exact position of $\lambda = s$. The wave P decreases asymptotically as $1/\sqrt{r}$. As the distance increases it reduces to a plane wave which results in a wave incident under the Brewster angle θ_B defined by

$$tg\ \theta_B = k_2/k_1 \tag{5}$$

(where k_1 and k_2 may be also complex). We may write the expression for P asymptotically (with a constant K)

$$P \sim \frac{K}{\sqrt{r}} e^{-ik_1 z\cos\theta_B + ik_1 r\sin\theta_B}. \tag{6}$$

At a time when the existence of the ionosphere was not yet known, it was hoped to explain in this way the propagation of the radio waves beyond the horizon.

B. Weyl's Solution in the Form Given by Noether

In 1919, Weyl published a paper[2] on the same problem. There was in his solution no term corresponding to a surface wave, and so Weyl questions the very existence of this wave in the dipole radiation. Weyl built up his solution, not as Sommerfeld did, by means of cylindrical waves, but with the aid of plane waves. It can be deduced, as Sommerfeld has pointed out already in his fundamental paper, from (2) by the transformation

$$\lambda = k_1 \sin\theta, \qquad \text{(see Fig. 3)} \tag{7}$$

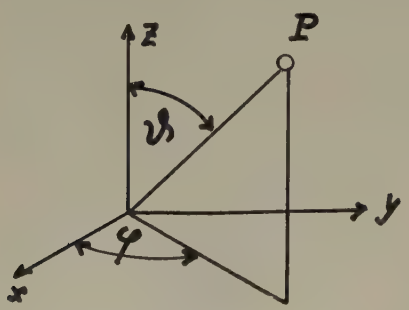

Fig. 3—Co-ordinate system used.

as well as by means of the integral representation of the Bessel funltion

$$J_0(\lambda r) = J_0(k_1 r \sin\theta) = \frac{1}{2\pi}\int_{-\pi}^{+\pi} e^{ik_1 r\sin\theta\cos\psi} d\psi. \tag{8}$$

Noether[3] expressed Weyl's double integral extended over ψ and θ in a form which is easier to discuss; it is

$$\pi_1 = \frac{ik_1k_2}{\pi}\int_{\text{I}} d\psi \int_{\text{II}} \frac{\cos\theta\sin\theta}{k_2\cos\theta + k_1\sin\eta} e^{ik_1(r\cos\psi\sin\theta + z\cos\theta)} d\theta \tag{9}$$

[3] F. Noether, "Ausbreitung elektrischer Wellen über der Erde," pp. 154–170 in "Funktionentheorie und ihre Anwendung in der Technik," Springer, Berlin, Germany; 1937.

where η is defined by

$$k_2 \sin\eta = k_1 \sin\theta. \tag{10}$$

The paths of integration over ψ and over θ are represented in Figs. 4 and 5, respectively. If we integrate

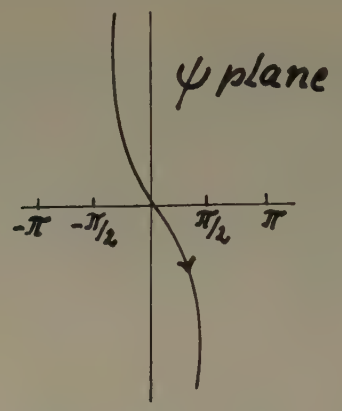

Fig. 4—Path of integration in the Ψ plane.

first over ψ, we would see that, with Sommerfeld, we should have obtained Hankel's function $H_0^{(1)}(kr\sin\theta) = H_0^{(1)}(\lambda r)$. Weyl treats his integral asymptotically according to the saddle-point method and obtains the space wave of Sommerfeld but not the surface wave. He contests thus the existence of the latter in the dipole radiation over a plane earth.

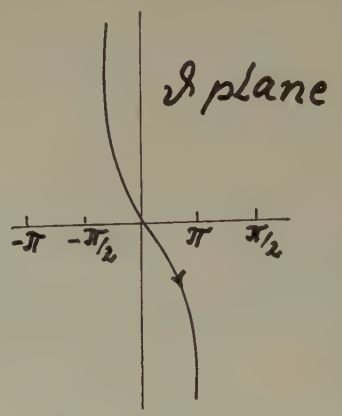

Fig. 5—Integration path in the θ plane.

C. The Papers of Norton, Burrows, Epstein, Wise, and Rice

This matter has been dealt with by different authors. Norton[4,5] established a solution which likewise contains no surface wave.

As a result of the realization that the mathematics contained an ambiguity, Burrows[6,7] attempted to decide the question experimentally by very careful measurements along a lake, employing ultra-short waves

[4] K. A. Norton, "Physical reality of space and surface waves in the radiation field of radio antennas," Proc. I.R.E., vol. 25, pp. 1192–1202; September, 1937.

[5] K. A. Norton, "Propagation of radio waves over a plane earth," *Nature*, vol. 135, p. 954; June, 1935.

[6] C. R. Burrows, "The surface wave in radio propagation over plane earth," Proc. I.R.E., vol. 25, pp. 219–229; February, 1937.

[7] C. R. Burrows, "Mechanisms of propagation," *Atti del Congresso Internazionale Marconiana* (Rome), pp. 43–51; 1948.

($\lambda = 2$ *m* with loaded quarter-wave doublets whose midpoints were 0.52 and 0.60 meter above the surface of the water). The curves of Fig. 6 represent a plot of the data so obtained. The smooth curves were calculated by means of the following formulas, using values of ϵ and σ determined by taking various parts of the lake along which measurements were carried out. The average value was found to be 4.988×10^8 electrostatic units. Taking into account the effect of temperature on the conductivity, $\sigma = 4.05 \times 10^8$ electrostatic units. Curve 1 is a plot of the received field strength that would result from transmission over a plane earth of perfect conductivity

$$E_0 = \frac{120\pi HI}{\lambda r}. \tag{11a}$$

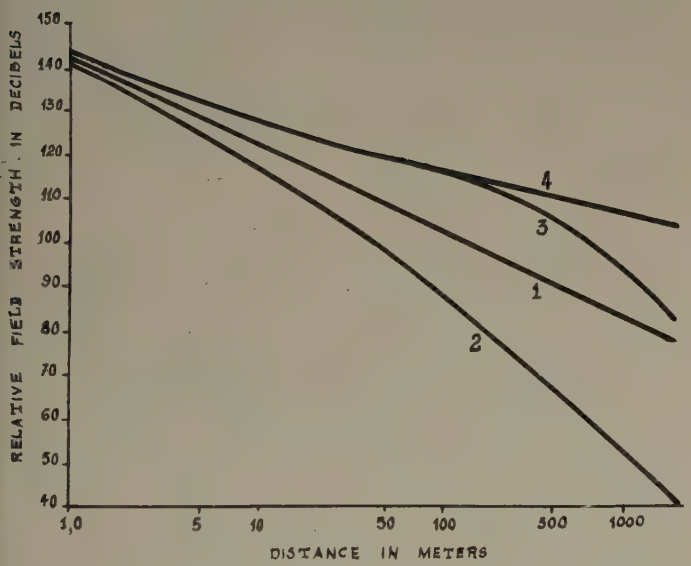

Fig. 6—Experimental results (Burrows).

Curves 2 and 3 result from multiplying (11a) by the magnitude of

$$W = A - \frac{B}{2} \approx C \tag{11b}$$

and

$$S = A + \frac{B}{2} \approx C + B, \tag{11c}$$

respectively, where

$$A = 1 + \sum_{n=1}^{\infty} \frac{x^n e^{2in(\delta+\pi/\lambda)}}{1 \cdot 3 \cdot 5 \cdots (2n-1)} \tag{11d}$$

$$B = \sqrt{2\pi x}\, e^{-(x/2)\sin 2\delta + i[(x/2)\cos 2\delta + \delta + \pi/4)]}, \tag{11e}$$

$$C = -\sum_{n=1}^{\infty} \frac{1 \cdot 3 \cdot 5 \cdots (2n-1)}{x^n e^{2in(\delta-\pi/4)}} \tag{11f}$$

$$xe^{2i\delta} = \frac{2\pi \dfrac{r}{\lambda}}{\sum - \dfrac{2i\sigma}{f}} \quad \text{and} \quad 0 \leqq \delta \leqq \frac{\pi}{4}. \tag{11g}$$

These follow from expressions given by Wise[8] when the magnitude of $\epsilon - (2i\sigma/f)$ is large compared to unity. $|W|$ is the attenuation factor corresponding to the formula derived by Weyl. $|S|$ is the attenuation factor as derived by Sommerfeld and used by him (and by Rolf) to calculate the variation of field strength with distance. B, the difference between S and W, corresponds to the surface-wave component. For a perfect dielectric, the exponent in B is a pure imaginary and curve 3 becomes curve 4. Fig. 6 represents a plot of the variation of the received field strength with distance. Curve 1 is a plot of (11a) showing the inverse distance field that would result from propagation over a plane earth of perfect conductivity. Curve 2 is a plot of (11b) showing variation of the received field strength according to Weyl, Norton, and the authors of the present paper. Curves 3 and 4 are plots of (11c) showing variation of the received field strength according to Sommerfeld. Curves 2 and 3 are based on a dielectric constant of 82.1, a conductivity of 4.05×10^8 electrostatic units and $\lambda = 2$ meters. Curve 4 refers to a perfect dielectric.

The experimental points are in good agreement with curve 2 which is a plot of (11b) and thus agree with Weyl, Norton, Wise, Rice and ourselves. At distances less than five meters (2.5 wavelength) the experimental points lie slightly below the theoretical curve and show a tendency toward oscillation. This is presumably due to the combined effects of the finite size of the antennas and the finite height above the water's surface. These oscillations may be, according to Burrows, a vestige of the pronounced interference patterns that extend to great distances with higher antennas. The discrepancy between the experimental points and curve 3, which is a plot of Sommerfeld's formula, is so great that there can be no doubt as to the incorrectness of the latter.

Burrows also determined the variation of field strength with antenna height. While the agreement between the experimental and theoretical curves is not as good as in the preceding case, it in no way introduces any doubt as to the error in the Sommerfeld curves which predict a field strength about 100 *times* that measured by Burrows.

Wise[9] developed Sommerfeld's integral in a series of increasing powers of r. He was able to show, by means of these developments, that the surface wave disappears. Neither is this surface plane contained in the series established by Rice.[10] One could still doubt here whether the integration path should not be conducted "ab initie" in such a way that the surface wave does appear. We shall see, however, that this is not the case. Moreover, these authors do not show where Sommerfeld's mistake lies.

[8] W. H. Wise, "The grounded condenser antenna radiation formula," PROC. I.R.E., vol. 19, pp. 1684–1689; September, 1931.

[9] W. H. Wise, "The physical reality of Zenneck's surface wave," *Bell Sys. Tech. Jour.*, vol. 16, pp. 35–44; January, 1937.

[10] S. O. Rice, "Series for the wave function of a radiating dipole at the earth's surface," *Bell Sys. Tech. Jour.*, vol. 16, pp. 101–109; January, 1937.

Burrows' results may be regarded now, in the light of our theoretical elucidation, as definitive. Epstein[11] asserts that the problem is not univocally set. Moreover, the surface wave would be a solution whose singularity does not correspond to the present problem; it is, namely, (cf. (2)) singular in $r=0$ for all values of z. Epstein therefore proposes to avoid the pole with the path of integration in $H_0^{(1)}$ as drawn in Fig. 7, i.e., to conduct the path of integration between the pole and the branch cut.

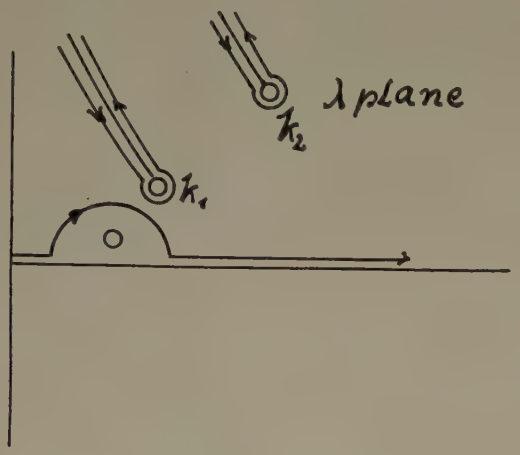

Fig. 7—Epstein's path of integration.

II. The Surface Wave Is Not Included in the Dipole Radiation

A. Its Singularity Does Not Correspond to the Problem

Now, the solution of the problem is as follows. First, we have Epstein's remark that the singularity of the surface wave is immediately contrary to the condition stated in (1d); this implies that the surface wave cannot belong to the solution. This fact had been overlooked so far because most of the authors have dealt exclusively with the asymptotic representation of the surface wave for great values of r, ($1/\sqrt{r}$ law) which states nothing about the behavior at $r=0$. It is however, as can be seen from (3), logarithmically singular along the whole z axis for $r=0$.

B. It Is Contrary to the Radiation Condition

Nevertheless, Epstein's remark that the problem is not uniquely determined is completely erroneous. The uniqueness is in any case guaranteed by a condition Sommerfeld published four years later;[12] it is the well-known radiation condition (Ausstrahlungsbedingung) which states that the solution at infinity must be made up only of divergent waves. Sommerfeld's condition stated in (1c) should be replaced by

$$\lim_{r\to\infty}\left(\frac{\partial\pi}{\partial n}-ik\pi\right)=0 \qquad \text{(1c-i)}$$

$$\lim_{r\to\infty} R\pi \neq \infty \qquad \text{(1c-ii)}$$

where n is the outward normal of a surface surrounding the whole radiatory device. Sommerfeld points out in the literature that this condition renders unique propagation problems and shows, above all, that for integrals extended over elementary waves, such as (2), the path of integration must be chosen so that the radiation condition is met. This would justify, as we shall see, the path proposed by Epstein if there were not another important point to take into account, as we shall see later. Rellich[13] has extended Sommerfeld's unique researches. If the surface wave is considered from this point of view, it may be seen that it does not meet the radiation condition. (Equation (6) shows that it corresponds to a wave coming from infinity and incident under the Brewster angle; it comes therefore from the outside. Its propagation $1/\sqrt{r}$ law would also contradict (1c-ii). For real values of k_1 and k_2 the field would outweigh the radiation of the dipole in the vacuum or over an infinitely conductive earth, which is physically impossible.

C. Sommerfeld's Error

It results therefore, from the preceding, that the path of integration is to be conducted so that the solution meets the radiation condition; that therefore it does not contain the surface wave. Now we shall see that Sommerfeld did not notice while computing his asymptotic development of the branch-cut integral that this contains, beside the space wave, the surface wave with negative sign and so cancels the residue of the pole, and that, therefore, the path taken primitively by Sommerfeld is the correct one and not the one proposed by Epstein.

In order to see this as simply and conveniently as possible, let us suppose that k_1 and k_2 are purely real in Figs. 8, 9, and 10. It is readily seen how the essential result is kept with $k_{1,2}$ complex. The cut issued from k_2 is taken directed vertically upwards. Sommerfeld chose as a cut from k_1 the equilateral hyperbola from $\lambda=k_1$ having as asymptotes the two axes; if k_1 is real, this hyperbola tends to follow more and more the axes. The branch cut in Fig. 8 is marked by a dashed line and a borderline is emphasized by short oblique hatching. The same kind of notation for corresponding points in the different planes of the following conformal mapping, as well as the same kind of hatching for corresponding domains and the same lines (dotted, dashed, and the like), makes it possible to discern the parts corresponding mutually to one another.

Let us study first the position of the pole. As k_1^2 and k_2^2 are situated (because $k_{1,2}^2=\omega^2\epsilon_0\epsilon_{1,2}\mu_0\mu+j\omega\mu_0\mu\sigma_{1,2}$) in the first quadrant, it is readily seen from (4) of Sommerfeld, which is correct, that

$$|s|\leqq|k_1|, \qquad |s|\leqq|k_2|, \qquad (12)$$

[11] P. S. Epstein, "Radio-wave propagation and electromagnetic surface waves," *Proc. Nat. Acad. Sci.*, vol. 33, p. 195; June, 1947.

[12] A. Sommerfeld, "Die Greensche Funktion der Schwingungsgleichen," *Jahr. der. D. Math. Vergg.*, pp. 309–353; 1912.

[13] F. Rellich, "Ueber das asymptotische Verhalten der Losungen von $\Delta u+\lambda u=0$ in unendlichen Gebieten," *Jahr. der D. Math. Vergg.*, vol. 53, p. 57; January, 1943.

this formula corresponding simply to the connection in parallel of impedances

$$\left(R = \frac{R_1 R_2}{R_1 + R_2}\right).$$

As in the physical case $|k_2| \gg |k_1|$, s lies in the half plane in the circle around the origin with $|k_1|$ as radius, and, therefore, not where Sommerfeld places it.[14,15] The same can be said for complex values of k_1 and k_2. We have yet to fix, for k_1 and k_2 real, the position of the pole relative to the branch cut. s is a solution of the equation

$$k_1^2\sqrt{\lambda^2 - k_2^2} + k_2^2\sqrt{\lambda^2 - k_2^2} = 0, \qquad (13)$$

whence (4) results by elevation to the second power. The solution must be situated in a point where both terms in the left side of (13) cancel one another. We already indicated in connection with (2) that for real $\lambda > k_{1,2}$ the signs of the roots are to be chosen positive.

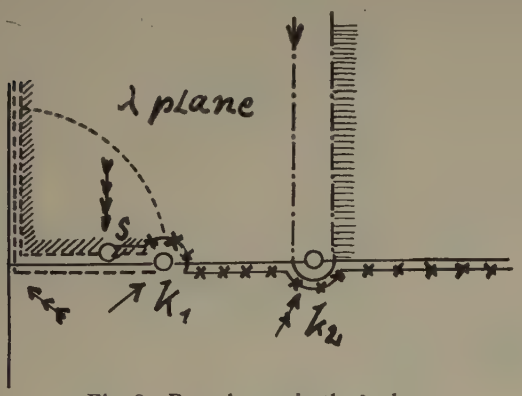

Fig. 8—Branch cuts in the λ plane.

Let us follow the values of the roots on the path marked by crosses in Fig. 8. $\sqrt{\lambda^2 - k_2^2}$ comes from the right with positive values; on circulating around the branch point k_2, it becomes negative imaginary and remains so on the remainder of the real axis till $\lambda = 0$ as it is not influenced by the cut from k_1. $\sqrt{\lambda^2 - k_1^2}$ is positive real from $\lambda = \infty$ till $\lambda = k_1$ and is not influenced by the branch point k_2. Now, in order to compensate in (13) the negative imaginary quantity $k_1^2\sqrt{\lambda^2 - k_2^2}$, we must go farther on the side of the branch cut through k_1 on which $k_2^2\sqrt{\lambda^2 - k_1^2}$ becomes positive imaginary, i.e., on the upper side. The pole is then in the point marked in Fig. 8. If k_1 and k_2 become complex, the branch cut chosen by Sommerfeld takes the position indicated in Fig. 2, and the pole lies in the position marked by a cross. If we now pull the cut vertically upwards (see Fig. 9), the pole disappears in the inferior sheet of the λ surface. We draw in Fig. 9 the path of integration around this branch cut. If we now map Sommerfeld's plane of Fig. 9 by means of $\lambda = k_1 \sin\theta$ on Weyl's θ plane, and if we hatch in the same way the corresponding regions on the two planes (see Fig. 10), we see that the path of integration $W\,W$ of Fig. 9 transforms into Weyl's path in the θ

[14] See Fig. 2 of footnote reference 1.
[15] See Fig. 28, p. 253, of footnote reference 9.

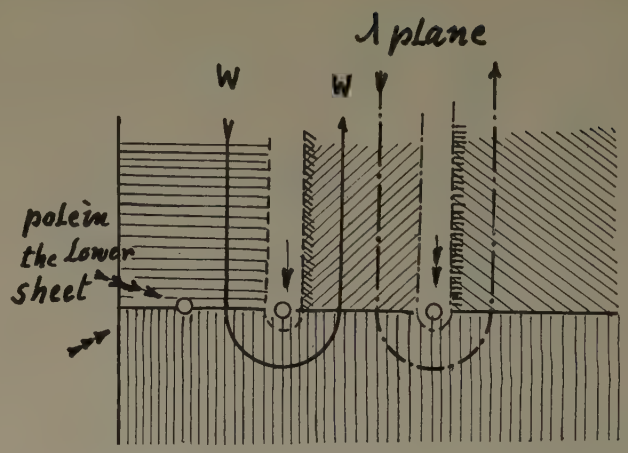

Fig. 9—Displacement of the branch cuts in the λ plane. Note: —=path; ---=cut.

plane of Fig. 5. It yields, according to Weyl's correct computation, the space wave and no surface wave. The lower sheet of the Riemannian λ surface which contains the pole thus transforms into the nonhatched part of the θ plane. Now, in order to establish the link with Sommerfeld's representation, we draw in Fig. 9 the path of integration, which therefore does not yield the surface wave, near the branch cut and displace the branch cut back again so that it sweeps again over the pole, which would be mapped in Fig. 10 in the nonhatched part. Now we place the branch cut into the position of Fig. 11. Then according to Cauchy's theorem the branch-cut integral plus residue of the overswept pole must yield the same as the integral along the cut which initially runs vertically upwards. The integral over the cut of Fig. 11 must consequently contain the surface wave with opposite sign. This proof is mathematically obligatory and is sufficient. However, to be complete, we shall compute again the asymptotic

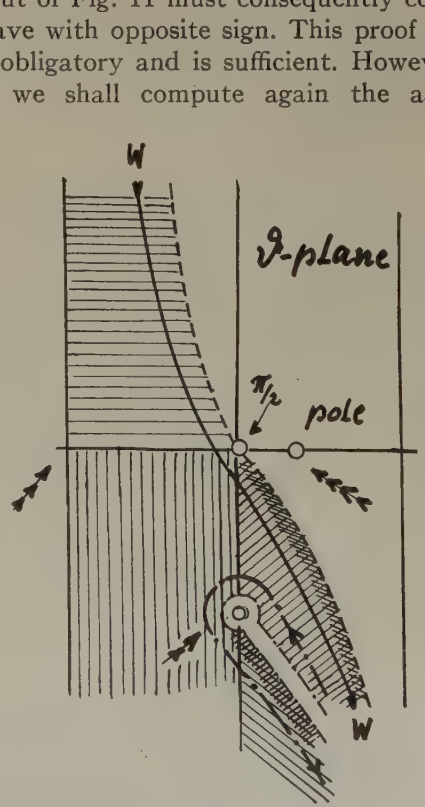

Fig. 10—Weyl's θ plane.

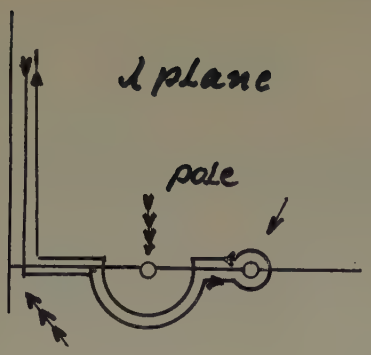

Fig. 11—Displaced branch cut in the λ plane.

representation of the branch-cut integral whereby the already-mentioned error of calculation of Sommerfeld will result. First we get, quite as Sommerfeld, the space wave which is yielded on the path of integration in the neighborhood of the point $\lambda = k_1$. To that, another contribution must be added which Sommerfeld overlooked and which originates from a saddle point immediately below the pole and which just compensates the residue. We develop the integrand of (2) in the immediate neighborhood of the pole $\lambda = s$ in the form

$$\frac{k_1^2 + k_2^2}{k_1^2\sqrt{\lambda^2 - k_2^2} + k_2^2\sqrt{\lambda^2 - k_1^2}} = \frac{a}{\lambda - s}. \qquad (14)$$

Then we get for integral (2), if we choose directly the form which it takes after the splitting of $J_0(\lambda r)$ with $H_0^{(1)}$ and if we substitute for $H_0^{(1)}(\lambda r)$, its asymptotic expression for great values of λr

$$\pi = M \int \frac{a\lambda d\lambda}{\sqrt{\lambda r}} e^{\lambda ir - ln(\lambda - s)} \quad (M = \text{constant}). \qquad (15)$$

If we differentiate the exponent with respect to λ and put it equal to zero, we get for the saddle point

$$\lambda_{\text{saddle point}} = s - \frac{i}{r}. \qquad (16)$$

That is, a point which lies a little below s. We want to check it yet in another manner (see Figs. 12 and 13). Let us follow in the λ plane the absolute values of the essential part of the integrand exp $(i\lambda r)/\lambda - s$ along a line AA' parallel with the imaginary axis. Owing to the factor $1/\lambda - s$ the absolute values decrease rapidly from s upwards and downwards. The factor $e^{i\lambda r}$ with the modulus $e^{-|Jm(\lambda r)|}$ for a positive imaginary part of λ decreases very rapidly upwards; for negative imaginary λ it has as modulus $e^{+|Jm(\lambda r)|}$ and decreases very rapidly downwards, so that, at some distance from the pole downwards, the modulus of $e^{i\lambda r}/\lambda - s$ increases again; between them lies the mentioned saddle point over which we conduct our path of integration. On pulling away the path over the pole, the integrals over the branch cut and around the pole are to be taken along the arrows marked in Fig. 12. Now we may think of computing the residue of the pole according to the saddle-point method, as the contribution of the saddle point must predominate also on the circle around the pole over which we can conduct the path. Then it is readily seen with the aid of the arrows of Fig. 12 that the residue and the branch-cut integral must compensate each other, and that, consequently, this saddle point brings with it a part in the branch-cut integral which just cancels the residue. Sommerfeld overlooked that, but we can now ascertain that thereby the contradiction between Sommerfeld and Weyl is removed.

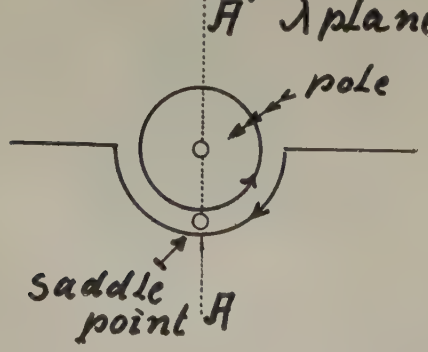

Fig. 12—Position of pole and saddle point in the λ plane.

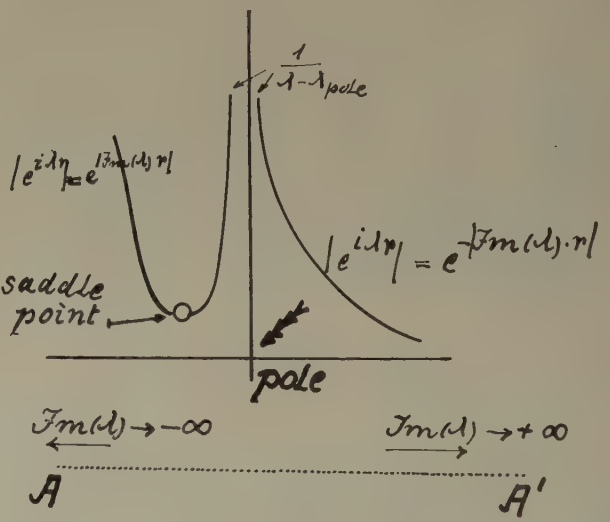

Fig. 13—Existence of a saddle point near the pole.

III. Conclusions

To summarize, we can say that the surface wave is not contained in the dipole radiation for the following reasons:

1. Its singularity contradicts the present problem.
2. It does not meet the radiation condition.
3. The theory discloses that it appears only through an inadvertency in Sommerfeld's calculation.
4. The experimental results of Burrows show the accuracy of the now consistent theory.

Bibliography

1. T. Kahan and G. Eckart, "L'onde de surface de Sommerfeld," *Compt. Rend. Acad. Sci.* (Paris), vol. 226, p. 1513; May, 1948.
2. T. Kahan and G. Eckart, "Sur le choise des chemins d'integration dans le problème relatif au rayonnement," *Compt. Rend. Acad. Sci.* (Paris), vol. 227, p. 969; November, 1948.
3. T. Kahan and G. Eckart, "La propagation des ondes electromagnétiques audessus du pol," *Jour. Phys.*, vol. 10, p. 165; May, 1949.
4. T. Kahan and G. Eckart, "On the electromagnetic surface wave of Sommerfeld," *Phys. Rev.*, vol. 76, p. 406; August, 1949.

An Analysis of Triple-Tuned Coupled Circuits*

NORMAN W. MATHER†, MEMBER, IRE

Summary—**An analysis is given of triple-tuned coupled circuits for high-Q cases in which the couplings between circuits are kept small and the response is symmetrical about a reference frequency. Both synchronously tuned and asynchronously tuned cases are investigated in detail. Universal response curves are derived and contour plots of gain bandwidth product are given.**

The results for the transitional and triple-peak response cases are compared with double-tuned coupled circuits. The advantages of triple-tuned circuits are shown to be their more uniform response in the pass band and fifty per cent better sideband selectivity.

I. Introduction

THE ANALYSIS of triple-tuned coupled circuits can be approached through image-parameter filter methods, or through general methods of network analysis. The latter approach is adopted here, since it more readily leads to general results. The published analyses[1–7] generally follow the same approach, but deal only with certain restricted special cases. The analysis given here involves less rigid conditions and, within the fairly broad limitations imposed, surveys the form of response that can be obtained and considers certain cases in quantitive detail. The limitations imposed are (1) that the magnitude of the response exhibit even symmetry about some reference frequency; (2) that the parts of the circuit are either tuned to the same frequency or are tuned closed to the same frequency; (3) that the parts of the circuit are high Q but not necessarily of equal Q; (4) that the couplings between the tuned parts be purely reactive with small coefficients of coupling; and (5) that only the response close to the pass band near the resonant frequencies be determined. With slight modifications, the last three of these restrictions can be greatly relaxed or eliminated completely for the case in which the three parts are tuned to the same frequency. A somewhat similar analysis of double-tuned coupled circuits has been made by Aiken.[8]

As is well known, high-Q coupled circuits can be put in many equivalent forms. Aiken,[8] Feldtkeller,[4] Dishal[5] and others have given the important equivalents for double-tuned circuits in a form that makes it possible to apply the analysis of one of them to them all. Similar triple-tuned equivalent circuits can be obtained by extension of the double-tuned circuit equivalents and, within the limitations of the approximations, the analysis of one of them is applicable to all of them. Thus the analysis which follows can be applied to many forms of equivalent circuits.

II. Circuit Equations

The circuit shown in Fig. 1 will be taken as representative of triple-tuned circuits with reactive couplings. Addition of reactive couplings in addition to, or in place of the mutual inductance couplings does not change the form of the equations obtained in the following analysis except as is noted in Section III *D*. The equations for the circuit of Fig. 1 are set up by the node-voltage method[9,10] as follows:

$$\left.\begin{aligned} Y_{11}E_1 - Y_{12}E_2 - Y_{13}E_3 &= I_1 \\ -Y_{21}E_1 + Y_{22}E_2 - Y_{23}E_3 &= 0 \\ -Y_{31}E_1 - Y_{32}E_2 + Y_{33}E_3 &= 0 \end{aligned}\right\} \tag{1}$$

where

$$\left.\begin{aligned} Y_{11} &= G_1 + j\left(\omega C_1 - \frac{1 - K_{23}^2}{\omega L_1 A}\right) \\ Y_{22} &= G_2 + j\left(\omega C_2 - \frac{1 - K_{13}^2}{\omega L_2 A}\right) \\ Y_{33} &= G_3 + j\left(\omega C_3 - \frac{1 - K_{12}^2}{\omega L_3 A}\right) \\ Y_{12} &= Y_{21} = j\,\frac{K_{23}K_{13} - K_{12}}{\omega\sqrt{L_1L_2}A} \\ Y_{23} &= Y_{32} = j\,\frac{K_{12}K_{13} - K_{23}}{\omega\sqrt{L_2L_3}A} \\ Y_{13} &= Y_{31} = j\,\frac{K_{12}K_{23} - K_{13}}{\omega\sqrt{L_1L_3}A} \end{aligned}\right\} \tag{2}$$

$$A = 1 - K_{12}^2 - K_{23}^2 - K_{13}^2 + 2K_{12}K_{23}K_{13} \tag{3}$$

$$K_{mn} = K_{nm} = \frac{M_{mn}}{\sqrt{L_mL_n}}, \qquad \begin{matrix}(n \neq m)\\ (m,\ n = 1,\ 2,\ 3).\end{matrix} \tag{4}$$

* Decimal classification: R142.3. Original manuscript received by the Institute, June 1, 1949; revised manuscript received, January 24, 1950. Presented, 1949 National IRE Convention, March 8, 1949, New York, N. Y.

† Princeton University, Princeton, N. J.

[1] E. A. Guillemin, "Communication Networks," vol. I, John Wiley & Sons, Inc., New York, N. Y., pp. 335–339; 1931.

[2] H. Wucherer, "Dreikreisige Bandfilter mit symmetrische ausgeglichener Übertragungskurve," *Telegraphen-Fersprech-Funk-und Fernseh-Technik*, vol. 28, pp. 231–238, June, 1939; pp. 324–329; August, 1939.

[3] M. R. Winkler, "A 3 resonant circuit transformer," *Electronics*, vol. 16, pp. 96–100 and 204; January, 1943.

[4] R. Feldtkeller, "Einführung in die Theorie der Rundfunksiebschaltungen," 3. Aufl., S. Hirzel, Leipzig, pp. 95–112; 1945.

[5] M. Dishal, "Exact design and analysis of double- and triple-tuned band-pass amplifiers," PROC. I.R.E., vol. 35, pp. 606–626; June, 1947. Also discussion of this paper, PROC. I.R.E., vol. 35, pp. 1507–1510; December, 1947.

[6] M. Dishal, "Design of dissipative band-pass filters producing desired exact amplitude-frequency characteristics," PROC. I.R.E., vol. 37, pp. 1050–1069; September, 1949.

[7] K. R. Spangenberg, "The universal characteristics of triple-resonant-circuit band-pass filters," PROC. I.R.E., vol. 34, pp. 629–634; September, 1946.

[8] C. B. Aiken, "Two-mesh tuned coupled-circuit filters," PROC. I.R.E., vol. 25, pp. 230–272; February, 1937.

[9] E. E. Staff, MIT, "Electric Circuits," John Wiley & Sons, Inc., New York, N. Y., chap. 8, 1940.

[10] M. F. Gardner and J. L. Barnes, "Transients in Linear Systems," vol. 1, John Wiley & Sons, New York, N. Y., chap. 2, 1942. The mutual inductance couplings are handled by extension of the method given on pp. 40–43.

The conductance parameters, G_m $(m=1, 2, 3)$, and the inductance parameters L_m, can be removed by using resonant-frequency parameters ω_m and dissipation factors D_m. These quantities are defined by the following equations:

$$\omega_m = \sqrt{\frac{1-K_{np}^2}{L_mC_mA}}, \qquad \begin{matrix}(m \neq n \neq p)\\ (m, n, p = 1, 2, 3)\end{matrix} \tag{5}$$

$$D_m = \frac{1}{Q_m} = \frac{G_m}{\omega_m C_m}, \qquad (m = 1, 2, 3). \tag{6}$$

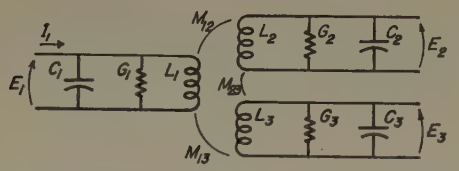

Fig. 1—Triple-tuned coupled circuit having mutual-inductance coupling between each of the three tuned parts.

When the foregoing relations are used in the Y's of (2), a simpler set of relations is obtained. These can be made still more convenient for the present purpose by normalization. The first equation in (1) is divided by $\frac{1}{2}\omega_1C_1D_T$, the second by $\frac{1}{2}\omega_2C_2D_T$, and the third by $\frac{1}{2}\omega_3D_3D_T$, where $D_T=D_1+D_2+D_3$ is the sum of the dissipation factors of the three parts of the circuit. The resulting expressions contain numerous quantities which are divided by D_T, and it therefore simplifies the notation to use lower-case letters for these quantities. Thus

$$d_m = \frac{D_m}{D_T}, \qquad (m = 1, 2, 3) \tag{7}$$

$$k_{mn} = k_{nm} = \frac{K_{mn}}{D_T} = \frac{K_{nm}}{D_T}, \qquad (m \neq n). \tag{8}$$

It should be noted that

$$d_1 + d_2 + d_3 = 1. \tag{9}$$

This property is used later in plotting gain-bandwidth-product contours.

Since the only cases to be investigated have the three parts of the circuit tuned near a reference frequency ω_r, a simplification is obtained by defining a frequency function Ω to be used in place of the frequency itself

$$\frac{\omega}{\omega_r} - \frac{\omega_r}{\omega} = 2\Omega. \tag{10}$$

The resonant frequencies ω_m of the parts of the circuit can be specified in the same way

$$\frac{\omega_m}{\omega_r} - \frac{\omega_r}{\omega_m} = 2\Omega_m. \tag{11}$$

Terms containing these functions divided by D_T can be put in simpler form by means of new frequency functions defined as follows:

$$x = \frac{4\Omega}{D_T} \tag{12}$$

$$x_m = \frac{4\Omega_m}{D_T}. \tag{13}$$

In all cases considered, Ω and Ω_m are small compared with unity. This allows terms containing the quantities ω_m/ω and $\omega/\omega_m-\omega_m/\omega$ to be approximated by the first few terms of series expansions of the quantities in terms of either the Ω's or D_Tx_m's. These expansions are obtained by application of the Binomial Theorem to expressions obtained from (10) and (11). The result up to and including second-degree terms is

$$\frac{\omega_m}{\omega} = 1-(\Omega-\Omega_m)+\frac{1}{2}(\Omega-\Omega_m)^2+\cdots$$

$$= 1-\frac{1}{4}D_T(x-x_m)+\frac{1}{32}D_T^2(x-x_m)^2+\cdots \tag{14}$$

$$\approx 1 \qquad \text{for} \quad (\Omega, \Omega_m \ll 1). \tag{15}$$

$$\frac{\omega}{\omega_m}-\frac{\omega_m}{\omega} \approx 2(\Omega-\Omega_m) = \frac{1}{2}D_T(x-x_m), \qquad (\Omega, \Omega_m \ll 1). \tag{16}$$

Using the approximations of (15) and (16), and the other parameters as defined above, the following system of equations is obtained from (1):

$$\left.\begin{aligned}
&[2d_1 + j(x-x_1)]E_1 + \left[j2\sqrt{\frac{C_2}{C_1}}\,y_{12}\right]E_2 + \left[j2\sqrt{\frac{C_3}{C_1}}\,y_{13}\right]E_3 = \frac{2I_1}{\omega_1C_1D_T}\\
&\left[j2\sqrt{\frac{C_1}{C_2}}\,y_{12}\right]E_1 + [2d_2 + j(x-x_2)]E_2 + \left[j2\sqrt{\frac{C_3}{C_2}}\,y_{23}\right]E_3 = 0\\
&\left[j2\sqrt{\frac{C_1}{C_3}}\,y_{13}\right]E_1 + \left[i2\sqrt{\frac{C_2}{C_3}}\,y_{23}\right]E_2 + [2d_3 + j(x-x_3)]E_3 = 0
\end{aligned}\right\} \tag{17}$$

where

$$\left.\begin{aligned}
y_{12} &= \frac{K_{12}-K_{23}K_{13}}{D_T\sqrt{(1-K_{23}^2)(1-K_{13}^2)}}\\
y_{23} &= \frac{K_{23}-K_{12}K_{13}}{D_T\sqrt{(1-K_{12}^2)(1-K_{13}^2)}}\\
y_{13} &= \frac{K_{13}-K_{12}K_{23}}{D_T\sqrt{(1-K_{12}^2)(1-K_{23}^2)}}.
\end{aligned}\right\} \tag{18}$$

In the high-Q cases considered here, the coefficients of coupling (the K's) are made small in order to obtain the desired response. As the K's become small, the quantities defined by (18) approach the limiting values

$$y_{12} = k_{12}$$

$$y_{23} = k_{23}$$

$$y_{13} = k_{13}.$$

Also as the K's become small, the resonant frequencies defined by (5) approach

$$\omega_m = \sqrt{\frac{1}{L_m C_m}}, \qquad (m = 1, 2, 3). \tag{19}$$

The response of the circuit will be investigated by considering the transfer impedance $Z_T = E_3/I_1$. If the input of the circuit is connected into the plate circuit of a vacuum tube in a conventional manner and the plate conductance of the tube is considered a part of G_1, the voltage gain E_3/E_g is given by $-g_m Z_T$ where E_g is the alternating grid voltage and g_m is the mutual conductance of the tube.

A completely general solution for Z_T is too unwieldy to be of much use; instead, only the solutions which give a response having symmetry about the reference frequency ($x=0$) are considered. Symmetry is obtained only approximately in the actual response, but fortunately the approximations made in (15) and (16) put the equations in a form for which exact criteria for symmetry may be specified. It may be shown that, when the parts of the circuit are tuned to the same frequency, i.e., synchronously tuned, it is necessary that one of the coefficients defined by (18) be zero in order to obtain a symmetrical response. Either y_{12} or y_{23}, when put equal to zero, results in less sideband selectivity than can be obtained with y_{13} equal to zero and, since no compensating advantage is apparent, only the latter case is considered. Methods of approximating this condition by making K_{13} almost zero have been developed and used.[3,11] A modification of the circuit of Fig. 1 which gives a zero value for y_{13} is shown in Fig. 2. In this case

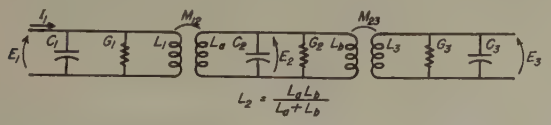

Fig. 2—Triple-tuned coupled circuit in which there is no mutual-inductance coupling between L_1 and L_3, nor between L_a and L_b.

inductance L_2 is split into two parts which causes the y's to be different than the values given in (18). For a zero y_{13}, the analysis shows that there must be no coupling between L_1 and L_3 nor between L_a and L_b.

In the asynchronously tuned case ($x_m \neq 0$), symmetry is not necessarily obtained by merely placing one of the y's of (18) equal to zero. The parameters x_m must be set to particular values depending upon the d's and y's of the circuit. Rather than consider all possible cases, most of which would seem to be of little practical importance, only the case for which y_{13} is zero is considered so that the resulting response can be directly compared with that obtained for the synchronously tuned case.

These considerations reduce the cases to be investigated to two, each of which has $y_{13}=0$: (1) the response in the synchronously tuned case and (2) the symmetrical response in the asynchronously tuned case.

III. Synchronously Tuned Case

The term "Synchronously Tuned" indicates that the three parts of the circuit are tuned to the same frequency: $\omega_1=\omega_2=\omega_3=\omega_r$ and, correspondingly, $x_1=x_2=x_3=0$. As indicated above, y_{13} is put equal to zero in order to obtain the best form of symmetrical response. When these conditions are applied to (17) and the resulting system of equations are solved to obtain the transfer impedance, the following is obtained:

$$Z_T = \frac{8 y_{12} y_{23}}{\omega_r \sqrt{C_1 C_3}\, D_T} \frac{1}{T} \tag{20}$$

where T is the negative of the determinant of the coefficients of (17)

$$T = 2x^2 - 8(d_1 d_2 d_3 + d_1 y_{23}^2 + d_3 y_{12}^2) + j[x^3 - 4(y_{12}^2 + y_{23}^2 + d_1 d_2 + d_2 d_3 + d_3 d_1)]. \tag{21}$$

Only the quantity T is a function of the frequency-deviation function x, so only it need be considered in investigating the form of the response. Obviously the response as given by Z_T is inversely proportional to T.

The magnitude of T can be written

$$|T| = [x^6 - 4f^2x^4 + 16g^4x^2 + ((f^2+1)^2 - 4g^4)^2]^{1/2} \tag{22}$$

where the parameters f^2 and g^4 are introduced to simplify the expression by reducing the number of parameters from five to two. It is easily determined from (21) and (22) that

$$f^2 = 2(y_{12}^2 + y_{23}^2 + d_1 d_2 + d_2 d_3 + d_3 d_1) - 1 \tag{23}$$

$$g^4 = \tfrac{1}{4}(f^2+1)^2 - 2(d_1 y_{23}^2 + d_3 y_{12}^2 + d_1 d_2 d_3). \tag{24}$$

Upon applying the relation $(d_1+d_2+d_3)^2=1$, (23) can be put in an alternate form

$$f^2 = 2(y_{12}^2 + y_{23}^2) - d_1^2 - d_2^2 - d_3^2. \tag{25}$$

These parameters are useful because once their magnitudes are specified the form of the response is likewise specified. It should be noted that increasing both of the coefficients of coupling increases f^2, the relation being clearly shown in (25).

If (21) is rewritten using these parameters, the result is

$$T = 2x^2 - (f^2+1)^2 + 4g^4 + j[x^3 - 2(f^2+1)x]. \tag{26}$$

This equation contains both the magnitude information of (22) and the phase information and forms the basis for a graphical analysis of triple-tuned circuits as given in another paper.[12]

[11] A. Crossley and H. E. Meinema, U. S. Patent No. 2,104,792, January 11, 1938.

[12] A. E. Harrison and N. W. Mather, "Graphical analysis of tuned coupled circuits," Proc. I.R.E., vol. 37, pp. 1016–1020; September, 1949.

It is evident from (23) and (24) that once the value of f^2 is set, the value of g^4 must lie between certain limits. To put this in more explicit terms, (23) and (24) can be rearranged as follows:

$$f^2 + 1 = 2(y_{12}^2 + y_{23}^2 + d_1d_2 + d_2d_3 + d_3d_1) \tag{23a}$$

$$g^4 = \tfrac{1}{4}(f^2 + 1)^2 - 2(d_3y_{12}^2 + d_1y_{23}^2 + d_1d_2d_3). \tag{24}$$

Since physically realizable d's in passive circuits are always positive and since, due to normalization, they can never be greater than unity, the terms inside the parentheses of (23a) are obviously equal to or larger than corresponding terms inside the second set of parentheses of (24). Furthermore, the minimum value of the quantity in the parentheses of (24) is zero. Using these relations, the limits of g^4 in terms of f^2 are given by

$$g_{min}^4 = \tfrac{1}{4}(f^2+1)^2 - (f^2+1) \leqq g^4 \leqq \tfrac{1}{4}(f^2+1)^2 = g_{max}^4. \tag{27}$$

The two limiting values of g^4 given by this expression converge toward zero as f^2 approaches -1. The limits as given by (27) have been plotted in Fig. 3. All of the physically possible solutions lie in the area defined by these limits.

The response within the allowed region of Fig. 3 can be divided according to the number of peaks in the magnitude of the response (minima in $|T|$) as the frequency-deviation function x varies. This can be done by investigating the minima and maxima of $|T|^2$. These occur

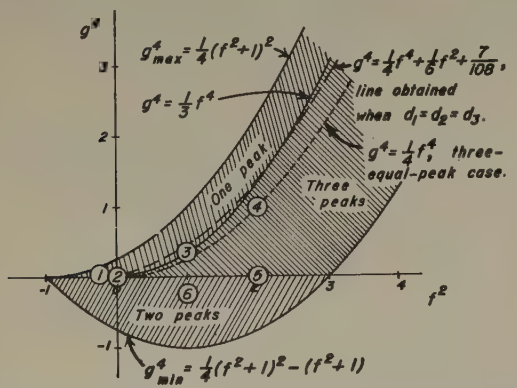

Fig. 3—Effect of parameters f^2 and g^4 on the form of the response. Response curves at the numbered locations are shown in Fig. 4.

at the same frequencies as those of $|T|$ since $|T|$ cannot be negative. The first derivative of $|T|^2$, when set equal to zero to give the condition for minima and maxima, yields

$$6x^5 - 16f^2x^3 + 32g^4x = 0 \tag{28}$$

whose roots are

$$\left.\begin{aligned} x &= 0 \\ x &= \pm\frac{2}{\sqrt{3}}(f^2 \pm \sqrt{f^4 - 3g^4})^{1/2} \end{aligned}\right\}. \tag{29}$$

Inspection of (29) indicates that one, two or three peaks in the response are possible. The results are summarized in Figs. 3 and 4.

The conditions required to obtain three peaks of equal amplitude can be determined by solving for the values of x for which the amplitude is equal to the amplitude at the resonant frequency at $x=0$. If the outer peaks are of greater amplitude than the center peak, there are four such values of x. If the outer peaks are of smaller amplitude, there are no such values of x. The three-equal-peak case lies between these extremes and has just two values of x for which the magnitude is equal to the magnitude at $x=0$. Thus, setting (22) equal to its value at $x=0$, yields

$$x^6 - 4f^2x^4 + 16g^4x^2 = 0 \tag{30}$$

whose roots are

$$\left.\begin{aligned} x &= 0 \\ x &= \pm\sqrt{2}(f^2 \pm \sqrt{f^4 - 4g^4})^{1/2} \end{aligned}\right\}. \tag{31}$$

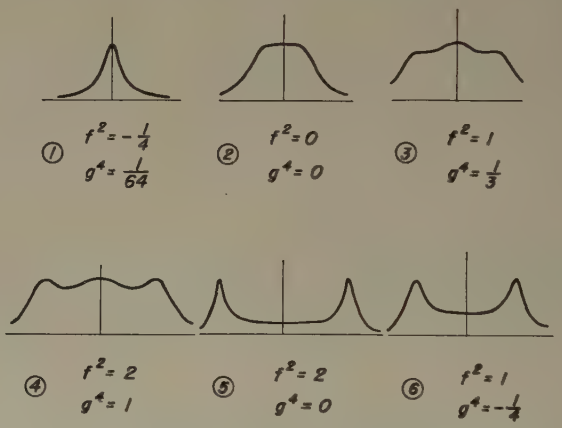

Fig. 4—Form of response for various values of the parameters f^2 and g^4.

The second of these expressions gives the values of x at which $|T|$ is equal to its value at $x=0$. The three-equal-peak case occurs when $g^4 = \frac{1}{4}f^4$ and $f^2 > 0$ and the outer peaks occur, as may be determined from either (29) or (31) at $x = \pm\sqrt{2}f$. The valleys in this case can be determined from (29) which yields their location as $x = \pm\sqrt{\frac{2}{3}}f$. The relation giving the three-equal-peak case is shown graphically in Fig. 3.

Also shown in Fig. 3 is the relation between the parameters g^4 and f^2 when the dissipation factors (and, therefore, the Q's) of the parts of the circuit are all the same. In such case, $d_1 = d_2 = d_3 = \frac{1}{3}$ which, when substituted into (23) and (24) gives the result

$$g^4 = \frac{1}{4}(f^2+1)^2 - \frac{1}{3}f^2 - \frac{5}{27}$$

$$= \frac{1}{4}f^4 + \frac{1}{6}f^2 + \frac{7}{108}. \tag{32}$$

The plot of this equation in Fig. 3 shows that it lies between the lines for $g^4 = \frac{1}{4}(f^2+1)^2$ and $g^4 = \frac{1}{4}f^4$ as is also evident by inspection of the equation. This result indicates that the three-equal-peak response cannot be obtained with the d's all the same.

A. Three-Equal-Peak Case

Further relations for the three-equal-peak case can be determined by substituting the condition for three equal peaks, $g^4=\frac{1}{4}f^4$, into the various relations already obtained for the more general synchronously tuned case. Equations (23) and (24) can be solved for the values of the y's in terms of the d's and an arbitrary value for f^2

$$\left.\begin{aligned} y_{12}^2 &= \frac{1}{8}\left(1-\frac{d_2}{d_1-d_3}\right)[(d_2+d_3)^2+3d_1^2+2f^2] \\ y_{23}^2 &= \frac{1}{8}\left(1+\frac{d_2}{d_1-d_3}\right)[(d_1+d_2)^2+3d_3^2+2f^2] \end{aligned}\right\}. \quad (33)$$

The relation between the y's and f^2 is clearly apparent here. These relations also show that the relation

$$d_2 < |\, d_1 - d_3\,| \quad (34)$$

must be satisfied if real, nonzero values of the y's are to be obtained when $f^2>0$. Thus the relation given by (34) must be satisfied if the three-equal-peak response is to be obtained in the synchronously tuned case.

A special case occurs in (33) when $d_1=d_3$ and $d_2=0$. The y's are then indeterminant from (33), but by examining (23) and (24) from which (33) is obtained, it is found that the condition $g^4=\frac{1}{4}f^4$ required for the three-equal-peak response is obtained independent of the values of the y's. This case is discussed by Dishal.[5] The only condition on the y's in this case is found from (23) to be

$$y_{12}^2 + y_{23}^2 = d_1^2 + \frac{f^2}{2} = 0.25 + \frac{f^2}{2}. \quad (35)$$

Substitution of the three-equal-peak condition $g^4=\frac{1}{4}f^4$ into (26) and (22) results in equations which represent all possible combinations in the synchronously tuned case that can give three equal peaks

$$T = 2x^2 - 2f^2 - 1 + j[x^3 - 2(f^2+1)x] \quad (36)$$

$$|T| = [x^6 - 4f^2x^4 + 4f^4x^2 + (2f^2+1)^2]^{1/2}. \quad (37)$$

The part of (37) inside the brackets can be written in terms of the Tschebyscheff polynomial[12] $T_6(\ )$ as follows:

$$|T|^2 = \frac{16}{27}f^6\left[T_6\left(\sqrt{\frac{3}{8}}\,\frac{x}{f}\right)+1\right] + (2f^2+1)^2, \quad (f^2>0). \quad (38)$$

Since the response can be written in this form, it would seem that the form of the response, except for the constant term, is the same as certain filters and stagger-tuned cascade amplifiers.

Equations (36) and (37) can be used as the basis for a set of universal response curves for the three-equal-peak case. Using the subscript "$_0$" to indicate quantities evaluated at $x=0$, the relative response can be written as

$$\frac{|Z_T|}{|Z_T|_0} = \frac{|T|_0}{|T|} = \left[\frac{x^2(x^2-2f^2)^2}{1+2f^2}+1\right]^{-1/2} \quad (39)$$

$$\theta_Z - (\theta_Z)_0 = -\tan^{-1}\frac{x^3-2(f^2+1)x}{2x^2-2f^2-1} \quad \text{(Leading angles positive).} \quad (40)$$

The universal curves based on these equations are shown in Figs. 5 and 6 and with logarithmic co-ordinates in Fig. 14. Of particular interest is the curve for $f^2=0$ which is the transitional case between a one- and a three-peak response and corresponds to the point at the origin of co-ordinates in Fig. 3. This curve has the same form as the monotonic response indicated by Baum[13] and Butterworth[14] for stagger-tuned amplifiers, and is for this circuit, the response having "maximal flatness."[15]

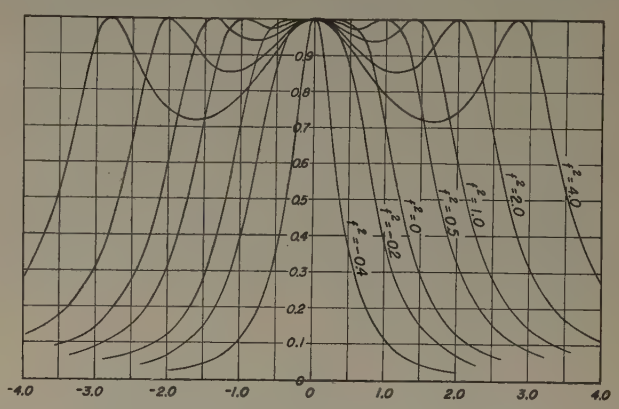

Fig. 5—Magnitude of response for three-equal-peak case as a function of the frequency deviation. (Plotted from (39).)

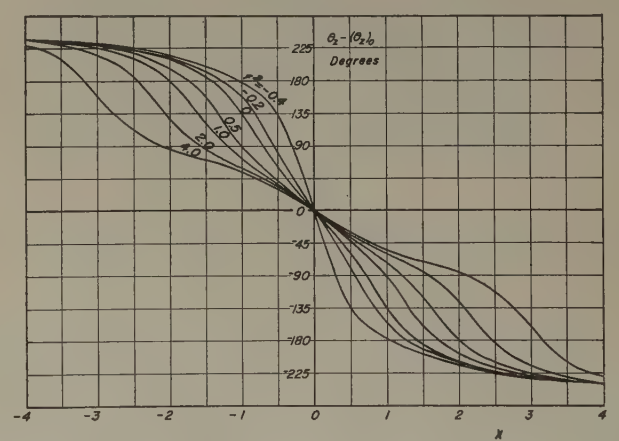

Fig. 6—Phase response for three-equal-peak case as a function of the frequency deviation. (Plotted from (40).)

[13] Tschebyscheff polynominals have been used in filter design and stagger-tuned amplifier designs. See, for example, W. Cauer, "Siebschaltungen," V.D.I.—Verlag, Berlin (1931); P. LeCorbriller, "Methode d'approximation de Tchebychef et application aux filtres de fréquences," *Rev. Gén. Élect.*, vol. 40, pp. 651–657, November 21, 1936; R. Feldtkeller (Ref. 4), pp. 54–77; R. F. Baum, "Design of broad band I.F. amplifiers," *Jour. Appl. Phys.*, vol. 17, pp. 519–529, June, 1946, and pp. 721–730; September, 1946.

[14] S. Butterworth, "On the theory of filter amplifiers," *Exp. Wireless and Wireless Eng.*, vol. 7, pp. 536–541; October, 1930.

[15] This is a term used in certain ladder-type filter designs to indicate this form of response. See, for example, V. D. Landon, "Cascade amplifiers with maximal flatness," *RCA Rev.*, pp. 347–363; January, 1941 and pp. 481–498; April, 1941. Also W. W. Mumford, "Maximally-flat filters in waveguides," *Bell Sys. Tech. Jour.*, vol. 27, pp. 684–713; October, 1948.

B. Gain and Bandwidth for Three-Equal-Peak Case

The bandwidth for any of the cases based on the three-equal-peak criterion can be obtained from the curves of Fig. 5. It is convenient, however, to specify the ratio of the bandwidth between -3 db points for m cascaded stages and the transitional ($f^2=0$) bandwidth for a single stage, also between -3 db points. A factor α_m is used for this purpose, the subscript m indicating the number of identical cascaded stages. Curves of α_1, α_2, and α_4 are shown in Fig. 7. Using the factor α_m, the bandwidth (BW) between -3 db points, in cycles per second, is

$$BW = \frac{\alpha_m D_T \omega_r}{4\pi} \text{ (cps)}. \tag{41}$$

Also shown in Fig. 7 is a curve for α_p which is the ratio of the bandwidth between the two outer peaks and the transitional bandwidth of a single stage between -3 db points.

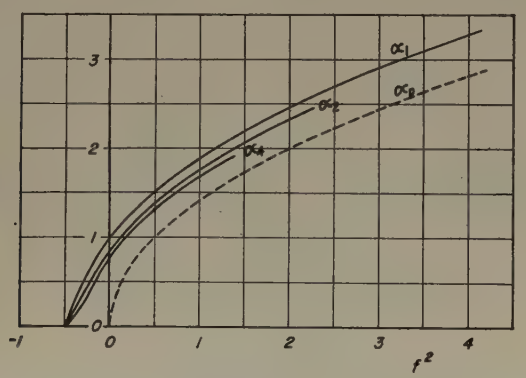

Fig. 7—Ratio of bandwidth for single and cascaded stages to transitional bandwidth of single stage as function of parameter f^2.

It has been shown that the gain-bandwidth product of amplifier circuits cannot exceed a limiting value irrespective of the complexity of the circuit.[16–18] The value given by Hansen[18] for four-terminal band-pass coupling networks (rearranged for comparison purposes) is

$$\frac{2\pi C}{g_m}(\text{Gain})_0(BW) = 5.06. \tag{42}$$

In the present case, with the three-equal-peak parameter relation $g^4=\frac{1}{4}f^4$ and a mutual conductance of unity, the gain-bandwidth product is given by the product of (20) evaluated at $x=0$ and (41) for a single stage

$$(\text{Gain})_0(BW) = \frac{\alpha_1 D_T \omega_r}{4\pi}\left|Z_T\right|_0 = \frac{2\alpha_1 y_{12} y_{23}}{\pi\sqrt{C_1 C_3}\,(2f^2+1)}. \tag{43}$$

[16] H. A. Wheeler, "Wide-band amplifiers for television," PROC. I.R.E., vol. 27, pp. 429–438; July, 1939.
[17] H. W. Bode, "Network Analysis and Feedback Amplifier Design," D. Van Nostrand Co., New York, N. Y., chap. 17; 1945.
[18] W. W. Hansen, "Maximum gain-bandwidth product in amplifiers," *Jour. Appl. Phys.*, vol. 16, pp. 528–534; September, 1945.

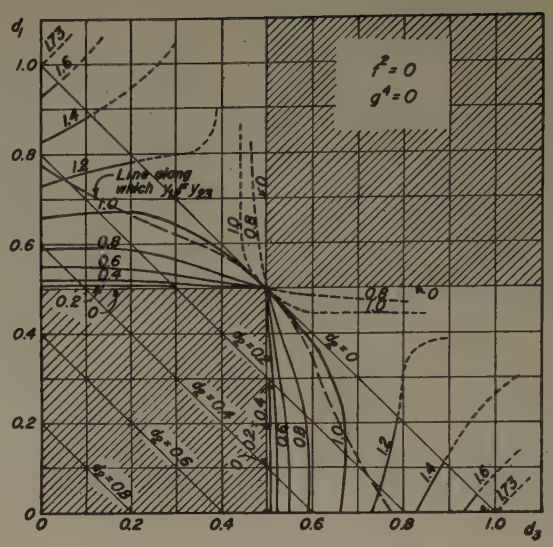

Fig. 8—Contour plot of $2\pi\sqrt{C_1C_3}\,(\text{Gain})_0(BW)$ for three-equal-peak case with $f^2=0$.

A rearrangement gives

$$2\pi\sqrt{C_1C_3}\,(\text{Gain})_0(BW) = \frac{4\alpha_1 y_{12} y_{23}}{2f^2+1}. \tag{44}$$

The right-hand side of this expression can be evaluated in terms of the normalized dissipation factors (the d's) by using (33) and values obtained from the curve for α_1 in Fig. 7. The results for three values of parameter f^2 are shown as contour plots in Figs. 8, 9, and 10. The region shown shaded in these figures has no solution giving real y's; it is the region for which the condition given in (34) does not hold. The plots have been extended into the negative d_2 region merely to show the form of the curves at the boundary. Also indicated in these figures are lines along which $y_{12}=y_{23}$. The point $d_1=d_3=0.5$, $d_2=0$ is indeterminant since, as already mentioned, the y's are independent of the d's at this point. However, the universal curves of Figs. 5, 6, and 14 hold at this point as well as for all other points which satisfy the relation $g^4=\frac{1}{4}f^4$.

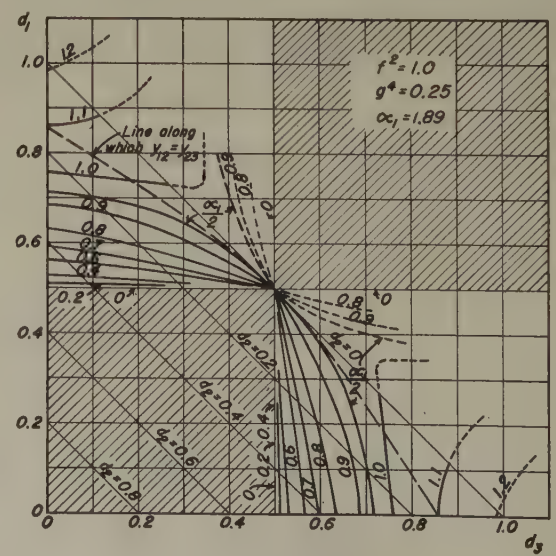

Fig. 9—Contour plot of $2\pi\sqrt{C_1C_3}\,(\text{Gain})_0(BW)$ for three-equal-peak case with $f^2=1.0$.

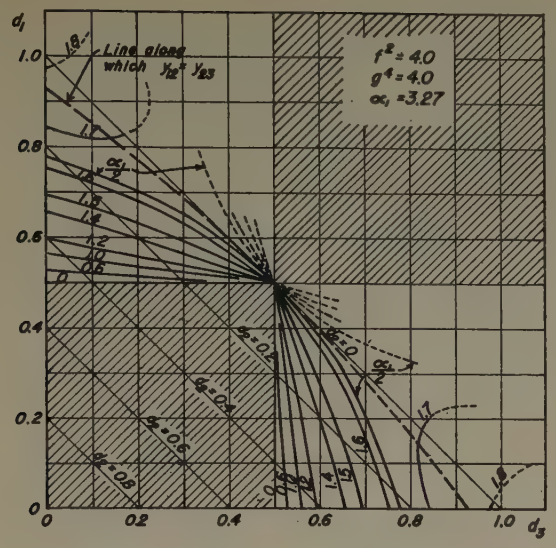

Fig. 10—Contour plot of $2\pi\sqrt{C_1C_3}\,(\text{Gain})_0(BW)$ for for three-equal-peak case with $f^2=4.0$.

C. Zeros on Complex Frequency Plane

Another point of interest is the location of the zeros of $-jT$ (poles of Z_T) on the complex x plane. Three cases have been determined and the results are shown in Fig. 11.

It may be noted that as f^2 is increased, the zero on the axis of imaginaries does not change position, and that the other two zeros become symmetrically oriented about the imaginary axis but always lying the same distance from the real axis. In the case of transitional coupling, $g^4=\frac{1}{4}f^4=0$, all three zeros are equidistant from the origin and thus lie on a circular arc of unit radius having a center at the origin. This is in agreement with the maximal-flatness analysis for ladder-type filter networks.[15]

D. Higher-Order Approximation

Equations (20) and (21) obtained for the synchronously tuned case are exact except for the approximation indicated in (15) for ω_m/ω which, in this case, is equal to

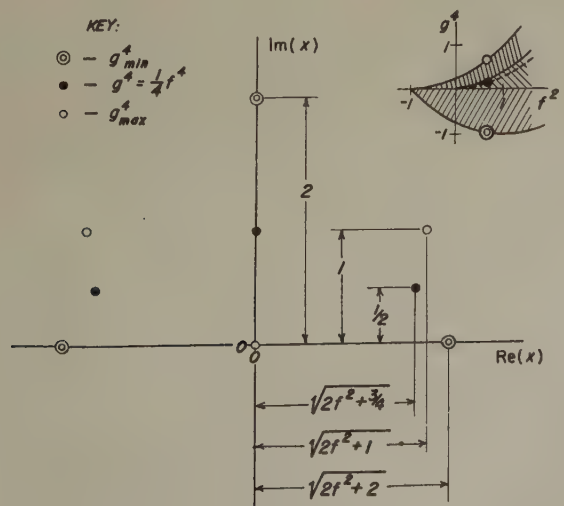

Fig. 11—Poles of Z_T (zeros of $-jT$) on complex x plane.

ω_r/ω. To make (20) and (21) exact, it is necessary to multiply each y_{12} and y_{23} in these expressions by ω_r/ω.

The errors in the previous approximate analysis due to taking ω_m/ω as equal to unity can be rather large, of the order of 5 to 10 per cent in cases of practical importance. These errors are also not evenly divided about the center of symmetry and result in a loss of symmetry in the response. The parameters f^2 and g^4 are likewise affected, so that on the plot of Fig. 3 they can no longer be represented by a point, but instead vary as a function of frequency.

Inspection of (23) and (24) indicates a possibility of keeping f^2 and g^4 nearly constant by changing one of the couplings so that one of the y's, say y_{23}, is multiplied by ω/ω_r instead of ω_r/ω. This would also eliminate the asymmetry indicated in (20). These results are obtained by making the coupling between L_2 and L_3 through a capacitance C_{23}, as shown in Fig. 12 instead of by mutual inductance. The system equations given by (17) still

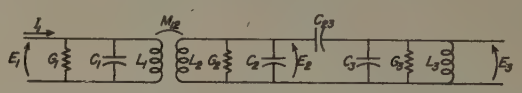

Fig. 12—Triple-tuned coupled circuit having both mutual-inductance and capacitance couplings in order to reduce effects of small asymmetries.

apply provided one changes the resonant frequency formulas of (5) so that C_2+C_{23} replaces C_2 in the formula for ω_2 and C_3+C_{23} replaces C_3 in the formula for ω_3. The same changes are made in the divisors used for normalizing. The y's, instead of (18), are

$$\left.\begin{aligned} y_{12} &= y_{21} = k_{12} \\ y_{23} &= y_{32} = -\frac{C_{23}}{D_T\sqrt{C_2C_3}} \\ y_{13} &= y_{31} = 0. \end{aligned}\right\} \tag{45}$$

To keep f^2 constant over a fairly wide range requires that $(\omega_r/\omega)^2y_{12}^2+(\omega/\omega)^2y_{23}^2=\text{Constant}$. To keep g^4 constant then requires that d_1 be equal to d_3. Unfortunately, this second condition makes the three-equal-peak condition as given by (34) unattainable. In section IV it will be shown that all three conditions can be realized by detuning the first and third parts of the circuit.

IV. Asynchronously Tuned Case

The case in which one or more of the resonant parts of the circuit are detuned so that $\omega_m=\omega_r$ and $x_m=0$ do not hold for all three values of the subscript m is called the asynchronously tuned case. Putting $y_{13}=y_{31}=0$, and solving (17) for the transfer impedance yields

$$Z_T = \frac{8y_{12}y_{23}}{\omega_1\sqrt{C_1C_3}\,D_T}\left(\frac{1}{T_a}\right), \tag{46}$$

where T_a is the negative of the determinant of the coefficients of (17). By considering only cases which give a symmetrical response about $x=0$, it is possible to specify that $|T_a|$ must be an even function of frequency.

The only nontrivial case which gives this result is the one in which the real part of T_a is an even function of x and the imaginary part is an odd function of x. This means that the coefficients of the odd powers in the real part and the coefficients of the even powers in the imaginary part must all be zero. Writing these conditions explicitly and solving the resulting equations for the detuning parameters x_1, x_2, and x_3 indicates that $x_1=x_2=x_3=0$ is a solution; it is the synchronously tuned case discussed in Section III.

Another solution is

$$\left.\begin{aligned} x_1 &= \pm 2\left[\frac{(d_2-d_3)}{(d_1-d_2)(d_3-d_1)}(d_1d_2(d_1-d_2)\right. \\ &\quad + d_2d_3(d_2-d_3)+d_3d_1(d_3-d_1) \\ &\quad \left. + y_{12}^2(d_1-d_2)+y_{23}^2(d_2-d_3))\right]^{1/2} \\ x_2 &= \frac{d_3-d_1}{d_2-d_3}x_1 \\ x_3 &= \frac{d_1-d_2}{d_2-d_3}x_1. \end{aligned}\right\} \quad (47)$$

An interesting special case occurs if d_1 is made equal to d_3 and y_{12}^2 is made equal to y_{23}^2. In that case the value of x_1 can be set arbitrarily, x_2 is zero, and $x_3=-x_1$.

When the parts of the circuit are detuned as specified by (47), T_a reduces to

$$T_a = 2x^2-(f_a^2+1)^2+4g_a^4+j[x^3-2(f_a^2+1)x] \quad (48)$$

where

$$f_a^2 = 2(y_{12}^2+y_{23}^2)-d_1^2-d_2^2-d_3^2 - \tfrac{1}{2}(x_1x_2+x_2x_3+x_3x_1) \quad (49)$$

$$g_a^4 = \tfrac{1}{4}(f_a^2+1)^2-2(d_1d_2d_3+d_1y_{23}^2+d_3y_{12}^2) + \tfrac{1}{2}(d_1x_1x_2+d_2x_3x_1+d_3x_1x_2). \quad (50)$$

Equation (48) is here purposely put in the same form as (26) in order to emphasize the similarity between this case and the synchronously tuned case. The parameters f_a^2 and g_a^4 are, except for an added constant in each case, the same as the parameters f^2 and g^4. Thus the results concerning the *form* of the response for the synchronously tuned case in terms of the parameters f^2 and g^4 apply also to this case except with the substitution of f_a^2 and g_a^4. The three-equal-peak case occurs when $g_a^4=\frac{1}{4}f_a^4$ and $f_a^2>0$, and the curves of Figs. 3–7, and 14 apply to this case. The response in the two cases differs only by a constant factor depending upon the relative ratio of $y_{12}y_{23}$ which appears in the numerators of (20) and (46). The ratio between ω_r and ω_1 in the two cases is so close to unity that it has no significance.

It is convenient to investigate the gain-bandwidth products rather than the products of $y_{12}y_{23}$ in the two cases. A comparison of relative gains is then possible by setting $f_a^2=f^2$ so that the bandwidths are the same. This is done by using the relations between x_1, x_2, and x_3 as given by (47) in the expression for f_a^2 of (49) and, by suitable manipulation, determining expressions which $|y_{12}y_{23}|_{a_{max}}$ and $|y_{12}y_{23}|_{max}$ cannot exceed. (The subscript a is used to denote quantities referring to the asynchronously tuned case.) The results are

$$|y_{12}y_{23}|_{a_{max}} < \tfrac{1}{4}(f_a^2+1) \quad (51)$$

$$|y_{12}y_{23}|_{max} \leqq \tfrac{1}{4}(f^2+1). \quad (52)$$

Using these values in (44) gives the result

$$[2\pi\sqrt{C_1C_3}\,(\text{Gain})\,(BW)]_{a_{max}} < \frac{\alpha_1(f_a^2+1)}{2f_a^2+1}$$

(Asynchronously tuned case). (53)

$$[2\pi\sqrt{C_1C_3}\,(\text{Gain})\,(BW)]_{max} \leqq \frac{\alpha_1(f^2+1)}{2f^2+1}$$

(Synchronously tuned case). (54)

A comparison of the values on the right-hand side of these two equations with the maximum values actually attained for the synchronously tuned case as shown in the contour plots of Figs. 8, 9, and 10 is shown in Table I. These figures indicate that there can be but little advantage in the asynchronously tuned case in so far as gain-bandwidth product is concerned.

TABLE I

Value of f^2 or f_a^2	Max. Value by (53) or (54)	Max. Value Obtained in Synchronously Tuned Case
0	1.00	0.865
1	1.26	1.22
4	1.82	1.81

It is possible, as was mentioned in Section III *D*, to cause the small first-order asymmetries in the response to cancel by using capacitive coupling to replace one of the mutual-inductance couplings as shown in Fig. 12, and then making $y_{12}^2=y_{23}^2$ and $d_1=d_3$. It is not then possible to obtain the three-equal-peak condition $g^4=\frac{1}{4}f^4$ in the synchronously tuned case except for the limiting condition $d_2=0$, but it is possible in the asynchronously tuned case as has been shown by Wucherer.[2] As previously indicated in connection with (47), when $d_1=d_3$, $y_{12}^2=y_{23}^2$, $x_1=-x_3$ and $x_2=0$ the conditions for symmetry (neglecting the small first-order asymmetries) are maintained. Thus the circuit arranged to cause the first-order asymmetries to cancel can be first synchronously tuned ($x_1=x_2=x_3=0$), and then the first and third parts detuned in opposite direction without destroying the symmetry of the response. As this is done the response tends to change in the direction of the three-equal-peak response, as is illustrated in Fig. 13. The co-ordinates in this figure are the same as those of Fig. 3, except with the addition of the subscript a to indicate the asynchronously tuned case. The condition for three-equal-

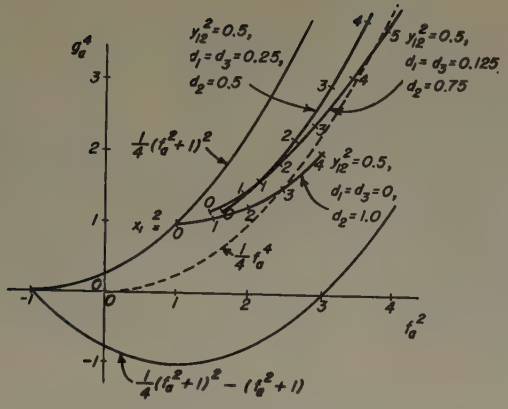

Fig. 13—Typical variation of f_a^2 and g_a^4 as the detuning parameter $x_1=x_3$ are increased with x, kept zero. Dotted line indicates three-equal-peak condition.

peaks is shown as a dotted line. It is apparent in this case that circuits having d_2 less than about 0.75 are of little value if the three-equal-peak condition is to be obtained with a moderate detuning of the first and third parts.

The gain-bandwidth product in this case is found to be

$$[2\pi\sqrt{C_1C_2}\,(\text{Gain})\;(BW)]_a = \frac{\alpha_1(f_a^2+2d_1^2+d_2^2-\frac{1}{2}x_1^2)}{2f_a^2+1}, \quad (d_1=d_3,\ x_1=-x_3). \tag{55}$$

The quantity $2d_1^2+d_2^2$ varies between $+0.375$ and $+1.0$ as d_2 is varied between 0.5 and 1.0. Thus it is evident that a small value of x_1^2 and a large value of d_2 are desirable. In the limit, when $d_2=1.0$, (55) gives 0.750, 0.788, 1.00, for $f_a^2=0$, 1.00, 4.00, respectively.

V. Comparison with Double-Tuned Circuits

Since the applications of triple-tuned circuits are likely to be similar to those of the familiar double-tuned circuit, it may be useful to compare the two circuits. For triple-tuned circuits the frequency function x is given by

$$x = \frac{4\Omega}{D_1+D_2+D_3}, \tag{12a}$$

while for double-tuned circuits the function

$$x_{do} = \frac{2\sqrt{2}\,\Omega_{do}}{D_1+D_2} \tag{56}$$

is used.[19] (The subscripts $_{do}$ are used to denote quantities which apply to double-tuned circuits.) The variable $\Omega=\Omega_{do}$ is defined by (10). The definitions for the x's are chosen so that when x or x_{do} is unity, the transitional response has dropped 3 db below its value at $x=0$.

Using the circuit of Fig. 1, with the third part omitted to make it a double-tuned circuit, the transfer impedance for the double-tuned circuit is found to be, when symmetry is specified,[20]

$$Z_{T\,do} = \frac{E_{2\,do}}{I_{1\,do}} = \frac{2(k_{12})_{do}}{\omega_1\sqrt{C_1C_2}\,(D_1+D_2)}\left(\frac{1}{T_{do}}\right) \tag{57}$$

where

$$T_{do} = -\sqrt{2}\,x_{do} + j[-x_{do}^2+f_{do}^2+1] \tag{58}$$

$$(k_{12})_{do} = \frac{K_{12}}{D_1+D_2} \tag{59}$$

and

$$f_{do}^2 = 2(k_{12})_{do}^2 + 2(d_1d_2)_{do} - 1 - (x_1x_2)_{do} \tag{60}$$

with

$$(d_1d_2)_{do} = \frac{D_1D_2}{(D_1+D_2)^2} \tag{61}$$

$$(x_1x_2)_{do} = \frac{8\Omega_1\Omega_2}{(D_1+D_2)^2}. \tag{62}$$

The quantities Ω_1 and Ω_2 are as defined by (11). Transitional response is obtained with $f_{do}^2=0$. The response relative to maximum response is given by

$$\frac{|Z_{T\,do}|}{|Z_{T\,do}|_{max}} = \frac{|T_{do}|_{min}}{|T_{do}|} = \left[\frac{2f_{do}^2+1}{x_{do}^4-2f_{do}^2x_{do}^4+(f_{do}^2+1)^2}\right]^{1/2}. \tag{63}$$

The curves for double-tuned circuits shown in Fig. 14 are based on this equation and a phase angle equation obtained in similar manner. In plotting Fig. 14 it has been assumed that $x=x_{do}$ when $\Omega=\Omega_{do}$. In each case the curves compared have been made to have equal bandwidth at -3 db points by suitable choice of the parame-

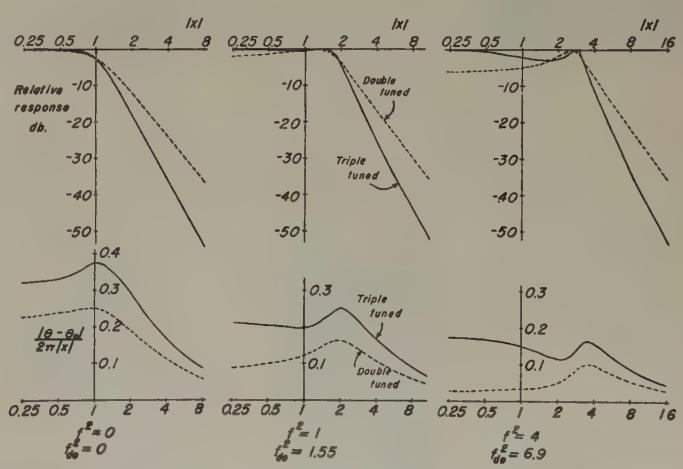

Fig. 14—Magnitude and phase comparison of triple-tuned and double-tuned circuit response.

[19] For a discussion of reasons for this choice, see footnote reference 11.

[20] The same results with different notation are given by E. S. Purington, "Single-and coupled-circuit systems," Proc. I.R.E., vol. 18, pp. 983–1016; June, 1930. Also in C. B. Aiken, footnote reference 7.

ter f_{do}^2. These curves show that the magnitude of the response is more uniform within the -3 db points for triple-tuned circuits, while outside this band the response approaches a rate of -18 db per octave of x as compared with -12 db per octave of x_{do} for double-tuned circuits.

If the assumption that $x=x_{do}$ when $\Omega=\Omega_{do}$ does not hold, the two curves of Fig. 14 are displaced horizontally, but are not changed in shape.

The gain-bandwidth product for double-tuned circuits can be derived analytically from the preceding expressions. The result of such calculation for various values of f_{do}^2 and with $x_1=x_2=0$ is shown in Fig. 15. For narrow bands, comparison with Figs. 8, 9, and 10 indicates an advantage for double-tuned circuits, but as the bandwidths are increased the advantage passes to triple-tuned circuits, provided proper values of the circuit parameters are chosen.

In summary, the advantages obtainable with triple-tuned circuits are more uniform response in the pass band between -3 db points and 50 per cent greater (in decibels) rejection of signals outside the pass band. For wide-band applications, the gain-bandwidth product can be made larger than for double-tuned circuits. Disadvantages are the use of more circuit elements and the necessity of adjusting D's and K's carefully in order to achieve desired characteristics.

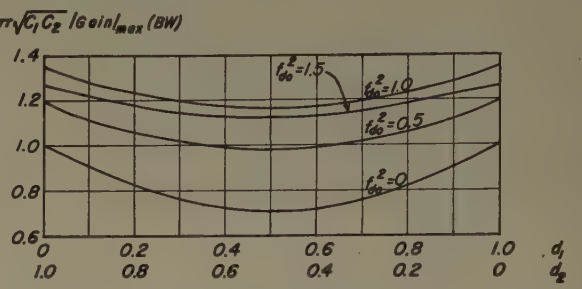

Fig. 15—Plot of $2\pi\sqrt{C_1C_2}|\text{Gain}|_{max}(BW)$ for double-tuned stages.

Contributors to the Proceedings of the I.R.E.

Howard E. Bussey was born at Tabor, S. Dak., in 1917. He received the B.A. degree in mathematics at George Washington University in 1943, and has pursued a graduate course in physics at the same school since 1948.

Howard E. Bussey

In 1942 he entered military service; after completing the cadet meteorology course at MIT and a brief radar-weather course at Spring Lake, N. Y., he served in the North Atlantic theater as radar weather coordinator, weather engineering and survey officer, and later as a weather forecaster. Since autumn of 1946 Mr. Bussey has been with the Central Radio Propagation Laboratory at the National Bureau of Standards, and at present is a physicist in the Tropospheric Propagation Research Section.

Mr. Bussey is a member of the American Physical Society, the American Meteorological Society, and Sigma Pi Sigma.

❖

For a photograph and biography of N. A. Begovich, see page 1345 of the November, 1949, issue of the Proceedings of the I.R.E.

Ralph I. Cole (A'29–SM'46) was born in St. Louis, Mo., on August 17, 1905. He received the B.S. degree in electrical engineering from Washington University, St. Louis, Mo., in 1927, and M.S. degree in physics from Rutgers University in 1936. During the period from 1929 to 1942, Mr. Cole was a civilian radio engineer at the Signal Corps Laboratories at Fort Monmouth, N. J., engaged in research and development of direction-finding equipments and modern tank communication apparatus. Directly commissioned a major in the Signal Corps in 1942, he supervised all research and development of direction-finding and vhf fighter control equipments during the war period. In 1945 he was transferred to the Air Force, Watson Laboratories, and assumed charge of its engineering division. Since leaving the armed services in 1947, Mr. Cole has been the chief engineer of the Base Directorate, Electronic Engineering, Watson Laboratories, at Red Bank, N. J.

Ralph I. Cole

While in the Air Force, he received the Legion of Merit medal for his efforts in the research and development field. He is now a colonel in the active Air Force Reserve, in charge of technical reserve training at Watson Laboratories. Mr. Cole is an Air Force member of the Radar Panel, Research and Development Board.

Seymour B. Cohn (S'41–A'44–M'46) was born at Stamford, Conn., on October 21, 1920. He received the B.E. degree in electrical engineering from Yale University in 1942; also the M.S. degree in communication engineering in 1946, and the Ph.D. degree in engineering sciences and applied physics in February, 1948, from Harvard University.

Seymour B. Cohn

From 1942 through 1945, Dr. Cohn was employed as a special research associate by the Radio Research Laboratory of Harvard University. During part of this time, he represented that Laboratory as a Technical Observer with the United States Army Air Force in the Mediterranean Theater of Operations.

Since March, 1948, Dr. Cohn has been employed by the Sperry Gyroscope Company as a project engineer in the microwave department. He is a member of Tau Beta Pi and an associate member of Sigma Xi. He is now serving on the Papers Review Committee of the IRE.

❖

For a photograph and biography of Norman W. Mather, see page 1029 of the September, 1949 issue of the Proceedings of the I.R.E.

Herbert J. Carlin (M'47) was born in New York, N. Y., in 1917. He attended Columbia University, receiving the B.S. degree in 1938, and the M.S. degree in 1940. In 1947 he was awarded the D.E.E. degree from the Polytechnic Institute of Brooklyn.

H. J. Carlin

From 1940 to 1945 Dr. Carlin was associated with the Westinghouse Company as a design engineer in the power-system relay section of the meter division, and has written several papers on power-system protection. He joined the Microwave Research Institute of the Polytechnic Institute of Brooklyn in 1945, and has made contributions in the field of microwave networks and microwave power measurements. He holds the position of research supervisor, and lectures in the Graduate School at the Institute.

Dr. Carlin is a member of the American Physical Society, the American Institute of Electrical Engineers, Tau Beta Pi, and Sigma Xi.

❖

Bernard M. Dwork (A'46) was born in New York, N. Y., on May 27, 1923. He received the B.E.E. degree from the College of the City of New York in 1943, the M.E.E. degree from Polytechnic Institute of Brooklyn in 1948, and is at present studying for the doctorate degree in mathematics at New York University. From 1943 to 1949 he was employed by the Federal Telecommunications Laboratory, where he worked on direction finders, radar countermeasures, and speech bandwidth compression systems. From 1944 to 1946 he served in the U. S. Army.

B. M. Dwork

Mr. Dwork is now on the staff of the Instruments Branch of the New York Operations Office of the U. S. Atomic Energy Commission, where he has been working on the development of radiation detection equipment.

❖

Gottfried Eckart was born at Munchen, Germany, on May 23, 1906. He received the E.E. degree from the Technical College of Munchen in 1929, and the Ph.D. degree in engineering in 1934. From 1934 to 1943, he was engaged in research at the Luftfahrt-Forschunsanstalt at Rechlin, and from 1943 to 1945, he was head of a radio technical institute.

G. Eckart

Since the war, Dr. Eckart has been engaged in research at the French Institute of Aeronautics, where he has been primarily concerned with research on electromagnetic wave propagation (very-short waves), radio navigation, and troposphere propagation. He is the author of a series of papers on these problems.

❖

B. Clifford Gardner was born in Jensen, Utah, on April 12, 1906. From 1926 to 1942, he was employed by the Farnsworth Television Laboratories, where he worked in the field of television-tube development. During the period from 1942 to 1949, he was engaged in development and production engineering on microwave, television, and storage-type tubes at the Raytheon Manufacturing Company. Since 1949 to the present time, he has been with Varian Associates in San Carlos, Calif.

B. C. Gardner

❖

R. C. Hergenrother (A'37) was born on September 5, 1903, in Chemnitz, Germany. He received the A.B. degree from Cornell University in 1925. During 1925 and 1926 he was employed in vacuum-tube development work at Westinghouse Lamp Company in Bloomfield, N. J. He went to the Pennsylvania State College in 1927 as an instructor in physics, and there received the M.S. degree in 1928. He was awarded the Ph.D. degree from the California Institute of Technology in 1931.

R. Hergenrother

Dr. Hergenrother held a Rockefeller Foundation Research Fellowship in physics at Washington University, St. Louis, Mo., from 1932 to 1934. From 1934 to 1935 he was employed by the Farnsworth Television Laboratories in Philadelphia, Pa., on research and development work on television tubes. From 1935 until 1945 he worked for the Hazeltine Corporation on electron-tube research and development. Since 1945 Dr. Hergenrother has been employed by the Raytheon Manufacturing Company, of Waltham, Mass., and is at present head of the klystron and storage-tube development laboratory in the power tube division.

He is a member of the American Physical Society, Sigma Xi, and Sigma Pi Sigma.

❖

Robert Hofstadter was born in New York, N.Y., on February 5, 1915. He received the B.S. degree in 1935 from the College of the City of New York, and the M.A. and Ph.D. degrees in 1938 from Princeton University. During the war, Dr. Hofstadter worked at the National Bureau of Standards on proximity fuzes, and at the Norden Laboratories Corporation on bomb director problems. He is currently studying the interaction of high-energy gamma rays with electrons.

R. Hofstadter

Dr. Hofstadter is the author of published articles on photoconductivity of crystals, infrared spectroscopy, and electronics, as well as on crystal conduction and scintillation counter studies. He expects to resign from his present position as assistant professor of physics at Princeton University on September 1, 1950, and to accept an appointment as associate professor in the physics department of Stanford University, Stanford, Calif.

❖

William H. Horton (S'42–A'45) was born in Pittsburgh, Pa., on April 6, 1921. He received the B.S. degree in electrical engineering from the Massachusetts Institute of Technology in 1943, and the E.E. degree from Stanford University in 1948. From 1943 through 1946 he was an officer in the United States Navy, working on airborne electronics. Since that time he has been a research assistant in the Microwave Laboratory at Stanford, working toward the Ph.D. degree.

W. H. Horton

Mr. Horton is a member of Sigma Tau and Sigma Xi.

John H. Jasberg (S'42–A'45) was born on November 3, 1917, in Telluride, Colo. He received the B.S. degree from the University of Idaho in 1943, and was employed by the Radio Research Laboratory at Harvard University during the period from 1943 until 1946.

JOHN H. JASBERG

Since that time, Mr. Jasberg has been a graduate student at Stanford University, in Stanford Calif., where he is now a research associate on the Staff of the Microwave Laboratory at Stanford.

❖

Theo Kahan was born in Sighet, Roumania, on August 4, 1904. He received the B.S., M.S., and Ph.D. degrees in France, and the E.E. degree from the École Superieure d'Electricité in Paris. As assistant to Pierre Weiss at Strasbourg for four years, he was engaged in research on ferromagnetism. Following this, he worked on wave mechanics with Louis de Broglie at the Institute Henri Poincaré, and on radioactivity with Madame Curie at the Institute of Radium.

THEO KAHAN

Dr. Kahan is the author of several books on nuclear physics, and he has published a series of papers on ferromagnetism, wave mechanics, nuclear physics, electromagnetic wave propagation, and microwave physics. At present he is the head of a research laboratory, and is engaged in nuclear and microwave studies.

❖

Werner J. Kleen was born in Hamburg, Germany, on October 29, 1907. He studied at the universities of Göttingen and Heidelberg and received the degrees of Dr. Phil. Nat. in 1931 and Dr. Habil. in 1936. From 1931 to 1945, he was member of the valve development laboratory of Telefunken Company, Berlin, where, from 1940, he was chief engineer in charge of the development of receiving and small transmitting tubes.

W. J. KLEEN

Since 1946, Dr. Kleen has been employed in the Centre de Recherches of the Compagnie Générale de T.S.F., Paris, where he is engaged in research and development of traveling-wave tubes. Together with H. Rothe, he is the author of a German standard work concerning electron tubes and their applications.

Editor's Note: Due to an oversight Dr. Kleen's biography and photograph were omitted from the Contributor's pages of the May, 1950, issue. We regret the error.

❖

Jerre D. Noe (S'43–M'49) was born at McCloud, Calif., in 1923. He received the B.S. degree in electrical engineering from the University of California in 1943, and the Ph.D. degree from Stanford University in 1948.

JERRE D. NOE

From 1943 to 1946 he was employed as a research associate by the Radio Research Laboratory of Harvard University. During 1944 and part of 1945 he worked in England at the American British Laboratory, associated with the Radio Research Laboratory. From 1946 to 1948 he was employed on a part-time basis in the development laboratory of Hewlett Packart Company, Palo Alto, Calif., during which time he was engaged in graduate study at Stanford University.

Since 1948, Dr. Noe has been a member of the electrical engineering staff of the Stanford Research Institute. He is a member of Sigma Xi, Tau Beta Pi, and Eta Kappa Nu.

❖

Irving E. Levy was born in Malden, Mass., on August 6, 1919. He received the B.S. degree in chemical engineering from Tufts College in 1941. Following graduation, he was employed by Raytheon Manufacturing Company as a process and development engineer. During the war, he served in the U. S. Navy as assistant navigator on an aircraft carrier, after which he returned to Raytheon to work in the general engineering division. He has been primarily concerned with special projects in connection with the processing and development of special-purpose tubes.

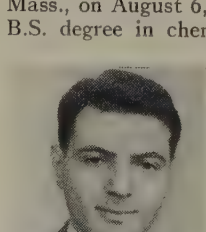

IRVING E. LEVY

Mr. Levy is an active amateur with the call letters W1SFR. He is a member of the American Society for Quality Control and the American Society for Testing Materials, for which he serves on subcommittee B4 of Section "A."

W. Eric Phillips (SM'45) was born in 1906, in Yorkshire, England. He received the degree of B.Sc. Engineering from the University of South Africa in 1928, followed by the M.Sc. Engineering degree in 1933 from the same institution. In 1931 he joined the staff of the department of electrical engineering of the Natal University College (now the University of Natal). During the years 1934 and 1935 he underwent a works training course at Metropolitan Vickers, Trafford Park, Manchester. This was followed by a three-year period during which he was a member of a research team investigating lightning phenomena in South Africa.

W. ERIC PHILLIPS

From 1940 until 1944 Dr. Phillips was on active service with the South African Defence Force, attached to the South African Corps of Signals as a technical officer in a radar unit. After demobilization he returned to the University of Natal, and was awarded the degree of D.Sc. Engineering in 1947 for research in the field of microwave propagation. He is a member of the Institution of Electrical Engineers, London, and president of the Natal Institute of Engineers.

❖

Glenn E. Tisdale (S'46–A'49) was born in Madison, Wis., on July 4, 1924. His undergraduate training was obtained at Princeton and Yale Universities, culminating in the B. Eng. degree in electrical engineering from the latter in 1944. Following graduation he was commissioned in the Navy Civil Engineer Corps, and spent a year in the Pacific area. In 1946 he resumed study at Yale, where he received the Master of Engineering degree in 1947, and the Ph.D. in 1949. While doing graduate work he taught mathematics at the New Haven YMCA Junior College. His summers were spent with the DuPont Company, in Wilmington, Del., working on problems of industrial electronics.

GLENN E. TISDALE

In June, 1949, Dr. Tisdale joined the Spencer-Kennedy Laboratories, Inc., in Cambridge, Mass., to design a commercial model of a variable electronic filter developed in connection with his doctoral thesis. Before joining the Servo Corporation he worked on problems of microwaves and ultra-high-frequency for the Raytheon Manufacturing Company, in Waltham, Mass. Dr. Tisdale is a member of Sigma Xi and Tau Beta Pi.

W. Saraga (SM'50) was born in Berlin Germany, in 1908. He studied telecommunications at the Berlin Technische Hochschule, and physics and mathematics at the Berlin University, where he received the Dr. Phil. degree in 1935.

W. Saraga

From 1929 to 1933 he was engaged in research at the Heinrich Hertz Institute in Berlin, which he left at the beginning of the Hitler regime. After a period of private research and technical journalism, he came to England in 1938 and joined the Telephone Manufacturing Company in 1939 as a research and development engineer.

Since 1944 Dr. Saraga has been in charge of a group for long-term network development and research. He is also a part-time lecturer in Network theory and mathematics at the South-East London Technical College.

Eugene N. Torgow (S'48–A'49) was born in New York, N. Y., on November 26, 1925. In 1946 he received the degree of B.E.E. from the Cooper Union School of Engineering in New York, N.Y. He spent the following year in the United States Army, engaged in radar repair and maintenance in the Pacific Theater. After being released from the Army, he entered the graduate school of the Polytechnic Institute of Brooklyn, where, in 1949, he received the degree of M.E.E.

Eugene N. Torgow

Since 1948, Mr. Torgow has been engaged in research on microwave attenuators and power measuring devices at the Microwave Research Institute of the Polytechnic Institute of Brooklyn. He is a member of Sigma Xi and the American Institute of Electrical Engineers.

❖

John Reed (A'48) was born in Cambridge, Mass., on March 9, 1922. He received the B.S. degree in applied physics at the Massachusetts Institute of Technology in February, 1943. From graduation until October, 1945, he was a staff member of the MIT Radiation Laboratory in the Radio Frequency Components Group. After graduate study at Cornell University, he joined the Antenna Group of Submarine Signal Company in January, 1947

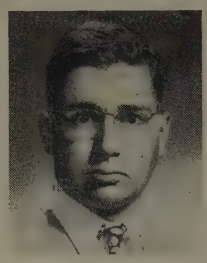

John Reed

He is now employed in the Microwave Section at Raytheon Manufacturing Company, in Newton, Mass.

❖

Correspondence

Cathode Neutralization of Video Amplifiers*

As stated by John M. Miller, Jr. in his analysis of "Cathode Neutralization of Video Amplifiers,"[1] the equations for gain are only approximate should a screen bypass capacitor return to ground, rather than to its corresponding cathode. A method of accommodating such circuit modifications to obtain exact solutions is evident from an examination of the simultaneous equations which form the basis of derivations given in the Appendix to this paper.

Should the screen grid capacitor of V-1 connect to ground, the current i_1 may be considered the cathode current of V-1 and $i_1(g_{m1}/g_{m1}')$ is then the plate current, where g_{m1}' is the cathode transconductance of V-1. Since the plate current is represented by i_1 only in simultaneous equation (6), and since it appears there as a factor of R_1, which in turn appears in no other simultaneous equation, one is justified in substituting $R_1(g_{m1}/g_{m1}')$ for R_1. If then g_{m1}' is substituted for g_{m1}, all of the simultaneous equations, and consequently the equations (1), (2), (3), and (4), will be exactly correct.

Similarly, i_2 represents V-2 cathode current in all simultaneous equations except (8) where it appears as a factor of R_2, which in turn appears in no other simultaneous equation. Equation (8) will then be correct for the case in which the screen grid of V-2 is bypassed to ground if $R_2(g_{m2}/g_{m2}')$ is substituted for R_2 and equation (6) will be correct if g_{m2}' is substituted for g_{m2}, where g_{m2}' is the cathode transconductance of V-2. It follows that these substitutions into equations (1), (2), (3), and (4) will result in exact solutions.

The corrections specified above may be applied singly or simultaneously, thus permitting exact solution of four combinations.

The use of a grounded bypass capacitor for V-1 will result in substantially lower input capacity because of positive feedback through R_{k0} to the cathode of this tube. The lower input capacity to V-2 will be obtained by a bypass capacitor between screen grid and cathode as a consequence of cathode circuit negative feedback.

Roger D. Thompson
Allen B. DuMont Labs.
Passaic, N. J.

* Received by the Institute, February 1, 1950.

[1] John M. Miller, Jr., "Cathode neutralization of video amplifiers," Proc. I.R.E., vol. 37, pp. 1070–1073; September, 1949.

Progression of Microwave Radio Scintillations at Wind Speed on an Overwater Path*

Summary

Fluctuations of 3.2-centimeter radio signals on a 26.5-mile overwater path were observed to progress at approximately wind speed from one receiver to another horizontal aligned normal to the radio path. In addition, the progression of the scintillations between two receivers vertically aligned normal to the path was observed to be downward.

* Received by the Institute, November 25, 1949. This work was done under Office of Naval Research Contract N5ori-136, P.O. I.

I. Introduction

During June and July of 1949, the Electrical Engineering Research Laboratory of the University of Texas made radio transmission studies at 3.2 centimeters wavelength on a 26-mile overwater path in the Gulf of Mexico. The results of previous studies have already been reported.[1,2] Receivers were located on the northeast end of Galveston Island, and the transmitter was located on the mainland beach near High Island, Texas.

During the course of these studies, two receivers were located in a line normal to the radio path. Part of the time these receivers were 65 feet apart horizontally and 16 feet mean sea level, and part of the time they were 10 feet apart vertically and various heights. The transmitter was at 15 feet msl. The received signals were recorded on Easterline-Angus meters driven by a single synchronous motor with timing markers placed simultaneously on both charts at one-minute intervals.

II. Horizontal Progressions

An example of the recordings is shown in Fig. 1. The recordings of the two receiver charts have been traced onto the same sheet with one recording displaced to prevent overlapping. These charts were analyzed in two ways. First, a number of points were identified as corresponding such as those marked with the same numbers in Fig. 1, and the time delays measured. Al-

[1] A. W. Straiton, "Microwave phase front measurements for over-water paths of 12 and 32 miles," Proc. I.R.E., vol. 37, pp. 808–813; July, 1949.

[2] A. W. Straiton, A. H. LaGrone, and H. W. Smith, "Comparison of measured and calculated microwave signal strength, phase and index of refraction," Proc. I.R.E., vol. 38, pp. 45–48; January, 1950.

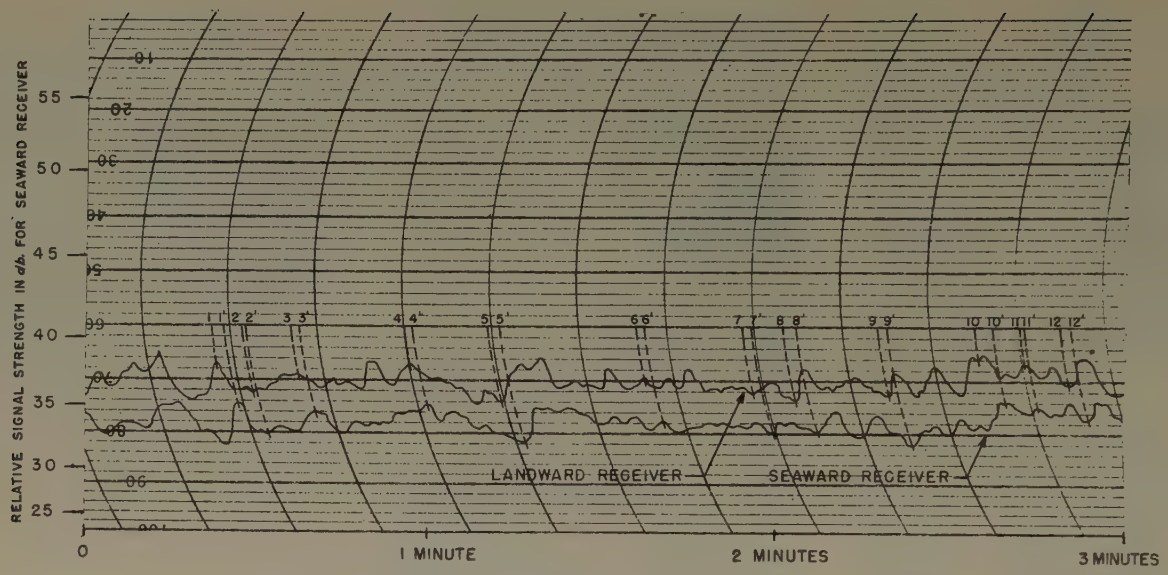

Fig. 1—Signal-strength recordings for horizontal separation of receivers.

though the sample lengths were too short for reliable conclusion, the time delays seemed to follow the normal distribution pattern.

Then, cross-correlation coefficients were determined for a number of time delays, and the time delay of the maximum coefficient noted. This time delay was in agreement with the average time delay obtained from correlating individual points. An autocorrelation function study indicated no periodicity in the scintillation.

Table I shows the average time delays noted for a number of different periods. The velocity of progression shown was calculated using the average time delay and the average path separation; i.e., 32.5 feet. This velocity of propagation is seen to agree within the accuracy of measurement with the average velocity of the component of wind normal to the path.

TABLE I

HORIZONTAL PROGRESSION DATA

Date	*Time*	*No. of Points Correlated*	*Average Progression Velocity in mph*	*Wind Velocity Normal to Path in mph*
6-28-49	1146	7	10.5	8.7 to 10.4
6-29-49	0342	9	14.8	18.0 to 14.7
6-29-49	2350	23	6.2	6.1 to 7.8
6-30-49	0322	10	5.7	6.1 to 7.3
7- 1-49	1924	10	6.4	6.9 to 8.6

All velocities are from seaward to landward

III. Vertical Progressions

Frequent measurements were made with two antennas displaced 10 feet vertically. Under nearly all circumstances, the characteristics of the signal strength-time variations at the two antennas were very similar. However, when corresponding points were identified or cross-correlation coefficients calculated, a downward progression of the scintillations was noted. In a number of cases, a pair of corresponding features occur simultaneously, but not a single case was found where the occurrence was noted at the lower antenna first. Table II shows the results of some of the vertical progression studies.

TABLE II

VERTICAL PROGRESSION DATA

Date	*Time*	*No. of Points Correlated*	*Average Time Diff. Sec.*	*Average Progression Velocity mph*
6-24-49	1610	35	0.59	5.8
6-28-49	1340	11	0.23	14.8
6-29-49	0342	13	0.33	10.3
6-29-49	0415	41	0.31	11.0
6-30-49	0322	16	0.41	8.3
6-30-49	1924	13	0.25	13.7
7- 1-49	0058	39	0.66	5.2

All average progression velocities are downward

IV. Discussion

In considering the progression of the scintillations, the propagation conditions under which the measurements were made should be kept clearly in mind. The radio path was distinctly beyond the line of sight, but a fairly strong duct existed producing very considerable trapping of the radio signal. The average signal strength was equal to or greater than the free-space value nearly all of the time. The temperature distribution of the air adjacent to the water was unstable.

It is felt that the scintillations are not due to additional signals from scattering areas outside of the duct, since overland ducts in Arizona produced no fluctuation while standard propagation beyond the line of sight scintillated badly.[3]

The fluctuations then seem to be due to regions of different dielectric constant moving across the radio path. Since the progression of individual occurrences could be traced while the wave forms were not identical, there seems to be more than one region of dielectric change in the path at any time, but not an extremely large number.

A proposed explanation of the downward progression of the fluctuation is that the surfaces of the dielectric changes were usually tilted forward, causing an effect at the upper antenna first. The tilt angle would need to be up to 45° to account for some of the apparent downward velocities noted.

It is hoped that more data on the nature of the progression of the scintillation will be obtained in the near future. Also, it is hoped that a theoretical explanation will be found which will give quantitative explanation to these observations.

[3] J. B. Smyth, "Signal fluctuation and scattering," presented, Symposium on Tropospheric Wave Propagation, Navy Electronics Laboratory, San Diego, Calif., July 28, 1949.

A. W. Straiton
H. W. Smith
Electrical Engineering
Research Laboratory
The University of Texas
Austin, Texas

Institute News and Radio Notes

Nominations—1951

At its May 10, 1950, meeting, the Board of Directors received the recommendations of the Nominations Committee and the reports of the Regional Committees for officers and directors for 1951. They are:

President, 1951: I. S. Coggeshall
Vice-President, 1951: Jorgen Rybner
Directors-at-Large, 1951–1953 (*two to be elected*): William H. Doherty, F. S. Howes, Dorman D. Israel, George R. Town
Regional Directors, 1951–1952 (*one to be elected in each Region*):
Region 2.—Harry F. Dart
Region 4.—William A. Dickinson, Paul L. Hoover, Hermann E. Kranz, W. E. Shoupp
Region 6.—W. M. Rust, Jr.
Region 8.—C. A. Norris, A. B. Oxley

According to Article VI, Section 1, of the Constitution, nominations by petition for any of the above offices may be made by letter to the Board of Directors, setting forth the name of the proposed candidate and the office for which it is desired he be nominated. For acceptance, a letter of petition must reach the executive office before twelve o'clock noon on August 14, 1950, and shall be signed by at least 100 voting members qualified to vote for the office of the candidate nominated.

IRE Will Inaugurate Plans For Annual Student Awards

Members of IRE Student Branches and Joint Student Branches in good standing will be eligible for an annual award to be given in each Branch by The Institute of Radio Engineers, according to a plan to become effective September 1.

The award will consist of a certificate provided by IRE headquarters and signed by the President of the Institute, together with a nontransferable voucher entitling the recipient to his first year's dues as Associate Member or Member, when presented with the student's application for transfer.

Awards will be made to students in the final year of their first undergraduate degree in engineering or science, and shall be based on the professional development, accomplishments, and interests of the students in those engineering and allied fields involved in activities of the Institute. The awards will also be based on the candidates' Student Branch or Joint Student Branch activities, student papers, original work, and scholarship. Meritorious extra-curricular activities will also be considered.

The judging of the recipient of the award will be undertaken by a committee appointed by the Section Chairman of the Section in which the Student Branch or Joint Student Branch is located. It shall include the IRE representative, and at least one other faculty member of the university whose Branch members are under consideration.

This award is intended to supplement student awards made by Sections of the Institute.

NAB Surveying Manufacturers for Information on FM Sets

Edward L. Sellers, who is in charge of the NAB FM-Radio Division, is making a survey of all FM set manufacturers, asking for information on the characteristics of their FM receivers.

The NAB resolution expresses the belief that "a number of FM receivers now being offered the public do not operate satisfactorily" within a field intensity range of 50 microvolts per meter, and that "some FM models are subject to excessive drift and are difficult to keep tuned."

He pointed out "that manufacture of FM home receivers with high sensitivity, effective limiting, and adequate antenna would go a long way in giving the country's some 700 FM broadcasters a new viewpoint on the role set manufacturers can play in providing the public with the full benefits of FM broadcasting on a nation-wide scale."

CAA Leases Biggest Contract For New Air Navigation Aids

The largest contract in the history of the Civil Aeronautics Administration was awarded recently to the Hazeltine Electronics Corp. for 450 distance-measuring equipment ground stations, the CAA announced. The equipment, known as "DME," will use radar-type radio pulse transmissions to inform pilots of their distance from a radio range.

Calendar of COMING EVENTS

Conference on Ionospheric Physics, Pennsylvania State College, Pa., July 24, 25 and 26

IRE West Coast Convention of 1950, Municipal Auditorium, Long Beach, Calif., September 13–15

IRE-AIEE Conference on Electronic Instrumentation in Nucleonics and Medicine, Hotel Park Sheraton, New York, N. Y., October 23–25

Radio Fall Meeting, Syracuse, N. Y., October 30, 31, November 1

Technical Committee Notes

The Electron Tubes and Solid-State Devices Committee held a meeting on April 5 under the chairmanship of L. S. Nergaard. Dr. Nergaard announced that electron tube definitions, in addition to those published in the April issue of the PROCEEDINGS OF THE I.R.E., will be available within a short time. *Standards on Electron Tubes; Methods of Testing, 1950*, prepared by this committee will be published in the August and September issues of the PROCEEDINGS OF THE I.R.E. The Committee, together with AIEE, sponsored a successful Conference on Electron Devices on June 22 and 23 at the University of Michigan. The University of New Hampshire has expressed its desire to become host to the 1951 conference. It was announced that A. L. Samuel has been appointed to serve as Vice-Chairman of the Committee. . . . Vice-Chairman C. H. Page presided at a meeting of the **Circuits Committee** on April 7. Work continues in the various subcommittees toward the compilation of definitions on circuit terms. A report on the progress of the Professional Group in Circuit Theory was given by Professor J. G. Brainerd. . . . Ernst Weber held a meeting of the **Measurements and Instrumentation Committee** on April 4. Reports of the activity in the subcommittees was given by the attending subcommittee chairmen. The Committee sponsored a **Symposium on Basic Circuit Elements** at the 1950 IRE National Convention. Four papers, "Performance and Measurement of Capacitors," by H. T. Wilhelm; "Behaviour of Resistors at High Frequencies," by G. R. Arthur, H. L. Krauss, and P. F. Ordung; "Inductors, Their Calculation and Losses," by Robert F. Field; and "Transformer Performance and Measurements," by Reuben Lee, were presented. The conference was attended by 350 people. . . . A **Symposium on Improved Quality Electronic Components** was held in Washington, D. C. on May 9, 10 and 11. It was sponsored jointly by IRE-AIEE-RMA with the active participation of various Federal agencies. The meeting was attended by approximately 750 people. The IRE wishes to thank Fred J. Given, Chairman of the Symposium Planning Group, J. G. Reid Jr., Chairman of the Technical Program Committee, and E. E. Zdobysz, Treasurer of the Symposium, and the committee personnel for their splendid work. . . . **Dr. Weber will represent the IRE on URSI Commission I.** F. J. Gaffney of the Committee on Measurements and Instrumentation will represent the National Research Council as a delegate at large at the URSI meeting in Zurich next year. He will also present a paper, a separate function. . . . **The Wave Propagation Committee** convened on April 20 at the National Bureau of Standards, Washington, D. C., with C. R. Burrows as Chairman. W. M. Goodall of

Bell Laboratories will represent the interest of the Wave Propagation Committee on the Task Group on Pulse. Chairman H. O. Peterson, of the Subcommittee 24.1, Standards and Practices, reported that substantial progress had been made in this subcommittee during the year and recommended that the same personnel continue during next year. The activities of Subcommittee 24.2, Theory and Application of Tropospheric Propagation, was given by Dr. Caroll for Dr. Booker. A report was also given by Mr. Wells for Chairman Waynick on the activities of Subcommittee 24.3. Subcommittee 24.4, Definitions and Publications, has prepared a list of definitions for presentation to the Standards Committee. . . . **The Video Techniques Committee** held a meeting on April 27 under the Chairmanship of J. E. Keister. A report on the activities of Subcommittee 23.1, Definitions and Symbols, was given by Chairman Daugherty. Dr. Garman, Chairman of Subcommittee 23.2, Utilization, Including Video Recording Methods of Measurement, reported on the activities of his group. Two papers written by R. L. Garman and H. J. Schafly have been submitted to the Technical Editor for possible publication in the PROCEEDINGS OF THE I.R.E. The activities of Subcommittee 23.3, Video Systems and Components: Methods of Measurement, was reported by Chairman Poch. . . . **The Joint IRE/AIEE Committee on High-Frequency Measurements** has been formed under the chairmanship of Professor Weber. Mr. Green will be Chairman of the IRE group on the Committee which will in turn act as Subcommittee 25.6 on Radio Frequency Measurements with respect to matters of standardization. The AIEE portion of the committee will be under the chairmanship of Harold Lyons of NBS and will constitute the AIEE Subcommittee on High-Frequency Measurements also. This Committee will be essentially an autonomous body. The major activity of this group will be a symposium on High-Frequency Measurements to be held next January in Washington, D. C., coincidental with the 50th Anniversary of the National Bureau of Standards. . . . **The Administrative Committee of the Professional Group on Instrumentation** held its first meeting at the 1950 IRE National Convention, held at the Hotel Commodore, New York, N. Y., on March 6–9 under the Chairmanship of Professor Weber. The activities of this Professional Group are closely associated with those of the Technical Committee on Measurements and Instrumentation. To date over 1,100 applicants have indicated interest. One of the activities of this group is to provide speakers to certain areas where required for section meetings or conferences. Names will be broken down geographically to show the location of the center of group interest. The Professional Groups Committee held a meeting on April 5, under the Chairmanship of W. R. G. Baker. Dr. Baker announced that 7,000 applications have been received. . . . **The Joint Technical Advisory Committee** held a meeting on April 26 at IRE headquarters, 1 East 79 St., New York, N. Y. John V. L. Hogan, Vice-Chairman, presided in the absence of Chairman Donald G. Fink.

Max F. Balcom Is Elected Head of Sylvania Directors

At a session of the Board of Directors of Sylvania Electric Products Inc., following the annual meeting, Max F. Balcom was elected chairman of the board to succeed the late Walter E. Poor, and Frank A. Poor, founder of the Company, was elect, ed vice-chairman.

MAX F. BALCOM

Mr. Balcom, the new chairman of the board, has been associated with Sylvania since 1918 when he became purchasing agent for a predecessor company, Novelty Incandescent Lamp Co., in Emporium, Pa. In 1931, with the formation of Hygrade Sylvania Corp., he was made assistant secretary of the new organization and placed in charge of radio costs and general corporate work. He became a director in 1934. Three years later he was elected vice-president in charge of the radio division and in 1944 was elected treasurer.

For many years Mr. Balcom has been active in various radio industry activities. He was president of the Radio Manufacturers Association in 1948 and 1949, and is presently chairman of the Association's television committee.

ASEE Committee Reports on Serious Engineer Shortage

Unless the percentage of high school graduates entering engineering colleges is increased, there is a strong probability that instead of a large surplus of engineering graduates, which has been prophesied rather widely, there will soon be fewer engineering graduates available than are needed annually by our national economy.

This is the conclusion drawn by a subcommittee of the Manpower Committee of the American Society for Engineering Education from a study of trends in engineering enrollments, and of statistics on 1949 graduations assembled jointly by the Society and the U. S. Office of Education. These statistics will be published soon by both organizations.

Baltimore Is Third Port To Install Harbor Radar System

Baltimore, Md., recently became the third major port in the world to put into operation a harbor radar system. The equipment will be used in a navigational aid research program designed to assist ships entering and leaving the port in fog and bad weather, to provide continuous observation of harbor shipping, and to give immediate information on the location of any shipping casualties in the harbor.

The radar equipment, a Westinghouse commercial marine radar unit, provides port operators with a 12½-inch radar "chart" of harbor shipping movements at ranges from 80 yards to 40 miles. It is installed at the City Recreation Pier in the radio control room, so that radar observations can be transmitted directly to harbor shipping over stations WMH and WJY, the city's ship-to-shore radio stations.

Quality Electronic Components Conference Held in Washington

Components for electronic equipment used in military aircraft and other weapons of war must be designed to serve without replacement throughout the life or normal use of the equipment if electronics is to continue to play its role of increasing importance in modern warfare, it was reported at the Conference on Improved Quality Electronic Components held May 9–11, in Washington, D.C.

FRED R. LACK

The conference, attended by 800 technicians from the industry and government, was sponsored jointly by The Institute of Radio Engineers, the Radio Manufacturers Association, and the American Institute of Electrical Engineers, with the co-operation of the Department of National Defense and the National Bureau of Standards. About 40 engineers and scientists from Canada, England, Australia, Sweden, and New Zealand attended the meeting.

Stressing the problem of the military services to train sufficient personnel to maintain electronic equipment, speakers told the industry engineers that in the past, maintenance of such equipment has cost from ten to one hundred times as much as the original apparatus and consumed valuable time and manpower.

Fred R. Lack, vice-president of Western Electric Co., New York, N. Y., gave the keynote address. More than forty technical papers were delivered during the three-day session, of which F. J. Given of the Bell Telephone Laboratories, Inc., served as chairman.

In his welcoming address Mr. Given said that the purpose of the conference was to promote and encourage the proper philosophies for obtaining a better all-around performance of electronic equipment.

"The meeting is important as a milestone marking the tremendous role which electronic components and equipment play in the present-day affairs of industry and government," Mr. Given said.

Industrial Engineering Notes[1]

Television News

Engineering testimony supplied by the Laboratory Division of the FCC during the color inquiry indicated that TV broadcasting in the uhf will "aggravate the oscillator radiation problem" now disturbing the industry and the Commission "because of the nature of the technical problems involved." Testifying on interference problems to be faced by color television, E. W. Chapin, Chief of the FCC Laboratory, said that the filling up of the spectrum through the use of more transmitters and receivers probably will increase interference and make it increasingly difficult or impossible to solve harmonic or local oscillator radiation problems by station allocations. He explained that the "economics are such as to tempt manufacturers to build cheaper and cheaper receivers without regard to the interference they may cause by oscillator radiation. It is especially unfortunate that oscillator radiation causes interference to somebody else's receiver and does not degrade the performance of the offender," he added. . . . **The FCC has announced that following the close of the color television hearing** it will take up the question as to whether the 470- to 500-Mc band should be allocated to TV or multichannel broad-band mobile radio communication. The hearings will begin not later than one week after the close of the color inquiry at a place to be announced. Permission was granted the National Mobile Radio System, an association of miscellaneous common carriers, to participate in this phase of the FCC allocation hearing in opposition to the grant of these frequencies to television broadcasting. Among others scheduled to participate are: Allen B. DuMont Laboratories, Inc.; Philco Corp.; Television Broadcasters Association; and several telephone companies. . . . **The FCC has granted in part an application of the Zenith Radio Corp. for a new transmitter** to be utilized with experimental TV station KS2XBS for Phonevision. The FCC allowed Zenith to change the location of its transmitter to 135 South La Salle St., Chicago, Ill., but held the transmission power of the station at 1 kw (visual) and 500 watts (aural). . . . A possibility that the **Columbia Broadcasting System, Inc., may promote a new corporation to manufacture or distribute television receivers** in the event the CBS color TV system is adopted by the FCC was disclosed during the cross examination of President Frank Stanton of Columbia. The witness said CBS might set up a new company if present receiver manufacturers refused to make sets capable of receiving CBS color transmissions. The CBS President said the possibility of forming a new company had been discussed with New York businessmen. It would be financed by a $50 million stock issue, consisting of 10 million shares at $5 a share. The stock would be "widely" held, he explained, and the company would probably not be controlled by CBS. The new company might confine its activities to distributing sets made to CBS specifications by other manufacturers, or it might make the receivers itself, under a license agreement with Columbia. . . . **CBS has told the FCC that patent royalties for CBS-type color receivers would not exceed $10 per set.** Total royalties payable to RCA, Hazeltine, and CBS would range from $9.00 per set to $9.77, depending upon the selling price of the receiver itself, according to information supplied the Commission by CBS Executive Vice-President Adrian Murphy. CBS based its estimates on figures reporting to show that the RCA license agreement provides for the payment of royalties at the rate of 2½ per cent of manufacturers' net selling price and the Hazeltine royalty of 1.05 per cent of the manufacturers' net selling price. . . . **Two manufacturers of television receivers—Air King and Teletone—who had previously testified as CBS witnesses were cross examined during the color TV hearing.** David H. Cogan, President of Air King Products, said his company would proceed "as rapidly as possible in whatever direction" the FCC should decide the current controversy. He explained that his company was prepared, if the FCC approves the CBS system, to produce color sets within 90 days of the Commission decision with a complete 100 per cent change-over to color set manufacturing within nine months to one year. Mr. Cogan suggested that the FCC allow six months of experimentation between the decision announcement and its effective date. Manufacturers could not switch over to the new production immediately, he said. The Air King President said the quality of TV programs is the "greatest single sales factor" in television receiver merchandising. S. W. Gross, President of the Teletone Corp., estimated that his concern could produce color TV sets for the CBS system at $200. In October, his estimate was $220 for a 10-inch color receiver, but the $20 was due to the reduced selling price of the company's present 10-inch black-and-white set, he said. Teletone has no plans to build color receivers until the hearings are over, he added. Other witnesses were John Schubert, vice-president of Bertman Electric Co., who testified that his firm would make a color converter to retail for $55 in the event of FCC's approval of the CBS system; and C. Cushway, executive vice-president of Webster-Chicago, who said that concern had manufactured a color "camera chain" and plans to manufacture others if the CBS system is adopted. Webster-Chicago has also manufactured about 20 disk-type converters and one or two scanning adapters. . . . **RMA and the television industry have won the 1st round of their fight against a 10 per cent excise tax on television receivers,** proposed by Treasury-Secretary John W. Snyder, when the House Ways and Means Committee rejected the Administration proposal in preliminary action on excise tax reduction legislation. The radio tax remains intact.

FCC Actions

While **radio and television stations showed increased revenues in 1949,** their **expenses also increased and their income dropped** 24 per cent, according to a tabulation released by the FCC. Total AM, FM, and TV station revenues in 1949 amounted to $459.8 million, an increase of 10 per cent over the preceding year, but expenses rose to $425.0 million, an increase of 14 per cent. Income of the three types of broadcasting stations before taxes amounted to $34.8 million compared with $46.1 million in 1948, a decrease of 24 per cent. Television stations had losses before taxes of $24.3 million compared with $14.9 million in 1948 . . . **FCC Chairman Wayne Coy told members of the Senate that he had "no intention of being available for reappointment"** as head of the Commission when his term expires in 1951. Mr. Coy said he will leave the FCC post while testifying before the Senate expenditures committee in behalf of the President's plan to reorganize the FCC and other Government agencies.

Statistics

Continued at a record-breaking pace, **television receiver production** by RMA member-companies **reached new highs** in both March and **the first quarter of 1950,** as more than a half-million sets were manufactured in a five-week reporting period and 1.2 million during the first quarter. Radio receiver production also was sustained at a high level, with the result that 1,505,641 radio and television sets were reported to RMA in the month and 3,618,882 during the first quarter of this year. Member companies reported production of 1,724,660 home radio receivers and 66,292 auto sets during the first three months of this year.

Sales of RMA parts manufacturers in March increased substantially over sales in the corresponding month of 1949, according to an indices compiled from company reports on sales to manufacturers and jobbers . . . **Sales of radio receiver sets by Canadian manufacturers totaled 728,680 units in 1949,** an increase of 22 per cent over the number sold in 1948, according to information received by the U. S. Department of Commerce. The value of 1949 sales at list prices was $55.3 millions. A breakdown of the 1949 sales showed table models accounted for 60 per cent of the total; automobile sets for 19 per cent; consoles for 13 per cent; and portables for eight per cent.

Radio and Television News Abroad

Although installation of a television transmitter in Rio De Janeiro, Brazil, has been delayed due to weather conditions and the fact that all materials have to be transported to a mountain location by cable car, a report to the Department of Commerce says **the station will go on the air in August.** The Embassy report states that the local office of General Electric has obtained special import license for 2,000 12½-inch and 19-inch receivers which it expects to have ready for sale in June. It is understood, the report states, that RCA, Philco, and Philips expect to be granted special import

[1] The data on which these NOTES are based were selected by permission from *Industry Reports*, issues of April 14, April 24, April 28, and May 5, published by the Radio Manufacturers Association, whose helpful attitude is gladly acknowledged.

licenses also . . . **Mexico,** which expects to have a television station in operation this summer, **has established new import tariff classifications** to permit the importation of television sets and parts. Previously, TV sets were considered as radios and were prohibited from importation . . . **Assembly of radio receivers in Mexico during 1949 totaled 116,000 sets,** compared with 71,500 in 1948. Ten firms were assembling radios at the end of the year, according to a report to the U. S. Department of Commerce. Imports of radio receivers totaled 7,404 sets in 1949, compared with 6,087 in 1948 and 185,225 in 1947. Imports of radio receiving tubes and components aggregated 25,883,454 pesos in 1949, representing an increase of 51 per cent over 1948 imports . . . **Approximately 95 per cent of all radio receivers imported into the Philippine Republic are of U. S. manufacture** and no sets or tubes are manufactured there, according to a report from the U. S. Embassy to the Department of Commerce. The report also notes that Philips is the principal European brand imported and that table model radios in plastic cabinets are preferred. Approximately 90 per cent of the radios in use are designed to receive short-wave broadcasts. Since electric power is available only in the large cities and environs, battery-operated sets are popular, accounting for 40 per cent of the sets in use.

TV Network Facilities Will Connect East and West in '51

The long-awaited linking of the east and west coasts for transcontinental television programs will be accomplished by the end of 1951 under tentative plans of the Bell System, according to testimony given the FCC during a recent hearing.

Frank A. Cowan, AT&T engineer, testifying on the FCC proposal to order the interconnection of the TV network facilities of the Bell System and other carriers, said that the intercity network facilities of the Bell System will total 23,000 miles by the end of next year. This will enlarge the network, which is expected to extend about 15,000 miles by the end of this year, by some 8,000 additional miles in 1951. At the end of next year, he said, the Bell System network is expected to be about equally divided between radio relay and coaxial cable.

The transcontinental link will be via Omaha, which is to be joined to the network this year, and San Francisco. The 1951 TV program also includes an extension to Miami as well as a connection with Binghamton, N. Y.

Glass Ribbons for Condensers Are Devised for Signal Corps

Through the use of glass ribbons in the place of mica sheets in miniature condensers, the U. S. Army Signal Corps expects to achieve a saving of 50 to 70 per cent in manpower during mass production.

The glass capacitors were developed by the Corning Glass Works under a Signal Corps research and development contract. Glass ribbon is used as the dielectric, and aluminum foil as the electrodes. They are sealed in a glass case that is impervious to atmospheric moisture and other troublesome climatic effects.

A huge manpower saving is anticipated in mass production because the glass ribbon will be of uniform thickness, whereas sheets of mica now have to be handsorted for uniform thickness and quality. From low frequency to self-resonant frequency, the Signal Corps said, the new miniature capacitators equal or exceed the performance of equivalent mica condensers. The glass condensers are a fifth to a sixth of the size of equivalent mica condensers. In addition, production and stocking problems will be simplified by a reduction of grade styles from 15 to two, the Signal Corps explained.

FCC Chairman Coy Uncertain About Lifting of TV Freeze

Devoting very little time to television problems and again refusing to predict when the TV freeze will be lifted, FCC Chairman Wayne Coy has told the National Association of Broadcasters that he is "less certain about the time when we will get out of the freeze" than he was a year ago.

He spoke during the 28th annual NAB convention in Chicago, and reminded his audience that a year had elapsed since he last spoke to the gathering and added: "In that year I have learned a lot about television, and I am even less certain of the answers to your questions than I was a year ago. I am even less certain about the time when we will get out of the freeze. I certainly hope—and let me repeat the word 'hope'—that we get out of the freeze before the end of the year. I pray that it will be earlier. I do not predict when," Mr. Coy emphasized.

Board of Directors Have Voted RMA Reorganization in Canada

Provisions for extensive reorganization and reconstruction of RMA were made by its Board of Directors at a meeting in Canada. Included in the reorganization plans were the following points: the engagement of a full-time paid president of national reputation, to succeed President R. C. Cosgrove in June; and the retirement of Bond Geddes, executive vice-president, general manager and secretary, on August 1. Mr. Geddes will continue as an advisory consultant to RMA for a period of years after nearly 23 years of service. Other points were the change of the RMA name to the "Radio-Television Manufacturers Association"; and the extensive reorganization of the RMA services and activities, with increased financial resources and strength.

The reorganization plans were presented to, and approved by, the RMA membership at its 26th annual convention, held on June 5–8, at Chicago, Ill.

Commissioner Hennock Advises Educators to Enter Television

FCC Commissioner Frieda B. Hennock has urged Pennsylvania educators to take full advantage of television as an educational medium. Miss Hennock participated in a recent "Meet The Press" forum of Philadelphia representatives of the press and educators at the University of Pennsylvania.

Miss Hennock deplored the decline in educational radio broadcasting and told the educators that they "must get in television at the beginning" and "stay in it."

Every educator, she said, should be alive to the potentialities of television and to the urgency of making himself heard right now. She stated that she could not urge them strongly enough to try to interest their respective schools and school systems in television.

German Patent Guide

A new "finding guide" to wartime German patent applications, which may now be used freely in Allied countries, has been made available by the Office of Technical Services, U. S. Department of Commerce. The guide is a subject index to the 200,000 German applications filed in Berlin over the period 1940–1945, and breaks them down into 13 major industrial groups, 89 classes, and some 500 subclasses. Copies of the guide, "Subject Outline of the Unpublished Applications for Patents filed at the German Patent Office—1940–1945," are available on request from the Office of Technical Services, U. S. Department of Commerce, Washington 25, D. C.

President Cosgrove Resigns From Executive Post Of AVCO

Victor Emanuel, President of Avco Manufacturing Corporation, has announced the resignation of R. C. Cosgrove as Executive Vice-President of the Company. Mr. Cosgrove will remain as a member of the Board of Directors and in a consulting capacity to the management. He also will continue to represent the Crosley Division of Avco in the Radio Manufacturers Association, of which he is President.

New *RMA Trade Directory* Is Mailed To Officers, Members

The 1949–1950 edition of the *RMA Membership List and Trade Directory* came off the press recently, and copies have been mailed to all RMA members, officers, and committees. In addition, copies are being sent to the radio trade press, to government agencies, military procurement officials, associated trade groups, technical libraries, and foreign purchasing commissions.

IRE People

L. M. Clement (A'14–M'17–F'26), formerly director of engineering, has been appointed technical adviser to the vice-president and general manager of the Crosley Division, Avco Manufacturing Corp. Because of the company's major expansions in both the appliance and electronic fields, the engineering department has been divided into two main divisions, with a manager in complete charge of each division's activities.

L. M. Clement

Mr. Clement's new duties will include liaison with trade associations and other key groups, investigations of new outside developments, and special assignments of a technical nature. Prior to joining Crosley as director of engineering in 1940, he had served in executive positions with RCA, Westinghouse, Western Electric Company, International Telephone and Telegraph Co., and the American Marconi Co.

❖

Frank E. Stoner (A'31–SM'45) who has retired as a Major General of the United States Army, has joined the firm of Weldon and Carr, consulting radio engineers, and is directing the new branch office in Seattle, Wash.

Frank E. Stoner

General Stoner has been prominent in the telecommunications field. A native of Vancouver, Wash., he was born on December 25, 1894, and received a public school education in the State of Washington.

During the first world war he was commander of the 14th Company, Philippine Scouts, and Wire Company, 1st Philippine Field Signal Battalion, 1917–1919. From 1919 to 1928 he served as Company Commander and Regimental Adjutant with the 46th Infantry, and 1st Infantry, Second Division, 7th Signal Service Company, Eighth Corps Area, and other organizations.

He was graduated from Signal School in 1928 and was officer in charge, War Department Message Center and Radio, from 1928 to 1932.

Other highlights of General Stoner's Army career include the following assignments: Executive Officer, Washington Alaska Military Cable and Telegraph System, 1932–1937; executive officer, The Army Signal School at Fort Monmouth, N. J., 1937–1939; graduate of Army Industrial College, 1940; Signal, Fifth Corps Area and Fifth Army Corps, 1940–1941; and Signal Officer, Third Army, 1941–42.

He was designated Chief, Army Communications Service, in February, 1942, and was appointed Major General in 1944. The following year he was named Assistant Chief Signal Officer.

He was appointed Chairman of the Panel of Communications Experts, United Nations General Assembly, on September 1, 1946, and has been Director of Telecommunications, United Nations.

Among the honors bestowed upon General Stoner during his distinguished career are: the Distinguished Service Medal; Cross of the British Empire, Commander Degree; French Legion of Honor, World War I and II Ribbons; European Theatre Ribbon; North American Ribbon; Victory Ribbon; Mexican Border; Defense Service Medals; Army of Occupation Ribbon. He was awarded the Marconi Medal of Achievement in 1946.

General Stoner served with Count Folke Bernadotte in Palestine, and installed an elaborate network of radio stations throughout the Middle East during the Palestine War.

❖

T. W. Jarmie (A'48), has joined the Electronic Engineering Company of California as resident project engineer at the Naval Air Missile Test Center, Point Mugu, Calif.

Mr. Jarmie was one of the original founders of Electronic Associates, Long Branch, N. J. He was their sales manager and a director from 1945 until leaving in February, 1950, for his new position.

Margaret S. Heagy (M'46), research engineer with the RCA Laboratories at Princeton, N. J., died recently. She was born on February 27, 1915, in New Jersey. The deceased was the wife of Professor Harry A. Heagy, a member of the faculty of the Peddie School in Hightstown, N. J.

Mrs. Heagy was a graduate of Alfred University and received the M.A. degree from Columbia University in 1936. During the early part of the war she worked in the development engineering department of Link Aviation Devices, Inc. at Binghamton, N. Y.

She joined RCA in 1944 and had been a member of the technical staff in the Tube Research Laboratories since that time, working on magnetrons, traveling-wave tubes, and microwave measurements.

James White (A'45) has been appointed manager of contract sales of Air King Products Co., Inc., manufacturers of radios, wire recorders, and television receivers. He will be in charge of sales to large contract accounts, including the engineering development and research phases in connection with these types of sales.

James White

Mr. White has played an important part in the installation of major radio and television stations throughout the country. Formerly he had been eastern manager of the Andrew Corp. of Chicago, and was also with the Gray Audograph Co. as assistant general manager before his association with Air King.

During the war he was commissioned lieutenant senior grade in the Naval Air Arm and saw action at Saipan, New Guinea, and the Philippine invasion aboard an aircraft carrier. After the German surrender he was appointed project engineer at the MIT Radiation Laboratory, working on new radar development.

A native of West Haven, Conn., Mr. White was graduated from Yale University with the electrical engineering degree. He has also completed work in advanced electronics at MIT, and in business administration at the graduate school of Chicago University.

Mr. White is a member of the Yale Club of New York, the Washington Engineering Society, and the National Office Management Association.

❖

D. B. Nason (A'41–M'44) has been advanced to manager of electronic engineering of the Crosley Division, Avco Manufacturing Corp. He will be in charge of research, development, and engineering on television and radio receivers and government projects.

D. B. Nason

He has been associated with the electronic engineering field for 15 years with RCA, Sylvania Electric Products Inc., and Eltron, Inc., as well as Crosley. He was with Crosley from 1940 to 1944 as chief receiver engineer in charge of development work on radio products for the armed forces. After leaving in 1944 to become vice-president in charge of engineering for Eltron, Inc., he returned to Crosley in 1948 to become manager of the Company's government engineering section.

Books

Recent Advances in Radio Receivers by L. A. Moxon

Published (1950) by Cambridge University Press, 51 Madison Ave., New York 10, N. Y. 168 pages+5-page index+10-page appendix+ix pages. 88 figures. 5½×8½. $4.00.

This book is the seventh in a series of monographs entitled "Modern Radio Techniques" edited by J. A. Ratcliffe. All the monographs in this series are written by men who were personally responsible for important advances in the subjects about which they write.

As the author states in his preface, the field covered by the title of the book is a wide one, and in such cases the selection of some of the material inevitably tends to be biased by the author's own personal experience and interests. The first 83 pages—just one-half of the text—is concerned with the concepts and aspects of noise factor and its measurement. Here the author speaks with considerable authority, and one wishes that he might have expanded this portion still further and made noise factor the subject of a complete monograph.

The second half of the book has one chapter dealing with wide-band intermediate-frequency amplifiers. The rest of the text, aside from citing a few receiver design trends, gives brief description of each of a somewhat heterogeneous (but no means complete) list of receiver circuits and circuit tricks. Some of these are not particularly "recent" and there are inaccuracies in the descriptions of others. Nevertheless, this reader found the book to be stimulating and worthwhile reading, and believes others will have the same reaction.

S. W. Seeley
Radio Corp. of America
711 Fifth Ave.
New York 22, N. Y.

Acoustical Designing in Architecture by Vern O. Knudsen and Cyril M. Harris

Published (1950) by John Wiley and Sons, Inc., 440 Fourth Ave., New York 16, N. Y. 404 pages+7-page index+45-page appendix+x pages. 222 figures. 5½×8½. $7.50.

For the radio engineer interested in architectural acoustics, this book comes as a welcome addition to the literature. It treats the special problems of noise control in buildings, the design of rooms, auditoriums school buildings, commercial and public buildings, homes, apartments, hotels, church buildings, and sound studios.

The text is easy to read and the authors have meticulously avoided mathematics. In many parts of the book, one gains the impression that he is sharing the personal experiences of Dr. Knudsen, who has contributed much to the growth of architectural acoustics in this country. In other parts of the book the authors have served more as reporters. The tables of sound absorption coefficients and of sound insulation data appearing in the appendices bring together much valuable data that previously existed only in bulletins of the Acoustical Materials Association, the National Bureau of Standards, and the National Physical Laboratory.

The radio engineer may feel that the chapter on sound-amplification systems is too abbreviated, or that more space might have been devoted to studio design, especially television studio design. However, this book is written for the architect, and the very fact that the architect is made aware of the basic problems makes it easier for the engineer to discuss the subject with him and to arrive at mutually satisfactory results.

The balance of the book yields a wealth of information on the principal phases of architectural acoustics. Without qualification, this text belongs in the library of everyone seriously interested in this subject.

Leo L. Beranek
Massachusetts Institute of Technology
Cambridge, Mass.

Television Simplified by Milton S. Kiver

Published (1950) by D. Van Nostrand Co., Inc., 250 Fourth Ave., New York 3, 556 pages+5-page index+18-page appendix+vii pages. 363 figures. 5½×8. $6.50.

This is the third edition of a popular type book in the field of television. The name, however, is a little too inclusive, since the book covers only the subject of television receivers. A brief mention of transmitter principles and a very limited discussion of television tubes is included. However, the basic principles of television have been explained in a very simplified manner which can be easily understood by a nonmathematical reader.

The author does a good job in simplifying some of the very complex problems involved in television circuitry. With the current tremendous expansion in personnel in this field, this is an important contribution.

The book starts with a short explanation of the television field and television principles and then goes on to explain the behavior of the vhf waves and antennas. From here, circuits are taken up with many illustrative examples. Circuit diagrams with actual values incorporated into commercial receivers are given. He discusses radio-frequency amplifiers, oscillators, mixers, intermediate-frequency amplifiers, detectors, and video amplifiers. Specialized subjects such as automatic gain control circuits, dc reinsertion, and synchronizing circuits are covered very carefully, inasmuch as their design is rather specialized. Enough is given, however, so that a serviceman may understand the functions of the parts he is handling. Frequency modulation is discussed only very briefly. Some new chapters have been added at the end of the book to cover inter-carrier television sound and color television.

The chapter on servicing and the discussions on installation are very brief and could have been expanded into a much more useful segment. However, it must be realized that the book is quite lengthy and too much material would make its cost prohibitive. Questions on each chapter are included at the end, as well as a glossary of television terms.

Almost eighteen pages are devoted to the allocation of television channels. With the great deal of material which could have been added to the book, this section could have been omitted, since its usefulness is very limited.

The book is well illustrated and is presented in easy, conversational manner. The author assumes that the reader has a knowledge of radio circuitry operation, but no knowledge of even the very fundamental operating principles of television. Those men interested in learning how to read and understand television circuit diagrams will find the book very interesting and informative. It should answer many questions that the serviceman has concerning the sets he is troubleshooting. Its very lack of mathematical treatment should make it welcome to many men whose mathematical knowledge is limited.

Nathan Marchand
Sylvania Electric Products Inc.
P.O. Box 6
Bayside, L. I., N. Y.

How to Become a Radio Amateur

Published, (1950) by the American Radio Relay League, West Hartford 7, Conn., 70 pages. 65 diagrams and photographs, 9 tables. 50 cents, postpaid in the United States.

"How to Become A Radio Amateur" is a complete beginner's guide to the hobby of amateur radio. What amateur radio offers, from message-handling to "rag-chewing," from communicating with distant countries to emergency communications work, from learning the code and theory to building a station, is explained fully in concise and understandable language.

The constructional sections, which feature receivers and transmitters suitable for the newcomer, make direct reference to the book's review of radio theory in order that the beginning amateur may acquire a basic knowledge of how and why his radio set functions.

A series of photographs of radio parts, together with their associated schematic symbols which represents the parts in a wiring diagram, is a new and helpful feature designed to aid the beginner in reading radio circuit diagrams.

The radio receivers and transmitters described in the book are suitable for any newcomer, but they have been especially designed with an eye toward the new Novice Class of amateur licenses which the Federal Communications Commission proposes to make available by next year. The Novice Class license will differ from other classes of amateur licenses in that the code test will be only 5 words per minute and the theory examination will be greatly simplified. Operation under this license will be limited to certain segments of the amateur bands under special regulations.

Sections*

Chairman		Secretary
H. R. Hegbar 2145 12th St. Cuyahoga Falls, Ohio	AKRON (4)	H. G. Shively 736 Garfield St Akron, Ohio
W. J. Miller 1074 Springdale Rd. Atlanta, Ga.	ATLANTA (6)	D. B. Buchanan 5130 Powers Ferry Rd. Atlanta, Ga.
E. W. Chapin 2805 Shirley Ave. Baltimore 14, Md.	BALTIMORE (3)	J. V. Lebacqz Johns Hopkins Un. Baltimore, Md.
J. Petkovsek 1015 Ave. E Beaumont, Texas	BEAUMONT-PORT ARTHUR (6)	C. B. Trevey 2555 Pierce St. Beaumont, Texas
W. H. Hausner WBZ, WBZ-FM, WBC-TV 1170 Soldiers Field Rd. Boston, Mass.	BOSTON (1)	L. E. Packard Technology Inst. Co. 1058 Main St. Waltham 54, Mass.
M. J. Kobilsky Fabrica Argentina De Prod. Vedia Y AR. Forest Buenos Aires, Argentina, S.A.	BUENOS AIRES (1)	H. T. Magno Mirasol 451 Buenos Aires, Argentina, S.A.
K. R. Wendt Colonial Radio Corp 1280 Main St. Buffalo 9, N. Y.	BUFFALO-NIAGARA (4)	H. G. Kuhn 211 Frankhauser Rd. R.F.D. #3 Williamsville, N. Y.
D. B. Harris 2003 Glenway Dr. Cedar Rapids, Iowa	CEDAR RAPIDS (5)	J. L. Hollis 2900 E. Ave. N.E. Cedar Rapids, Iowa
Kipling Adams General Radio Co., 920 S. Michigan Ave. Chicago 5, Ill.	CHICAGO (5)	R. M. Krueger Am. Phenolic Corp. 1830 S. 54 Ave. Chicago 50, Ill.
F. W. King 6249 Banning Rd. Cincinnati 24, Ohio	CINCINNATI (5)	J. P. Quitter 509 Missouri Ave. Cincinnati 26, Ohio
J. B. Epperson Scripps-Howard Radio Box 228 Berea, Ohio	CLEVELAND (4) July 27–Aug. 24	J. L. Hunter John Carroll Univ. Cleveland, Ohio
R. B. Jacques 226 W. Como Ave Columbus, Ohio	COLUMBUS (4) July 14–Aug. 11	S. N. Friedman 144 N. Edgevale Columbus, Ohio
Lawrence Grew S. N. E. Telephone Co New Haven, Conn.	CONNECTICUT VALLEY (1)	John Merrill 16 Granada Terr. New London, Conn.
J. H. Homsy 6022 Vanderbilt Dallas, Texas	DALLAS-FORT WORTH (6)	R. A. Arnett Box 7166 Dallas, Texas
C. J. Marshall 2412 Rosewood Ave. Dayton 9, Ohio	DAYTON (5)	R. W. Ittelson 551 Daytona Pkwy. Fairfield, Ohio
T. G. Morrissey Radio Station KFEL Albany Hotel Denver, Colo.	DENVER (5)	Hubert Sharp Box 960 Denver 1, Colo.
G. A. Richardson Dept. of Elec. Eng. Iowa State College Ames, Iowa	DES MOINES-AMES (5)	A. D. Parrott Northwestern Bell Tel. Co. 604—Ninth St. Des Moines 9, Iowa
N. C. Fisk 3005 W. Chicago Ave. Detroit 6, Mich.	DETROIT (4)	P. L. Gundy 55 W. Canfield Ave. Detroit, Mich.
W. J. Peterson 322 E. Allegheny Ave. Emporium, Pa.	EMPORIUM (4)	W. R. Rolf 364 E. Fifth St. Emporium, Pa.
R. E. Moe Eng. Dept. General Elec. Co. Owensboro, Ky.	EVANSVILLE-OWENSBORO	H. W. A. Chalberg 316 W. Ninth St. Owensboro, Ky.
B. H. Ratts 2506 Terrace Rd. Ft. Wayne 3, Ind.	FORT WAYNE (5)	R. B. Jones 4322 Arlington Ave. Ft. Wayne, Ind.
C. R. Wischmeyer 808 N. Rice Ave. Bellaire, Texas	HOUSTON (6)	Wayne Phelps 26 N. Wynden St. Houston 19, Texas
G. H. Fathauer 4125 E. 10 St. Indianapolis 1, Ind.	INDIANAPOLIS (5)	J. H. Shultz Indianapolis Elec. School 312 E. Washington St. Indianapolis 4, Ind.
F. M. Ashbrook 111-A Ellis China Lake, Calif.	INYOKERN (7)	D. L. Ewing 309-B Fowler China Lake, Calif.
C. F. Heister Fed. Com. Comm. 838 U. S. Court House Kansas City 6, Mo.	KANSAS CITY (5)	Mrs. G. L. Curtis 6005 El Monte Mission, Kan.
G. L. Foster Sparton of Canada London, Ont., Canada	LONDON, ONTARIO (8)	G. R. Hosker Richards-Wilcox Co. Ltd. London, Ont., Canada
R. L. Sink Consolidated Eng. Co. 620 N. Lake Ave. Pasadena 4, Calif.	LOS ANGELES (7)	W. G. Hodson 524 Hampton Rd. Burbank, Calif.
S. T. Fife Univ. of Louisville Louisville, Ky.	LOUISVILLE (5)	I. W. Lyle Route 3 Jefferson Town, Ky.
E. J. Limpel A. O. Smith Corp. 3533 N. 27 St. Milwaukee 1, Wis.	MILWAUKEE (5)	W. H. Elliot 4747 N. Larkin St. Milwaukee 11, Wis.
A. B. Oxley R.C.A. Victor Co. 1001 Lenoir St. Montreal, P.Q. Canada	MONTREAL, QUEBEC (8)	H. A. Audet Canadian Broadcasting Corp. 1231 St. Catherine St. Montreal, Que, Canada
C. W. Carnahan 3169—41 Place Sandia Base Branch Albuquerque, N. M.	NEW MEXICO (7)	T. S. Church 3325 49th Loop Sandia Base Branch Albuquerque, N. M.
H. F. Dart 33 Burnett St. Glen Ridge, N. J.	NEW YORK (2)	Earl Schoenfield W. L. Maxson Corp. 460 W. 34th St. New York 1, N. Y.
C. M. Smith Radio Station WMIT 419 N. Spruce St. Winston Salem, N. Car.	NORTH CAROLINA-VIRGINIA (3)	V. S. Carson Elec. Eng. Dept. N. C. State College Raleigh, N. Car.
M. W. Bullock Capital Broadcasting Co. 501 Federal Securities Bldg. Lincoln 8, Neb.	OMAHA-LINCOLN (5)	C. W. Rook Dept. of Elec. Eng. Univ. of Nebraska Lincoln, Nebr.
J. T. Henderson 11 Primrose St. Ottawa, Ont., Can.	OTTAWA, ONTARIO (8)	E. L. R. Webb National Res. Council Sussex St. Ottawa, Ont., Canada
J. T. Brothers Philco Radio and Television Tiogo and 'C' Sts. Philadelphia 34, Pa.	PHILADELPHIA (3)	L. M. Rodgers 400 Wellesley Rd. Philadelphia 19, Pa.
M. Glenn Jarrett 416 Seventh Ave. Pittsburgh 19, Pa.	PITTSBURGH (4)	W. P. Caywood, Jr. 23 Sandy Creed Rd. Pittsburgh 21, Pa.
F. E. Miller 3122 S.E. 73 Ave. Portland 6, Ore.	PORTLAND (7)	Henry Sturtevant 8211 S.W. Westgard Ave. Portland 19, Ore.
L. J. Giacoletto RCA Laboratories Princeton, N. J.	PRINCETON (3)	W. H. Surber School of Engineering Princeton University Princeton, N. J.
J. A. Rodgers Huntington Hills Rochester, N. Y.	ROCHESTER (4)	J. C. O'Brien 283 Malden St. Rochester 13, N. Y.

* Numerals in parentheses following Section designate Region number.

Sections

	Chairman	Secretary
Sacramento (7)	N. D. Webster 515 Blackwood N. Sacramento, Calif.	J. R. Miller 3991 3rd Ave. Sacramento, Calif.
St. Louis (5)	L. A. Mollman Union Electric Co. 12 and Locust Sts. St. Louis 1, Mo.	H. G. Wise 1705 N. 48 St. E. St. Louis, Ill.
Salt Lake (7)	C. R. Evans Radio Station KSL Salt Lake City, Utah	E. C. Madsen Dept. of Elec. Eng. University of Utah Salt Lake City, Utah
San Antonio (6)	F. E. Brooks 143 Eng. Bldg. University of Texas Austin, Texas	A. H. La Grone Box F University Sta. Austin 12, Texas
San Diego (7)	E. W. Thatcher 2661 Poinsettia Dr. San Diego 6, Calif.	J. P. Day 3565 Ingraham St. San Diego 9, Calif.
San Francisco (7)	W. R. Hewlett 395 Page Mill Rd. Palo Alto, Calif.	J. R. Whinnery Elec. Engr. Dept University of Calif. Berkeley, Calif.
Seattle (7)	S. D. Bennett 3437-36 Ave W. Seattle 99, Wash.	J. E. Mason 2318 Tenth St. Bremerton, Wash.
Schenectady	H. L. Thorson General Elec. Co. Bldg. 269 Schenectady, N. Y.	J. D. Cobine General Elec. Res. Lab. The Knolls Schenectady, N. Y.
Syracuse (4)	L. R. Fink 416 Cherry Rd. Syracuse 9, N. Y.	Samuel Seely Dept. of Applied Science Syracuse University Syracuse, N. Y.
Toledo (4	M. W. Keck 2231 Oak Grove Pl. Toledo, Ohio	E. V. Birk 723 Ledge Ave. Toledo, Ohio
Toronto, Ontario (8)	C. Graydon Lloyd Canadian General Electr c Co., Ltd. 212 King St., W. Toronto, Ont., Canada	Walter Ward Canadian General Electric Co., Ltd. 212 King St., W. Toronto, Ont., Canada
Twin Cities (5)	W. G. Pree 2500 W. 66 St. Minneapolis, Minn	O. A. Schott 4224 Elmer Ave. Minneapolis 16, Minn.
Washington (3)	H. W. Wells Carnegie Inst. of Wash. 5241 Broad Branch Rd. N.W. Washington, D. C.	Mark Swanson 8704 Maywood Ave. Silver Spring, Md.
Williamsport (4)	Richard Blythe Dept. of Physics Bucknell Univ. Lewisburg, Pa.	R. C. Walker Box 414, Bucknell Univ. Lewisburg, Pa.

SUBSECTIONS

	Chairman	Secretary
Amarillo-Lubbock (6) (Dallas-Ft. Worth Subsection)	C. E. Houston Dept. of Elec. Engr. Texas Tech. College Lubbock, Texas	R. F. Lee 2704-31 St. Lubbock, Texas
Centre County (4) (Emporium Subsection)	F. T. Hall Dept. of Elec. Engr. Pennsylvania St. College State College, Pa.	J. H. Slaton Dept. of Eng. Research Pennsylvania St. College State College, Pa
Hamilton (8) (Toronto Subsection)	A. H. Sievert Canadian Westinghouse Co. Hamilton, Ont., Canada	J. H. Pickett Aerovox Canada Ltd. 1551 Barten St. E Hamilton, Ont., Canada
Lancaster (3) (Philadelphia Subsection)	R. B. Ayer RCA Victor Division New Holland Pike Lancaster, Pa.	J. L. Quinn RCA Victor Division New Holland Pike Lancaster, Pa.
Long Island (2) (New York Subsection)	O. M. Dunning Hazeltine Elec. Corp. 5825 Little Neck Pkwy. Little Neck, L. I., N. Y.	David Dettinger Wheeler Labs. 259–09 Northern Blvd. Great Neck, L. I., N. Y.
Monmouth (2) (New York Subsection)	A. C. Beck Bell Telephone Labs. Holmdel, N. J.	W. M. Goodall Bell Telephone Labs. Whalepond Rd. Deal, N. J.
Northern N. J. (2) (New York Subsection)	A. W. Parkes, Jr. Aircraft Radio Corp. Boonton, N. J.	A. G. Richardson 180 Vreeland Ave. Boonton, N. J.
South Bend (5) (Chicago Subsection)	George Weiler 1429 E. Monroe South Bend, Ind.	A. R. O'Neil Radio Sta. WSBT 1525 N. Adams South Bend 16, Ind.
Urbana (5) (Chicago Subsection)	R. M. Wainwright Elec. Eng. Department University of Illinois Urbana, Ill.	M. H. Crothers Elec. Eng. Department University of Illinois Urbana, Ill.
Winnipeg (8) (Toronto Subsection)	R. D. Cahoon C.B.C. Winnipeg, Man., Canada	J. R. B. Brown Suite 2 642 St. Marys Rd. Winnipeg, Man., Canada

Professional Groups

	Chairman
Antennas and Propagation	Newbern Smith National Bureau of Standards Washington 25, D. C.
Audio	Leo L. Beranek Massachusetts Institute of Technology Cambridge 39, Mass.
Broadcast and Television Receivers	Virgil M. Graham Sylvania Electric Products Inc. 40-22 Lawrence St. Flushing, L. I., N. Y.
Broadcast Transmission Systems	Lewis Winner Bryan Davis Publishing Co., Inc. 52 Vanderbilt Ave. New York 17, N. Y.
Circuit Theory	J. G. Brainerd University of Pennsylvania Philadelphia, Pa.
Instrumentation	Ernst Weber Polytechnic Institute of Brooklyn Brooklyn, N. Y.
Nuclear Science	Harner Selvidge Bendix Aviation Corporation Fisher Building Detroit 2, Mich.
Quality Control	R. F. Rollman Allen B. DuMont Laboratories 1000 Main Ave. Clifton, N. J.
Vehicular and Railroad Radio Communications	A. B. Buchanan 2000 Second Ave. Detroit 26, Mich.

Abstracts and References

Prepared by the National Physical Laboratory, Teddington, England, Published by Arrangement with the Department of Scientific and Industrial Research, England, and *Wireless Engineer*, London, England

NOTE: The Institute of Radio Engineers does not have available copies of the publications mentioned in these pages, nor does it have reprints of the articles abstracted. Correspondence regarding these articles and requests for their procurement should be addressed to the individual publications, and not to the IRE.

Acoustics and Audio Frequencies 835
Antennas and Transmission Lines 836
Circuits and Circuit Elements 836
General Physics 839
Geophysical and Extraterrestrial Phenomena 840
Location and Aids to Navigation 840
Materials and Subsidiary Techniques ... 840
Mathematics 841
Measurements and Test Gear 842
Other Applications of Radio and Electronics 843
Propagation of Waves 843
Reception 845
Stations and Communication Systems ... 845
Subsidiary Apparatus 846
Television and Phototelegraphy 847
Transmission 847
Vacuum Tubes and Thermionics 847
Miscellaneous 848

The number in heavy type at the upper left of each Abstract is its Universal Decimal Classification number and is not to be confused with the Decimal Classification used by the United States National Bureau of Standards. The number in heavy type at the top right is the serial number of the Abstract. DC numbers marked with a dagger (†) must be regarded as provisional.

The Annual Index to these Abstracts and References, covering those published in the PROC. I.R.E. from February, 1949, through January, 1950, may be obtained for 2s.8d. postage included from the *Wireless Engineer*, Dorset House, Stamford St., London S. E., England. This index includes a list of the journals abstracted together with the addresses of their publishers.

ACOUSTICS AND AUDIO FREQUENCIES

534+621.395.62 **1319**

1950 IRE National Convention Program—(PROC. I.R.E., vol. 38, pp. 192–211; February, 1950.) Summaries are given of the following papers:

14. Representations of Speech Sounds and Some of their Statistical Properties—Sze-Hou Chang, G. E. Pihl, and M. W. Essigmann.
127. Sound-System Design for Reverberant Auditoriums—L. L. Beranek, W. H. Radford, and J. B. Wiesner.
128. High-Efficiency Loudspeakers for Personal Radio Receivers—H. F. Olson, J. C. Bleazey, J. Preston, and R. A. Hackley.
129. A Review of Direct Radiator Loudspeakers—F. H. Slaymaker.
130. Loudspeaker Housings—W. F. Meeker.
131. A Miniature Condenser-Type Microphone—J. K. Hilliard.
148. Noise Considerations in Audio Systems—F. L. Hopper.
149. Considerations of Noise in Sound Recording and Reproducing Systems—A. W. Friend.
150. Magnetic Recording Frequency Response—Measurement Procedures and Pitfalls—R. E. Zenner.
151. Distortions in Recording Systems—H. E. Roys.
152. Perceptibility of Flutter in Recorded Speech and Music—H. Schecter.

534.231 **1320**

On the Energy Flux in the Fields of Spherical Sound Radiators—S. N. Rzhevkin. (*Zh. Tekh. Fiz.*, vol. 19, pp. 1380–1396; December, 1949. In Russian.) Using Bessel and Neumann spherical functions, a generalized expression is derived determining the sound field of a complex spherical radiator. A relation is established between the Stokes-Rayleigh functions $f(jkr)$ and $F(jkr)$ normally used and the more convenient new functions $G(kr)$, $D(kr)$, $\epsilon(kr)$, and $\delta(kr)$. Tangential energy fluxes are absent in the fields of simple radiators but are always present in the fields of complex radiators. As an example, the radiator with two modes of oscillation is discussed in detail. Zonal and sectoral radiators are also considered.

534.231:534.26 **1321**

On the Freely Vibrating Circular Disk and the Diffraction by Circular Disks and Apertures—C. J. Bouwkamp. (*Physica's Grav.*, vol. 16, pp. 1–16; January, 1950. In English.) A theory is developed for the acoustic field produced by a freely vibrating rigid disk when the wavelength is large compared with the radius a of the disk. By analysis based on integral equations, an expression for the field is derived in the form of a series of ascending powers of ka, where k is the wave number. The results are equally applicable to the diffraction of plane scalar waves incident normally upon a circular disk or aperture.

534.232+534.39 **1322**

Powerful Acoustic Waves—P. Alexander. (*Research* (London), vol. 3, pp. 68–73; February, 1950.) Discussion of various methods of producing high-power ultrasonic oscillations, and of the chemical and physical effects produced by such oscillations in solids and liquids. The many diverse phenomena occasioned by ultrasonic irradiation are ascribed either to cavitation or to the enormous acceleration of particles in the sound field.

534.321.9 **1323**

Ultrasonic Vibrations—E. Skudrzyk. (*Elektrotech. u. Maschinenb.*, vol. 67, pp. 76–84; March, 1950.) Discussion of the production and effects of ultrasonic vibrations in gases, liquids, and solids, the conditions being fundamentally different in the three cases.

534.321.9:534.373 **1324**

Ultrasonic Reverberation Measurements in Liquids: Part 2—C. E. Mulders. (*Appl. Sci. Res.*, vol. B1, pp. 341–357; 1950.) Measurements of the absorption of ultrasonic waves in various solutions suggest that the high absorption in sea water may be due to perturbation of the reaction $MgSO_4 \rightleftarrows Mg + SO_4$ and is not associated with NaCl, as has been suggested by Liebermann (613 of 1949). Part 1: 932 of 1949.

534.6:621.395.632.11 **1325**

Acoustical Study of Telephone Bells of the French P.T.T. Administration—(*Ann. Télécommun.*, vol. 5, pp. 21–28; January, 1950.) Description of the apparatus and methods used to study telephone ringing, with a view to establishing new standards for intensity and spectral composition of the sound emitted.

534.62 **1326**

Room for Acoustic Tests of Loudspeakers and Microphones—M. Milosevic. (*Rev. Tech. Comp.* (Franç), no. 13, pp. 33–42; February, 1950.) The room is constructed according to principles discussed in 2699 of 1949. Over-all dimensions are: length 5.5 m, width 2.7 m, height 3 m. The test chamber, about 3 m long, is paraboloidal at the end which houses the loudspeaker and opens out to cylindrical shape. The walls of the chamber are thickly lined with glass wool. Test results are shown in many diagrams. Measurements in the test chamber on loudspeakers and microphones give results in good agreement with free-field measurements.

534.771 **1327**

The Development of Hearing-Test Methods—W. Beindorf. (*Funk. und Ton.*, vol. 4, pp. 76–84; February, 1950.)

534.78:621.395.822:629.13 **1328**

Telephony and the Problem of Noise in Aircraft—P. Chavasse and R. Lehmann. (*Ann. Télécommun.*, vol. 3, pp. 45–56; February, 1948.) Discussion of the noise level and noise spectra in different types of aircraft and their combined effect in masking speech sounds.

534.782 **1329**

The Reproduction of Natural Speech Sounds—H. Koschel. (*Fernmeldetech. Z.*, vol. 3, pp. 48–53; February, 1950.) A review of methods of producing artificial speech sounds for technical purposes.

534.782.07 **1330**

The Phonetic Steno-Sonograph—J. Dreyfus-Graf. (*Tech. Mitt. Schweiz. Telegr.-Teleph. Verw.*, vol. 28, pp. 89–95; March 1, 1950. In French, with German summary.) Electroacoustic apparatus which records the spoken word in written characters, examples of which are shown.

534.84 **1331**

The Intelligibility Ratio as the Criterion of the Acoustic Quality of a Hall—A. Moles. (*Ann. Télécommun.*, vol. 5, pp. 57–64; February, 1950.) Reverberation time and sound distribution are insufficient to determine precisely the acoustic quality of a hall. A better criterion is provided by measurements of the intelligibility of articulated sounds at different points in the hall. Based on an analysis of the occurrence of different sounds in speech, two lists are compiled of 100 French logatoms, each

consisting of two consonants and a vowel, suitable for use in such measurements.

534.862.4 1332
Direct Methods of Frequency Linearization of the Output from the Reproducing-Head Circuit—F. Grammelsdorff and W. Gulckenburg. (*Funk. und Ton.*, vol. 4, pp. 66–75; February, 1950.) The effects of introducing resistance, capacitance, and inductance in the reproducing-head circuit on the shape of the response curve are examined and shown in diagrams. With a suitable combination the output voltage can be kept nearly constant at about 3 mv from 40 cps to 50 kc. With better design of the equipment, the output voltage can be raised to about 10 mv. Any further increase depends on improvement of the magnetic properties of the tape used.

621.3.012:621.317.089 1333
A Modern Electroacoustic Frequency-Response Recording Unit—Lehner. (*See* 1449.)

621.395.625.2 1334
Disc-Recording Standards—B. E. G. Mittell. (*Proc. I.R.E.* (Australia), vol. 11, pp. 5–14; January, 1950.) 1948 Australian I.R.E. Convention paper reviewing the development of standards for commercial disk recording. Present standards and methods of testing used in the laboratories of Electric and Musical Industries Ltd., Hayes, Middlesex, are discussed. A comprehensive table is given of current practice and recommended standards. See also 1243 of 1948.

621.395.92 1335
Crystal Earpieces for Portable Hearing-Aids—W. Güttner. (*Z. Angew. Phys.*, vol. 2, pp. 33–39; January, 1950.) The construction is described of an earpiece in which a double crystal plate of Rochelle salt is coupled to a Helmholtz resonator. From the equivalent electrical circuit the sound pressure produced in the earpiece may be simply calculated. The characteristics of two such earpieces are plotted. The range of coupling, tuning, and damping of the crystal and resonator combination is relatively narrow for linearity of the response curve.

621.396.645.37:621.395.623.7:621.3.018.8 1336
Ouput Impedance Control—D. W. Thomasson. (*Wireless World*, vol. 56, pp. 116–117; March, 1950.) Comment on 1070 of June (Roddam).

621.396.645.37:621.395.623.7:621.3.018.8 1337
Output Impedance Control—T. Roddam, P. J. Baxandall, H. Pursey, E. Jeffery, and H. J. Pichal. (*Wireless World*, vol. 56, pp. 155–157; April, 1950.) Author's reply to 1336 above, and further comment on 1070 of June.

ANTENNAS AND TRANSMISSION LINES

621.392.26†+621.396.67 1338
1950 IRE National Convention Program—(Proc. I.R.E., vol. 38, pp. 192–211; February, 1950.) Summaries are given of the following papers:

32. Waveguide Applications of Artificial Metallic Dielectrics—W. E. Kock.
33. The Effects of Anisotropy in a Three Dimensional Array of Conducting Disks—G. Estrin.
34. A Study of Single-Surface Corrugated Guides—W. Rotman.
35. A Study of the Current Distribution on the Helix—J. A. Marsh.
36. Diffracted Beams in Metal Lenses—A. E. Heins.
57. On the Relation between the Geometry and the Impedance Characteristics of Typical Radiating Systems—T. H. Crowley and V. H. Rumsey.
58. A Method for Studying the Response of Loops to the Electromagnetic Field—B. C. Dunn, Jr.
59. Measurement of the Radiation Efficiency of Elliptically and Linearly Polarized Antennas—J. Rowen.
60. Broad-Band Unidirectional Antenna 50 to 170 Mc—V. J. Colaguori and R. Guenther.
61. Antenna System for Very High-Frequency Radio Ranges and Direction Finding—F. J. Lundburg and F. X. Bucher.
73. Radiation from Circular Current Sheets—W. R. LePage, C. S. Roys, and S. Seely.
74. Radiation Patterns of Circular and Cylindrical Arrays—J. E. Walsh.
75. Properties of Guided Waves on Inhomogeneous Cylindrical Structures—R. Adler.
79. A Supergain UHF Television Transmitting Antenna—O. O. Fiet.
122. Surface-Wave-Transmission Lines—G. Goubau.
123. Frequency-Modulation Distortion in Linear Systems having Small Sinusoidal Irregularities in Transfer Characteristics, with Application to Lossless Waveguides—F. Assadourian.
124. The Representation, Measurement, and Calculation of Equivalent Circuits for Slots in Rectangular Waveguide—J. Blass, L. Felsen, H. Kurss, N. Marcuvitz, and A. A. Oliner.
125. Dielectric Tube Antennas—R. E. Beam and D. G. Harman.
126. Measurement of Current and Charge Distributions on Antennas and Open-Wire Lines—D. J. Angelakos.

621.392.43 1339
Two-Band Antenna-Matching Networks—J. G. Marshall. (*QST*, vol. 34, pp. 36–39, 90; February, 1950.) Continuation of 34 of February. To demonstrate the use of the design formulas previously given, numerical examples are calculated for a simple antenna operating on its fundamental and second-harmonic frequencies, using different types of transmission line.

621.396.67:621.315.625.015 1340
Investigation of the Voltages on Insulators in the Guy Wires of Tower Aerials—A. A. Metrikin. (*Radiotekhnika* (Moscow), vol. 4, pp. 59–62; November and December, 1949. In Russian.)

621.396.671 1341
The Transmission and Reception of Elliptically Polarized Waves—G. Sinclair. (Proc. I.R.E., vol. 38, pp. 148–151; February, 1950.) A vector parameter is defined which represents a generalization of the effective length of an antenna to include a specification of the polarization of the field radiated by the antenna. The parameter so defined is also useful in calculating the voltage at the terminals of the antenna when it is used to receive plane waves of arbitrary (elliptical) polarization.

621.396.677 1342
Triplet Reflector Array—R. W. Hogg. (*Wireless Eng.*, vol. 27, pp. 47–53; February, 1950.) The basic system described consists of a horizontal dipole with a reflector system in which the usual single parasitic element is replaced by three elements spaced vertically $\lambda/8$ apart; arrays of one and two such units are considered. From theoretical considerations this design was expected to give not only an improved back-to-front ratio, but also, due to its decreased sensitivity to frequency variation, a bandwidth over twice that for the single reflector system. The improvement observed in practice fell short of that predicted theoretically, the bandwidth for a wavelength of 6 m increasing from 2 Mc for a 2-stack single reflector array to 3 Mc for the corresponding triplet array.

621.396.677 134
Calculations for [parabolic] Reflectors—F. Brendel. (*Funk. und Ton.*, vol. 4, pp. 93–9 February, 1950.) A general formula is derive for the gain of a parabolic reflector, and th direct radiation and the reaction of the reflecto on the transmitting dipole are discussed. Th field distribution is calculated for paraboli and cylindro-parabolic reflectors of variou apertures and the resulting curves are compare with Köhler's results for sheet-metal and gri type reflectors (1932 Abstracts, p. 525). Th radiation characteristics are determined for parabolic reflector without assuming a uniform intensity distribution over the surface of th reflector.

621.396.677 134
An Experimental Verification of the Theor of Parallel-Plate Media—C. A. Cochran (*Proc. IEE* (London), Part III, vol. 97, p 72–76; March, 1950.) The transmission coeff cient and deviation for various angles of inc dence of a plane wave on a parallel-plat prism were measured. The results obtaine are compared with values calculated from a idealized theory in which plate thickness an resistivity are neglected and an infinite numbe of plates is assumed. This theory explain qualitatively the action of the prism, but th plate thickness must be taken into accoun to obtain quantitative agreement with ex perimental results.

621.396.677 134
Wide-Angle Metal-Plate Optics—J. Ruz (Proc. I.R.E., vol. 38, pp. 53–59; January 1950.) 1949 IRE National Convention pape A description of microwave metal-plate lens of the "constrained" type, in which focusin takes place normal to the electric vector. The are shown to have exceptional wide-ang scanning properties. General design formula and expressions for phase aberration and th effect of refocusing are derived. Particula designs are investigated and their properti tabulated, together with a graph giving max mum scanning angle as a function of ban width for each type. A wide-angle 2-mediu lens is also discussed.

621.396.67 13
The A.R.R.L. Antenna Book [Book Revie —Publishers: American Radio Relay Leagu West Hartford, Conn., 1949, 265 pp., $1.0 (Proc. I.R.E., vol. 38, p. 191; Februar 1950.) "Amateurs, experimenters, and pra tical radio men will find this book replete wi useful information on antennas intended chief for amateur applications. The book is thoroughly revised version of the previo edition."

CIRCUITS AND CIRCUIT ELEMENTS

621.3.07:621.396.645.37 13
Control, Positive and Negative Feedba and Negative Resistance Coordinated—W Reichardt. (*Elektrotechnik* (Berlin), vol. pp. 47–53 and 73–80; February and Marc 1950.) A "control theory" is developed a different applications of feedback are co sidered as special cases of the basic contr circuit.

621.314.3† 13
The Magnetic Amplifier—N. R. Castelli (Proc. I.R.E., vol. 38, pp. 151–158; Februar 1950.) "The 'small-signal' theory of the ma netic amplifier is developed under certa simplifying assumptions. Expressions for t amplification are derived in terms of electric and magnetic quantities, and conditions f

optimum amplification are obtained. The predictions of the theory are found to agree qualitatively with experimental results of other workers."

621.316.729 1349
Synchronization of Quasi-Sinusoidal Oscillators—G. Francini. (*Alta Frequenza*, vol. 18, pp. 125–133; June–August, 1949. In Italian, with English, French, and German summaries.) The equation representing the behavior of the fundamental types of oscillator is examined by considering the effect of injecting an external voltage or current. By limiting the study to the steady state, and by the use of a simplifying hypothesis, the performance of the oscillator can be determined and, in particular, the limits within which the frequency and amplitude of the applied signal must lie for synchronization to be effected. Various possible circuits for the injection of the synchronizing signal are considered.

621.316.86 1350
The Application of Thermistors to Control Networks—J. H. Bollman and J. G. Kreer. (Proc. I.R.E., vol. 38, pp. 20–26; January, 1950.) Equations are developed for the relations between current, voltage, resistance, and power in thermistors under steady-state conditions. Voltage/current characteristics are illustrated for directly heated thermistors in series or parallel with external resistance. Their behavior for zero incremental circuit resistance is studied. The complete differential equation for the time variation of resistance of a directly heated thermistor is obtained in a form which can be solved by use of various linear approximations.

621.318.4:621.396.615.17 1351
Nonlinear Coil Generators of Short Pulses—L. W. Hussey. (Proc. I.R.E., vol. 38, pp. 40–44; January, 1950.) The construction is described of small permalloy coils for the production of pulses of duration <0.1 μs at repetition rates up to a few megacycles per sec. Circuits suitable for various frequency ranges are discussed.

621.318.423.013.78:621.3.017.22 1352
The Eddy-Current and Screen Losses of a Screened Single-Layer Solenoid—F. M. Phillips. (*Proc. IEE* (London), Part III, vol. 97, pp. 77–87; March, 1950.) Butterworth's method for determining the hf resistance of an isolated single-layer solenoid is outlined. A modification is proposed which, however, increases the discrepancy between the theory and experimental measurements. The effect of a concentric screening can is also considered and the losses arising in the can itself are calculated. The calculations are in good agreement with Bogle's empirical formula (821 of 1941). The effect of the screening can on the Q value is determined for a particular coil for which all the losses are calculated.

621.318.572 1353
Speed of Electronic Switching Circuits—E. M. Williams, D. F. Aldrich, and J. B. Woodford. (Proc. I.R.E., vol. 38, pp. 65–69; January, 1950.) "Methods of analysis of electronic switching circuits are described which lead to determination of triggering delay and switching wave forms. These methods are illustrated with particular reference to multivibrators."

621.385.12:621.318.572 1354
The Use of Cold Cathode Relay Valves with Grid-Cathode Circuits of High Resistance—R. J. Hercock and D. M. Neale. (*Brit. Jour. Appl. Phys.*, vol. 1, pp. 53–55; February, 1950.) The grid current drawn by a cold-cathode relay tube near the critical grid potential normally precludes the use of a tube of this type where the grid circuit contains a high series resistance. By superimposing a train of voltage pulses on the applied grid potential this limitation may be removed. The instantaneous grid current may then be high while the mean value is much less. The value of the limiting resistance in the grid circuit may then be increased a hundredfold or more. In many cases the pulses may conveniently be derived from the rectifier ripple. Practical applications of the principle are described.

621.39 1355
1950 IRE National Convention Program—(Proc. I.R.E., vol. 38, pp. 192–211; February, 1950.) Summaries are given of the following papers:

9. Transistor Trigger Circuits—H. J. Reich and P. M. Schulteiss.
12. Mathematical Theory and Applications of Silicon Crystals for Mixing and Harmonic Generation at Microwave Frequencies—P. D. Strum, J. W. Kearney, and J. C. Greene.
28. A Comparison of Frequency and Time Domain Viewpoints in Circuit Design—W. H. Huggins.
29. Study of Transient Effects by a New Method of Integral Approximation—M. V. Cerrillo.
30. Applications of the Integral Approximation Method of Transient Evaluation—W. H. Kautz.
52. Frequency Analysis of Variable Networks—L. A. Zadeh.
53. Distortion Bandpass Considerations in Angular Modulation Systems—A. A. Gerlach.
54. Concerning the Lowest Possible Unloaded Resonant Circuit Q's which can be used in Multiple Resonant Circuit Filters—M. Dishal.
55. Tunable Microwave Waveguide Filters—W. Sichak and H. A. Augenblick.
56. Filters for Television Interference—A. M. Seybold.
70. Modern Methods of Servo Synthesis—R. McCoy and D. Herr.
80. Design of a Hybrid Ring Diplexer for Ultra-High-Frequency Television Use—W. H. Sayer and J. M. De Bell, Jr.
84. The Design of Diode Gate Circuits—R. J. Slutz.
88. Monoformer—A. C. Munster.
93. The Analysis and Design of a Band-Pass Distributed Amplifier—V. C. Rideout and T. P. Tung.
94. An Investigation of the 400-Mc Amplifier Performance of the Type SN-973B Subminiature RF Pentode—N. B. Ritchey.
95. An Extension to Stagger-Tuned Amplifier Design—J. M. Pettit.
96. Ultra-High-Gain Direct-Coupled Amplifier Circuits—W. K. Volkers.
97. Analysis and Design of Self-Saturable Magnetic Amplifiers—S. Cohen.
99. Behavior of Resistors at High Frequencies—G. R. Arthur, H. L. Krauss, P. F. Ordung, and S. E. Church.
100. Inductors, their Calculation and Losses—R. F. Field.
101. Transformer Performance and Measurements—R. Lee.
163. Miniaturization Techniques: A Discussion and Proposal—M. Abramson and S. Danko.
164. The Exponential-Line Pulse Transformer—E. R. Schatz and E. M. Williams.
168. The Transient Behavior of a Class-C Oscillator—C. H. Page.
169. Mode Suppression in Broad-Band Reflex Klystron Oscillators—A. H. Sonnenschein and H. A. Finke.
170. Telemetering Blocking Oscillator—W. Todd.
171. Some Aspects of RF Phase Control in Microwave Oscillators—E. E. David, Jr.
172. Seven-League Oscillator—F. B. Anderson.

621.392 1356
Synthesis of Wideband Two-Phase Networks—H. J. Orchard. (*Wireless Eng.*, vol. 27, pp. 72–81; March, 1950.) "Hitherto networks providing a two-phase supply from a single-phase supply over a wide band of frequencies have been designed empirically. A synthesis technique is now available which gives exact design formulas both for the network components and also for the relations between the design parameters. It is shown that the most general circuit meeting the requirement is essentially a pair of all-pass networks. By utilizing elliptic functions, such networks can be designed to have a Tchebycheff approximation to the ideal requirement: this represents the most efficient condition. Simple computing schemes, design curves, and a numerical example are included."

621.392 1357
Recurrent Network with Inductively Coupled Elements—G. G. Sacerdote. (*Alta Frequenza*, vol. 18, pp. 268–276; December, 1949. In Italian, with English, French, and German summaries.) For certain ranges of frequency the operation of such networks with purely reactive elements is analogous to that of networks consisting of elements not purely reactive.

621.392.011.2 1358
Reciprocity Between Generalized Mutual Impedances for Closed or Open Circuits—A. G. Clavier. (Proc. I.R.E., vol. 38, pp. 69–74; January, 1950.) Equations are developed for the relations between voltages and currents in a pair of open wires of any shape. For sinusoidal voltages, the mutual impedances are reciprocal for closed networks, and also for open wires provided the points of application of voltage and measurement of current are exactly interchanged. Extensions to transient currents and n-coupled circuits are suggested. Applications to quadripoles, linear antennas, and wave projectors are discussed. Limitations of the theory are indicated.

621.392.4.018.12 1359
Realization of a Constant Phase Difference—S. Darlington. (*Bell Sys. Tech. Jour.*, vol. 29, pp. 94–104; January, 1950.) Analysis of the problem of obtaining over a wide frequency range the best approximation to a constant phase difference between the outputs of a pair of constant-resistance phase-shifting networks fed from a common source. The phase variation over a frequency range of ratio ω_1/ω_1 is derived generally for networks of n sections with optimum circuit constants, using Cauer's functions based on a Tchebycheff approximation. The determination of the parameters of the network sections is described.

621.392.41:621.317.729 1360
An Electrolytic Tank for the Measurement of Steady-State Response, Transient Response and Allied Properties of Networks—A. R. Boothroyd, E. C. Cherry, and R. Makar. (*Proc. IEE* (London), Part III, vol. 97, pp. 126–128; March, 1950.) Long summary of 2743 of 1949.

621.392.43 1361
Theoretical Limitations on the Broadband Matching of Arbitrary Impedances—R. M. Fano. (*Jour. Frank. Inst.*, vol. 249, pp. 139–154; February, 1950.) Conclusion of 1094 of June.

621.392.43 1362
Two-Band Antenna-Matching Networks—Marshall. (*See* 1339.)

621.392.43:621.396.67 1363
Design Procedures for Pi-Network Antenna Couplers—L. Storch. (PROC. I.R.E., vol. 38, p. 158; February, 1950.) Correction to 571 of April.

621.392.5 1364
Method of Calculating the Response of a Linear System to an Arbitrary Stimulus—M. D. Indjoudjian. (*Ann. Télécommun.*, vol. 3, pp. 34–44; February, 1948.) The concept of admittance of a network is generalized by the introduction of a response factor and methods are indicated for determining the response of a system to an arbitrary stimulus from its response to certain particular stimuli. Comparison is made between Fourier series, the Fourier integral and Laplace integral, indicating their fields of application and explaining the successful results obtained by means of the Laplace transformation, closely related to the fact that the Laplace transforms of voltages and currents follow Ohm's law. The most important formulas connected with the Laplace transformation are listed and the method is applied to determine the response of a linear system to an impulsive, transient, or suddenly applied sinusoidal stimulus, introducing Heaviside developments in series. The particular case of a low-pass filter is considered. The relation between the continuous spectrum of an isolated signal and the line spectrum of a train of recurrent signals is discussed. Other applications of the Laplace transformation to differential and integral equations and to finite-difference equations are explained.

621.392.52 1365
The Analysis of Broad-Band Microwave Ladder Networks—M. C. Pease. (PROC. I.R.E., vol. 38, pp. 180–183; February, 1950.) When line effects are present, analysis of multi-element networks by normal methods is complicated. Pauli spin matrices are applied to structures with 2, 3, 4, or 5 elements, and explicit formulas for the transmission function of quarter-wave coupled filters are derived. Curves for the mid-band $\lambda/4$-spacing case are given; from these the exact voltage SWR of a low-Q filter can be readily calculated.

621.392.52:621.315.212 1366
Spurious Modes in Coaxial-Transmission-Line Filters—D. E. Mode. (PROC. I.R.E., vol. 38, pp. 176–180; February, 1950.) Poor agreement between observed and calculated lower TEM cut-off frequencies is shown to be due to the transmission of higher, or spurious, modes past the shunt rods, or to resonances occurring when the circumference of either coaxial conductor is a multiple of the wavelength. A more exact method for calculating the TEM cut-off frequencies is given.

621.392.52:621.397.82 1367
Eliminating TVI with Low-Pass Filters—G. Grammer. (*QST*, vol. 34, pp. 19–25, 20–25, 104, and 23–30; February–April, 1950.) Part 1 deals with the installation and operation of amateur transmitting equipment to minimize interference with television reception. Part 2 discusses operating characteristics of filters and practical design considerations. Part 3 describes simplified graphical methods for filter design.

621.392.52.029.63 1368
A Coupled 'Coaxial' Transmission-Line Band-Pass Filter—J. J. Karakash and D. E. Mode. (PROC. I.R.E., vol. 38, pp. 48–52; January, 1950.) Design of a microwave filter formed by two parallel conductors within a conducting cylinder. Expressions are derived for cut-off frequencies, attenuation, and impedances, and matching conditions are considered. Experimental results are in fair agreement with theory.

621.392.53:621.397.645 1369
The Design of Complex Correcting Circuits for Television Amplifiers—G. V. Braude, K. V. Epaneshnikov, and B. Ya. Klimushev. (*Radiotekhnika* (Moscow), vol. 4, pp. 24–33; November and December, 1949. In Russian.) The operation of the correcting circuit using inductances in the grid and anode circuits of the tube (Fig. 5) is discussed. Use is made of the method of transient characteristics determining the transmission of a single impulse by the amplifier, and parameters of the circuit are so chosen as to ensure the best compromise between the frequency and phase corrections. The characteristics so obtained are much better than those of a simple circuit (inductance in the anode circuit only) and approach very near the ideal characteristics.

621.395/.396.665:621.3.015.33 1370
Transient Response of a Regulator Chain—H. Jefferson. (*Wireless Eng.*, vol. 27, pp. 83–85; March, 1950.) An expression is derived which characterizes the output of a chain of identical automatic level regulators following a change of input level. A system having n sections has an output response characteristic which crosses the reference-level axis $n-1$ times. The time scale depends only on a constant k, a characteristic of the regulators, but the amplitude is independent of k and depends only on the magnitude of the initial disturbance. Further expressions are derived for the case when k is not the same for all the regulators in the chain, and for the practical case when the integration process is imperfect owing to leakage.

621.396.6 1371
1950 Components Exhibition, Paris—J. Rousseau. (*TSF Pour Tous*, vol. 26, pp. 91–96; March, 1950.) Short review with classification of exhibits, and descriptions and illustrations of tubes, cr tubes, coils, assembled units, and capacitors. Other types of equipment will be considered in subsequent articles. For other accounts see *Radio Prof.* (Paris), vol. 19, pp. 20–29; February, 1950 and *Toute la Radio*, vol. 17, pp. 128–137; March and April, 1950.

621.396.6 1372
The Design of Electronic Equipment using Subminiature Components—M. L. Miller. (PROC. I.R.E., vol. 38, pp. 130–135; February, 1950.) A general survey with particular attention to the heat dissipation of the units and the operating temperatures of the components.

621.396.611.1:536.49 1373
Nomographic Determination of Temperature Compensation for Oscillatory Circuits—H. Geschwinde. (*Funk. und Ton.*, vol. 4, pp. 85–89; February, 1950.) Values of compensating ceramic capacitors are given by a simple abac.

621.396.611.1.015.3:621.3.012 1374
Detuned Resonant Circuits—D. G. Tucker and H. Elger. (*Wireless Eng.*, vol. 27, pp. 64–65; February, 1950.) Comment on 1102 of June (Elger) and Elger's reply.

621.396.611.21 1375
Crystal-Controlled Oscillators—C. V. Chambers. (*QST*, vol. 34, pp. 28–33; March, 1950.) An investigation to determine optimum operating conditions using the new small type of crystal in three popular oscillator circuits: (a) grid-anode circuit, (b) triode-tetrode circuit, and (c) modified Pierce circuit. Tubes used were Types 6AG7, 6F6, 6V6GT, and 6L6. Circuits are shown and performance curves are analyzed. The 6AG7 was found the best tube from every standpoint. The triode-tetrode circuit gives the highest output and the modified Pierce circuit the lowest crystal current. Screen-voltage regulation is recommended for good keying.

621.396.611.3:621.365.5 1376
Output Coupling of Valve Generators for Industrial Heating Purposes—M. Krüger. (*Arch. Elektrotech.*, vol. 39, pp. 619–632; 1950.) A systematic study of various methods of coupling to the load circuit, particularly transformer coupling, for which graphical design methods are given.

621.396.611.4 1377
On Avoiding Low Frequencies in a Rectangular Cavity Resonator used as Part of a Triode Generator—K. F. Niessen. (*Appl. Sci. Res.*, vol. B1, pp. 325–340; 1950.) Reprint. See 1330 of 1949.

621.396.615 1378
Phase-Shift Oscillator—W. R. Hinton and W. P. N. Court. (*Wireless Eng.*, vol. 27, pp. 65–66; February, 1950.) Comments on 324 of March (Vaughan).

621.396.615 1379
On the Design of RC Oscillators—V. G. Kriksunov. (*Radiotekhnika* (Moscow), vol. 4, pp. 49–58; November and December, 1949. In Russian.) Several variants of the RC oscillator are examined critically and the advantages of the type in which the feedback voltage from the load resistance is applied to the phase-shift circuit through a cathode follower (Fig. 2) are pointed out. The operation of this type of oscillator is discussed in detail and separate design formulas are derived for the cases when the phase-shift circuit consists of three and four links respectively. Formulas are also derived for determining the frequency stability and amplitude of steady-state oscillations. A diagram is given of the oscillator with which the theoretical conclusions were verified.

621.396.615 1380
Investigations of a Transitron Relaxation Oscillator—V. V. Migulin and T. N. Yastrebtsova. (*Elektrotechnik* (Berlin), vol. 4, pp. 42–45; February, 1950.) German account of 3054 of 1948.

621.396.615.12:621.365.5 1381
High-Power, High-Frequency Oscillators for Industrial Uses—C. Beurtheret. (*Rev. Tech. Comp.* (Franç), no. 13, pp. 5–16; February, 1950.) Two design principles have been adopted for simplifying industrial heating apparatus. These are: (a) the intermittent operation of tubes with high thermal inertia, permitting a tenfold increase of the normal maximum anode dissipation; and (b) the coupling of thyratron or other rectifiers direct to hv polyphase mains. Illustrations of a 12-120-kw and a 50-500-kw generator incorporating these principles are shown.

621.396.619.23 1382
Non-Linear Effects in Rectifier Modulators—D. G. Tucker and E. Jeynes. (*Wireless Eng.*, vol. 27, p. 66; February, 1950.) Comment on 2184 of 1949 (Belevitch).

621.396.615.17 1383
High-Power Sawtooth Current Synthesis from Square Waves—H. E. Kallmann. (PROC. I.R.E., vol. 38, pp. 60–64; January, 1950.) 1949 IRE National Convention paper. A high-power sawtooth oscillation may be obtained by adding a series of square waves whose amplitudes and periods decrease as $1/2^n$. For n square waves, the first (2^n-1) harmonics of the true and synthesized sawtooth waves are identical, and a basic circuit using push-pull connections for addition of four square waves is illustrated. The requirements of filters for smoothing the step-ripple of the output are discussed. The efficiency of the basic circuit is <50 per cent,

but by a gating system which permits only addition of the current in the 'push' and 'pull' tubes, this can be raised to nearly 100 per cent.

621.396.615.17:621.315.612.4 1384

Aperiodic Frequency-Doubling by Means of 'Pluri-Terminal' Titanate Capacitors—A. A. Pascucci and H. W. Stawski. (*Nature* (London), vol. 165, p. 441; March 18, 1950.) The dependence of the permittivity of titanate ceramic dielectrics upon applied field strength holds both for crossed and for parallel superimposed fields. In measurements demonstrating this effect, application of a sufficiently high ac voltage to one pair of opposite faces of a parallelepiped of the material, and a polarizing voltage to the orthogonal pair, produced a frequency-doubled output, the fundamental frequency being almost completely suppressed. See also 1612 of 1949 (no. 53: Pascucci).

621.396.645 1385

New High-Efficiency Methods of Amplifying Modulated Oscillations—N. V. Trunova. (*Radiotekhnika* (Moscow), vol. 4, pp. 63–73; November and December, 1949. In Russian.) A modified Doherty modulation circuit is proposed in which two modulated channels with a single impedance inverter are provided (Fig. 2). This method is compared with the one used in the Dutch (Nozema) 125-kw transmitter in which four modulated channels with three impedance inverters are used (Fig. 5). The operation of both systems is discussed and the design of the grid circuit is considered in detail. The Nozema system is expensive and gives only a slight increase (from 3 to 6 per cent) in the efficiency. The single inverter system on the other hand ensures a sufficiently high efficiency (approximately 60 per cent) and a low level of nonlinear distortion.

621.396.645 1386

Graphical and Analytical Study of Cathode Follower Problems—S. Malatesta. (*Alta Frequenza*, vol. 18, pp. 134–147; June–August, 1949. In Italian, with English, French, and German summaries.) Considering anode current as a function of the grid/anode voltage rather than of the grid/cathode voltage, a family of characteristic curves and a set of differential parameters are derived; by means of these, cathode-follower problems can be solved by the conventional methods used for amplifiers.

621.396.645 1387

A New Phase-Inverter Stage for a Push-Pull Amplifier—J. Lignon. (*TSF Pour Tous*, vol. 26, pp. 102–105; March, 1950.) Description of a circuit using a double-triode for feeding an aperiodic amplifier. Chief advantages of such a stage are: (a) the voltage gain of about 30 dispenses with the need for a driver stage in an lf power amplifier; and (b) the phase relation of the two output voltages remains constant from zero up to several megacycles per sec., so that phase distortion is eliminated.

621.396.645 1388

RC-Coupled Power Stage—M. G. Scroggie. (*Wireless Eng.*, vol. 27, pp. 81–82; March, 1950.) Conditions are derived for maximum output.

621.396.645:534.85 1389

Phonograph Reproduction: Part 2—C. G. McProud. (*Audio Eng.*, vol. 34, pp. 20–22; March, 1950.) Continuation of 1117 of June, giving full details of the preamplifier and equalizer circuits, with a complete list of components, for a control unit to be used with the Musician's Amplifier (70 of February).

621.396.645.37 1390

Combining Positive and Negative Feedback—J. M. Miller, Jr. (*Electronics*, vol. 23, pp. 106–109; March, 1950.) Description, with full circuit details, of a 2-stage af amplifier using a combination of local positive feedback in the first stage and a moderate amount of over-all negative feedback. Results of distortion measurements for many different combinations of operating conditions are tabulated and shown graphically. Characteristics approaching those of more complex amplifiers with a greater degree of negative feedback can be obtained.

621.396.822:621.316.8 1391

The Linear Theory of Fluctuations Arising from Diffusional Mechanisms—An Attempt at a Theory of Contact Noise—J. M. Richardson. (*Bell Sys. Tech. Jour.*, vol. 29, pp. 117–141; January, 1950.) A general analysis of the power spectral density $S(\omega)$ of the fluctuations of the resistance of a contact which are linearly determined by thermally-excited concentration fluctuations in a diffusing medium. Special physical models are considered and the theoretical spectra derived are compared with Christensen and Pearson's experimental results: $S(\omega) = KV^{a-2}\overline{R}^{b+2}\omega^{-1}$, where V is the applied dc voltage, $\overline{R}$ the average value of the contact resistance and $a \approx 1.85$, $b \approx 1.26$. A system involving the contact between relatively large areas of rough surfaces covered with diffusing surface layers should have $S(\omega) \propto \omega^{-1}$ and a reasonable dependence of $S(\omega)$ on $\overline{R}$. A refinement of the theory removes the divergence at $\omega = 0$ of the integral of $S(\omega)$. The analysis is intended to elucidate the mechanism of voltage fluctuations in granular resistors, thin films, rectifying crystals, and transistors when a dc voltage is applied.

GENERAL PHYSICS

53 1392

1950 IRE National Convention Program—(Proc. I.R.E., vol. 38, pp. 192–211; February, 1950.) Summaries are given of the following papers:

5. News of the Nucleus—U. Liddel.
76. Scattering of Plane Electromagnetic Waves by a Perfectly Conducting Hemisphere or Hemispherical Shell—E. Kennaugh.
77. Diffraction by a Prolate Spheroid—F. V. Schultz.

531.8:621.396.619 1393

From Linear to Nonlinear Mechanics—J. Loeb. (*Ann Télécommun.*, vol. 5, pp. 65–71; February, 1950.) By analogy with the linear transformation of a telecommunication signal by a nonlinear system, the modulator, a similar process can be used to linearize nonlinear electromechanical or mechanical systems such as relays, radiogoniometers, etc. A 'sweep function' in this case serves the same purpose as the radio carrier wave.

534.2+538.566 1394

Field Due to a Point Radiator in a Medium of Non-Homogeneous Layers—L. M. Brekhovskikh. (*Bull. Acad. Sci.* (URSS), vol. 13, pp. 505–545; September and October, 1949. In Russian.) In previous papers the author investigated the propagation of sound and em waves in layers with plane parallel boundaries. In the present paper the more general case is considered of a layer, the upper and lower boundaries of which are not sharply defined. A new method is proposed for determining the field due to a point radiator. In this method the radiated spherical wave is resolved into a number of plane waves and the propagation of each of these is examined separately. Equations determining the propagation of the waves are derived and their solutions found in the form of integrals. These integrals are discussed in detail and it is shown that the results obtained can be presented in a form suitable for calculation. Different combinations of waves become predominant at different distances from the radiator. The dependence of the sound pressure or intensity of the em field on distance from the radiator is determined. Illustrative examples are given.

537.291+538.691]621.385.029.63/.64 1395

Electron Beams in Axially Symmetrical Electric and Magnetic Fields—C. C. Wang. (Proc. I.R.E., vol. 38, pp. 135–147; February, 1950.) Equations are obtained for the trajectories of electrons along the outer edges of beams for the general case in which both axial and radial fields are present. The effects of the combined fields can be expressed as a single generalized potential function depending only on the axial and radial space coordinates, thus permitting the force components to be expressed as components of the gradient of the potential function. Numerical solutions are obtained and normalized curves are given for practical cases. An equilibrium radius exists for which the net radial forces acting on the electron are zero and the outer radius of the beam oscillates about this value, the amplitude being nonsymmetrical and the distance between successive maxima depending on the amplitude.

538.322 1396

Attraction between Two Parallel Currents of Unlimited Length—A. Liénard. (*Jour. Phys. Radium*, vol. 11, pp. 1–6; January, 1950.) The degree of approximation of known formulas for the force of attraction is determined by combining Kelvin's inversion method and the Schwartz method of alternation. Making use of the fact that the field around each conductor is the same as that due to doublets comprising two equal and opposite currents, an expression for the attraction is derived in the form of a rapidly converging series. Simple modifications of the formulas are indicated for the case in which the medium surrounding the conductors is not a vacuum.

538.56:537.71 1397

The Intrinsic Impedance of Space—T. Tanasescu and É. Brylinski. (*Wireless Eng.*, vol. 27, pp. 63–64; February, 1950.) Further discussion. See also 607 of April (Budeanu), 876 of May (Foch), and 877 of May (Brylinski).

538.569.4:523.755 1398

On the Absorption of Radio Waves in the Solar Corona—V. L. Ginzburg. (*Astrnom. Zh.*, vol. 26, pp. 84–96; March and April, 1949. In Russian.) Formulas for the absorption of radio waves in an ionized gas are discussed; they may be applied to the ionosphere, the solar corona, and the interstellar gas. Differences between the absorption of radio waves and light waves are considered. The 'radiative depth' of the solar corona for wavelengths in the range 0.6–50 m is determined and the results are tabulated. Discussion of the effect of magnetic fields shows that both the ordinary and extraordinary waves are elliptically polarized and that they originate from different layers and can have very different intensities.

537.212+538.12 1399

Electric and Magnetic Fields [Book Review]—S. S. Attwood. Publishers: Chapman and Hall, London, and J. Wiley and Sons, New York, 3rd edn 1949, 475 pp., 44s. or $5.50. (*Wireless Eng.*, vol. 27, p. 94; March, 1950; Proc. I.R.E., vol. 38, p. 191; February, 1950.) Intended to provide "training in the development of the fundamental concepts, formulas, terminology, and units used in electric and magnetic field study." "The rationalized mks system of units has been adopted, but tables are given showing the relations between the units in the various systems."

GEOPHYSICAL AND EXTRA-TERRESTRIAL PHENOMENA

523.72:621.396.812.3 1400
Sudden Enhancements [of atmospherics] on Very Long Waves—Bureau. (*See* 1499.)

523.72.029.64:621.396.822 1401
Distribution of Radiation from the Undisturbed Sun at a Wave-Length of 60 cm—H. M. Stanier. (*Nature* (London), vol. 165, pp. 354–355; March 4, 1950.) Measurements made at this wavelength with spaced antennas showed that no apparent increase in radiation occurs at the limb and the intensity there is about 66 per cent of that near the center of the disk. About 30 per cent of the total radiation comes from the region outside the visible disk.

621.396.11:523.74 1402
Unusual Ionospheric Storm—Bennington. (*See* 1500.)

523.755 1403
The Solar Corona—H. v. Klüber. (*Elektron Wiss. Tech.*, vol. 4, pp. 77–88; March, 1950.) Observations made during eclipses are reviewed and the temperature and electron distribution in the corona are studied. Radiation intensity at different wavelengths is discussed. The 'betatron theory' may explain the heating of the corona to a temperature 10^6 degrees above that of the sun's surface, 6,000 degrees.

523.755:538.569.4 1404
On the Absorption of Radio Waves in the Solar Corona—Ginzburg. (*See* 1398.)

523.856:621.396.822 1405
Point Sources of Radio Noise—D. H. Menzel and D. J. Crowley. (*Nature* (London), vol. 165, p. 443; March 18, 1950.) A brief discussion of the origin of noise observed in radio-astronomy. It is tentatively suggested that the point sources may be comets within the solar system, which absorb ionizing energy from the sun and re-radiate it after conversion.

551.510.535:621.396.1 1406
Physical Society Conference [on the ionosphere] at Cambridge, 14th to 16th July 1949—(*Proc. Phys. Soc.*, vol. 63, pp. 141–150; February 1, 1950.) Abstracts are given of 17 papers presented at the conference; these are all noted below, in this section or in the 'Propagation of Waves' section.

551.510.535 1407
Theoretical Considerations Regarding the Formation of the Ionized Layers—D. R. Bates and M. J. Seaton. (*Proc. Phys. Soc.*, vol. 63, pp. 129–140; February 1, 1950.) Physical Society Summer Conference paper. The detailed mechanisms involved in the formation of the E, F_1, F_2, and D layers by solar ultraviolet radiation are discussed. Use is made of the results of some recent calculations on the continuous absorption cross-section of atomic oxygen and nitrogen, and of the evidence on the ionic composition of the layers that is provided by the analysis of the emission spectrum of the upper atmosphere during twilight. The uncertainties existing at present are emphasized.

551.510.535 1408
The Formation of the Ionized Regions—K. Weekes. (*Proc. Phys. Soc.*, vol. 63, pp. 147–148; February 1, 1950.) Summary of Physical Society Summer Conference paper. Close comparison of observed results with Chapman's simple theory of absorption of ultraviolet light in an isothermal atmosphere reveals discrepancies, examination of which leads to a revision of the assumption that the electron recombination rate is independent of gas pressure. Gases which may be concerned in the various layers are discussed.

551.510.535 1409
Irregularities in the Horizontal Plane in Region E of the Ionosphere—J. W. Findlay. (*Proc. Phys. Soc.*, vol. 63, p. 148; February 1, 1950.) Summary of Physical Society Summer Conference paper. Experiments are described for measuring phase and amplitude variations of 2.4-Mc signals reflected from region E at vertical incidence, and the rapidity of phase fluctuation is taken as a measure of the irregularity of the reflecting region; daily and seasonal variations of this irregularity are shown. Measurements of the amplitudes of pulse signals returned to three ground receiving points about 100 m apart fit in with the assumption that the irregularities in region E have at any time random motions among themselves and also an over-all horizontal drift. Theories are developed for determining these motions.

551.510.535:523.5 1410
Meteor Ionization in the Upper Atmosphere—A. C. B. Lovell. (*Proc. Phys. Soc.*, vol. 63, p. 149; February 1, 1950.) Summary of Physical Society Summer Conference paper. Recent progress in the study of the scattering of radio waves from meteor trails is described. Two significant facts are (a) the discovery of the great daytime meteor radiants active from May to September, and (b) the appreciation that only about 10^{-6} of the energy of the meteor is spent in ionization. Reflections from meteor trails have been investigated at various high frequencies, and it is established that all transient echoes in the altitude range 80 to 120 km are due to meteor ionization.

551.510.535:523.75 1411
Irregular Behaviour of the Ionosphere Associated with Solar Events—W. R. Piggott. (*Proc. Phys. Soc.*, vol. 63, p. 146; February 1, 1950.) Summary of Physical Society Summer Conference paper. Phenomena occurring in the lower regions of the ionosphere associated with solar flares are briefly discussed; the types of experimental data obtained are summarized, and the geophysical significance of the results is indicated. Two main types of ionospheric disturbance are identified, viz., type A, quasi-auroral, and type R, regular. Type A produces marked effects in the F region, associated with fluctuations in the local magnetic field; its relaxation time is a few minutes to one or two hours. Type R consists of a positive phase (ionization density above normal) and a negative phase (ionization density below normal and recovering); it has not been found to be connected with magnetic variations; its relaxation time may be some hours or days.

551.510.535:621.396.11 1412
Scattering of Radio Waves from Region E—Millington. (*See* 1488.)

551.510.535:621.396.11 1413
Scattered Echoes Near the Critical Frequencies of the F_2 region—Rivault. (*See* 1481.)

551.510.535:621.396.81 1414
Measurements on Long and Very Long Waves—Bracewell. (*See* 1495.)

551.510.535 (98) 1415
(P', f) Records at Spitsbergen—A. B. Whatman. (*Proc. Phys. Soc.*, vol. 63, p. 145; February 1, 1950.) Summary of Physical Society Summer Conference paper. Sixty (P', f) records are shown, made with Admiralty Type-249 equipment in Spitsbergen in 1942–1943. These illustrate all the interesting normal and abnormal effects met with and supplement those recently published (2796 of 1949).

LOCATION AND AIDS TO NAVIGATION

621.396.9 1416
1950 IRE National Convention Program—(PROC. I.R.E., vol. 38, pp. 192–211; February, 1950.) Summaries are given of the following papers:

18. The Statistical Properties of Noise Applied to Radar Range Performance—S. M. Kaplan and R. W. McFall.
61. Antenna System for Very-High-Frequency Radio Ranges and Direction Finding—F. J. Lundburg and F. X. Bucher.
120. Measurement and Analysis of Noise in a Fire-Control Radar—R. H. Eisengrein.
143. Analysis of Course Errors in the VHF Omnidirectional Radio Range—J. W. Leas.
144. Dynamic Aspect of Errors in Radio Navigation Systems, particularly in Case of Fast-Moving Receivers and Transmitters—H. Busignies.
145. A New Basis for Analyzing Radio Navigation and Detection Systems—N. L. Harvey.
146. Stochastic Processes as applied to Aerial Navigation and Direction Finders—L. A. de Rosa.
147. 1000-Mc Crystal-Controlled Airborne Transmitter for Distance Measuring Equipment—B. Warriner.

621.396.9:371.3 1417
Aids to Training—The Design of Radar Synthetic Training Devices for the R.A.F.—G. W. A. Dummer. (*Proc. IEE* (London), Part III, vol. 97, pp. 124–125; March, 1950.) Discussion on 2230 of 1949.

621.396.93 1418
Fixed H-Adcock Direction Finder for V.H.F.—B. G. Pressey and G. E. Ashwell. (*Wireless Eng.*, vol. 27, pp. 54–58; February, 1950.) "The paper describes an investigation into the practicability of the fixed type of H-Adcock direction finder for use at very high frequencies (30–100 Mc) under conditions in which the antenna system is remote from the operator. The experimental equipment consisted essentially of two crossed H-Adcock antennas mounted on a wooden tower 10 m high. The antenna system was connected by rf transmission lines to a goniometer and receiver situated in a hut near the base of the tower. By making adjustments to the length of the transmission lines and their point of connection to the antenna feeders a high instrumental accuracy was obtained on signals of mixed as well as vertical polarization. The sensitivity was such that bearings with a silent swing of $\pm 5°$ could be taken on field strengths varying between 0.5 and 14 μv/m over the frequency range."

621.396.93 1419
The Specification and Measurement of Polarization Errors in Adcock-Type Direction Finders—W. Ross. (*Elektrotechnik* (Berlin), vol. 4, pp. 90–92; March, 1950.) German version of 3143 of 1949.

621.396.93:621.396.11 1420
The Effects of Sky-Wave on the Planning of Navigational Aids using Frequencies in the 70–130-kc Band—Sanderson. (*See* 1490.)

621.396.93:621.396.11 1421
The Characteristics of Low-Frequency Radio Waves Reflected from the Ionosphere, with particular reference to Radio Aids to Navigation—Williams. (*See* 1489.)

621.396.93:621.396.11.029.58 1422
Very-Low Frequency Propagation—Smith and Tremellen. (*See* 1493.)

MATERIALS AND SUBSIDIARY TECHNIQUES

531.788 1423
Construction and Applications of a New Design of the Philips Vacuum Gauge—F. M. Penning and K. Nienhuis. (*Philips Tech. Rev.*,

vol. 11, pp. 116–122; October, 1949.) By modification of the electrode structure of the original design (1525 and 4265 of 1937) the range of the instrument has been extended to below 10^{-6} mm Hg. Its application as a leak detector is described.

535.215.4 1424

The Photoconductivity of Bismuth Sulphide and Bismuth Telluride—A. F. Gibson and T. S. Moss. (*Proc. Phys. Soc.*, vol. 63, pp. 176–177; February 1, 1950.) Independent investigations by the two authors on Bi_2S_3 and Bi_2Te_3 photoconductive and photovoltaic layers of considerable sensitivity do not confirm the suggestion made by Fink and Mackay (U. S. Patent No. 2406139, 1946) that these substances may be photosensitive to wavelengths as great as 7μ. The measurements indicate that the Bi compounds behave in a similar way to the corresponding Pb compounds but are inferior to them.

535.37 1425

The Fluorescence of Zinc Sulphide Activated with Copper—F. A. Kröger, J. E. Hellingman, and N. W. Smit. (*Physica, 's Grav.*, vol. 15, pp. 990–1018; December, 1949.) In English.) Experimental study, using controlled atmospheres at different temperatures, of the variation in the relative concentration of the fluorescence and quench centers with the conditions of preparation. Effects of refiring at a lower temperature are described. The physical behavior of the system is discussed on the basis of the Schön-Klasens theory of energy transfer between centers.

537.122:621.315.6 1426

Time Dependence of Electronic Processes in Dielectrics—H. Fröhlich and J. O'Dwyer. (*Proc. Phys. Soc.*, vol. 63, pp. 81–85; February 1, 1950.)

537.228.1:548.0 1427

Superpolarizable (Piezoelectric) Materials—E. Granier. (*Rev. Gén. Élec.*, vol. 59, pp. 33–45; January, 1950.) Study of the dielectric, hysteresis, and piezoelectric properties of crystals derived from Rochelle salt.

537.228.1:548.0 1428

On the Ferroelectricity of KH_2PO_4 and KD_2PO_4 Crystals—J. Pirenne. (*Physica,'s Grav.*, vol. 15, pp. 1019–1022; December, 1949. In English.) A new theory is proposed to explain the unusual isotopic effect observed with these crystals.

537.529 1429

The Time Delay in Conduction and Breakdown Processes in Amorphous Solids—J. H. Simpson. (*Proc. Phys. Soc.*, vol. 63, pp. 86–100; February 1, 1950.) Theoretical determination of the time delay from Fröhlich's theory, and comparison with experimental values.

539.23:537.311.31 1430

The Resistivity of Thin Metallic Films—R. A. Weale. (*Proc. Phys. Soc.*, vol. 62, pp. 135–136; February 1, 1949.) A formula derived for the effective temperature coefficient α' of resistivity indicates that for a film of certain thickness α' will be zero and will be negative if the thickness is further reduced. Negative values are to be expected for comparatively thick films of Bi, in which the mean free path of the electrons is exceptionally long. The formula also shows that the temperature at which α' is zero is lower the thicker the film. The results of van Itterbeek and de Greve (343 and 3305 of 1946) for Ni films are in good agreement with the formula.

539.23:537.311.31 1431

Conductivity of Thin Metallic Films—D. A. Wright and R. A. Weale. (*Proc. Phys. Soc.*, vol. 63, pp. 173–175; February 1, 1950.) Wright disagrees with Weale's treatment of the problem and points out that according to Appleyard and Lovell (1940 of 1937) metallic films, however thin, should have a positive temperature coefficient. Semiconductor effects could explain the existence of a negative coefficient below a certain temperature. Weale indicates a way of reconciling the two points of view.

620.197 1432

Tropicalization of some Materials and Assemblies used in the Construction of Valves—G. Trebuchon. (*Le Vide* (Paris), vol. 5, pp. 748–752 and 777–780; January and March, 1950.) Discussion of materials affected, various specifications of methods to meet different conditions of use, test methods, and practical techniques.

621.3.011.5:532 1433

Refractive Indices and Dielectric Constants of Liquids and Gases under Pressure—J. S. Rosen. (*Jour. Chem. Phys.*, vol. 17, pp. 1192–1197; December, 1949.) Interpolation formulas are discussed.

621.3.011.5:[546.815.831+546.431.831 1434

Dielectric Properties of Lead Zirconate and Barium-Lead Zirconate—S. Roberts. (*Jour. Amer. Ceram. Soc.*, vol. 33, pp. 63–66; February 1, 1950.) Methods are described for preparation of ceramic samples. The dielectric properties are measured at 1 Mc in the temperature range 25° to 350° C for samples with different proportions of lead and barium. High dielectric constants, of the order of 7,000, are obtainable even at room temperatures. Nonlinear dielectric properties and piezoelectric effects are also investigated.

621.315.61.011.5.029.62/.64:621.317.335.3 1435

Measurement of Dielectric Constant and Power Factor at Ultra High Frequencies—Briganti. (*See* 1452.)

621.385.032.21+666.1.037.5 1436

1950 IRE National Convention Program—(Proc. I.R.E., vol. 38, pp. 192–211; February, 1950.) Summaries are given of the following papers:

158. A Vacuum Seal between Metals and Ceramics for High Temperature Applications—H. W. Soderstrom and K. H. McPhee.
159. Effect of Coating Composition of Oxide-Coated Cathodes on Electron Emission—E. G. Widell and R. A. Hellar.
160. Effects of Controlled Impurities in Nickel Core Metal on Thermionic Emission from Oxide-Coated Cathodes—G. Hees.
161. Investigation of Contaminant in Vacuum Tubes—P. D. Williams.
162. Hot Strength Properties of Filamentary Alloys—B. Wolk.

666.968:621.315.612.6:621.315.613.1 1437

Vacuum-Tight Sealing of Glass and Mica—J. Labeyrie. (*Jour. Phys. Radium*, vol. 11, p. 20; January, 1950.) Mica laminas as thin as 0.01 mm can be sealed to glass by means of a powdered enamel (G50) which softens at 354° and melts at 550° C. The same enamel may be used to seal mica to alloys with coefficients of expansion between 85 and 110×10^{-7} per degree C.

MATHEMATICS

51:621.396 1438

Mathematics in Radio—E. Roubine. (*Rev. Tech. Comp.* (Franç), no. 13, pp. 17–32; February, 1950.) The subject is considered from two aspects: (a) the assistance given to the technician by different branches of mathematics; and (b) the application of radio principles in the solution of mathematical problems. The processes of classical analysis, symbolic, tensorial, and matrix calculus, and infinitesimal geometry are outlined. Examples are given of their use. The principles of servomechanisms and computing machines are briefly examined. As an example of the difficulties which may occur in the application of analytical methods, the case of the cylindrical dipole radiator is discussed.

517.56:621.3 1439

Origin and Meaning of Circular and Hyperbolic Functions in Electrical Engineering—A. Boyajian. (*Jour. Frank. Inst.*, vol. 249, pp. 117–131; February, 1950.)

517.9 1440

Determination of the Stable Periodic Solutions of Certain Quasi-Harmonic Differential Equations—T. Got. (*Compt. Rend. Acad. Sci.* (Paris), vol. 230, pp. 612–614; February 13, 1950.)

681.142 1441

1950 IRE National Convention Program—(Proc. I.R.E., vol. 38, pp. 192–211; February, 1950.) Summaries are given of the following papers:

83. Static Magnetic Pulse Control and Information Storage—An Wang.
84. The Design of Diode Gate Circuits—R. J. Slutz.
85. Marginal Checking as an Aid to Computer Reliability—N. H. Tayler.
86. Development of the California Digital Computer—D. R. Brown and P. L. Morton.
90. M.I.T. Electroatatic Storage Tube—S. H. Dodd, H. Klemperer, and P. Youtz.
117. A Discussion revealing some Late Developments in Electronic Analog Computer Techniques—H. I. Zagor.
118. An Electronic Storage System—E. W. Bivans and J. V. Harrington.
119. Experimental Determination of System Functions by the Method of Correlation—J. B. Wiesner and Y. W. Lee.
121. A Digital Electronic Correlator—H. E. Singleton.
166. A Compact Magnetic Memory—P. L. Morton.

681.142 1442

Electrical Computer for Higher-Order Equations—H. Glubrecht. (*Z. Angew. Phys.*, vol. 2, pp. 1–8; January, 1950.) Seventh-order equations of the general form

$$w=a_n\cdot z^n+a_{n-1}\cdot z^{n-1}+\cdots+a_1\cdot z+a_0=0$$

may be solved by the apparatus described. The unknown complex quantity z is represented by two sinusoidal oscillations with a phase difference of 90°. By combining the proposals of Tischner and Rasch, the z and w planes are displayed on a cr tube screen and the passage of the polar curves through zero is used to give the solution points in the z plane.

681.142 1443

On a General Type of Algebraic Mathematical Machine—F. H. Raymond. (*Ann. Télécommun.*, vol. 5, pp. 2–20; January, 1950.) Further discussion of Type-OME machines (919 of May), their principles and applications. Type OME 14 can solve up to 10 simultaneous equations and uses one matrix of linear potentiometers. Types OME 12 and OME 13 use four such matrices and are designed for the solution of integro-differential equations.

501 1444

Introduction to Applied Mathematics [Book Review]—F. D. Murnaghan. Publishers: Chapman and Hall Ltd., London, 1948, 389 pp., 30s. (*Beama Jour.*, vol. 57, pp. 12–13; January, 1950.) "The standard of the book is that of a graduate course in applied mathematics." It is

the first of a series to be published on mathematical theories underlying physical science and on advanced mathematical techniques required for the solution of scientific problems. A "well-printed, well-produced" volume "suited to the needs of scientific workers in mathematics, physics, chemistry, and engineering."

517 1445

Höhere Mathematik für Mathematiker, Physiker, Ingenieure [Book Review]—R. Rothe. Publishers: B. G. Teubner Verlagsg., Leipzig. Vol. 1: Differential Calculus and Basic Formulas of Integral Calculus, with Applications. 8th edn 1948, 208 pp., 6.20 DM. Vol. 2: Integral Calculus, Infinite Series. Vector Calculus, with Applications. 6th edn 1949, 208 pp., 6.20 DM. Vol. 4: Exercises with Solutions Nos. 1/2, 5th edn 1949, 109 pp., 3.50 DM. Nos. 3/4, 4th edn 1949, 108 pp., 3.40 DM. (*Elektrotechnik* (Berlin), vol. 4, p. 64; February, 1950.)

MEASUREMENTS AND TEST GEAR

529.78:621.396.91 1446

The Synchronization of Clocks by means of Periodic Signals—M. Lavet. (*Rev. Gén. Élec.*, vol. 59, pp. 22–32; January, 1950.) Past and present systems of time-signal transmissions are reviewed and their application in various branches of science and industry is discussed. Methods are described for applying the accurate time signals now available to the synchronization of master clocks and recording chronometers, and to the regulation of ancient pendulum clocks in church towers or public buildings.

529.786+621.3.018.4 (083.74) 1447

Adjustment of High-Precision Frequency and Time Standards—J. M. Shaull. (Proc. I.R.E., vol. 38, pp. 6–15; January, 1950.) The basic equipment used by the C.R.P.L. of the National Bureau of Standards for broadcasting standard frequency and time signals is described and the application of these signals in the calibration of similar equipment is discussed. Several methods are described for checking the frequency of precision oscillators and the performance of precision clocks. Methods of recording performance data for such standards are suggested. Expected improvements in constancy and accuracy, and possible changes in the types of standards used in time measurement, are considered.

539.16.08.621.083.72 1448

A Pulse-Amplitude Analyser of Improved Design—E. H. Cooke-Yarborough, J. Bradwell, C. D. Florida, and G. A. Howells. (*Proc. IEE* (London), Part III, vol. 97, pp. 108–121; March, 1950.) A discussion of the requirements and a detailed description are given of an instrument designed to measure the amplitude distribution of pulses in an ionization chamber or other source. There are five channels, so that the pulses are divided into five groups of different level. The instrument consists of an amplifying and pulse-expanding unit, a ladder sorting circuit, and five scaling units and registers. The circuits include a combined discriminator and cancelling circuit, and an automatic dc level control, which are new and contribute effectively to stability and simplicity of adjustment.

621.317.089:621.3.012 1449

A Modern Electroacoustic Frequency-Response Recording Unit—H. Lehner. (*Funk. und Ton.*, vol. 4, pp. 53–65; February, 1950.) The construction and operation of the instrument are described. Impedances of passive 2-pole networks, quadripole and transmission-line attenuations, microphone and loudspeaker response curves can be recorded automatically.

621.317.32 1450

A Negative-Feedback D.C. Amplifier with D.C.-Polarized Chokes and Grid-Controlled Valves—W. Geyger. (*Arch. Tech.* (Messen), vol. 169, pp. T22–T24; February, 1950.) An instrument is described in which the direct voltage to be measured is applied to the control windings of a magnetic amplifier and is opposed by the voltage across a compensating resistor in the circuit of a moving-coil recorder. The recorder is operated from a symmetrical double-triode circuit to which the output from the magnetic amplifier is applied. The range of the instrument is from zero to 0.5 mv.

621.317.321.027.2 1451

Method of Measurement of Small Direct Voltages—H. H. Rust and H. Endesfelder. (*Z. Angew. Phys.*, vol. 2, pp. 39–41; January, 1950.) The method consists in converting the direct voltage into a proportionate alternating voltage. A carbon microphone is energized by the voltage to be measured and responds to tone of constant frequency and amplitude from a loudspeaker. By suitable amplification of the microphone output, voltages down to 1 μv can be measured. Variable direct voltages may be measured if their pulsation frequency is lower than that of the tone source.

621.317.335.3:621.315.61.011.5.029.62/.64 1452

Measurement of Dielectric Constant and Power Factor at Ultra-High Frequencies—E. Briganti. (*Alta Frequenza*, vol. 18, pp. 243–253; December, 1949. In Italian, with English, French, and German summaries.) Description of a method of measurement based on determining the Q factor of a coaxial transmission line sustaining standing waves, with and without the dielectric. Simple formulas are given for calculating dielectric constant and power factor from the different lengths of the resonant line. Results obtained on 10-cm and 22.5-cm wavelengths are given for a few modern insulating materials.

621.317.361:621.396.611.21 1453

Crystal Resonators as Frequency Substandards—F. J. M. Laver. (*Proc. IEE* (London), Part III, vol. 97, pp. 93–99; March, 1950.) The phase response of a crystal resonator is a more sensitive indication of its resonance point than the amplitude response. Equipment using the phase-difference principle is described which enables the resonance frequency of quartz vibrators of frequency 100 kc$\pm$10 cps to be determined to $\pm$1 part in 10^8, provided that the Q factor of the vibrator is greater than 10^5. Some results of long-period tests of vibrators with this equipment are given. Quartz resonators may usefully supplement the oscillator units of a large frequency-standard installation.

621.317.7 1454

1950 IRE National Convention Program—(Proc. I.R.E., vol. 38, pp. 192–211; February, 1950.) Summaries are given of the following papers:

19. Accelerated Life Testing of Vacuum Tubes—J. Rothstein.
20. Statistical Evaluation of Life Expectancy of Vacuum Tubes designed for Long-Life Operation—E. M. McElwee.
26. Specifications for Quality of the Visual Output of Picture Tube Screens—A. E. Martin.
42. Oscillographic Presentation of Time Delay and Distortion in Broad-Band FM Systems—A. R. Vallarino.
44. New Test Equipment for the UHF Television Band—J. Ebert and H. A. Finke.
45. Direct Reading Phasemeter—L. H. O'Neill and J. L. West.
46. Measuring Procedure for Radioteletype Converters—H. C. Hawkins.
98. Performance Measurement of Capacitors—H. T. Wilhelm.
101. Transformer Performance and Measurements—R. Lee.

621.317.71 1455

New Method of Measurement of Very Heavy Direct Currents.—R. Servant. (*Rev. Gén Élec.*, vol. 59, pp. 45–47; January, 1950.) Two flat arms at right angles, with hyperbolic profiles, are pivoted at the vertex and serve as formers for special windings fed by an auxiliary current source adjustable within wide limits. When held so that a conductor carrying heavy current is included in the angle between the two arms, the device is subjected to a couple proportional to the cable current and this couple is neutralized by adjustment of calibrated torsion springs. Partial readings obtained at various positions around the conductor are added. Currents in the range 1–10 ka can be measured.

621.317.733:621.317.37 1456

Development of Bridges for Dielectric Measurements—T. Gast. (*Z. Angew. Phys.*, vol. 2, pp. 41–48; January, 1950.) A review of ac bridges from the fixed-frequency hand-operated instrument to the fully-automatic two-component bridge with a wide frequency range. An automatic system of loss equalization for a pure capacitance bridge by means of an auxiliary current is described.

621.317.733.029.62/.63 1457

Two Simple Bridges for Very-High-Frequency Use—D. D. King. (Proc. I.R.E., vol. 38, pp. 37–39; January, 1950.) Two bridges for impedance measurement are described: (a) a hybrid junction tunable over the range 100–500 Mc and capable of great sensitivity; and (b) an untuned Wheatstone bridge for use in the same frequency range. Design features and performance characteristics are given for both units.

621.317.755 1458

Simple Cathode-Ray Oscilloscope—M. G. Scroggie. (*Wireless World*, vol. 56, pp. 82–83; March, 1950.) Design details of a circuit comprising tube controls, variable-frequency time base and single-tube amplifier. The time-base operates at frequencies from 12 cps to 40 kc, while the amplifier has a flat response over the range 20–20,000 cps and a continuously variable gain up to about 41 db at af and to 26 db at higher frequencies.

621.317.755 1459

An Easily Portable Cathode-Ray Oscillograph—E. E. Carpentier. (*Philips Tech. Rev.*, vol. 11, pp. 111–115; October, 1949.) Description of the Type-GM5655 cro of dimensions $4\frac{1}{2}\times11\frac{1}{2}\times9\frac{1}{2}$ in. and weight 14 lb. The normal frequency limit is 100 kc. Separate amplifiers are used for the horizontal and vertical diflections.

621.317.755:621.396.6.001.4 1460

Curve Tracer with Electronic Graph Lines—J. W. Balde, J. C. Bregar, and K. L. Chapman. (*Electronics*, vol. 23, pp. 100–103; March, 1950.) The response curve of the apparatus under test is displayed on the screen of a cro together with marker lines indicating the tolerance limits. Only a short time is required to adapt the equipment for testing a different type of apparatus. Production testing and adjustment of filters, amplifiers, discriminators, etc., are greatly facilitated.

621.317.755.089.6 1461

The Dynamic Sensitivity and Calibration of Cathode-Ray Oscilloscopes at Very-High Frequencies—H. E. Hollmann. (Proc. I.R.E., vol. 38, pp. 32–36; January, 1950.) The basic formula for dynamic sensitivity in terms of the

transit-time angle of electrons in the deflecting field is modified to take account of (a) their displacement on leaving the field and (b) stray-field effects. Good agreement with experimental values is obtained.

621.317.761 1462
Measuring a Varying Frequency—R. L. Chase. (*Electronics*, vol. 23, pp. 110–112; March, 1950.) A pulse-shaping circuit is used to convert the wave of unknown frequency to a series of sharp pulses. Measurement is initiated by an external starting pulse and the number of cycles of a standard 5-Mc oscillator occurring in an interval corresponding to a selected integral number of the derived pulses is counted. Frequencies in the range 100 kc–5 Mc can be measured to within 0.1 per cent in about 200 μs. The equipment was designed to measure the frequency of the rf oscillator in an FM particle accelerator, but many other applications are possible.

621.395.813.083 1463
Intermodulation Distortion—T. Roddam. (*Wireless World*, vol. 56, pp. 122–125; April, 1950.) A simplified method of measurement not requiring a harmonic analyzer.

621.396.615:621.316.726.078.3 1464
A Variable-Frequency Oscillator stabilized to High Precision—L. F. Koerner. (*Bell Lab. Rec.*, vol. 28, pp. 66–71; February, 1950.) The oscillator is stabilized by locking to a combination of the nth harmonic of a standard frequency source and an lf interpolation oscillator. This stabilized frequency may then be multiplied by means of an harmonic generator. The ultimate accuracy is limited only by that of the frequency standard. Curves obtained by means of the equipment are given showing the response of a quartz-crystal network for frequencies near its 10-Mc fundamental and third harmonic.

621.396.822:621.316.8 1465
Resistor Noise—E. Paolini and G. Canegallo. (*Alta Frequenza*, vol. 18, pp. 254–267; December, 1949. In Italian, with English, French, and German summaries.) Study of the noise produced by spontaneous voltage fluctuations across resistors of different types. Two instruments for measurement of such noise are described.

OTHER APPLICATION OF RADIO AND ELECTRONICS

535.322.1:539.165 1466
Theory of a Magnetic-Lens Type Beta-Ray Spectrometer—N. F. Verster. (*Appl. Sci. Res.*, vol. B1, pp. 363–378; 1950.)

539+621.3 1467
1950 IRE National Convention Program—(Proc. I.R.E., vol. 38, pp. 192–211; February, 1950.) Summaries are given of the following papers:

6. Particle Accelerators—M. S. Livingston.
7. Radio-Frequency Problems associated with Particle Accelerators—J. P. Blewett.
8. Detection of Nuclear Radiations—J. R. Dunning.
43. Rockets Range Instrumentation—E. R. Toporeck and F. M. Ashbrook.
51. Industrial Television System—R. C. Webb and J. M. Morgan.
64. A High-Capacity Matrix-Commutated Radio Telemetering System—J. P. Chisholm, E. F. Buckley, and G. W. Farnell.
67. Use of Image Converter Tube for High-Speed Shutter Action—A. W. Hogan.
68. Ultrasonic Pulse Instruments for Automatic Continuous Measurement of Physical Properties of Solids and Liquids—S. R. Rich.
69. Electronic Duplicator Attachments for Automatic Machine Tool Operation—W. Roth.
70. Modern Methods of Servo Synthesis—R. McCoy and D. Herr.
71. An Electronic Flowmeter and its Industrial Applications—E. Mittelmann and V. J. Cushing.
132. Effects of Intense Microwave Radiation on Living Organisms—J. W. Clark.
133. A Differential Vectorcardiograph—S. A. Briller and N. Marchand.
134. Electronic Mapping of the Electrical Activity of the Heart and Brain—S. Goldman.
167. Synchro-Cyclotron Field Regulator—C. S. McKown and W. P. Caywood, Jr.

539.16.08 1468
Fluctuations in Proportional Counters—W. F. G. Swann. (*Jour. Frank. Inst.*, vol. 249, pp. 133–137; February, 1950.)

621.3.07+621.396.645.37 1469
Control, Positive and Negative Feedback and Negative Resistance Coordinated—Reichardt. (*See* 1347.)

621.365.5:621.396.611.3 1470
Output Coupling of Valve Generators for Industrial Heating Purposes—Krüger. (*See* 1376.)

621.384.6 1471
A New Method for Particle Injection into Accelerators—W. B. Jones, H. R. Kratz, J. L. Lawson, G. L. Ragan, and H. G. Voorhies. (*Phys. Rev.*, vol. 78, pp. 60–62; April 1, 1950.) A method involving rapid damping of the radial or vertical oscillations for as large a number of revolutions as possible, and subsequent removal of this damping.

621.384.61 1472
The Electron Cyclotron—P. A. Redhead, H. LeCaine, and W. J. Henderson. (*Canad. Jour. Res.*, vol. 28, pp. 73–91; January, 1950.) A magnetic-resonance electron accelerator is described which is based on the principles suggested by Veksler (1913 and 2315 of 1945). A constant magnetic field and an accelerating rf field of frequency 2800 Mc are used. Final energies of 5 Mev have been obtained in an experimental accelerator with a vacuum chamber of diameter 14 in.

621.384.611.2 1473
Validity of Two-Dimensional Design of Synchrotron Pole-Faces—J. J. Wilkins. (*Proc. Phys. Soc.*, vol. 63, pp. 177–178; February 1, 1950.)

621.385.833 1474
Work carried out with the Magnetic Electron Microscope—G. Dupouy. (*Rev. d'Optique*, vol. 29, pp. 89–100; February, 1950.)

621.385.833 1475
Proton Microscope Design. Application of Ion Optics in Mass Spectrography—C. Magnan. (*Rev. d'Optique*, vol. 29, p. 100; February, 1950.) Summary only.

621.385.833 1476
Electron-Optics of Electrostatic Lenses. Comparison of Theoretical Resolving Powers of Electron and Proton Microscopes—P. Chanson. (*Rev. d'Optique*, vol. 29, p. 111; February, 1950.) Summary only.

621.385.833 1477
Simple Expression for the Focal Length and Chromatic Aberration of an Extensive Group of Electrostatic Lenses—É. Regenstreif. (*Compt. Rend. Acad. Sci.* (Paris), vol. 230, pp. 630–632; February 13, 1950.) See also 1213 of June.

621.385.833:530.12 1478
Electron Lenses in Relativistic Mechanics—J. Laplume. (*Rev. d'Optique*, vol. 29, pp. 106–111; February, 1950.)

621.386.1 1479
Application of Electron Optics to X-Ray Tubes of Great Intensity—S. Goldsztaub. (*Rev. d'Optique*, vol. 29, pp. 101–105; February, 1950.)

PROPAGATION OF WAVES

538.566.2 1480
Solution of a Transcendental Equation by Means of Conformal Representation—G. Eckart and T. Kahan. (*Rev. Sci.* (Paris), vol. 86, pp. 723–726; December, 1948.) The equation considered, which occurs in wave propagation theory, is

$$[\sqrt{(\lambda^2-k_1^2)}-\sqrt{(\lambda^2-k_2^2)}]/[\sqrt{(\lambda^2-k_1^2)}+\sqrt{(\lambda^2-k_2^2)}]=-\exp[+2h\sqrt{(\lambda^2-k_1^2)}]$$

where k_1^2, k_2^2 and h are real and positive and $k_1^2>k_2^2$. By conformal transformation of the Riemann surface λ, the real positive roots of the equation seen to lie on the real axis of λ in the interval $k^2\leqq\lambda<k_1$. Graphical methods are given for determining the values of the roots.

621.396.1+551.510.535]:061.3 1481
Physical Society Conference [on the ionosphere] at Cambridge, 14th to 16th July 1949—(*Proc. Phys. Soc.*, vol. 63, pp. 141–150; February 1, 1950.) Abstracts are given of 17 papers presented at the conference; these are all noted below, in this section or in the "Geophysical and Extraterrestrial Phenomena" section.

621.396.11+621.396.81 1482
1950 IRE National Convention Program—(Proc. I.R.E., vol. 38, pp. 192–211; February, 1950.) Summaries are given of the following papers:

135. Calculation of Effective Phase, Group, and Pulse Velocities of Wave Propagation—A. Fischler, G. H. Sloan, and D. Goldenberg.
137. Radio Wave Propagation in a Curved Ionosphere—J. M. Kelso.
153. A Microwave Propagation Test—J. Z. Millar and L. A. Byam, Jr.

621.396.11+621.396.81 1483
Comparison of Measured and Calculated Microwave Signal Strengths, Phase, and Index of Refraction—A. W. Straiton, A. H. LaGrone, and H. W. Smith. (Proc. I.R.E., vol. 38, pp. 45–48; January, 1950.) Experimental signal-strength/height curves and phase-change/height curves for 3.2-cm waves are compared with those derived from the corresponding curves showing the variation of the measured modified refractive index with height. The latter curves and attenuation factors determined from radio observations are also compared with the corresponding curves and attenuations deduced from meteorological observations. Four sets of radio data, for path lengths of 12.3, 31.6, 40, and 47 miles, are considered.

621.396.11 1484
The Speed of Radio Waves and Its Importance in Some Applications—R. L. Smith-Rose. (Proc. I.R.E., vol. 38, pp. 16–20; January, 1950.) 1949 IRE National Convention paper reviewing present knowledge. The available data on the velocity of light are noted. Recent measurements of the velocity of 3-kMc radio waves in vacuo have given higher values than that for light, indicating an unresolved discrepancy. Investigations associated with navigation-aid systems have given values for radio wave velocities over land and sea paths. A table of mean velocity values, with estimated measurement accuracies is given for both pulsed and cw radio trans-

missions at frequencies between 100 kc and 3.3 kMc.

621.396.11 1485

The Application of Ionospheric Data to Short-Wave Transmission Problems—W. J. G. Beynon. (*Proc. Phys. Soc.*, vol. 63, p. 145; February 1, 1950.) Summary of Physical Society Summer Conference paper. "A short survey is presented of the fundamental theory underlying the application of normal-incidence ionospheric data to short-wave communication problems, with particular reference to calculating the maximum usable frequency (muf). Some aspects of the problem of applying normal-incidence data on ionospheric absorption to the calculation of field strength in long distance transmission are also discussed."

621.396.11 1486

The Regular Behaviour of Long and Very Long Waves Returned from the Ionosphere—J. A. Ratcliffe. (*Proc. Phys. Soc.*, vol. 63, p. 142; February 1, 1950.) Summary of Physical Society Summer Conference paper, defining the scope of the first session, indicating how the main contributions fit into the plan of the discussion and outlining some of the work carried out in Cambridge. The frequencies considered lie between 10 kc and 300 kc. Observations have mainly been near the frequencies of 16 kc (GBR, Rugby) and 100 kc (Decca), the academic workers generally concentrating on reflection effects at nearly vertical incidence, while commercial organizations have been mainly concerned with experiments at oblique incidence.

621.396.11:551.510.535 1487

Scattered Echoes Near the Critical Frequencies of the F_1 region—R. Rivault. (*Proc. Phys. Soc.*, vol. 63, pp. 126–128; February 1, 1950. In French.) Physical Society Summer Conference paper. Two types are observed in vertical soundings at Poitiers, France: (a) when the scattering is not too diffuse, several components can be seen at frequency intervals of about $\frac{1}{4}$ or $\frac{1}{8}$ of the gyro-frequency. This type of scattering is most frequent during long nights and disappears at sunrise. It may be connected with the breakdown of the regular day-time stratification; and (b) a *G* layer is sometimes in evidence as a diffuse pattern extending from about 3 Mc up to 5.2 Mc; it disappears near sunrise. Such scattering is associated with magnetic storms and meteor showers. Many phlotographic pecords are reproduced.

621.396.11:551.510.535 1488

Scattering of Radio Waves from Region *E*—G. Millington. (*Proc. Phys. Soc.*, vol. 63, p. 149; February 1, 1950.) Summary of Physical Society Summer Conference paper. Sporadic echoes scattered directly back from the *E* layer show no definite correlation with visible meteors; it is suggested that they may be caused either by the sun or by the stars of the galaxy. Long-distance scattering, in which the sources are illuminated and the scattered signals received by reflection from the *F* layer, may be due to scattering centers in the *E* layer or on the ground. The risk of interference from an unwanted signal on a shared frequency as a result of long-distance scattering is discussed.

621.396.11:621.396.93 1489

The Characteristics of Low-Frequency Radio Waves Reflected from the Ionosphere, with particular reference to Radio Aids to Navigation—C. Williams. (*Proc. Phys. Soc.*, vol. 63, pp. 143–144; February 1, 1950.) Summary of Physical Society Summer Conference paper. Observations at fixed and mobile (airborne) receiving points are used to determine changes of amplitude and phase in signals reflected by the *E* layer. From the results the relative amplitudes of ground and reflected waves are established as a function of distance from the transmitters, and the height of the reflecting layer and the reflection coefficient at oblique incidence during day and night are estimated.

621.396.11:621.396.93 1490

The Effects of Sky-Wave on the Planning of Navigational Aids Using Frequencies in the 70–130 kc/s Band—W. T. Sanderson. (*Proc. Phys. Soc.*, vol. 63, p. 143; February 1, 1950.) Summary of Physical Society Summer Conference paper. The accuracy of the Decca system depends on the stability of the phase-locked transmissions and observations have been made to determine the phase variation which can be expected at various ranges and times. Results indicate that in English latitudes the night sky wave effects persist throughout the day during mid-winter on 70 kc, falling to about half the night value at 120 kc. During the summer daylight (April–September) the effects are so small up to 300 miles that they are difficult to measure. Hawker has found that the secant of the sun's zenithal distance at noon gives a good approximation to the relative amplitude of the daylight errors throughout the year. The bearing of these results on the planning of medium-range cw navigation aids is discussed.

621.396.11.029.45+621.396.81.029.45 1491

The Ground Interference Pattern of Very-Low-Frequency Radio Waves—K. Weekes. (*Proc. IEE* (London), vol. 97, pp. 100–107; March, 1950.) Measurements in an aircraft of the strength of 16-kc signals at distances up to 850 km from the transmitter are described. At distances up to 300 km the results agree with those of previous experiments by Budden, Ratcliffe, and Wilkes (3441 of 1939). The ionospheric reflection conditions which would account for these results are found to be no longer valid at the greater distances, and there appears to be a considerable change in these conditions at about 400 km. This applies to reflection coefficient, equivalent height (or phase change at reflection), and also polarization, which becomes approximately linear at 500 km.

621.396.11.029.58/.64 1492

Propagation of Short Radio Waves over Desert Terrain—J. P. Day and L. G. Trolese. (Proc. I.R.E., vol. 38, pp. 165–175; February, 1950.) The vertical distribution of field over a 190-ft interval was measured during daytime, when the atmosphere was well mixed, and at night, when a small-scale duct was formed, over an optical 26.7-mile path and a non-optical 46.3-mile path on various frequencies between 25 and 24,000 Mc. Transmitters and receivers were fitted in elevator cabs in 200-ft towers. The results are discussed and correlated with simultaneous meteorological measurements. Diffraction and partial-reflection effects were also studied. With frequencies up to 1,000 Mc the duct affects the magnitude but not the shape of the height/gain curves; with microwaves the shape is altered considerably.

621.396.11.029.58:621.396.93 1493

Very-Low-Frequency Propagation—S. B. Smith and K. W. Tremellen. (*Proc. Phys. Soc.*, vol. 63, p. 143; February 1, 1950.) Short summary of Physical Society Summer Conference paper. Earlier experiments during 1920–1926 are discussed, with particular reference to (a) apparent abnormalities and other little known phenomena, (b) world atmospheric noise centers, seasonal, and diurnal variations in direction and intensity, and (c) df using different techniques, with special reference to reception along various geomagnetic paths.

621.396.81 1494

On the Deduction of the Refractive Index Profile of a Stratified Atmosphere from Radio Field-Strength Measurements—J. W. Green. (Proc. I.R.E., vol. 38, pp. 80–88; January, 1950.) A method due to Macfarlane (2894 of 1947) derives the refractive index profile from the variations of received amplitude with height and range. Application to amplitudes calculated from standard diffraction theory and duct propagation theory confirmed the formal accuracy of the method, but suggested that it would be very sensitive to small measurement errors. Application to field-strength values observed over water and land for standard and non-standard atmospheric conditions confirmed this and showed that the formula was unsatisfactory except in a limited frequency range under standard conditions.

621.396.81:551.510.535 1495

Measurements on Long and Very Long Waves—R. N. Bracewell. (*Proc. Phys. Soc.*, vol. 63, p. 144; February 1, 1950.) Summary of Physical Society Summer Conference paper. Details are given of the regular daily and seasonal variations of waves of frequencies 16 kc and 100 kc observed, after reflection from the ionosphere, at distances of 90, 200, and 500 km. The night reflection coefficient for a 16-kc wave is found to be about 0.5 in all seasons; that for 70- and 113-kc waves is markedly lower, and decreases in summer. From round about sunrise the reflection coefficient for the 16-kc wave drops in summer, but not in winter; for the 70- and 113-kc waves the fall occurs both in summer and winter, though that in summer is far more marked. The reflection height, about 90 km at night in all seasons, exhibits corresponding decreases. Polarization conditions are also noted. When observations are made at a distance of 500 km from the transmitter, multiple reflections are important and the sunrise variations are more rapid.

621.396.81.029.6 1496

Radio Propagation Variations at VHF and UHF—K. Bullington. (Proc. I.R.E., vol. 38, pp. 27–32; January, 1950.) 1949 IRE National Convention paper. Long-period observations of field-strength variation as a function of distance from the transmitter, of fading effects, and of the influence of irregular terrain, buildings, and trees are analyzed and checked against theory where possible. Using median values together with a measure of the spread of values for fading and shadow losses, empirical formulas are obtained for the service area of and distance required between co-channel stations for any assigned ratio of signal to interference.

621.396.812.3 1497

The Variations in Direction of Arrival of High-Frequency Radio Waves—W. Ross. (*Proc. Phys. Soc.*, vol. 63, pp. 149–150; February 1, 1950.) Summary of Physical Society Summer Conference paper. Bearings observed on hf transmissions are subject to continuous fluctuations, apart from those due to variable instrument errors. Both rapid and slow fluctuations occur, the latter with periods from a few minutes up to half an hour. These slow fluctuations are similar for bearings on neighboring frequencies and transmission paths; they are apparently due to fairly localized tilting of the ionosphere layers. The rapid fluctuations are observed even when pulses are used, and hence may be caused by ionosphere irregularities of smaller scale than those causing slow fluctuations. The random irregularities may be due to the spreading of disturbances produced by perturbations in the regular diurnal changes

in the ionosphere. See also 3424 of 1949 (Ross and Bramley).

621.396.812.3 1498

Some Work at Cambridge on Radio Fade-Outs—K. Weekes. (*Proc. Phys. Soc.*, vol. 63, pp. 146–147; February 1, 1950.) Summary of Physical Society Summer Conference paper. Observations on the changes of "phase path" and amplitude of the pulse reflected from the E region during fade-out were made (a) at vertical incidence on 2.0 and 2.4 Mc, (b) near vertical incidence on 70 and 113 kc, and (c) near vertical incidence on 16 kc and 40 kc. The "phase path" may decrease initially by 2 to 4 km in case (a), and by as much as 20 km in cases (b) and (c); the amplitude decreases initially by a factor which is at least 200 in case (b), but is only of the order of 3 in case (c). There is rapid recovery to normal values as the fade-out ends. An ionization distribution which would account for the observed results is suggested.

621.396.812.3:523.72 1499

Sudden Enhancements [of atmospherics] on Very Long Waves—R. Bureau. (*Proc. Phys. Soc.*, vol. 63, pp. 122–126; February 1, 1950. In French.) Physical Society Summer Conference paper. The increased level of atmospherics received on wavelengths of 11,000 m during a solar flare is usually accompanied by a Dellinger fade-out on short-wave circuits. Several instances have been found where the fade-out is preceded by an apparent short increase in recorded field-strength, which may be caused by the reception of solar radiation for a few seconds before it is absorbed by the increased ionization in the *D* region. Many photographic records are reproduced.

621.396.812.3:523.74 1500

Unusual Ionospheric Storm—T. W. Bennington. (*Wireless World*, vol. 56, pp. 131–132; April, 1950.) A giant sunspot crossing the sun's meridian on February 20, 1950, was associated not only with the usual phenomena of an ionospheric storm, but with strong reception in Great Britain of transmissions from Leningrad and Stockholm in the 6-m band, and by very rapid fading of the medium-wave London Home Service transmission. The first phenomenon is probably due to the "auroral" type of sporadic *E* and the second to exceptional turbulence of the *F* layer.

RECEPTION

621.396.621 1501

1950 IRE National Convention Program—(Proc. I.R.E., vol. 38, pp. 192–211; February, 1950.) Summaries are given of the following papers:

13. Considerations in Low Noise Figure Microwave Receiver Design—M. T. Lebenbaum and P. D. Strum.
66. Highly Selective Mobile Receiver—R. T. Adams, R. A. Felsenheld, and G. W. Sellers.
107. Frequency-Modulation Interference—L. B. Arguimbau.
108. The Theory of Amplitude-Modulation Rejection in the Ratio Detector—B. D. Loughlin.
109. An Improved Method of Frequency Conversion—V. H. Aske and J. Grund.
110. Common-Frequency Carrier-Shift Radio-Teletype Converter—R. R. Turner.
136. An Atmospherics Waveform Receiver—W. J. Kessler and S. E. Smith.
154. Diversity Reception Techniques—S. H. Van Wambeck and A. H. Ross.
155. Experimental Evaluation of Diversity Receiving Systems—J. L. Glaser and S. H. Van Wambeck.

621.396.621:[537.228.1:548.0 1502

Piezoelectric Crystals in Receiver Construction—F. C. Saic. (*Electrotech. u. Maschinenb.*, vol. 67, pp. 44–50; February, 1950.) A brief review of the characteristics of piezoelectric crystals and a discussion, illustrated by reactance diagrams, of their application in the if stage of wide-band radio receivers.

621.396.621:621.396.619.11/.13 1503

Signal-to-Thermal Noise Ratio—M. V. Callendar. (*Wireless Eng.*, vol. 27, pp. 96–100; March, 1950.) Curves are given of output signal-to-thermal-noise ratio for an FM receiver. The signal-to-noise ratios range from very large values to values <1. Corresponding curves are also given for an AM receiver, and a comparison is made, emphasizing the effect of the ratio of pre-detector to post-detector bandwidth in each case. FM can give results at least equal to AM in respect of signal-to-noise ratio for communication work, provided that the pre-detector bandwidth is no greater than is necessary to accept the full deviation, and that the limiter is fully efficient: the deviation ratio for such work should not exceed a value of about 4. In practice, an AM receiver will in some instances give a slightly better result than a corresponding FM receiver, particularly if any slight mistuning is present.

621.396.621:621.396.822 1504

Design Factors in Low-Noise-Figure Input Circuits—M. T. Lebenbaum. (Proc. I.R.E., vol. 38, pp. 75–80; January, 1950.) 1948 IRE National Convention paper. A method is described for calculating the minimum noise figure attainable by the use of double-tuned circuits in the inputs of hf amplifiers; this provides simple data for designing the network. For active and passive tube input loading a graphical method is given for determining the constants of a double-tuned input circuit with minimum noise figure.

621.396.621.54 1505

The Diode as a Mixing Device in the U.H.F. Band—H. F. Mataré. (*Electron Wiss. Tech.*, vol. 4, pp. 48–52; February, 1950.) Analysis indicating the conditions under which the large reactive effect of a diode mixer may be used to advantage.

621.396.621.54:621.396.828 1506

Elimination of Radio Interference by Off-Frequency Inversion—S. Freedman. (*Radio and Telev. News*, vol. 43, pp. 53–57, 154; March, 1950.) Circuit, description, and performance details of the Type-MCL4 signal splitter. Crystal oscillators operating respectively on frequencies 50 kc above and below the receiver if frequency, and an asymmetrical high-pass filter, with cut-off frequency 50 kc, permit selection of the sideband giving greatest interference attenuation and give high selectivity. A further 1-kc heterodyne and filter give additional selectivity for cw reception. See also 811 of 1948 (McLaughlin).

621.396.822 1507

Induced Grid Noise and Noise Factor—R. L. Bell. (*Nature* (London), vol. 165, pp. 443–444; March 18, 1950.) Assuming that all the induced grid noise is correlated with cathode /anode shot noise, the minimum noise factor obtained on adjusting conductive and susceptive components of grid-ground admittance is independent of lead inductance effects, space-charge capacitance, transit-time damping, and induced grid noise itself. In this hypothetical case, the optimum detuning at the grid required for minimum noise factor is very nearly equal to the space-charge capacitance.

621.396.828 1508

The Main Principles of the Protection of Radio Receivers against Interference Due to H.F. Oscillators for Induction Heating—F. E. Il'gekit and K. V. Bazhenov. (*Radiotechnica* (Moscow), vol. 4, pp. 14–23; November and December, 1949. In Russian.)

621.396/.397].828:621.327.43 1509

Interference from Fluorescent Tubes—"Diallist." (*Wireless World*, vol. 56, pp. 93–94; March, 1950.) Production of rf oscillations in fluorescent tubes is investigated and a possible explanation given. Suppression of these oscillations is discussed and a suitable practical method described.

621.397.828 1510

Interference from Television Receivers—M. G. Scroggie. (*Wireless World*, vol. 56, pp. 126–129; April, 1950.) The line-scanning system of a television receiver is a source of magnetic and electric interference fields. Modern trends in design tend to decrease the magnetic but increase the electric field. The magnetic field chiefly affects portable receivers, but these can fortunately be moved out of the interference region. The electric field can be substantially decreased by the use of simple screening in the television receiver.

STATIONS AND COMMUNICATION SYSTEMS

621.39 1511

1950 IRE National Convention Program—(Proc. I.R.E., vol. 38, pp. 192–211; February, 1950.) Summaries are given of the following papers:

15. Speech Transmission through Restricted Bandwidth Channels—M. J. DiToro, W. Graham, and S. Schreiner.
16. Application of Communication Theory to Periodic Radio Systems—M. Leifer and N. Marchand.
17. Some Aspects of Data Transmission over Narrow-Band Communication Circuits—M. M. Brenner.
31. Transient Response of Asymmetrical Carrier Systems—G. M. Anderson and E. M. Williams.
37. Signal Corps High-Frequency Radio Communication Research and Development—J. Hessel and H. F. Meyer.
38. Military Single-Sideband Equipment Development—R. A. Kulinyi.
39. Radio Relay Design Data 60 to 600 Mc—R. Guenther.
40. Multiplex Microwave Radio Relay—D. D. Grieg and A. M. Levine.
41. Cross Talk in Frequency- and Phase-Modulated Radio Relays used in Conjunction with Multichannel Telephony Equipment—S. Fast.
62. Product Phase Modulation and Demodulation—D. B. Harris and D. O. McCoy.
63. Some Novel Methods for the Generation of PCM—N. R. Castellini, D. L. Jacoby, and B. Keigher.
65. Techniques for Closer Channel Spacing at VHF and Higher Frequencies—C. F. Hobbs and W. B. Bishop.
110. Common-Frequency Carrier-Shift Radio-Teletype Converter—R. R. Turner.
156. Comparison of Modulation Methods for Voice Communication over Ionospheric Radio Circuits—M. G. Crosby, H. F. Meyer, and A. H. Ross.
157. Comparison of Modulation Methods for Facsimile Communication over Ionospheric Radio Circuits—M. Acker and B. Goldberg.

621.39.001.11 1512

Communication in the Presence of Noise—Probability of Error for Two Encoding Schemes—S. O. Rice. (*Bell Sys. Tech. Jour.*, vol. 29, pp. 60–93; January, 1950.) "Recent work by C. E. Shannon and others has led to an expression for the maximum rate at which information can be transmitted in the presence of random noise. Here two encoding schemes are

described in which the ideal rate is approached when the signal length is increased. Both schemes are based upon drawing random numbers from a normal universe, an idea suggested by Shannon's observation that in an efficient encoding system the typical signal will resemble random noise. In choosing these schemes two requirements were kept in mind: (1) the ideal rate must be approached, and (2) the problem of computing the probability of error must be tractable."

621.39.001.11 1513
Calculation of Transmission Efficiency according to Hartley's Definition of Information Content—A. G. Clavier. (*Ann. Telecommun.*, vol. 5, pp. 29–34; January, 1950.) French version of 2045 of 1949 correlated with 1241 of June (Aigrain).

621.391.63 1514
Comparative Study of the Propagation of Optical Radiations of Different Wavelengths in the Atmosphere—G. Goebel. (*Fernmeldetech. Z.*, vol. 3, pp. 43–47; February, 1950.) Measurements were made of the received intensity of a light signal modulated at 1 kc and transmitted over a 3.2-km path, under different atmospheric conditions. No general inferiority of short waves to long waves was observed. Air movements and humidity variations had no measurable effect; warm air layers in the propagation path caused a 1-50-cps short-duration scatter. Storms affected propagation only when accompanied by rain or electric discharges. No clearly defined parameters for distance attenuation were found. High ground-temperature caused short-term fading, while smoke and mist caused selective fading. Even in cloudy conditions the ratio of the received intensities of ultraviolet and deep-red did not exceed 10^2, so that with a receiving amplifier compensated for fading a sufficiently constant signal level should be ensured for communication over the whole optical range.

621.396.5 1515
Ten Years of Radio-Telephone Communications with Mountain Stations—P. Hani. (*Tech. Mitt. Schweiz. Telegr.-Teleph. Verw.*, vol. 28, pp. 112–121; March 1, 1950. In German and French.) A short account of developments since 1933–1936, when the first R/T links were installed, together with a description of the equipment now in use. The central transmitter gives about 4-w output at 57 to 75 Mc. The installation is mains operated and incorporates an automatic calling system by which the subscriber can call any station on the central network. Output from subscriber stations, which are battery operated, is 0.3 w at a frequency adjustable from 40 to 60 Mc.

621.396.619.13:621.396.41 1516
The Application of Frequency Modulation to V.H.F. Multi-Channel Radiotelephony—J. H. H. Merriman and R. W. White. (*Proc. IEE* (London), vol. 97, pp. 123–124; March, 1950.) Discussion on 3513 of 1948.

621.396.619.16 1517
Pulse Communication—A. Bloch and E. Fitch. (*Proc. IEE* (London), vol. 97, p. 107; March, 1950.) Comment on 2079 of 1948 (Cooke, Jelonek, and Fitch; Oxford) and 2619 of 1948 (Fitch), pointing out the essential equivalence of the method of deriving the spectrum of a pulse transmission described by Fitch and the method previously given by Bloch.

621.396.619.16 1518
The Optimum Pulse-Shape for Pulse Communication—J. H. H. Chalk. (*Proc. IEE* (London), vol. 97, pp. 88–92; March, 1950.) The optimum pulse shape is determined for minimum adjacent-channel interference. The method is also applied to find the pulse shape making the energy available for detection a maximum for a receiver with a given pass band. In either case the optimum pulse shape depends only on the product of pulse length and bandwidth.

621.396.619.16 1519
Pulse Code Modulation—D. G. Holloway. (*Electrician*, vol. 144, pp. 679–683 and 763–765; March 3 and 10, 1950.) An outline of fundamental theory.

621.396.619.24:621.396.828 1520
Folded Sideband Modulation—J. L. A. McLaughlin. (*Electronics*, vol. 23, pp. 88–91; March, 1950.) The basic principles are described of a system in which bands of frequencies several kilocycles wide are transmitted sequentially in a narrow band on one side of a carrier. The width of the frequency spectrum used is less than the information bandwidth. Interfering beat notes produced by unwanted carriers falling within the sideband used are eliminated by shifting them to the other side of the carrier. See also 1782 of 1949.

621.396.65 1521
Résumé of V.H.F. Point-to-Point Communication—F. Hollinghurst and C. W. Sowton. (*Proc. IEE* (London), vol. 97, pp. 121–123; March, 1950.) Discussion on 2080 of 1948.

621.396.65:621.396.5 1522
Multiplex Telephony Systems and Radio Links—J. P. Voge. (*Ann. Telecommun.*, vol. 5, pp. 73–88 and 90–97; February and March, 1950.) Analysis of modulation methods and comparison of different multiplex systems. Factors considered are number of channels available, signal-to-noise ratio, power and bandwidth required, reliability, and secrecy. Characteristics of recently constructed radio multiplex systems are given, including two systems in use in the United States for communicating television programs.

621.396.65:621.397.5 1523
A Microwave System for Television Relaying—J. Z. Millar and W. B. Sullinger. (PROC. I.R.E., vol, 38, pp. 125–129; February, 1950.) IRE 1949 National Convention paper. Requirements for television radio relay links are discussed and a Philco system is described. This operates in the 6-kMc common-carrier band and uses heterodyne modulation with a klystron, Type SAC-19, developed by the Sperry Corporation specially for this application. The equipment has been installed by Western Union for transmission between New York and Philadelphia. Photographs show the repeater, the type of antenna used, and a square-wave signal and CBS test pattern after transmission from one terminal to the other and back again. See also 1185 of 1949 (Forster).

621.396.712 1524
The National Transmitter at Beromünster with Unmodulated Aerial Power of 100–200 kW—H. Affolter. (*Tech. Mitt. Schweiz. Telegr.-Teleph. Verw.*, vol. 28, pp. 95–104; March 1, 1950. In German.) Illustrated description of the new transmitter and the general layout, showing particularly the hv and rectifier equipment with simple switching arrangements for supplying either the old or the new transmitter, the water-cooling system, and the special tubular hf feeder line. The installation incorporates the latest ideas in high-power transmitter design. Performance figures are tabulated. Frequency range is 520–1580 kc; overall efficiency at maximum power and 100 per cent modulation is 40.8 per cent.

621.396.931 1525
Small-Town Mobile F.M. Operation—E. Cook. (*Tele-Tech*, vol. 9, pp. 26–28, 55; February, 1950.) Circuit details are given of a two-way R/T installation operating on 37.74 Mc. All receivers are tuned to a common frequency and their af stages are biased to cut-off until a signal is received. An individual receiver responds when the carrier of the calling transmitter is modulated by a particular tone.

SUBSIDIARY APPARATUS

621–526+621.316.722 1526
1950 IRE National Convention Program—(PROC. I.R.E., vol. 38, pp. 192–211; February, 1950.) Summaries are given of the following papers:

70. Modern Methods of Servo Synthesis—R. McCoy and D. Herr.
114. High-Voltage Regulation by means of Corona Discharge between Coaxial Cylinders—S. W. Lichtman.
165. Universal Precision Resolvers—D. L. Herr.

621.3.027.3:621.3.032.4 1527
Heating the Filaments of Valves in a Cascade Generator by Means of High-Frequency Current—T. Douma and H. P. J. Brekoo. (*Philips Tech. Rev.*, vol. 11, pp. 123–128; October, 1949.) Considerable simplification of the hf filament-heating circuits is made possible by the use of filament-current transformers with ferroxcube cores.

621.314.63 1528
Characteristics of Compound Barrier-Layer Rectifiers—E. Billig and P. T. Landsberg. (*Proc. Phys. Soc.*, vol. 63, pp. 101–111; February 1, 1950.) "The assumptions involved in Mott's and Schottky's theories of rectification are analyzed and a potential barrier at the metal/semiconductor interface is proposed which enables one to pass continuously from one theory to the other."

621.316.721.076.7 1529
An Electronic Current Regulator—N. F. Verster. (*Appl. Sci. Res.*, vol. B1, pp. 358–362; 1950.) A method for stabilizing the magnet current of a β-ray spectrometer, derived from a 20-kw dc generator. A vibrating-contact dc amplifier is used to amplify the error voltage and control the field of an exciting generator which energizes the fields of the main generator. Stabilization is within 0.1 per cent throughout the range 2–120 a.

621.316.722.1 1530
Design of a Voltage-Stabilizing Circuit with the Regulating Valve Connected in Parallel—K. B. Mazel'. (*Radiotechnica* (Moscow), vol. 4, pp. 74–79; November and December, 1949. In Russian.)

621.316.73 1531
A Magnetic Field Stabilization Circuit—L. Katz, P. A. Forsyth, L. F. Cudney, G. W. Williams, H. E. Johns, and R. N. H. Haslam. (*Canad. Jour. Res.*, vol. 28, pp. 67–72; January, 1950.) A rotating coil in the air gap of a large electromagnet generates an alternating voltage proportional to the field strength. A fraction of this voltage is balanced against a reference voltage derived from a similar coil rotating between the poles of a permanent magnet. Departures from balance are used to control the current supplied to the electromagnet so as to maintain a steady field. By varying the fraction used for balance, the field may be controlled at any value within a wide range.

621.396.682 1532
Stabilized Anode Supply Unit Using Mazda-2050 Thyratrons—L. Chrétien. (*TSF Pour Tous*, vol. 26, pp. 53–58; February, 1950.) A simple circuit including two thyratrons and also two Type-VR150 stabilizing tubes. The voltage change is about 3 per cent for load

variation from 50 ma to 300 ma or supply-voltage variation from 80 v to 160 v.

TELEVISION AND PHOTOTELEGRAPHY

621.396/.397].828:621.327.43 1533
Interference from Fluorescent Tubes—"Diallist." (*See* 1509.)

621.397.5 1534
1950 IRE National Convention Program—(PROC. I.R.E., vol. 38, pp. 192–211; February, 1950.) Summaries are given of the following papers:

26. Specification for Quality of the Visual Output of Picture Tube Screens—A. E. Martin.
27. The Importance of Practical Design and Specifications for Effective Production and High Quality—J. Manuele.
47. 5-kw Visual and 2.5-kw Aural Television Amplifiers—P. Breen.
48. Design Considerations in TV Transmitters—L. Pollack, E. Bradburd, and I. Krause.
49. Wideband RF Problems in Television Transmitters—E. Bradburd and L. Pollack.
50. The Vidicon—A New Photoconductive Television Pickup Tube—P. K. Weimer, S. V. Forgue, and R. R. Goodrich.
51. Industrial Television System—R. C. Webb and J. M. Morgan.
56. Filters for Television Interference—A. M. Seybold.
78. A 1-kw UHF Television Transmitter—T. M. Gluyas.
79. A Supergain UHF Television Transmitting Antenna—O. O. Fiet.
80. Design of a Hybrid Ring Diplexer for Ultra-High-Frequency Television Use—W. H. Sayer and J. M. De Bell, Jr.
81. Construction and Operation of an Experimental UHF Television Station—R. F. Guy and F. W. Smith.
82. Electro-Optical Filters for Color Television—V. A. Babits and H. F. Hicks, Jr.
102. Use of Miniature Pentode RCA-6CB6 in Television Intermediate-Frequency Amplifiers—W. E. Babcock.
103. Noise Suicide Circuit—H. E. Beste and G. D. Hulst.
104. Quality Rating of Television Images—P. Mertz, A. D. Fowler, and H. N. Christopher.
105. Television Image Reproduction by Use of Velocity-Modulation Principles—M. A. Honnell and M. D. Prince.
106. Design of Printed-Circuit Television Tuner—D. Mackey and E. J. Sass.

621.397.5 1535
Colour Television in the U. S. A.—Comparison of Different Methods—L. Chretien. (*TSF Pour Tous*, vol. 26, pp. 108–111; March, 1950.) Critical review of different systems, based on an article in *Electronics*, December, 1949, entitled "New Directions in Color Television." See 763 of April (D.G.F.).

621.397.5:621.396.65 1536
A Microwave System for Television Relaying—Millar and Sullinger. (*See* 1523.)

621.397.5 (083.74) 1537
Report on the International Television Standards Conference—(PROC. I.R.E., vol. 38, p. 116; February, 1950.) Extracted from a report by D. G. Fink on the C.C.I.R. conference at Zürich, July, 1949. National attitudes on television standards are reviewed and conference conclusions and questions for further study are noted.

621.397.5(083.74) 1538
Television Standards—Y. Delbord. (*Ann. Télécommun.*, vol. 4, pp. 388–396; and 425–429; November and December, 1949. vol. 5, pp. 35–47 and 50–56; January and February, 1950.) In four parts: (a) historical review of the development of the various standards, including a comprehensive chart showing the systems adopted in different countries; (b) relative importance of the different standards; (c) reasons for international divergence; and (d) the French point of view.

621.397.6 1539
New Television Equipment at Alexandra Palace—(*Engineer* (London), vol. 189, pp. 146–147; February 3, 1950.) General description of (a) film-dubbing suite for the production of newsreels and other films to which the sound track is added after filming; (b) telefilm recording room where television programs are recorded on cinematograph film; (c) central room where films are televised for transmission in the program; and (d) the accommodation and proposed development of the television studio center at Lime Grove, Shepherds Bush, London.

621.397.61 1540
The New Eiffel Tower [television] Sound Transmitter—L. Thourel. (*Électronique* (Paris), no. 40, pp. 27–31; March, 1950.) Description of the circuits and constructional features of the rf amplifier chain which delivers 5-kw useful carrier power at 42 Mc. It comprises three units housed in one case. The 7-Mc crystal-oscillator drive unit and the first amplifier/frequency-multiplier unit are removable; the main amplifier and power stages are built in. The anodes of the tubes in the final stage are water-cooled. Efficiency of this stage is 54 per cent with anode voltage 5.4 kv.

621.397.62 1541
Television Spot-Wobble—R. W. Hallows. (*Wireless World*, vol. 56, pp. 84–86; March, 1950.) Discussion of a method of eliminating the horizontal lines usually seen in a television picture, by giving the spot a rapid vertical oscillation of small amplitude so as not to overlap to any large extent the boundaries of a single scanning line. A slight loss of vertical definition results.

621.397.62 1542
Selectivity in Television—W. T. C. (*Wireless Eng.*, vol. 27, pp. 69–71; March, 1950.) Selectivity is discussed in relation to television reception in Britain, the main problem being to prevent the sound signal from interfering with the picture signal. This is particularly difficult when, as in the Midlands transmission, only the lower of the vision sidebands, which lies between the vision and sound carriers, is transmitted. The merits of tuned-rf and superheterodyne receivers are compared. The choice between the two depends on whether or not it is feasible to obtain rejector circuits of sufficiently high Q at signal frequency, the important factor being the relation of the product of bandwidth and circuit Q to signal frequency.

621.397.62:[621.385.2:621.315.59 1543
Application of Germanium Diodes in Veryhigh and Ultrahigh TV Sets—J. H. Sweeney. (*TV Eng.*, vol. 1, pp. 10–11, 36; February, 1950.) Discussion of the relative merits of the crystal diode as a replacement for the tube diode, particularly in video-detector, dc-restorer and af discriminator circuits.

621.397.81 1544
Fringe-Area Television—(*Wireless World*, vol. 56, pp. 87 and 139; March and April, 1950.) Two maps show values of the video field-strength recorded with mobile equipment at many places about 70 miles from the Sutton Coldfield transmitter. The greatest variations observed were, as might be expected, in the hilly country of Wales.

621.397.813:621.397.62 1545
The Distortion of Video and Audio Signals in a Television Receiver—G. I. Byalik. (*Radiotechnica* (Moscow), vol. 4, pp. 34–46; November and December, 1949. In Russian.) The use of a single receiving channel for AM video signals and FM audio signals is limited by the presence of the nonlinear element, the detector, which causes intermodulation distortion. A mathematical analysis of this effect on the quality of the image and the sound is presented and suggestions are made for rendering the distortion of the audio signals negligible and reducing that of the video signals to a few per cent. It is shown by this analysis and also by experiments that a second if amplifier is not required for the sound channel.

621.397.82:621.392.52 1546
Eliminating TVI with Low-Pass Filters—Grammer. (*See* 1367.)

621.397.828 1547
Television Interference Suppression—L. Varney. (*RSGB Bull.*, vol. 25, pp. 290–294; March, 1950.) Synopsis of a paper read at a meeting of the Radio Society, October, 1949. Achievements in this field are reviewed and some recent improvements in technique are described. See also 2356 of 1949.

621.397.62 1548
The Principles of Television Reception [Book Review]—A. W. Keen. Publishers: Pitman and Sons, London, 319 pp., 30s. (*Wireless Eng.*, vol. 27, pp. 94–95; March, 1950.) "The book can be recommended for those who have little or no knowledge of television but who have a good background of ordinary wireless theory and practice. It will enable them to obtain a good general, but hardly a detailed, knowledge of television."

TRANSMISSION

621.3.016.35:621.396.61 1549
Static and Dynamic Temperature Compensation of Transmitters—E. Roske. (*Fernmeldetech. Z.*, vol. 3, pp. 53–61; February, 1950.) Discussion of the effect of temperature change on frequency stability and the possibilities of compensation by the use of ceramic components.

621.316.726:621.396.615 1550
1950 IRE National Convention Program—(PROC. I.R.E., vol. 38, pp. 192–211; February, 1950.) A summary is given of the following paper:

111. A Simple Crystal Discriminator for FM Oscillator Stabilization—J. Ruston.

621.396.61.029.58 1551
Continuously-Tuned 50-kw Transmitter—J. L. Hollis. (*Electronics*, vol. 23, pp. 70–73; March, 1950.) Circuit and construction details of the U. S. Navy transmitter Type AN/FRT-5 and AN/FRT-6. Motor-driven, servo-positioned units are used to tune individual stages and allow operation on any frequency from 4 to 26 Mc without tuned-circuit switching. Frequency changing is effected in less than two minutes.

621.396.619.23 1552
Non-Linear Effects in Rectifier Modulators—D. G. Tucker and E. Jeynes. (*Wireless Eng.*, vol. 27, p. 66; February, 1950.) Comment on 2184 of 1949 (Belevitch).

621.397.61 1553
The New Eiffel Tower [television] Sound Transmitter—Thourel. (*See* 1540.)

TUBES AND THERMIONICS

621.385+621.396.615.14 1554
1950 IRE National Convention Program—(PROC. I.R.E., vol. 38, pp. 192–211; February,

1950.) Summaries are given of the following papers:

10. Glass-Sealed Germanium Diodes—S. F. Amico.
11. High-Temperature Characteristics of Germanium Diodes—L. S. Pelfrey.
19. Accelerated Life Testing of Vacuum Tubes—J. Rothstein.
87. A New Class of Switching Tubes for Digital Applications—J. Katz.
89. A New Type of Frequency-Control Tube —R. W. Slinkman.
90. MIT Electrostatic Storage Tube—S. H. Dodd, H. Klemperer, and P. Youtz.
91. Performance and Analysis of a Transverse Current Traveling-Wave Amplifier and Limiter—L. M. Field.
92. An Experimental Electron Tube using Space-Charge Deflection of the Electron Beam—J. T. Wallmark.
112. A New "Soft Structure" for Rugged Receiving Tubes to Improve Resistance to Shock and Electron Emission—G. W. Baker.
113. Hydrostatic Pressure in an Electron Gas: its Application to Electron-Beam-Electromagnetic Wave Interaction—P. Parzen and L. Goldstein.
115. Thyratron Grid Emission and the Trigger-Grid Thyratron—L. Malter and M. R. Boyd.
116. High-Intensity Pulse-Distribution Tube—P. M. G. Toulon.
138. Development of 10-cm High-Power Pulsed Klystron—M. Chodorow, E. L. Ginzton, I. Neilsen, and S. Sonkin.
139. Space-Charge Effects in Reflex Klystrons —V. Westberg and M. Chodorow.
140. Recent Development in High-Power Klystron Amplifiers—C. Veronda and V. Learned.
141. A New Super-Power Beam Triode—W. N. Parker, W. E. Harbaugh, M. V. Hoover, and L. P. Garner.
142. External-Cathode Inverted Magnetron—J. F. Hull.
158. A Vacuum Seal between Metals and Ceramics for High Temperature Applications—H. W. Soderstrom and K. H. McPhee.
159. Effect of Coating Composition of Oxide-Coated Cathodes on Electron Emission—E. G. Widell and R. A. Hellar.
160. Effects of Controlled Impurities in Nickel Core Metal on Thermionic Emission from Oxide-Coated Cathodes—G. Hees.
161. Investigation of Contaminant in Vacuum Tubes—P. D. Williams.
162. Hot-Strength Properties of Filamentary Alloys—B. Wolk.

621.385.029.63/.64:537.291+538.691 1555

Electron Beams in Axially Symmetrical Electric and Magnetic Fields—Wang. (*See* 1395.)

621.385.15 1556

A New Secondary Cathode—C. S. Bull and A. H. Atherton. (*Proc. IEE* (London), vol. 97, pp. 65–71; March, 1950.) The emission from the secondary cathode in a multiplier stage gradually decreases during its life; this is due to bombardment by the primary electron beam, which causes disintegration of the surface oxide layer and gradual exposure of the clean base metal of the secondary cathode. To avoid this, thicker coatings of MgO were tried but had too high a resistance. A new type of cathode, made from a mixture of MgO and $BaCO_3$, was found to be sufficiently conducting and gave a secondary emission ratio of about 3. The emission remained sensibly constant for over 1,000 hours, with an operating temperature of 400° C and a primary bombarding current density of 20 ma/cm². The use of this cathode has made possible the development of an orbital-beam single-stage thermionic multiplier tube with a mutual conductance of 20 ma/volt and input capacitance of 8 pF.

621.396.615.141.2 1577

The Behaviour of Multiple Circuit Magnetrons in the Neighbourhood of the Critical Anode Voltage—W. E. Willshaw and R. G. Robertshaw. (*Proc. Phys. Soc.*, vol. 63, pp. 41–45; January 1, 1950.) The mechanism of operation of the multiple circuit magnetron oscillator in the region of minimum magnetic field and voltage, where the efficiency is commonly to approach zero, should approach that of an oscillator of the traveling-wave-tube type, providing that a cathode of suitable size is used. Useful efficiencies should thus be obtainable under these conditions. Details of experiments are given in which an electronic efficiency of 12 per cent was obtained at a wavelength of 3 cm at values of magnetic field and voltage several times lower than those used for high efficiency operation. The mode of operation was determined by the value of the magnetic field, a given mode being maintained over a range of magnetic field of the order of 8 per cent. The anode voltage was about 70 per cent of the critical value. The experimental results generally support the hypothesis and suggest that the minimum voltage regime should be of extreme importance for work at the highest radio frequencies.

621.396.615.142.2 1558

Two-Cavity Klystron—B. Meltzer. (*Wireless Eng.*, vol. 26, pp. 365–369; November, 1949.) Two fundamental differential equations governing electron flow in the drift space are derived. They are valid only while the motion preserves its single-stream character, the limiting condition being when overtaking occurs. Thermal variations of velocity and forces due to the magnetic field of the current are neglected. The equations are integrated and applied to discussion of the plane diode, effects in the drift space of the klystron and in the klystron with space-charge-limited cathode.

MISCELLANEOUS

539+658 1559

1950 IRE National Convention Program—(PROC. I.R.E., vol. 38, pp. 192–211; February, 1950.) Summaries are given of the following papers:

1. Evolution and Growth of Industrial Designing—J. Vassos.
2. Procedure in Industrial Designing—C. Peterson.
3. Cost Reduction Possibilities in Industrial Design—W. B. Donnelly.
4. Sales Attitude towards Industrial Design —E. P. Toal.
5. News of the Nucleus—U. Liddel.
20. Statistical Evaluation of Life Expectancy of Vacuum Tubes designed for Long-Life Operation—E. M. McElwee.
21. Application of Statistics to Acceptance Specifications—B. Koslow.
22. Statistical Methods in Research and Development—L. Lutzker.
23. Statistical Engineering of Tolerances—E. D. Goddess.
24. Top Management Evaluates Quality in Terms of Sound Engineering—A. B. DuMont
25. Statistics—A New Tool for the Planning and Analysis of Laboratory Experiments —E. B. Ferrell.
163. Miniaturization Techniques: A Discussion and Proposal—M. Abramson and S. Danko.